APPENDIX NUMBER F HAS BEEN

OMITTED FROM THIS FICHE BECAUSE IT

IS OF POOR REPRODUCTIVE QUALITY

L'APPENDICE NUMÉRO F A ÉTÉ

OMIS DE CETTE FICHE ÉTANT DONNÉ SA

PIÈTRE QUALITÉ DE REPRODUCTION

TP 7738E

DEMONSTRATION OF RAIL FREIGHT TRUCKS USING FRAME-BRACING TECHNOLOGY

By

J.W. Horwat, P.Eng.
Project Engineer

B.T. Whitten
Project Engineer

B.H. Willoughby
Mechanical Technician

Transportation Technology Limited

April 1986

Library and Information Centre / Centre de documentation (CSLA)
RECEIVED / REÇU LE
OCT 3 1986
Transport Canada / Transports Canada

K6-10478

87-02428/

The contents of this report reflect the views of the contractor and not necessarily the official views of the Transportation Development Centre of Transport Canada

Un sommaire en français de ce document est inclus avant la table des matières.

PROJECT TEAM

The project team for UTDC R&D Ltd. consisted of:

John W. Horwat	Program Manager/Project Chief Engineer
Roy E. Smith	Project Chief Engineer
Brian T. Whitten	Analyst
Bruce H. Willoughby	Technician
Gerald H. Poelwyk	Designer/Draftsman

THIS PAGE LEFT BLANK INTENTIONALLY.

Transport Canada / Transports Canada

Development / Développement

REPORT DOCUMENTATION FORM

1. Transport Canada Report No.	2. TDC Project No.	3. Recipient's Catalogue No.
TP 7738E	4729	

4. Title and Subtitle	5. Report Date
DEMONSTRATION OF RAIL FREIGHT TRUCKS USING FRAME-BRACING TECHNOLOGY	April 1986
	6. Performing Organization Report No. 42-TR-7100-001
7. Author(s) J.W. Horwat, B.T. Whitten, B.H. Willoughby	8. Transport Canada File No. D 1465-384
9. Performing Organization Name and Address Transportation Technology Ltd.(formerly UTDC R&D Ltd.) P.O. Box 160, Station 'A' Kingston, Ontario K7M 6R1	10. DSS File No. 10SD-T8200-2-2510
	11. DSS or Transport Canada Contract No. OSD82-00089
12. Sponsoring Agency Name and Address Transportation Development Centre (TDC) Guy Favreau Complex 200 Dorchester Blvd. West, Suite 601, West Tower Montreal, Quebec H2Z 1X4	13. Type of Report and Period Covered Final; Oct. 82-Aug. 85
	14. Sponsoring Agency Code TDC 4729
15. Supplementary Notes This project was co-sponsored by the Ministries of Northern Affiars and Transportation and Communications, Government of Ontario	16. TDC Project Officer D.W. Dibble

17. Abstract

The design, installation, testing and demonstration of the UTDC frame-braced three-piece rail freight trucks is the subject of this report. Two test and two control 100-ton gondola cars were produced at the Ontario Northland Transportation Commission (ONTC). These cars were subjected to yard and mainline testing and placed in revenue ore service to confirm the results of the mathematical analyses. The tests showed that the stable speed of the frame-braced truck was some 20 percent greater than that of the conventional truck; the angle-of-attack was improved by 55-60 percent; and the wheel wear of a frame-braced truck was reduced by 25-30 percent over the conventional truck after only 24,000 km of travel at ONTC, and 55% after 100,000 miles at Burlington Northern. It was found that BN could achieve a payback on frame-braced trucks in two to three years.

18. Key Words	19. Distribution Statement
Rail frame-braced, three piece car truck	Copies available on request from the Transportation Development Centre

20. Security Classification (of this report)	21. Security Classification (of this page)	22. No. of Pages	23. Price
Unclassified	Unclassified	82	--

TDC/CDT 79-005
Rev 86

Canada

Transports Canada / Transport Canada

Développement / Development

FORMULE DOCUMENTAIRE DU RAPPORT

1. Nº du rapport Transports Canada	2. Nº de l'étude — CDT	3. Nº de catalogue du destinataire
TP 7738E	4729	

4. Titre et sous-titre	5. Date du rapport
DEMONSTRATION OF RAIL FREIGHT TRUCKS USING FRAME-BRACING TECHNOLOGY	avril 1986
	6. Nº du rapport de l'organisme exécutant: 42-TR-7100-001
7. Auteur(s): J.W. Horwat, B.T. Whitten, B.H. Willoughby	8. Nº de dossier Transports Canada: D 1465-384
9. Nom et adresse de l'organisme exécutant: Transportation Technology Ltd.(formerly UTDC R&D Ltd.) C.P. 160, Station 'A' Kingston, Ontario K7M 6R1	10. Nº de dossier — ASC: 10SD-T8200-2-2510
	11. Nº de contrat — ASC ou Transports Canada: OSD82-00089
12. Nom et adresse de l'organisme parrain: Centre de développement des transports (CDT) Complexe Guy-Favreau 200 ouest, boul. Dorchester, Suite 601, Tour Ouest Montréal, Québec H2Z 1X4	13. Genre de rapport et période visée: Final; oct. 82-août 85
	14. Code de l'organisme parrain: CDT 4729
15. Remarques additionnelles: Ce projet était co-parrainé par les Minisitères des Affaires du Nord et de Transporation et Communications, Gouvernement de l'Ontario.	16. Agent de projet — CDT: D.W. Dibble

17. Résumé

Ce rapport concerne l'étude, la réalisation, l'essai et l'exploitation expérimentale par UTDC de bogies marchandises trois pièces à liaison croisé des longerons. Deux wagons tombereaux de 100 tonnes de charge ont été munis de ce type de bogies dans les installations de l'Ontario Northland Transportation Commission (ONTC) et deux autres, de bogies trois pièces non modifiés, ces deux derniers devant servir de wagons témoins. L'ensemble a été soumis à des essais en gare de triage et sur voies principales avant d'être mis en service minéralier payant pour valider les résultats des analyses mathématiques. Les essais ont montré que les bogies modifiés demeuraient stables à une vitesse de 20 p. 100 supérieure à celle des bogies classiques et que leur angle d'inscription était amélioré dans une proportion de 55-60 p. 100. Côté usure des roues, les bogies modifiés ont affiché une diminution de 25-30 p. 100 après seulement 24 000 kilomètres sur le réseau ONTC et de 55 p. 100 après environ 160 000 kilomètres sur le réseau Burlington Northern (B.N.). Il a été calculé que B.N. pourrait récupérer le coût de la modification sur une période de deux à trois ans.

18. Mots-clés	19. Diffusion
Chemin de fer, bogies trois pièces, liaison croisée des longerons	Pour obtenir un exemplaire, s'adresser au Centre de développement des transports

20. Classification de sécurité (de ce rapport)	21. Classification de sécurité (de cette page)	22. Nombre de pages	23. Prix
non classifié	non classifiée	82	--

CDT/TDC 79-005 Rev 86

Canada

ACKNOWLEDGEMENTS

UTDC R&D Ltd. wishes to acknowledge the aid and advice given by the personnel of the Ontario Northland Transportation Commission, in particular G.A. Payne, Chief Mechanical Officer, O. Buffett, A. Woodley and the shop artisans. UTDC wishes to acknowledge the aid and support of the National Research Council Railway Laboratory, in particular, C.A.M. Smith, Director, and W. Watson, and CP Rail, especially V. Katchadourian and W. Pale.

SUMMARY

This program was inaugurated to continue and expand on the earlier work carried out by UTDC. The program objective was to build, test, and demonstrate in revenue service a modification to rail freight trucks known as frame-bracing. The modification was designed to improve the dynamic stability and the curving ability of the truck at a reasonable cost.

Four 90-tonne (100 ton) freight trucks were fitted with the frame-braced modification. These were then teamed up with an equal number of unmodified "control" trucks in two two-car consists. Test results confirmed the analytical predictions that the frame-bracing modifications resulted in an improved truck: more stable at high speeds and with better curving performance than the standard trucks.

It is evident from revenue service measurement that the wheel wear, espectially tread wear, on the modified trucks is less than that of the standard trucks.

From the wear measurements and other referenced data, it was determined that a payback period of five years or less could be realized by a broad range of railroads and car owners, especially those whose cars travel high annual distances and where current wheel life is less than three times the annual distance.

The modified and control carsets continue in normal revenue service.

SOMMAIRE

Ce programme constitue le prolongement des travaux antérieurs faits par UTDC. Objectif: construire, tester et mettre en service payant des bogies marchandises du type à liaison croisée des longerons. Il s'agissait en fait de modifier à coût raisonnable des bogies existants de manière à en améliorer la stabilité dynamique et le comportement en courbe.

Quatre bogies marchandises de 90 tones métriques de charge ont été modifiés et testés en même temps qu'un nombre égal de bogies "témoins" non modifiés, répartis entre deux rames de deux wagons chacunes. Les résultats des essais ont confirmé les prévisions analytiques voulant que la liaison croisée des longerons ait pour effet d'améliorer la stabilité à haute vitesse et le comportement en courbe par rapport aux bogies conventionnels.

Les mesures faites en cours d'exploitation en service payant montrent clairement que l'usure des roues, et spécialement des bandes de roulement, est moins prononcée avec les bogies modifiés.

Se basant sur l' sure constatée et sur d'autres données, les chercheurs ont calcule que la période nécessaire pour récupérer le coût de la modification serait d'au plus cinq années pour un large éventail de chemins de fer et de propriétaires de wagons. Cela est particulièrement vrai pour ceux dont les wagons roulent beaucoup et affichent une durée utile des roues inférieure à trois fois le kilométrage annuel parcouru.

Les bogies modifiés ainsi que les bogies témoins continuent d'être exploités en service payant normal.

THIS PAGE LEFT BLANK INTENTIONALLY.

TABLE OF CONTENTS

		PAGE NO.
	SUMMARY	
1.0	INTRODUCTION	1
	1.1 BACKGROUND	1
	1.2 OBJECTIVE	2
2.0	DESCRIPTION OF DESIGN	3
3.0	DYNAMIC STABILITY AND CURVING ANALYSIS	9
4.0	TESTING	15
	4.1 TEST CONFIGURATION	15
	4.2 TEST DESCRIPTION	16
5.0	FATIGUE ANALYSIS	27
6.0	ECONOMIC STUDY	29
7.0	RESULTS	39
	7.1 STABILITY AND CURVING ANALYSES	39
	7.2 TEST RESULTS	53
8.0	DISCUSSION	71
	8.1 STABILITY AND CURVING	71
	8.2 TESTING	74
9.0	CONCLUSIONS	79
10.0	RECOMMENDATIONS	81

TABLE OF CONTENTS (cont'd)

APPENDIX A Properties of Cross Braced Trucks

APPENDIX B Frame-Braced Modification Parts List

APPENDIX C Test Plan; Mass, Moment of Inertia, Stiffness Testing

APPENDIX D Test Plan; Static and Dynamic Testing

APPENDIX E Reports; Fatigue Analysis of the Frame Braced Truck; Fatigue Test of Cross Braced Truck

APPENDIX F Cost/Benefit Analysis of Frame Braced Trucks, UTDC R&D Technical Note 42-TN-7100-015.

APPENDIX G Results of the Stability and Curving Analysis

APPENDIX H Reports; Mass, Inertia, Linear and Stiffness Measurement Tests on the Barber S-2 Truck at ONR North Bay; Measured Values of Inter-axle Lateral and Yaw Stiffness for the UTDC Cross-Braced Truck

APPENDIX I Stability and Curving Test Results at Canadian Pacific

APPENDIX J Wheel Profiles for Reprofiled and Worn Wheels, Standard and Modified Trucks

APPENDIX K Wheel Profiles from Burlington Northern Coal Cars

TABLE OF CONTENTS (cont'd)

LIST OF FIGURES		PAGE NO.
2.1-1	Illustration of a Conventional Three-piece Freight Truck	4
2.1-2	Axle Shear	4
2.1-3	Axle Bending (Yaw)	4
2.1-4	Frame Bracing Concept	6
2.1-5	Frame Bracing Retrofit	7
2.1-6	Welding Jig	8
3.1-1	Critical Speed Characteristics Unsteered Trucks (conicity = .2)	10
3.1-2	Plots of Angle of Attack of the Leading Axle (Shaded Area is Flange Free)	11
3.1-3	Angle of Attack Defined	13
3.1-4	Three Piece Truck Model for Analyses	14
4.1-1	Test Consist	17
4.1-2	Instrumentation Location at ONTC	20
4.1-3	Map Showing Test Areas	21
4.1-4	Wheel Profile Measuring Device	24
7.1-1	Critical Speed Versus K_S, K_B	43
7.1-2	Angle of Attack for Curve Radius of 300 m, Conicity of 0.05	44
7.1-3	Angle of Attack for 300 m Curve, Conicity of 0.20	45
7.1-4	Tread Wear Index, 300 m Curve Radius, 0.05 Conicity	46
7.1-5	Tread Wear Index, 300 m Curve Radius, 0.20 Conicity	47
7.1-6	Flange Wear Index, 300 m Curve Radius, 0.05 Conicity	48

TABLE OF CONTENTS (cont'd)

LIST OF FIGURES

		PAGE NO.
7.1-7	Flange Wear Index, 300 m Curve Radius, 0.2 Conicity	49
7.1-8	Loaded Car Curving Performance - Angle of Attack	50
7.1-9	Loaded Car Curving Performance - Tread Wear Index	51
7.1-10	Loaded Car Curving Performance - Flange Wear Index	52
7.2-1	Chart Recorder Readout - 60 mi/hr	57
7.2-2	Brace Forces vs. Track Curvature, Empty Car	58
7.2-3	Brace Forces vs. Track Curvature, Loaded Car	59
7.2-4	Lateral Acceleration on Lead Axle Bearing Endcap	62
7.2-5	Angle of Attack Test Comparison, Frame Braced to Standard Truck	63
7.2.6	Angle of Attack, 100-ton Trucks, 3 Speeds	64
7.2-7	Overlay of Wheel Profiles, Wheel Position 3L, First Married Pair at ONTC	68
7.2-8	Overlay of Wheel Profiles, BN Cars, 100,000 miles	70

LIST OF TABLES

6.1-1	Cost/Benefit - ONTC - 5520 miles per year	34
6.1-2	Cost/Benefit - ONTC - 50,000 miles per year	35
6.1-3	Cost/Benefit - BN - AAR Interchange Rates	36
6.1-4	Cost/Benefit - BN - 1985 Estimate Rates	37
7.2-1	Inertia Test Data	53
7.2-2	Angle of Attack of Leading and Trailing Axles Measured at 37 mph	65
7.2-3	Quantitative Wheel Wear Results	69

1.0 INTRODUCTION

1.1 BACKGROUND

The rail truck currently installed under 1.5 million railway freight cars in North America was conceived and developed some fifty years ago. Although improvements have been made to this three-piece truck, it changed little until the late seventies, when two models of a major change, known as "cross-bracing", appeared under test cars. Cross-bracing describes a linking of diagonally opposite axle journals permitting axle yaw while inhibiting axle parallel shear (lozenging). Trucks employing this concept have been called "radial" trucks since the designers' intention was to improve curving through the promotion of radial alignment of the axles.

To further explore and understand the properties of cross-bracing leading to some performance improvement, UTDC R&D carried out an internally funded program of analysis and design. From this work, an alternative method of controlling freight truck axle positions and improving the stability and curving of the standard three-piece unit was developed. This method appeared to achieve performance levels equivalent to the cross-braced truck but with a simpler and less costly apparatus. The results of the study appear in a paper by R.E. Smith and R.J. Anderson entitled "Properties of Cross Braced Trucks", which is contained in Appendix A.

A single laboratory version of the design hardware was fabricated and, with the cooperation of the National Research Council (NRC), tested at the NRC facilities in Ottawa. The tests achieved sufficient success to warrant further development and testing. Proposals to that effect were made to Transportation Development Centre, Ontario's Ministry of Transportation and Communications, and Ontario's Ministry of Northern Affairs. Each agreed to share in the sponsorship of this program.

1.2 OBJECTIVE

The objectives of the program were:

- to build and install the UTDC R&D-designed frame bracing modification on rail freight trucks;
- to test the modified trucks under standard cars comparing the results to those of unmodified trucks also under standard cars; and,
- to demonstrate the frame bracing technique and its potential benefits in extended revenue service.

2.0 DESCRIPTION OF DESIGN

In the analysis of the three piece North American freight truck (Fig 2.1-1), there are only two wheelset actions which can occur. These are interwheelset shear (Fig 2.1-2) and interwheelset yaw (Fig 2.1-3). Any other actions can be characterized by a combination of these two.

The control of interwheelset shear is dependent on the truck shear stiffness (K_S), while the control of interaxle yaw is a function of truck bending stiffness (K_B). The shear stiffness KS is defined as the ratio of the force required to displace the axles in shear and the shear displacement (Figure 2.1-2) i.e.

$$K_S = \frac{F}{X}$$

The bending stiffness K_S is defined as the ratio of the moment required to yaw the axles antiparallel and the angle of that yaw (Figure 2.1-3) i.e.

$$K_B = \frac{M}{\theta}$$

The analysis of dynamic stability and curving may be performed by considering K_S, K_B, truck and carbody geometry and classical wheel/rail interface phenomena. Because of the design of the three piece truck, K_S, resulting primarily from the sideframe/bolster interconnection is quite low permitting truck lozenging, while K_B, resulting

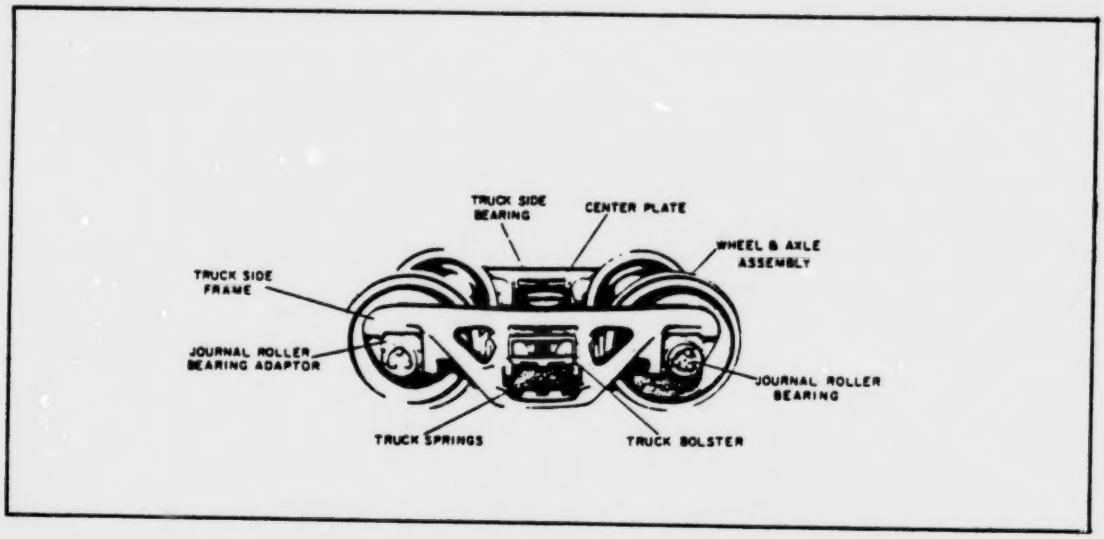

FIGURE 2.1-1 - ILLUSTRATION OF A CONVENTIONAL THREE-PIECE FREIGHT TRUCK

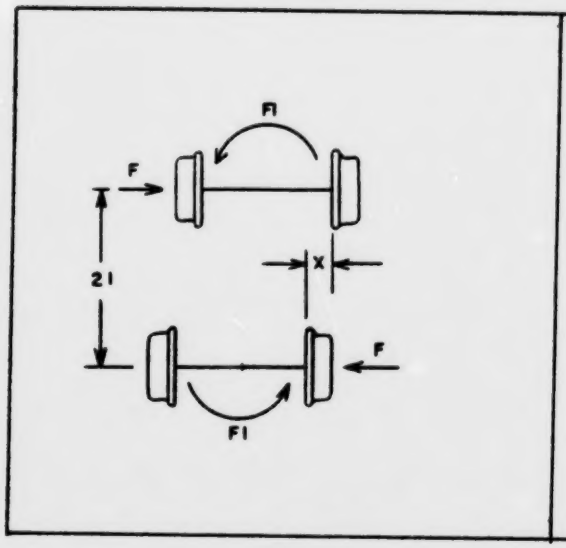

FIGURE 2.1-2 - INTERAXLE SHEAR

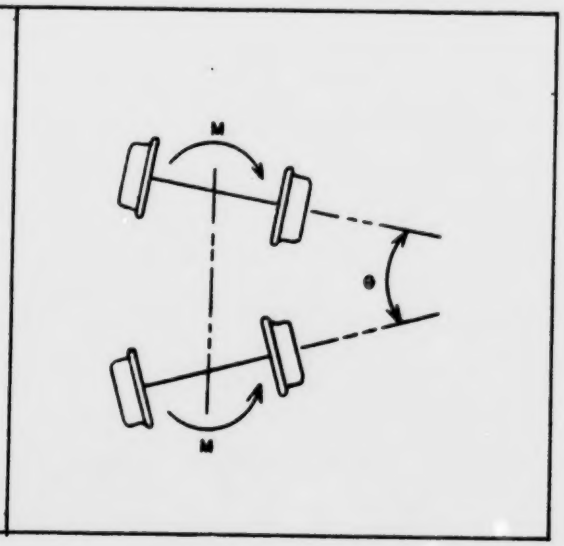

FIGURE 2.1-3 - INTERAXLE BENDING (YAW)

from the solid axle bearing adapter to sideframe connection is very high, resisting inter-axle yawing, thus resisting any axle-to-curve radial positioning.

It becomes apparent that allowing for the radial positioning of the axles while inhibiting axle shear would encourage better curving ability. Both motions must also be resisted adequately to produce the required stability.

The frame-bracing concept (Figure 2.1-4) introduces mechanical elements which reduce K_B while increasing K_S to achieve better steerability while providing increased stability.

The elements of the design are shown in Figure 2.1-5. Appendix B contains a complete list of parts for the design.

The resiliently-mounted braces (4) provide for increased K_S while the primary resilient pads (1) provide for reduced K_B.

To ensure the proper placement of the brackets with respect to the sideframe, and eliminate brace adjustment, a welding jig (Figure 2.1-6) was designed and manufactured. It was designed to support the sideframe, centre it and place the brackets in proper position for welding.

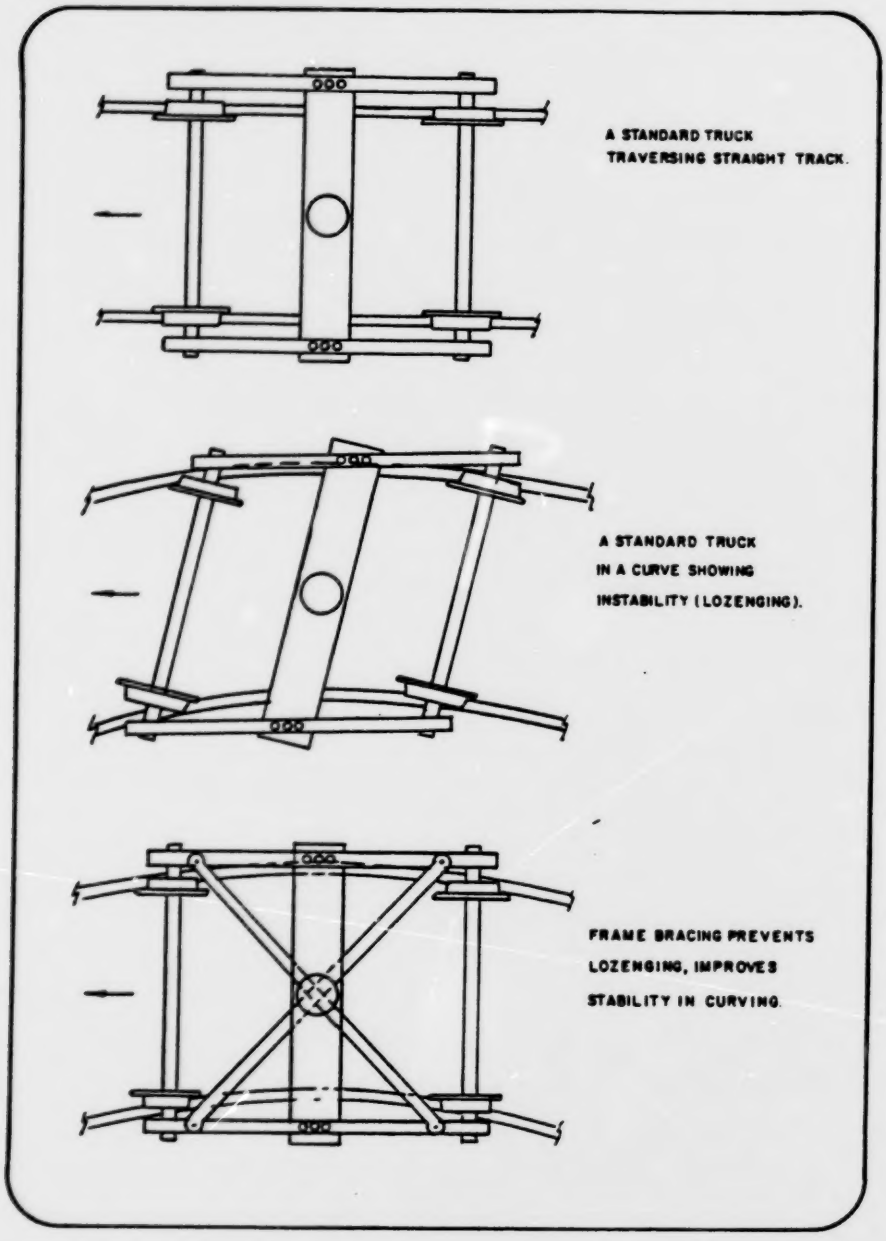

FIGURE 2.1-4 - FRAME BRACING CONCEPT

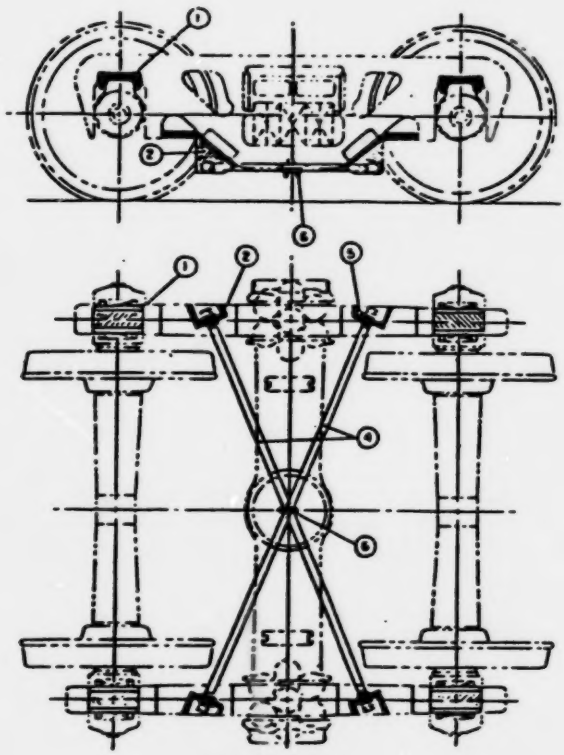

ITEM	DESCRIPTION
1	Primary (LC) Pad
2	Bracket Assembly
4	Braces
5	Centre Bonded Bushing
6	Clamp

FIGURE 2.1-5 - FRAME-BRACING RETROFIT

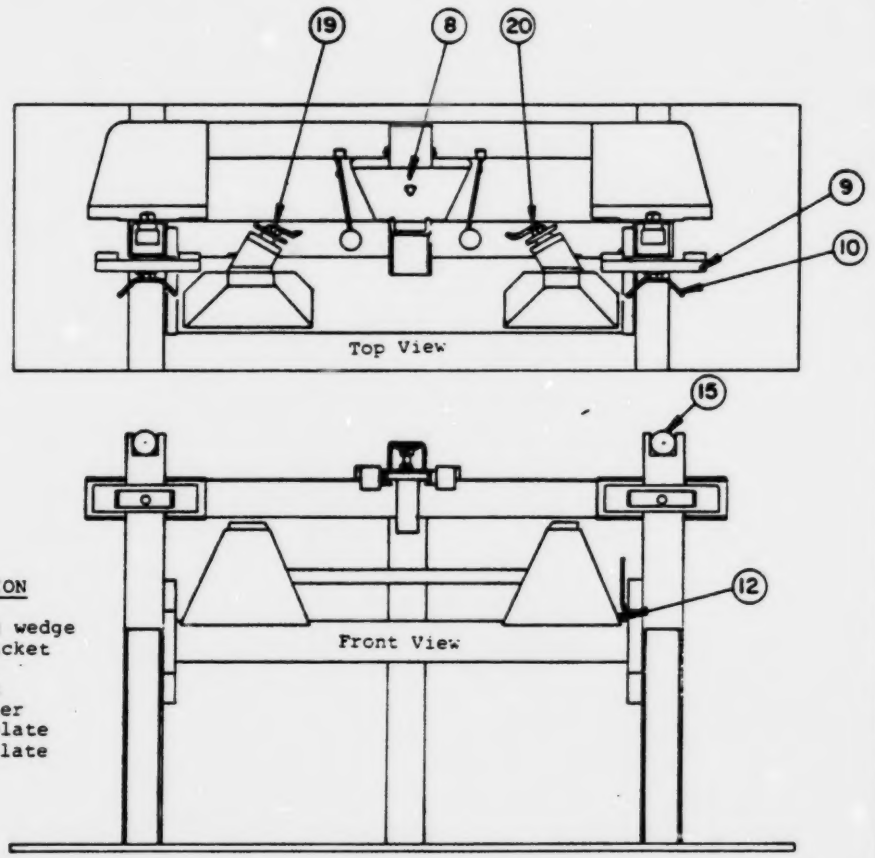

ITEM	DESCRIPTION
8	Centering wedge
9	Clamp bracket
10	Wing nut
12	Stop bolt
15	Load Runner
19	Holding plate
20	Holding plate

FIGURE 2.1-6 - WELDING JIG

3.0 DYNAMIC STABILITY AND CURVING ANALYSES

In the Smith and Anderson paper (Appendix A) it was shown that the classical unsteered truck analyses are based on axle-to-axle generalized stiffness parameters of K_S (shear) and K_B (bending). Through creation of a lumped mass/spring/damper model of the truck with the mass elements (bolster, sideframe, wheelsets) of infinite stiffness, joined together through parallel springs and dampers, a series of second order linear differential equations may be written which become an eigenvalue problem, the solution of which will produce critical speed field plots based on values of K_S and K_B as shown in Figure 3.1-1.

Critical speed is defined as the speed of the vehicle at which the perturbed motions of the vehicle system become undamped.

Each curve represents a constant critical speed, and can be seen to increase as K_s and K_B are increased up to an optimum, above which further stiffness increases result in decreased critical speeds. For the model analyzed, the highest critical speed is slightly greater than 95 m/s on the right and 100 m/s at the top.

It was shown in the paper that, using the same model in a quasi-static non-linear curving analysis, the leading axle angles of attack were as shown in Figure 3.1-2 with the angles increasing as KS and K_B increased, somewhat contrary to the critical speed curve behaviour.

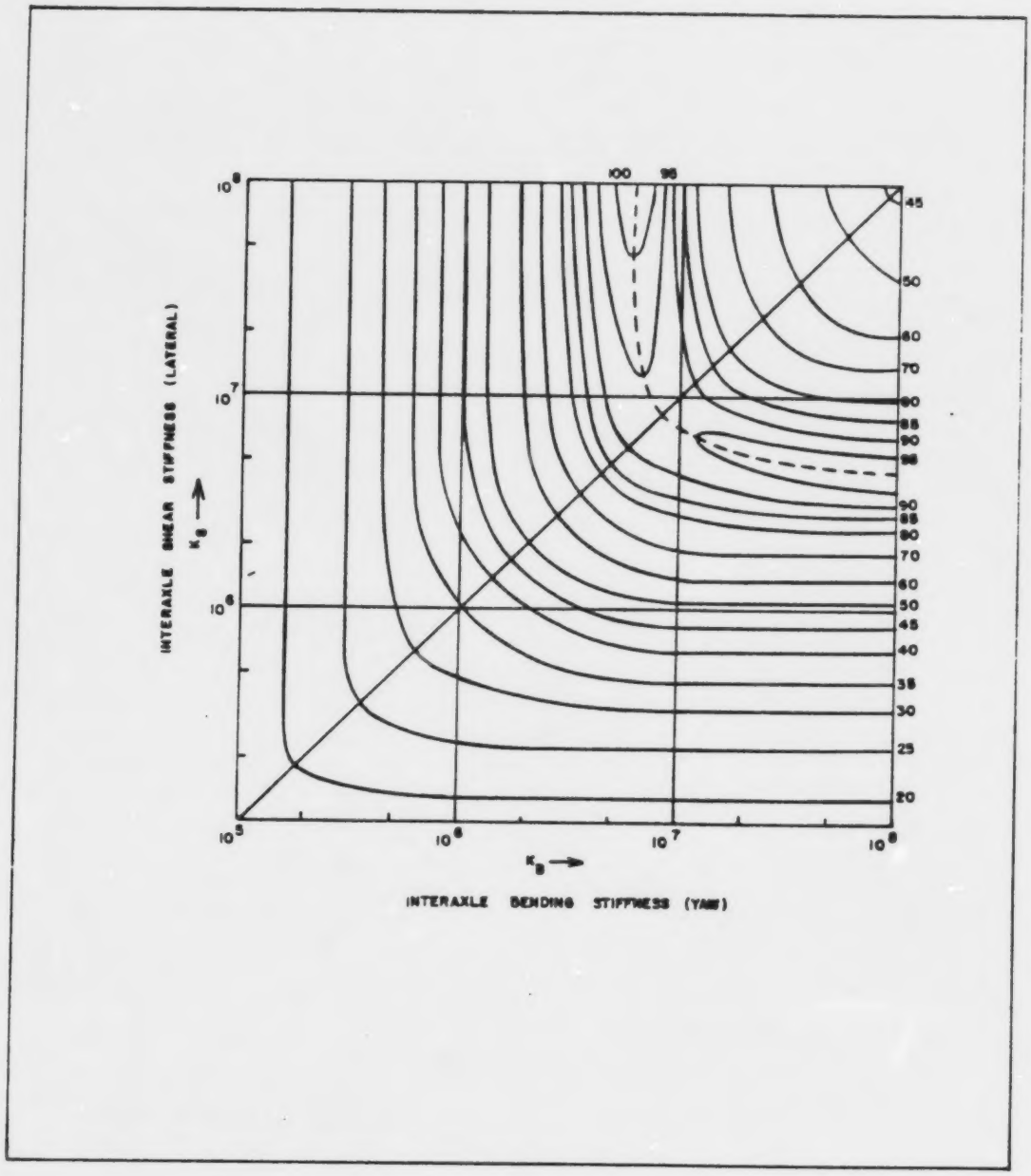

FIGURE 3.1-1 - CRITICAL SPEED CHARACTERISTICS UNSTEERED TRUCKS
(conicity = 0.2)

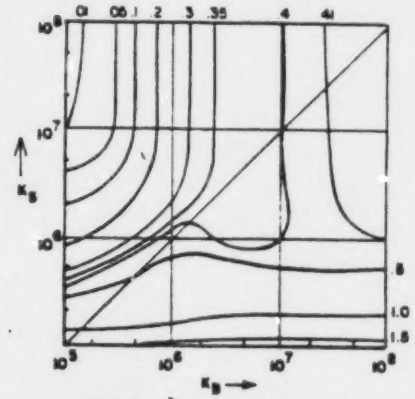

FIG 17 - λ = 0.05, R = 300 M

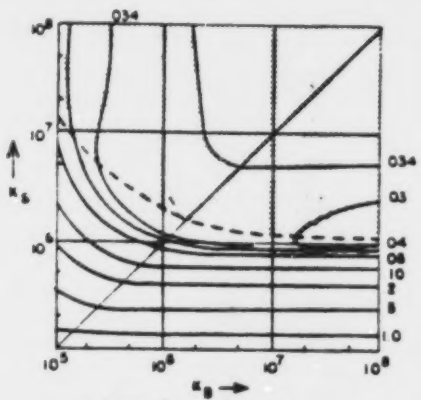

FIG 23 - λ = 0.05, R = 300 M

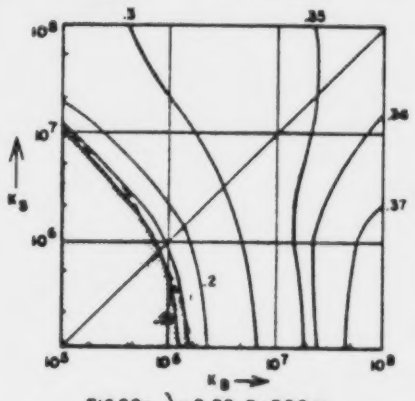

FIG 20 - λ = 0.20, R = 300 M

ANGLE OF ATTACK (LEADING AXLE)

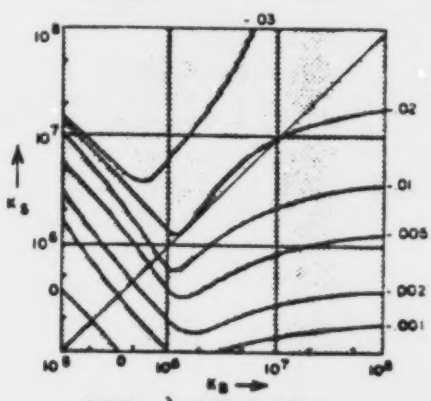

FIG 26 - λ = 0.20, R = 300 M

ANGLE OF ATTACK (TRAILING AXLE)

FIGURE 3.1-2 - PLOTS OF ANGLE OF ATTACK
(SHADED AREA IS FLANGE FREE)

The axle angle of attack is defined as the angle between the axis of the wheelset and a radial from the centre of curvature of the track as illustrated in Figure 3.1-3.

It was concluded that there existed a tradeoff relationship between high critical speeds and good curving.

The analyses performed in this program began with the creation of a 29 degree-of-freedom full vehicle model as shown in Figure 3.1-4. The connections between each element featured parallel springs and velocity-dependent dampers in lateral, longitudinal and yaw, where warranted, totalling 48.

It was decided to continue the K_S - K_B field analysis concept but utilizing data based on the dimensions of the 100 ton freight car application of this project.

The model was then expanded to include the braces as spring elements between frame corners and changing the stiffnesses of the primary elements. The K_S - K_B field plotting continued, and the results are contained in 7.1.

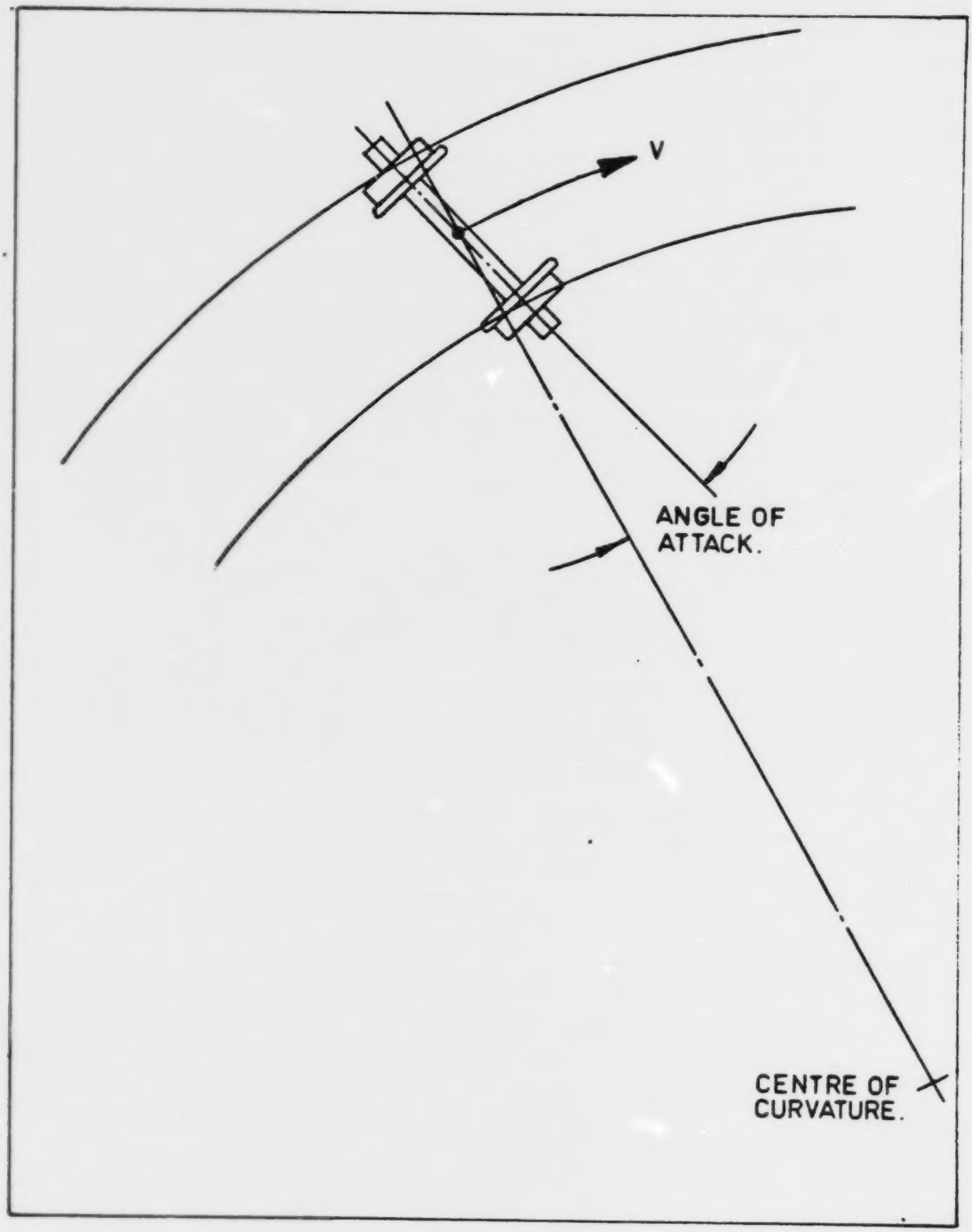

FIGURE 3.1-3 - ANGLE OF ATTACK DEFINED

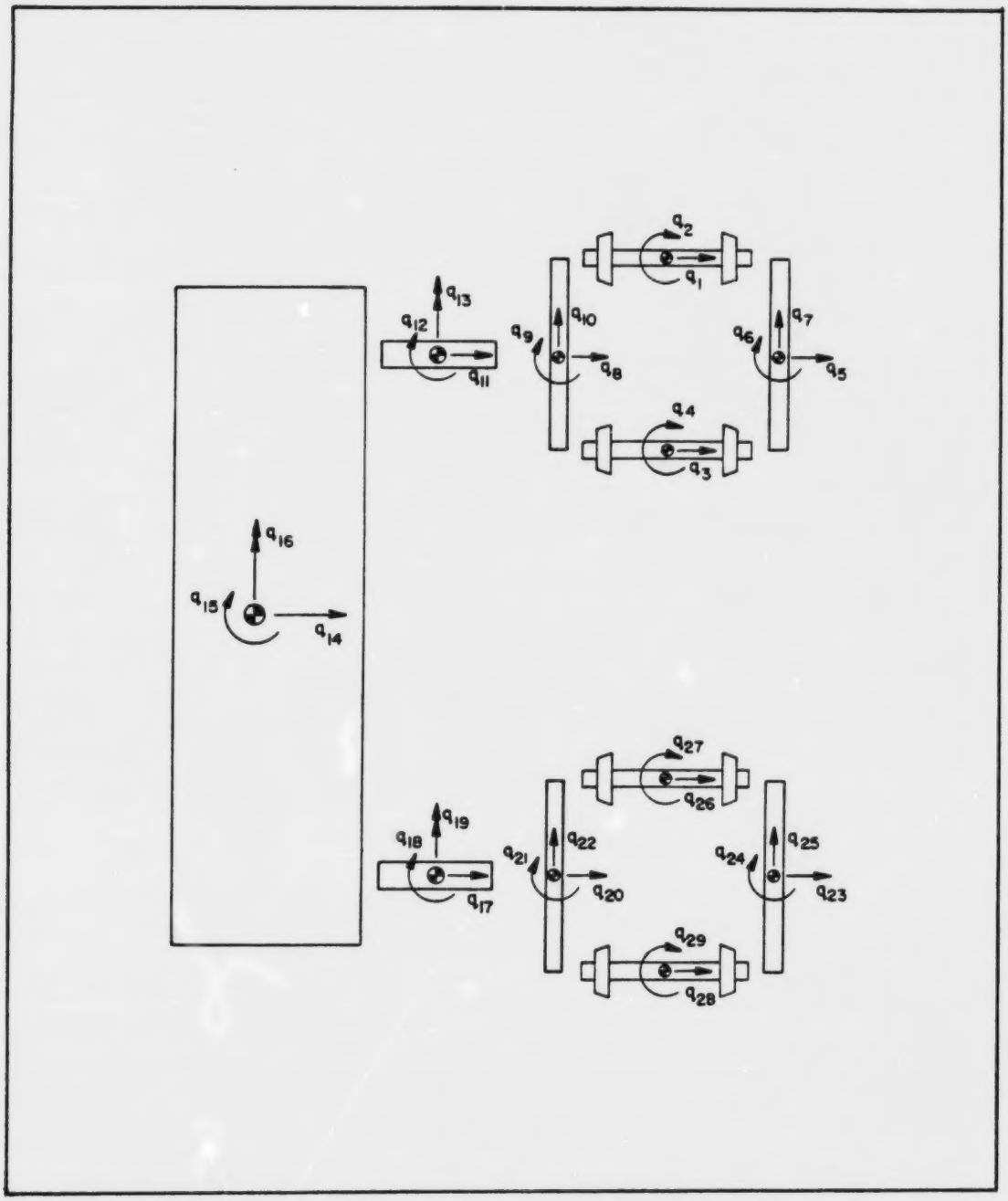

FIGURE 3.1-4 - THREE PIECE TRUCK MODEL FOR ANALYSES

4.0 TESTING

The following tests were carried out during the course of this program:

- measurement of truck component mass, centre of mass, mass moments of inertia, and stiffness;
- truck clearance and low-speed yard test;
- high-speed stability and brace forces, empty and loaded;
- low speed small radius curve angle of attack;
- modified brake performance; and
- wheel profile measurements.

4.1 TEST CONFIGURATIONS

Four 90-tonne (100-ton) Barber S-2-C trucks were fitted with the frame bracing modification. The sideframes had been reconditioned and matched "button-for-button" to ensure the closest tolerance on axle parallelism (standard practice is within one button). Two of the trucks were equipped with wheelsets of 1:20 conicity once-reprofiled wheels. The other two trucks were equipped with new 1:20 wheelsets. The trucks were then fitted under two gondola cars, identified as test cars, and considered the experimental sample.

Four other 90 tonne Barber S-2-C trucks were reconditioned, matched, assembled with once-reprofiled and new wheelsets and fitted to two gondola cars. These were also identified as test cars and became the control sample.

For test purposes, a control car and an experimental car with once-reprofiled wheels became Married Pair 1 and the cars with new wheels became Married Pair 2. On high speed tests, the consist was composed of a locomotive, control car, experimental car, instrumentation van and a caboose, as shown in Figure 4.1-1.

4.2 TEST DESCRIPTION

4.2.1 Truck Mass, Moment of Inertia, Stiffness

The truck component masses etc. were measured because no current data were available for these specific trucks. These data were required as input for the stability, curving and fatigue analyses.

The mass of each component was ascertained by placing the component on three (3) calibrated load cells and summing the recorded readings of weight.

The mass centre of each component was determined through accurate measurement of the load cell position and performance of a moment balance.

The mass moment of inertia of each component was found using the simple pendulum technique.

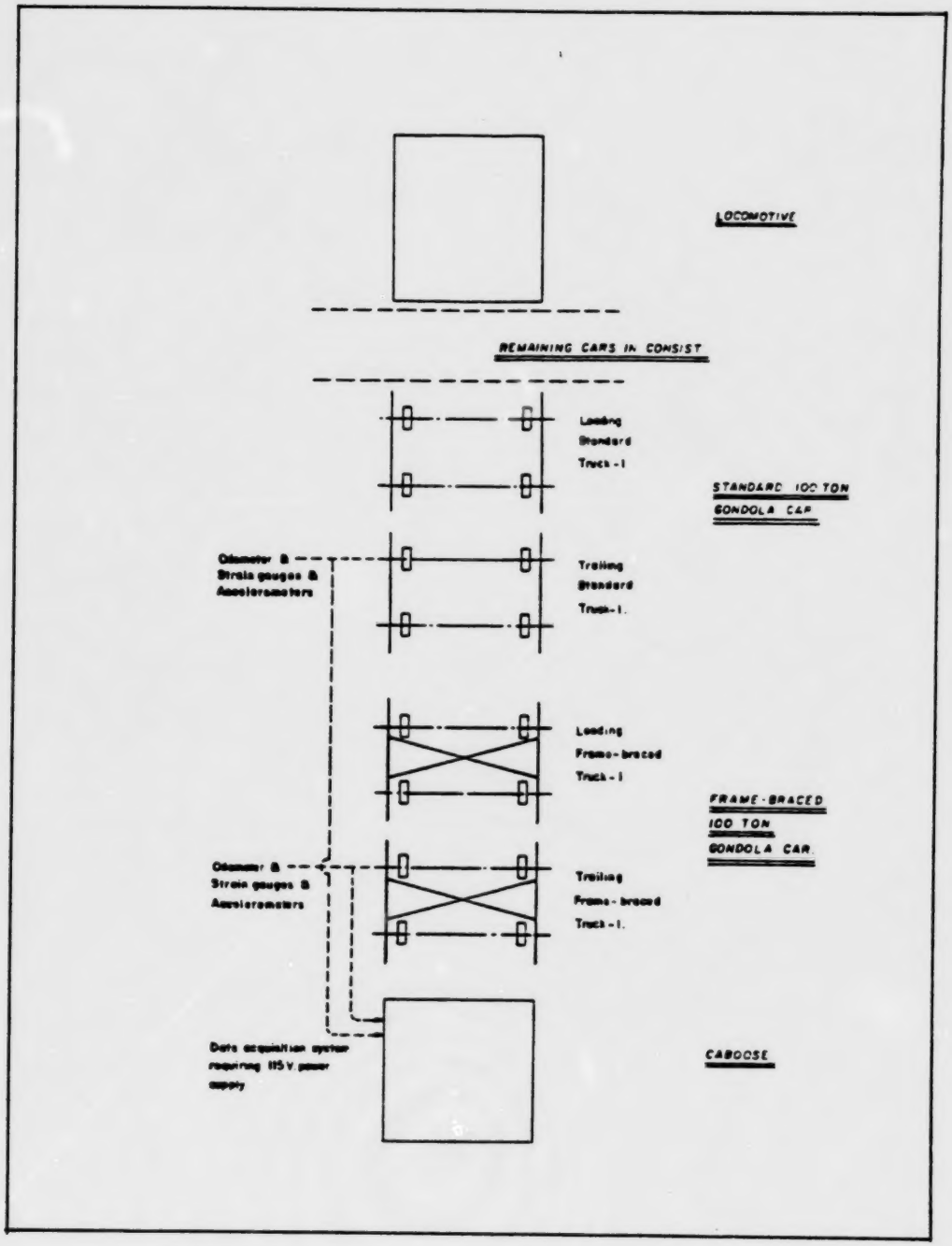
LOCOMOTIVE
REMAINING CARS IN CONSIST
Leading Standard Truck - 1
STANDARD 100 TON GONDOLA CAR
Odometer & Strain gauges & Accelerometers
Trailing Standard Truck - 1.
Leading Frame-braced Truck - 1
FRAME-BRACED 100 TON GONDOLA CAR
Odometer & Strain gauges & Accelerometers
Trailing Frame-braced Truck - 1.
Data acquisition system requiring 115 V power supply
CABOOSE

FIGURE 4.1-1: TEST CONSIST

The stiffness parameters of the truck were to be determined by applying a known force at the area in question while the remainder of the truck was held stationary and the displacement recorded.

A further test to determine shear stiffness and bending stiffnes of the truck was carried out at the NRC Railway Laboratory.

A detailed description of the foregoing tests is contained in Appendix C. The test results appear in 7.2.1.

4.2.2 Truck Clearance and Low Speed Yard Tests

Clearance and yard tests were carried out to ensure that minimum AAR standard vertical rail clearance of 70 mm (2.75 in) was achieved by all modification parts; and that all moving and working parts of the truck were free of any interference.

The tests were performed using visual inspection and flat bars with measuring tapes and rulers.

4.2.3 High-Speed Mainline Tests

High speed tests of the modified and unmodified cars were carried out to ensure that:

- the vehicle critical speed was greater than that seen in normal service (near 45 mph);
- the stresses placed on the braces were within the design range of 12,000 lb (53,000 N); and

- o the stresses placed on the sideframes near the bracket welds were of acceptable magnitude when analyzed.

One modified and one unmodified truck were instrumented with accelerometers on a leading axle bearing adaptor and each of the two leading truck bolsters. Strain gauges were installed on the braces and a sideframe of the leading modified truck. The locations are shown in Figure 4.1-2. Acceleration and strains were recorded on a Sangamo-Weston Sabre VI multi-track chart recorder.

Speed was recorded manually as called by the train engineer. The chosen speeds were 48, 64, 80 and 96 km/h (30, 40, 50, 60 mph).

The tests were carried out on two sections of track featuring similar conditions for curvature and speed between North Bay and Temagami (Fig 4.1-3).

A copy of the Test Plan appears as Appendix D. The results appear in 7.2.3.

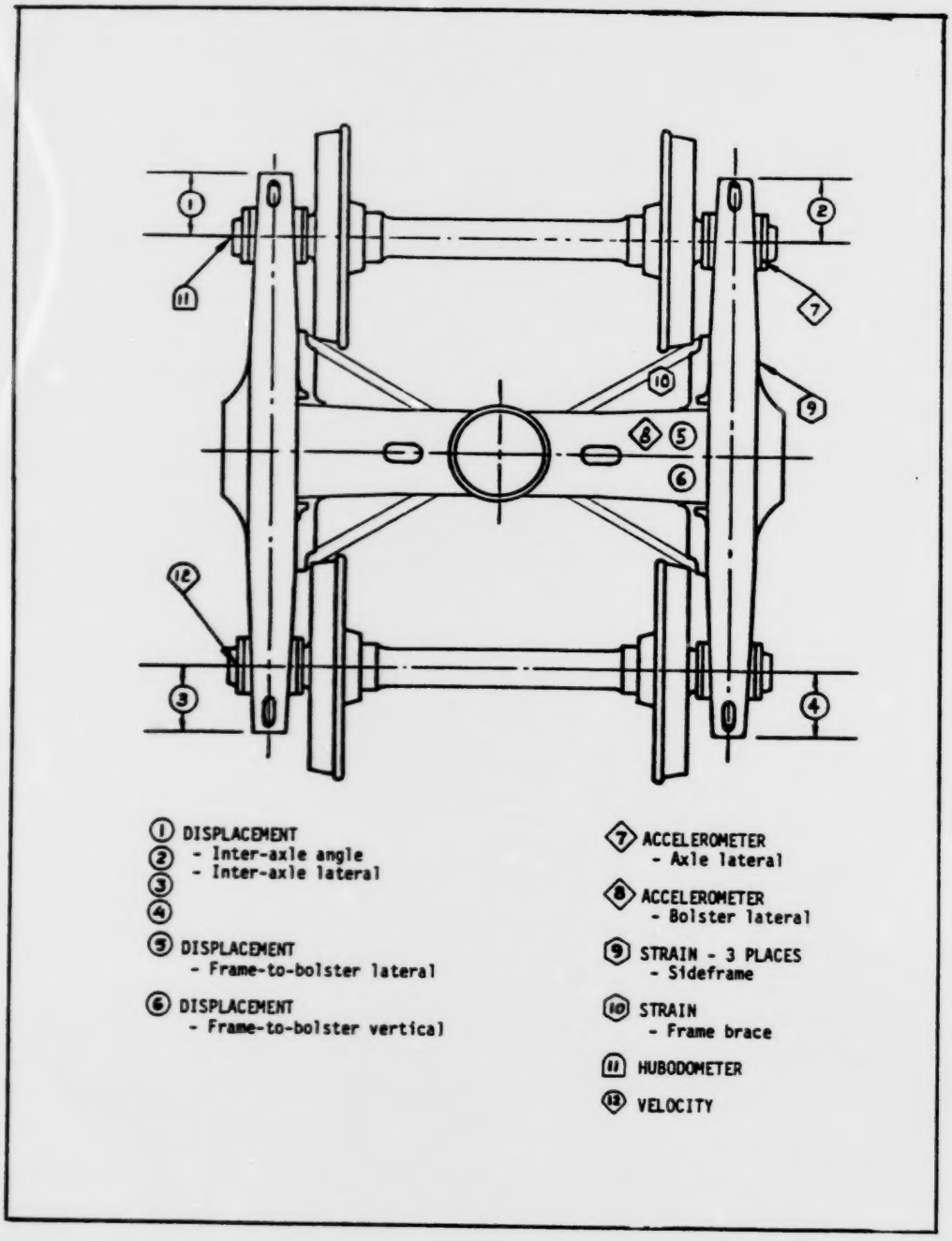

FIGURE 4.1-2: INSTRUMENTATION LOCATION AT ONTC

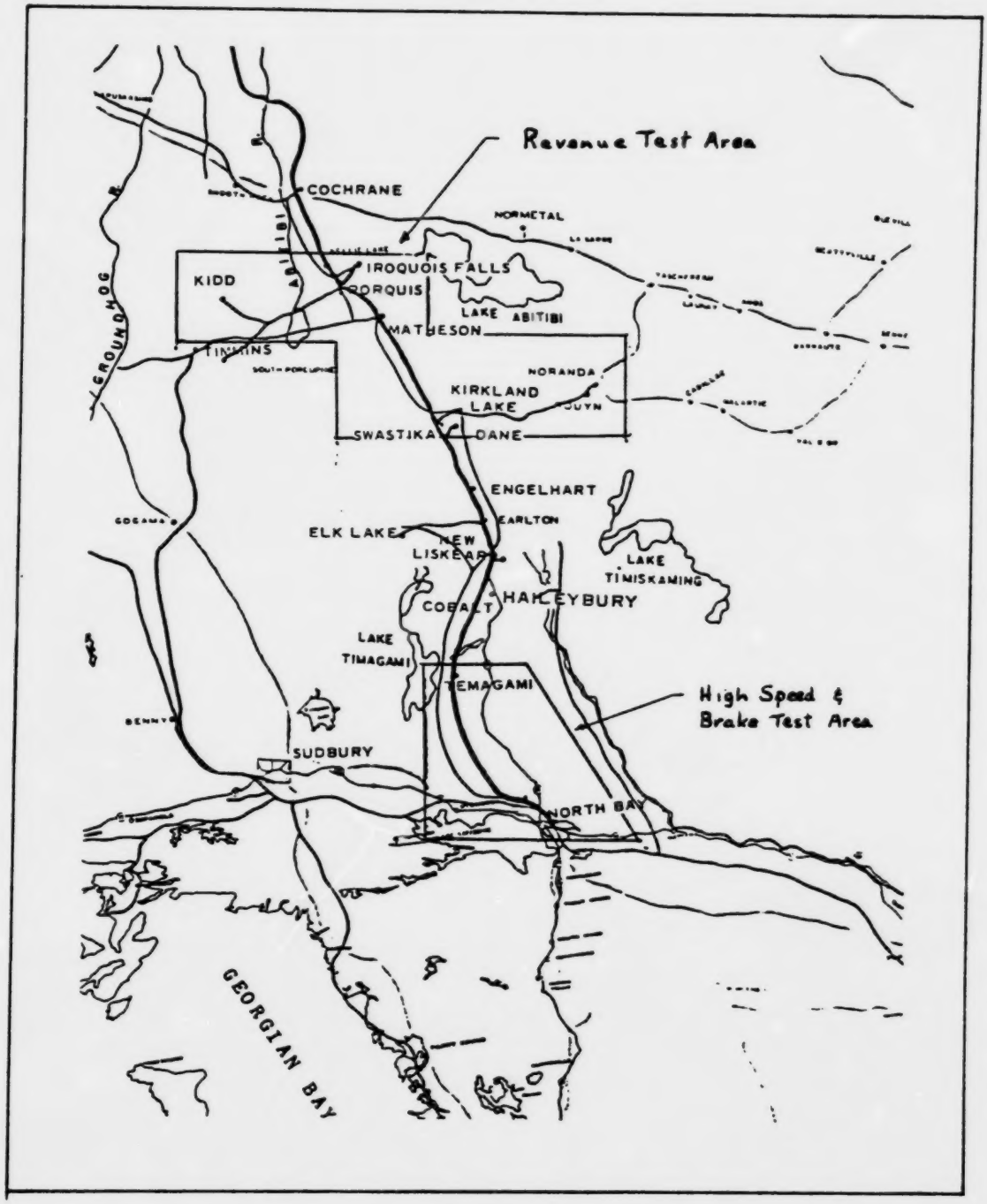

FIGURE 4.1-3: MAP SHOWING TEST AREAS

4.2.4 Low Speed, Small Radius Curve Angle of Attack

As one measure of the improvement in performance of the frame-braced truc , axle angle of attack measurements were carried out on a 19 degree curve near the North Bay maintenance building. The objective was to measure the angle of attack of the leading axle of the leading truck of each of the modified and unmodified cars at various constant speeds through the test section both loaded and empty.

Instrumentation consisted of a computer assisted electro-mechanical system designed by UTDC R&D that features powered ground mounted toggles and truck-mounted conducting strikers. A complete description is contained in Report No. TP4869E, Axle Angle of Attack Comparison, Frame-Braced vs. Conventional Freight Truck.

4.2.5 Modified Brake Performance Test

The inclusion of the primary suspension LC pad displaces the sideframe 25 mm vertically with respect to the wheels. Since the tread brake beams move along guide slots in the sideframe, the beam ends were reworked to allow conformal contact of the brake shoe with the wheel. The ONTC then required that the brakes be tested to ensure normal effectiveness.

The tests were carried out some 65 km north of North Bay over a 16 km section at various speeds to the locomotive maximum, and with various brake pressures to the maximum service level.

Instrumentation consisted of a video camera focused on one brake shoe, a video monitor and recorder and locomotive speed and brake air pressure called out by the crew. The results are summarized in 7.2.5.

4.2.6 Wheel Profile Measurements

To assess the wear quantity and wear pattern of the modified and unmodified truck wheels, periodic wheel profile measurements were carried out.

The measuring tool was a Seiki TS-3D tread wear measuring device as shown in Figure 4.1-4, that is capable of tracing, on paper, the full width of the tread.

The measurements taken in May 1985 were reduced to ascertain metal removed to quantitatively compare wheel wear life. The traces were digitized and those values were used as data for a computer program which calculated the wear in volume and mass of metal removed.

The measurements have been carried out in North Bay, Englehart and Rouyn.

In addition, three carsets of Frame Braced trucks have been in service on the Burlington Northern Railroad since November 1984. These tests are not part of this program but are mentioned because the travel distance has accumulated at a much faster rate than that of the ONTC cars, thus the results give an indication of what is to be expected at ONTC in the future.

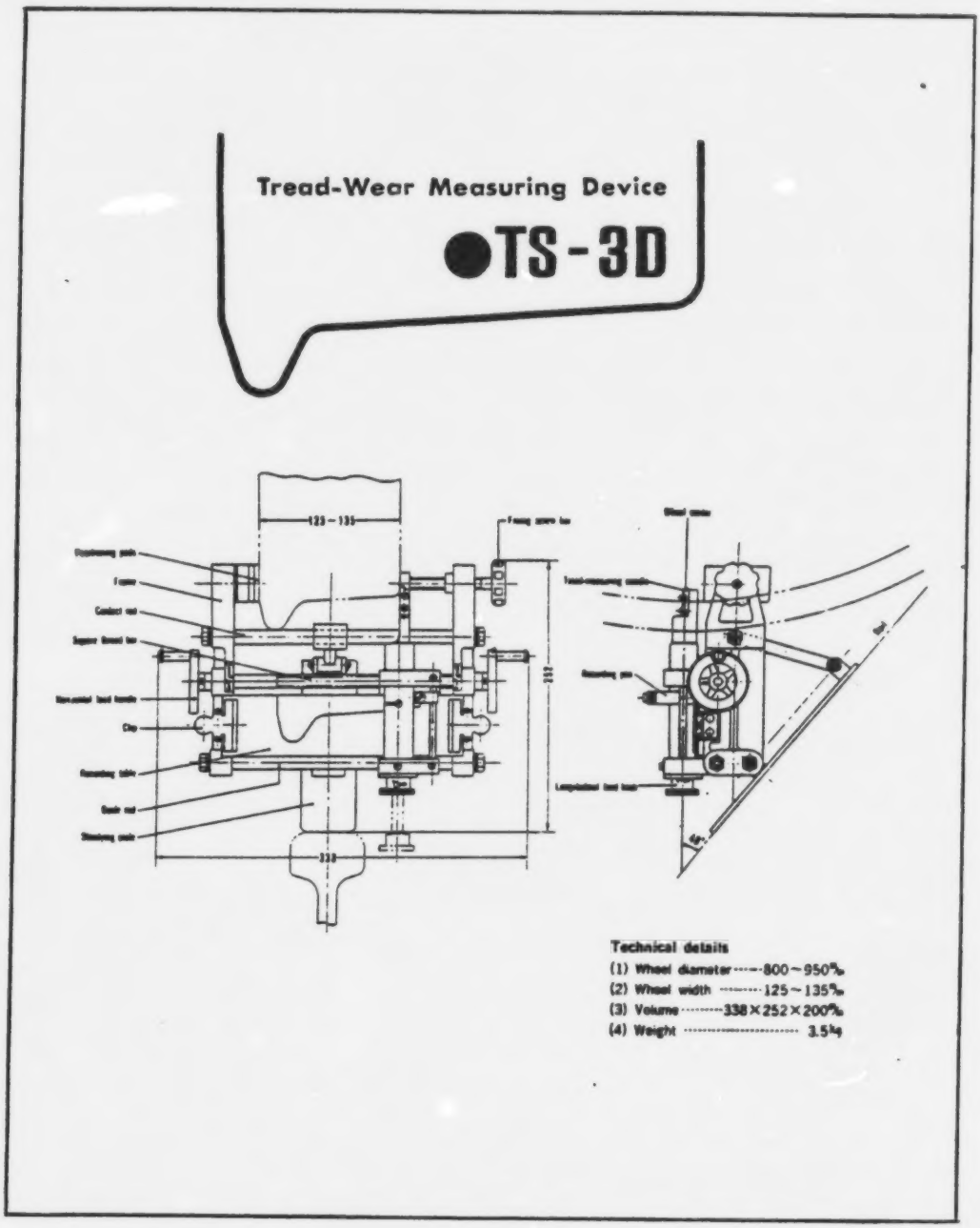

FIGURE 4.1-4 WHEEL PROFILE MEASURING DEVICE

Wheel tracings of these cars have been taken at 50,000 m (80,000 km), and 100,000 miles (160,000 km) of service travel, as have tracing of new wheels. A comparison of these are made in 7.2.6.

4.2.7 Although not a part of this program, a full truck fatigue test was carried out at the Norfolk Southern Railway Laboratories in Alexandria, Virginia, USA. The description of the test as well as the results are contained in Appendix E. The results are summarized in Section 5. The test set-up is shown on the cover of Progressive Railroading, July 1985 issue.

THIS PAGE LEFT BLANK INTENTIONALLY.

5.0 FATIGUE ANALYSIS

As shown in Part 2, Design, the frame-bracing modification calls for attaching channel brackets to the sideframe. Through the brace connections, the brackets will impose non-vertical stresses on the sideframes for which the sideframes have not been designed.

It was therefore considered essential to perform a fatigue analysis of the sideframe in the area of the bracket weldment. Of interest in the analysis were the fatigue life and safety factor based on the accepted methods of analysis. To maintain a high level of accuracy, the stress values to be used in the analysis were those actually measured in testing after the modification incorporation.

The data used in the analysis were collected from calibrated strain gauge measurements under actual running conditions at ONTC and recorded on a chart pen recorder.

Using generally accepted methods of analysis such as those of von Mises and Manson's Method, it was concluded that the modified member has an infinite fatigue life with a factor of safety of 1.5 for the worst loads recorded.

The analysis was carried out by Chadwick Engineering Ltd., a subcontractor to UTDC R&D Ltd. The report is attached as Appendix E.

Subsequent to the first revenue service installation in the U.S.A., a fatigue test was carried out on a complete truck frame at the request of and by the Norfolk Southern Railway Laboratories in Alexandria Virginia.

The Frame-Braced truck was assembled in the test fixture in the following manner:

- o one sideframe clamped allowing no movement:
- o one sideframe free to move longitudinally to provide brace stressing;
- o normal secondary springs replaced by steel tubes to minimize vertical displacement;
- o two 100,000 lb hydraulic rams acting vertically on the bolster to provide a 56% overload condition;
- o one hydraulic ram acting horizontally on the sideframe to provide a 9000 lb tension/compression on the braces.

At the end of 1,000,000 vertical load cycles at 0.65 Hz and 153,750 longitudinal cycles at 0.1 Hz, a close inspection showed no failure at the sideframe connections. Cracks were found on the FB channels where the holding rings are stitch welded to the channel. The holding rings are now welded to the channel all around.

The Norfolk Southern considered the test as successful. The laboratory report is also included in Appendix E.

6.0 ECONOMIC STUDY

The purpose of the economic study was to establish the cost/benefits of this frame-bracing modification to the railroads. The study would be based on computer simulation using actual test results. The computer economic model was developed at the Canadian Institute of Guided Ground Transport (CIGGT) who were subcontracted to perform the work. The work consisted of:

- consultation on experimental design;
- generation of cost and wear data;
- analysis of UTDC R&D test results with respect to costs of wheel and track wear;
- economic/financial analysis of the costs and benefits of the frame-braced trucks; and,
- preparation of a report to UTDC R&D summarizing the findings.

As part of the work, CIGGT were to collect historical data from the ONR in the areas of:

- distance travelled on the system;
- rate of track replacement and cost;
- other track maintenance and cost;
- rate of wheel replacement and cost; and
- other truck maintenance and cost.

From the testing, UTDC R&D would supply:

- o wheel profiles and wear data;
- o distance travelled by each test car; and,
- o angle of attack test results.

CIGGT submitted Report No. 84-6 to UTDC R&D on July 16 1984. The test cars had accumulated less than 10,000 miles (16,000 km), which CIGGT considered to be insignificient travel. In addition, records normally used as data in the CIGGT analysis, such as actual wear measurements of revenue cars, were not available. The report concluded that preliminary analysis was not feasible because of the computer program's dependence on comparative wear rate results.

Some of the data supplied by CIGGT were:

- o ONR billing records for wheel repair;
- o other Railroads' billing records for ONR cars including charges; and,
- o annual travel of ONR Series 5000 cars.

From the above data, CIGGT Report 82-3 titled Rail Wear Economic Analysis for Type II Trucks, and the test and demonstration data gathered from this program, an economic/benefit analysis was completed and is contained in UTDC R&D Technical Note 42-TN-7100-015, which appears as Appendix F.

The Technical Note (Appendix F) concluded that retrofitting frame bracing to ONR Series 5000 100 ton cars was not economically justified yielding a direct payback period of 129 years (Table 6.1-1).

Tables 6.1-1,-2,-3, and -4 were derived as follows:

- Hardware Costs - Retro parts is price as set by UTDC at the time;
- Hardware Costs - Labour is assumed as 16 manhours per carset at $15 per manhour (varies with case study);
- Yearly Savings - Downtime is the cost of a car lost to maintenance for wheel changeouts, which for Table 6.1-1 is negligible for costs each 18.1 years;
- Yearly Savings - Rail wear comes from a table of values shown in Appendix F, the annual travel and an inflation to account for the 1982 table;
- Yearly Savings - Ties etc. is a complex function of average loads over the designated route and the frequency of the loads, more comprehensively explained in the referenced CIGGT report;
- Yearly Savings - Fuel is a function of a tabled fuel savings value from the CIGGT report, the average load hauled and the distance travelled.

- Yearly Savings - Pads and Bushes prorates the cost of replacing all of the Frame-Braced Truck rubber components every 10 years;

- Yearly Savings - Spares Stocking assumes a cost to stock bolts, braces and rubber components to effect unscheduled repairs;

- Wheel Chge Costs - c/w Labour is the estimated cost to change four wheelsets;

- Wheel Chge Costs - Average Annual - Conv. (records) is the recorded cost per year for wheel maintenance (estimated in Tables 6.1-3 and -4);

- Wheel Chge Costs - Average Annual - FB @ 1.57 is the above cost for the conventional truck divided by the Frame Braced Truck wheel life improvement factor of 1.57;

- FB 15 Yr Cost - Installation is the Hardware Cost

- FB 15 Yr Cost - Annual Cost is the total yearly savings multiplied by 15;

- FB 15 Yr Cost - Wheel Chge Costs is the average Annual FB cost over 15 years;

- Conv. 15 Yr Cost - Wheel Chge Costs is the average annual - conv. costs over 15 years.

The remainder is self-explanatory.

It should be noted that no taxes or cost of money calculations are included in any of these analyses.

With the same conditions prevailing except increased annual travel of 50,000 miles (80,000 km) (Table 6.1-2), the payback for ONTC would be just under four years, showing clearly that high mileage cars reap the most benefits from Frame Bracing.

It was concluded that an operation such as the Burlington Northern Railroad (on which three test cars with Frame Bracing are running) which accumulate 100,000 miles per year on coal cars on a 776 mile route, would achieve direct payback in some three to four years (Tables 6.1-3 & 6.1-4).

The analysis produced a cost/benefit model that runs on an Apple II+ microcomputer, thus creating an in-house capability to produce cost/benefit estimates quickly for any potential customer.

The analysis clearly show that high mileage heavy haul carriers can benefit from frame bracing.

A complete report on the economics of the frame braced truck appears as Appendix F.

Cost Benefit Analysis of The Frame-Braced Freight Truck

ASSUMED: TRACK CONDITIONS: 132 lb steel, jointed, wood ties, average maintenance.

100 TON CAR CLASS:EMPTY (TON)	= 28.5		LOADED (TON)	= 128.5	
TRAFFIC MIX: EMPTY	= .5		LOADED = .5	CAR QTY =	99
CURVATURE (%):	= 30		CURVE-TO-TANGENT RATIO		0.43
ROUTE TRAFFIC (MMGT)	= .228		ROUTE (MILES)	=	100
TDOP RAIL SAVINGS(@1 MMGT)	=$ 9.36				
FUEL CONVERSION (L/US GAL)	= 3.785		FUEL COST (1985US$/L)	=$	0.33
FUEL SAVINGS FACTOR	= 3.549E-4				
WHEEL LIFE FACTOR	= 1.57		WHEEL COST (1985)	=$	379.00
LABOUR RATE (1985$/MHR)	=$ 15				
LABOUR PER WHEELSET CHANGEOUT	= 10.33				
WHEELSET CHANGEOUT COST ESTIMATE	$ 1196.00(1985)				
US$ EXCHANGE RATE	= 1.35	INFLATION RATE (COMPOUND FROM 1983)=			1.0816
MOD PRICE PER CARSET	=US$ 2222.22				

CASE:	WHEEL LIFE / ANNUAL TRAVEL		18.1
	ANNUAL VEHICLE TRAVEL (MILES)		5520
	CURRENT WHEEL LIFE (MILES)		100000
HARDWARE COSTS	RETRO PARTS		3000.00
	LABOUR		240.00
		TOTAL	3240.00
YEARLY SAVINGS	DOWNTIME		0.00
	RAIL WEAR		2.79
	TIES ETC.		6.45
	FUEL		3.03
	PADS & BUSHES (ANN RATE) = .1		-78.84
	SPARES STOCKING		-5.00
		TOTAL	-71.56
WHEEL CHGE COSTS	C/W LABOUR		4704.00
	AVGE ANNUAL - CONV(RECORDS)		266.07
	AVGE ANNUAL - FB @ 0		169.47
FB 15 YR COST	INSTALLATION		3240.00
	ANNUAL COST		1073.46
	WHEEL CHGE COSTS		2542.10
		TOTAL	6855.56
CONV 15 YR COST	WHEEL CHGE COSTS		3991.10
	NPV OF SAVINGS		-2864.46
ROI & PAYBACK-	AVGE ANNUAL COST -CONV		266.07
	-FB		-169.47
	-ADDED		-71.56
	ANNUAL SAVINGS(DOLLARS)		25.04
GROSS PAYBACK (YEARS) =HOME COSTS/ANNUAL SAVINGS			129.41

TABLE 6.1-1: COST/BENEFIT - ONTC - 5520 MILES PER YEAR

COST BENEFIT ANALYSIS OF FRAME BRACED FREIGHT TRUCK

ASSUMED:	TRACK CONDITIONS:	132 LB.STD STEEL(260BHN),JOINTED, WOOD TIES,AVGE MAINTENANCE.			
	100 TON CAR CLASS:	EMPTY (TON)	= 28.5	LOADED (TON)	= 128.5
	TRAFFIC MIX:	EMPTY = .5		LOADED = .5	CAR QTY = 99
	CURVATURE (Σ):	30		CURVE-TO-TANGENT RATIO	0.43
	ROUTE TRAFFIC (MMGT)	2.067		ROUTE (MILES)	= 188
	RAIL SAVINGS(@2.067 MMGT)$	10.34			
	FUEL CONVERSION (L/US GAL)	3.785		FUEL COST (1985US$/L)	=$ 0.33
	FUEL SAVINGS FACTOR	3.549E-4			
	WHEEL LIFE FACTOR	1.57		WHEEL COST (1985)	=$ 379.00
	LABOUR RATE (1985$/MHR)	$ 15.00			
	LABOUR PER WHEELSET CHANGEOUT	= 10.33			
	WHEELSET CHANGEOUT COST ESTIMATE	$ 1197.00(1985)			
	MOD PRICE PER CARSET	US$ 2222.22			
	US$ EXCHANGE RATE	1.35		INFLATION RATE (COMPOUNDED) 1.0816 (FROM 1983)	

CASE:	ANNUAL TRAVEL/WHEEL LIFE		2
	ANNUAL VEHICLE TRAVEL (MILES)		50000
	CURRENT WHEEL LIFE (MILES)		100000
HARDWARE COSTS	RETRO PARTS		3000.00
	LABOUR		240.00
		TOTAL	3240.00
YEARLY SAVINGS	DOWNTIME		3.03
	RAIL WEAR		27.96
	TIES ETC.		79.56
	FUEL		27.42
	PADS & BUSHES (ANN RATE) = .1		-78.84
	SPARES STOCKING		-5.00
		TOTAL	54.14
WHEEL CHGE COSTS	C/W LABOUR		4788.00
	AVGE ANNUAL - CONV		2394.00
	AVGE ANNUAL - FB @ 1.57		1524.84
FB 15 YR COST	INSTALLATION		3240.00
	ANNUAL COST		-812.10
	WHEEL CHGE COSTS		22872.61
		TOTAL	25300.51
CONV 15 YR COST	WHEEL CHGE COSTS		35910.00
	NPV OF SAVINGS		10609.49
ROI & PAYBACK-	AVGE ANNUAL COST -CONV		2394.00
	-FB		-1524.84
	-ADDED		54.14
	ANNUAL SAVINGS(DOLLARS)		923.30
GROSS PAYBACK (YEARS) =HDWE COSTS/ANNUAL SAVINGS			3.51

TABLE 6.1-2: COST/BENEFIT - ONTC - 50,000 MILES PER YEAR

Cost Benefit Analysis of Frame-Braced Trucks on Freight cars.

100 TON CAR CLASS:	EMPTY (TON)	= 31.5	LOADED (TON)	= 131.5	
TRAFFIC MIX:	EMPTY = .5		LOADED = .5	CAR QTY =	100
CURVATURE (Z):	30		CURVE-TO-TANGENT RATIO		0.43
ROUTE TRAFFIC (MMGT)	1.05		ROUTE (MILES)	=	776
TDOP RAIL SAVINGS - - - - $	15.48				
FUEL COST (1986US$/US GAL)	.78		FUEL COST (1985US$/L)	=$	0.21
FUEL SAVINGS FACTOR	3.549E-4				
WHEEL LIFE FACTOR	2.2		WHEEL COST (1985)	=$	275.00
LABOUR RATE (1985$/MHR) $	24.00				
LABOUR PER WHEELSET CHANGEOUT =	7.25				
WHEELSET CHANGEOUT COST ESTIMATE $	1005.00(1985)				
MOD PRICE PER CARSET	US$ 2500.00				
INFLATION RATE (COMPOUNDED)	1.1248(FROM 1982)				

CASES: ANNUAL TRAVEL/WHEEL LIFE		2.5
ANNUAL VEHICLE TRAVEL (MILES)		100000
CURRENT WHEEL LIFE (MILES)		250000
HARDWARE COSTS — RETRO PARTS		2500.00
LABOUR		192.00
	TOTAL	2692.00
YEARLY SAVINGS — DOWNTIME		6.30
RAIL WEAR		87.06
TIES ETC.		132.33
FUEL		35.25
PADS & BUSHES (ANNUAL RATE= 0.10)		-58.40
SPARES STOCKING		-5.00
	TOTAL	197.54
WHEEL CHGE COSTS — INCLUDING LABOUR		4020.00
AVGE ANNUAL - CONVENTIONAL		1600.00
AVGE ANNUAL - FB @ 2.2		730.91
FB 15 YR COST — INSTALLATION		2692.00
ANNUAL COST		-2963.16
WHEEL CHANGE COSTS		10963.64
	TOTAL	10692.48
CONV 15 YR COST — WHEEL CHANGE COSTS		24120.00
NPV OF SAVINGS		13427.52
ROI & PAYBACK- AVGE ANNUAL COST -CONV		1600.00
-FB		-730.91
-ADDITIONAL		197.54
ANNUAL SAVINGS(DOLLARS)		1074.63
GROSS PAYBACK (YEARS) =HDWE COSTS/ANNUAL SAVINGS		2.51

TABLE 6.1-3: COST/BENEFIT - BN - AAR INTERCHANGE RATES

Cost Benefit Analysis of Frame-Braced Trucks on Freight cars.

100 TON CAR CLASS:	EMPTY (TON)	= 31.5	LOADED (TON)	= 131.5
TRAFFIC MIX:	EMPTY = .5		LOADED = .5	CAR QTY = 100
CURVATURE (Z):	3@		CURVE-TO-TANGENT RATIO	0.43
ROUTE TRAFFIC (MMGT)	1.05		ROUTE (MILES)	= 776
TDOP RAIL SAVINGS - - - - - $	15.48			
FUEL COST (1986US$/US GAL)	.78		FUEL COST (1985US$/L)	=$ 0.21
FUEL SAVINGS FACTOR	3.549E-4			
WHEEL LIFE FACTOR	2.2		WHEEL COST (1985)	=$ 275.00
LABOUR RATE (1985$/MHR)	$ 14.00			
LABOUR PER WHEELSET CHANGEOUT	= 7.25			
WHEELSET CHANGEOUT COST ESTIMATE	$ 696.00(1985)			
MOD PRICE PER CARSET	US$ 2500.00			
INFLATION RATE (COMPOUNDED)	1.1248(FROM 1982)			

CASES:	ANNUAL TRAVEL/WHEEL LIFE		2.5
	ANNUAL VEHICLE TRAVEL (MILES)		100000
	CURRENT WHEEL LIFE (MILES)		250000
HARDWARE COSTS	RETRO PARTS		2500.00
	LABOUR		112.00
		TOTAL	2612.00
YEARLY SAVINGS	DOWNTIME		6.30
	RAIL WEAR		87.06
	TIES ETC.		132.33
	FUEL		35.25
	PADS & BUSHES (ANNUAL RATE= 0.10)		-58.40
	SPARES STOCKING		-5.00
		TOTAL	197.54
WHEEL CHGE COSTS	INCLUDING LABOUR		2784.00
	AVGE ANNUAL - CONVENTIONAL		1113.60
	AVGE ANNUAL - FB @ 2.2		506.18
FB 15 YR COST	INSTALLATION		2612.00
	ANNUAL COST		-2963.16
	WHEEL CHANGE COSTS		7592.73
		TOTAL	7241.57
CONV 15 YR COST	WHEEL CHANGE COSTS		16704.00
	NPV OF SAVINGS		9462.43
ROI & PAYBACK-	AVGE ANNUAL COST -CONV		1113.60
	-FB		-506.18
	-ADDITIONAL		197.54
	ANNUAL SAVINGS(DOLLARS)		804.96
GROSS PAYBACK (YEARS) =HDWE COSTS/ANNUAL SAVINGS			3.24

TABLE 6.1-4: COST/BENEFIT - BN - 1985 ESTIMATE RATES

THIS PAGE LEFT BLANK INTENTIONALLY

7.0 RESULTS

7.1 STABILITY AND CURVING ANALYSES

The stability and curving analyses produced predictions of:

- o critical speed (dynamic stability limit);
- o wheel/rail angle of attack by curve radius;
- o tread wear index; and
- o flange wear index.

Tread Wear Index (TWI) is the product of wheel tread lateral forces (FT) and the angle of attack ( ); i.e.:

$$TWI = F_T \times$$

Flange Wear Index (FWI) is defined as the product of wheel flange lateral forces (FF) and the angle of attack ( ); i.e.:

$$FWI = F_F \times$$

Those parameters varied in the analyses were:

- o wheel conicity (1:20, 1:5);
- o vehicle weights (loaded, unloaded);
- o curve radius (300 m, 1000 m);
- o primary suspension lateral stiffness (K_x);
- o primary suspension longitudinal stiffness (K_y);
- o frame brace stiffness (K_{23}); and
- o bolster sideframe torsional stiffness (K_t).

The computer programs were enhanced to calculate K_s and K_B, K_{23} and K_t to locate the truck position on the characteristic curve, or to calculate values of K_x and K_y based on inputs of K_s, K_B, K_{23}, and K_t to solve for the required primary suspension specifications.

The complete set of results appears as Appendix G. Typical examples follow.

Figure 7.1-1 shows curves of constant critical speed against shear stiffness K_s and bending stiffness K_B at a wheel conicity of 0.2. The conventional truck has K_s at $10^{5.5}$ (316,228) N/m while K_B is 10^8 (100,000,000)N.m/rad. This point would appear at the extreme right and below the horizontal line for a critical speed below 22.5 m/s (49.5 mi/hr). The frame-braced truck with K_s of $10^{6.25}$ (1,778,279) N/m and K_B of $10^{6.64}$ (4,365,158) N.m/rad, should attain a critical speed in excess of 27.5 m/s (60.5 mi/hr). The inherent friction damping at the sideframe/bolster interface which was not included in either analysis, could cause the actual critical speeds of both trucks to be somewhat greater.

The predicted angle of attack is shown in Figures 7.1-2 and 7.1-3 for curve radius of 300 m (5.8 deg). At a conicity of 0.05, the conventional truck would exhibit an angle of attack greater than 0.55 deg while the frame braced truck would show 0.35. For a wheel conicity of 0.20 (worn wheel), the angle of attack of the conventional truck would be greater than 0.30 deg, while the frame-braced truck would show slightly less than 0.2 degree.

The predicted tread wear indices are shown in Figures 7.1-4 and 7.1-5 for a curve radius of 300 m. For a wheel conicity of 0.05, the conventional truck would have an index in excess of 70 N, while the frame-braced truck would show slightly less than 35 N. With a conicity of 0.20, the conventional truck would show more than 32 N, while the frame-braced would exhibit less than 25 N.

The predicted flange wear index is shown in Figure 7.1-6 for a curve radius of 300 m and a conicity of 0.05. The conventional truck shows an index in excess of 140 N while the frame-braced position is less than 90 N. With a conicity of 0.2, as shown in Figure 7.1-7, the flange wear index for the conventional truck can be expected to be greater than 45 N while the frame braced truck would yield near 27.5 N.

Figures 7.1-8, 7.1-9, and 7.1-10, contain the results of three cases of analytical curving performance of a loaded car with new 1:20 wheels. The results are in the form of Angle of Attack, Tread Wear Index and Flange Wear Index versus curve radius. The shear (log k_S) and bending stiffnesses (log K_B) are 5.53/8.00, 6.14/6.42; and 6.34/6.64, corresponding to the stiffness of the conventional truck and the Frame Braced truck with primary LC pads of nominally 15,000 lb/in and 30,000 lb/in respectively.

In Figure 7.1-8, the conventional truck achieves an analytical angle of attack of 0.693 deg on a 5.82 deg (300 m radius) curve and an angle of attack

of 4.11 deg on a 19.5 deg (90 m radius) curve. The Frame Braced truck with 15,000 lb/in LC pads achieves angle of 0.354 deg and 1.36 deg on the same curves while the Frame Braced truck with 30,000 lb/in pads achieves angles of attack of 0.322 and 1.12 deg on the same curves.

In Figure 7.1-9, the tread wear indices accomplished by the conventional truck are 388 N on the 5.82 deg curve and 2100 N on the 19.5 deg curve. The indices attained by the Frame Braced truck are 179 N and 687 N for the 15,000 lb/in configuration and 148 N and 571 N for the 30,000 lb/in unit.

The loaded car curving performance shown in Figure 7.1-10 is in the form of Flange Wear Indices where it can be seen that the conventional truck attains indices of 912 N and 3600 N on curves of 5.82 deg (300 m radius) and 19.5 deg (90 m radius). On these same curves, the Frame Braced trucks with 15,000 lb/in pads achieve indices of 605 and 1170 N while the Frame Braced truck with 30,000 lb/in pads attains indices of 525 and 975 N respectively.

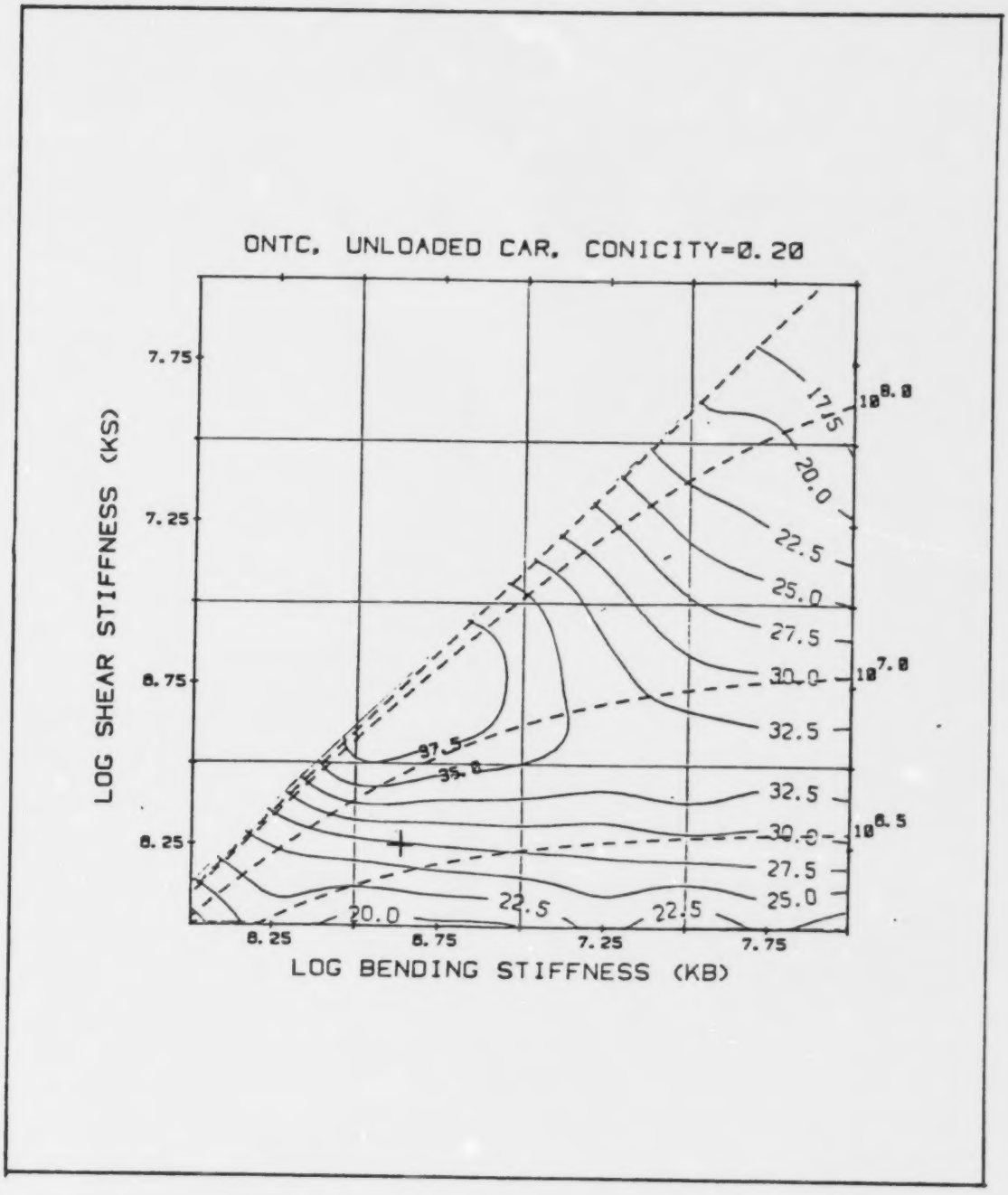

FIGURE 7.1-1: CRITICAL SPEED VERSUS K_S, K_B

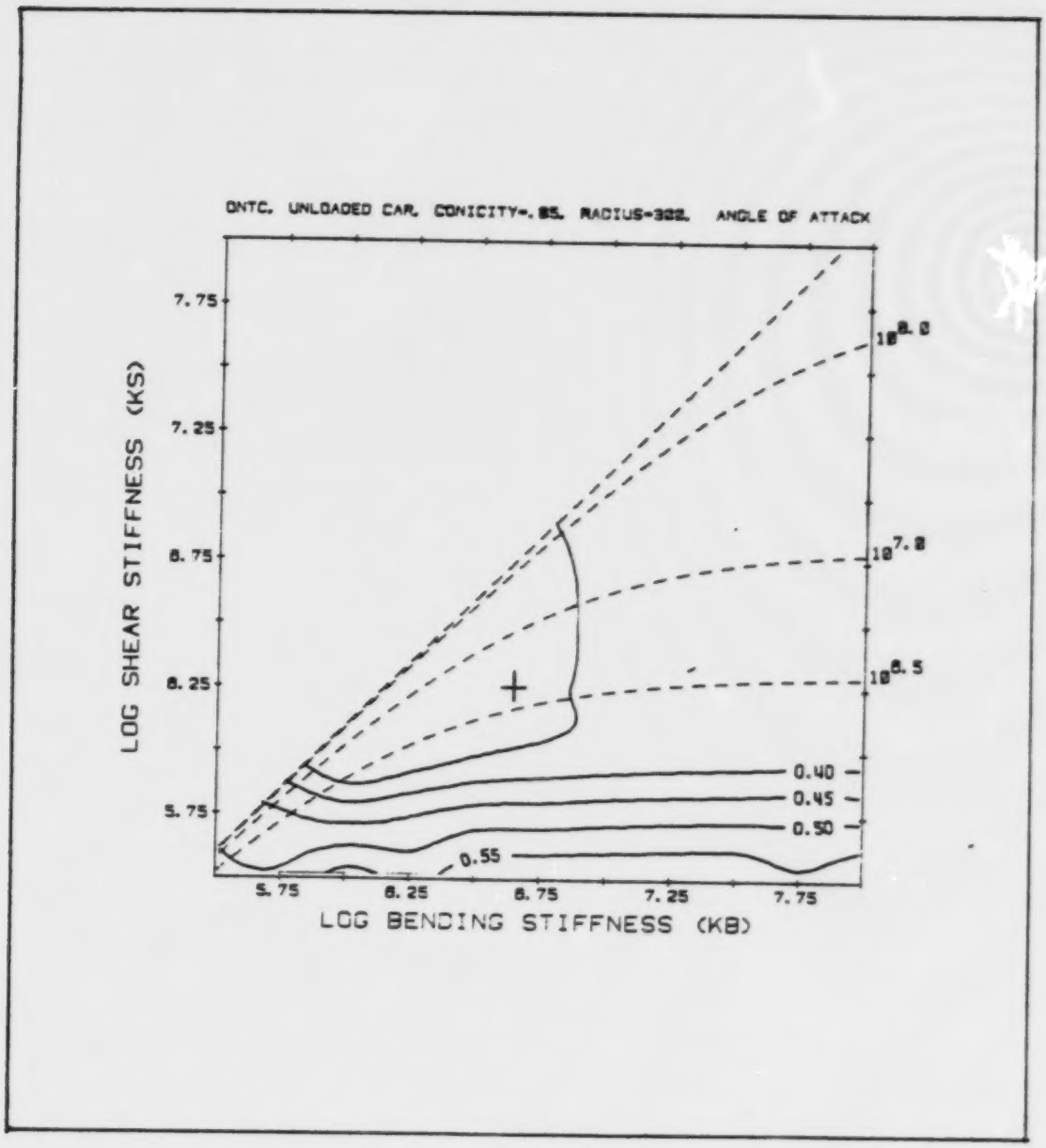

FIGURE 7.1-2: ANGLE OF ATTACK FOR CURVE RADIUS OF 300 M, CONICITY OF 0.05

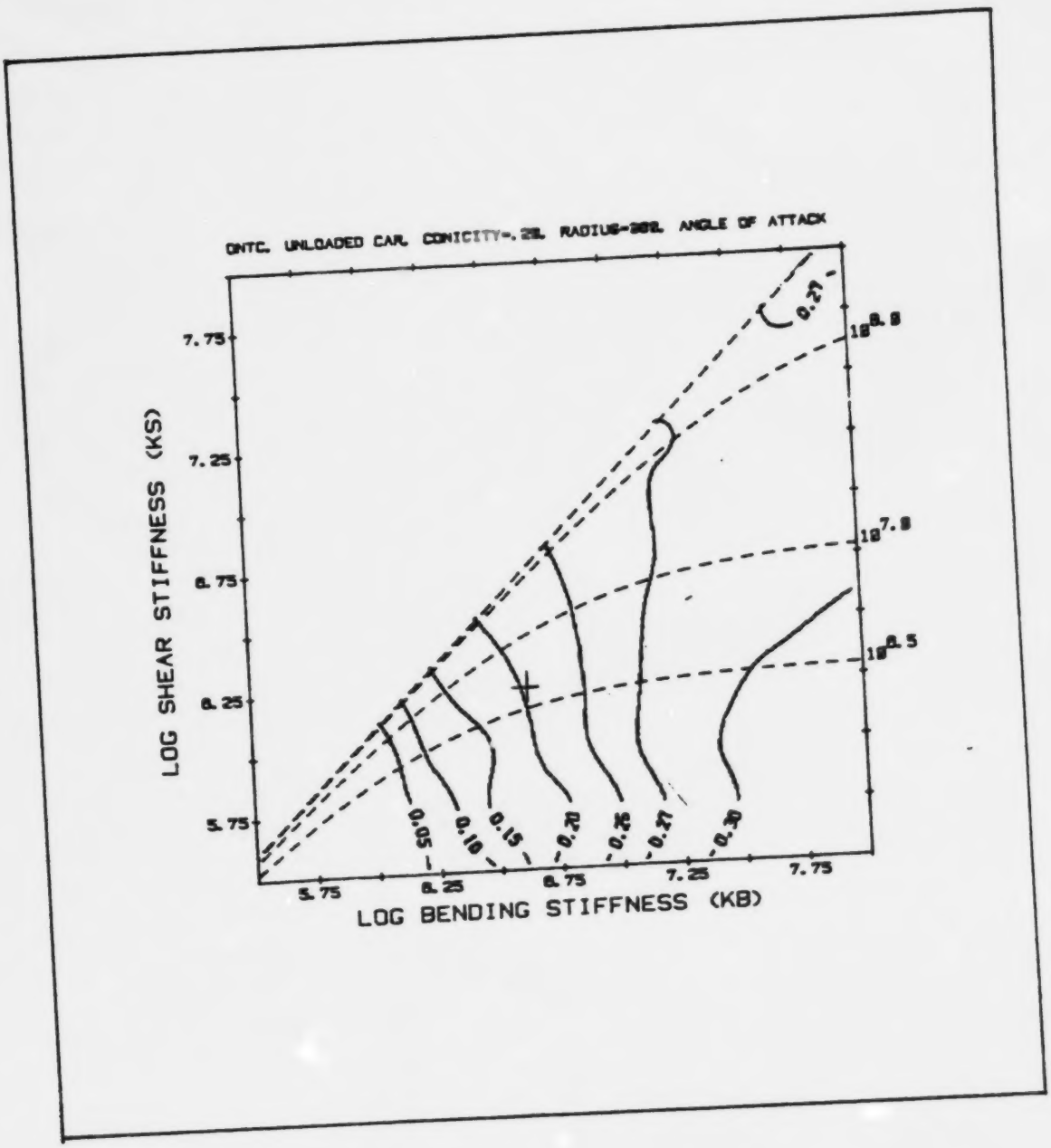

FIGURE 7.1-3: ANGLE OF ATTACK FOR 300 M CURVE, CONICITY OF 0.20

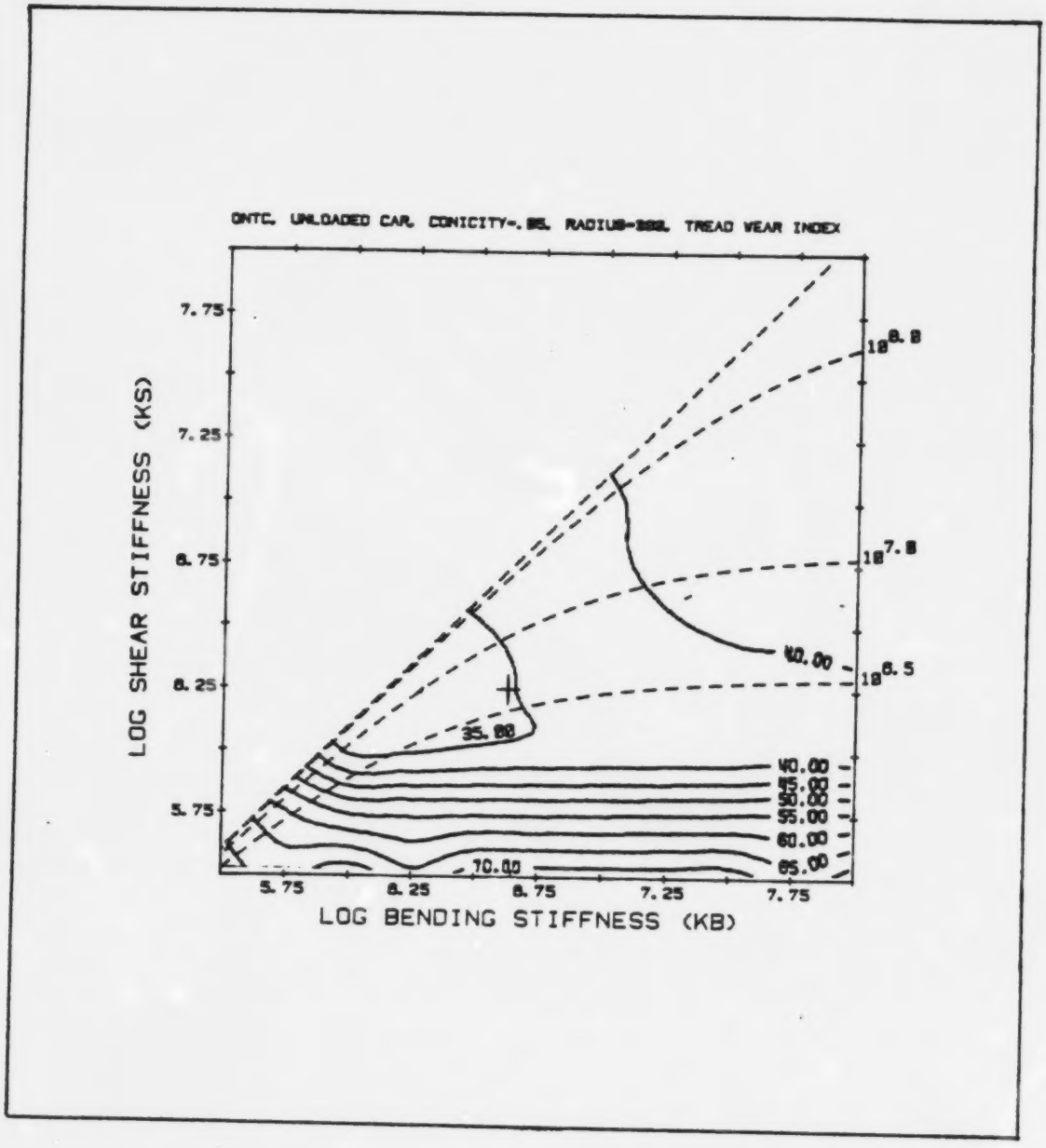

FIGURE 7.1-4: TREAD WEAR INDEX, 300 M CURVE RADIUS, 0.05 CONICITY

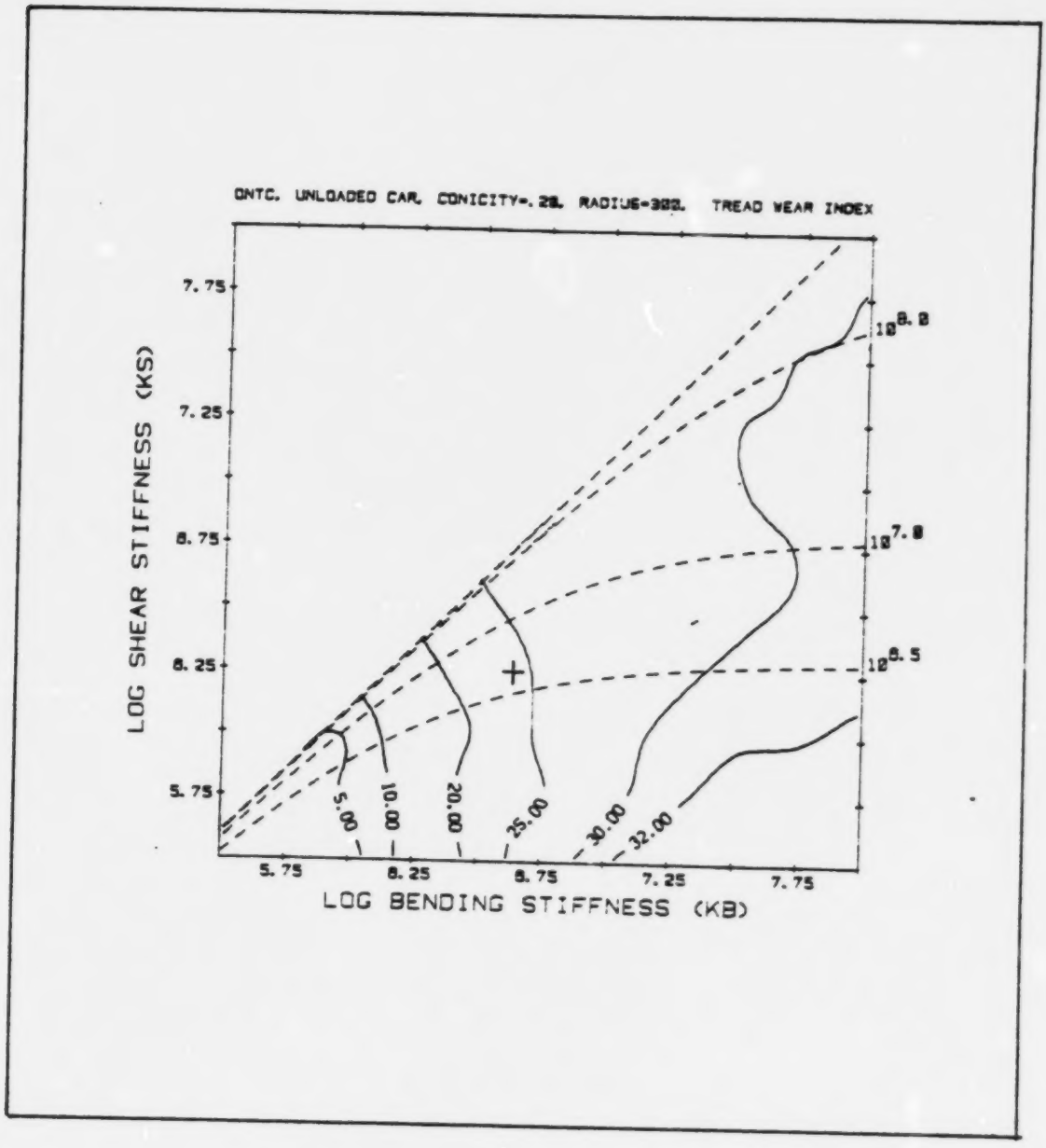

FIGURE 7.1-5: TREAD WEAR INDEX, 300 M CURVE RADIUS, 0.20 CONICITY

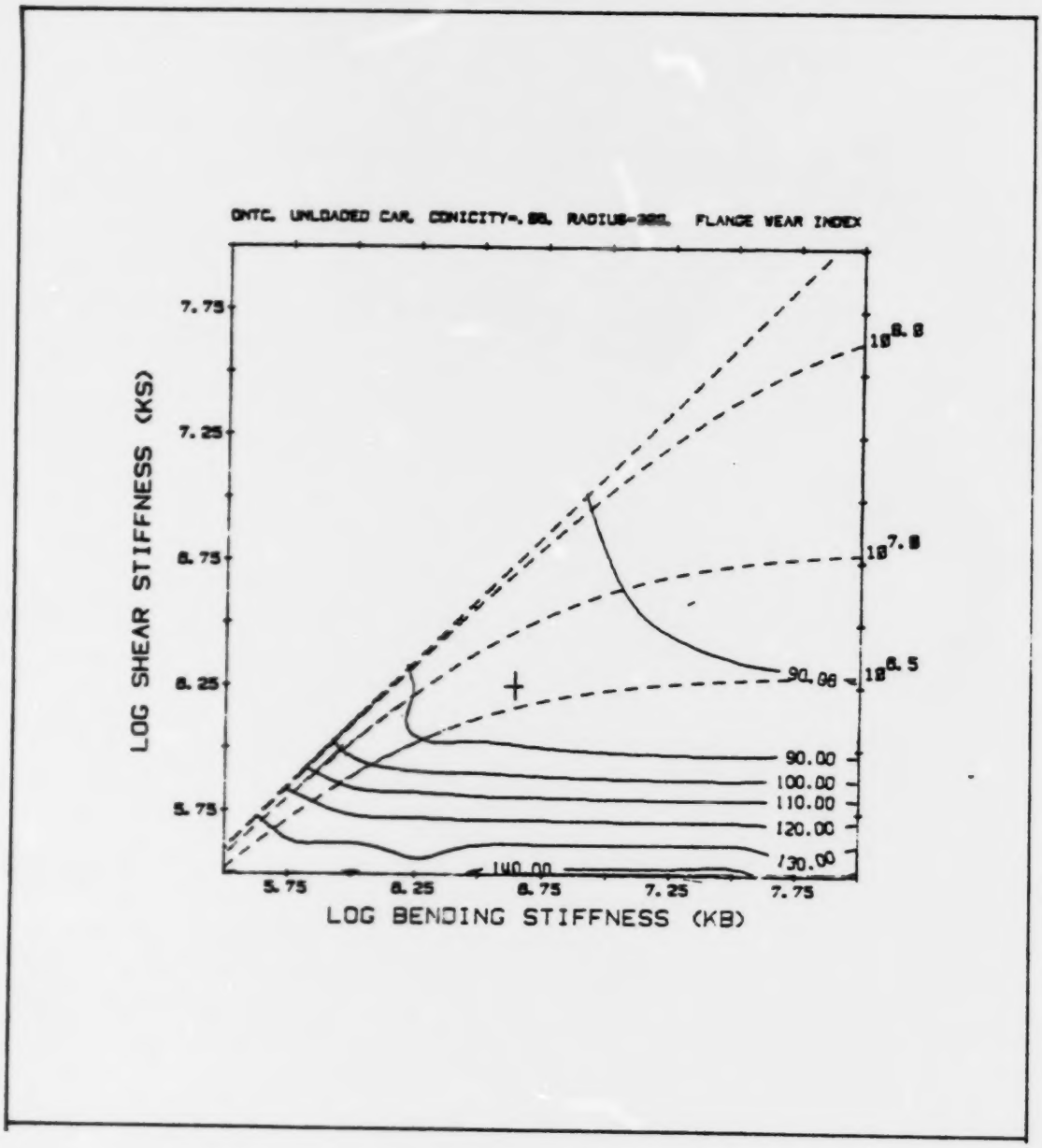

FIGURE 7.1-6: FLANGE WEAR INDEX, 300 M CURVE RADIUS, 0.05 CONICITY

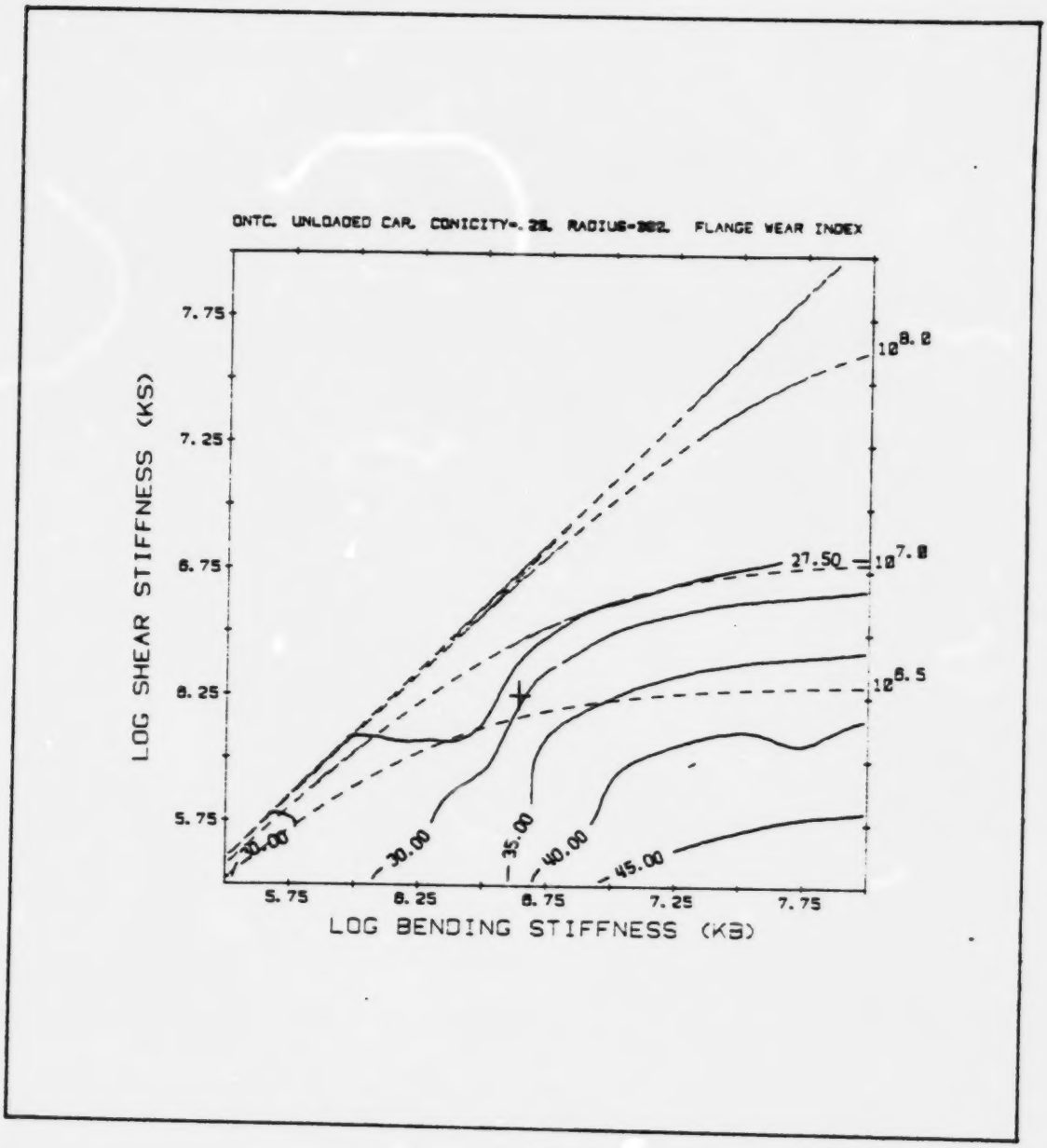

FIGURE 7.1-7: FLANGE WEAR INDEX, 300 M CURVE RADIUS, 0.2 CONICITY

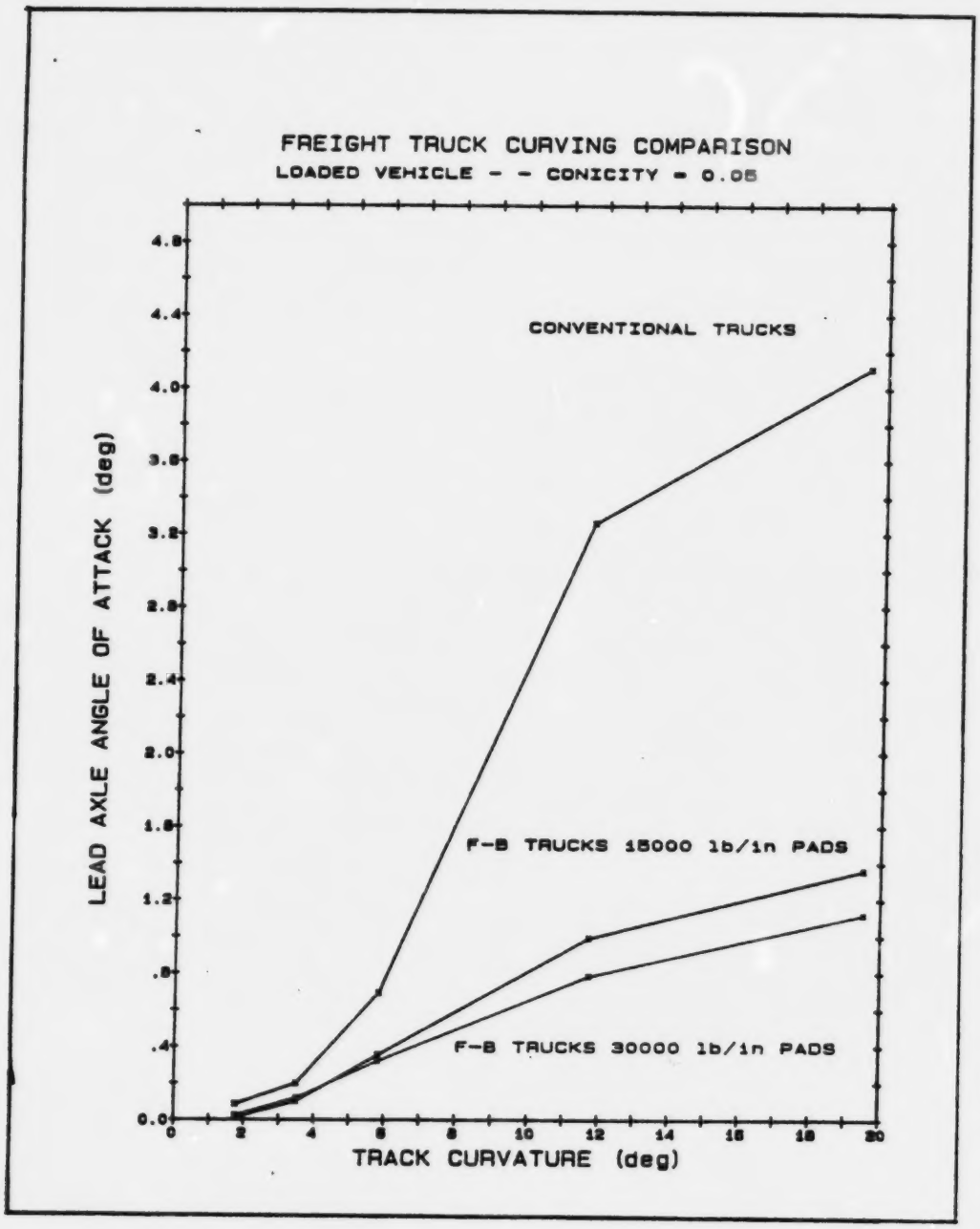

FIGURE 7.1-8: LOADED CAR ANALYTICAL CURVING PERFORMANCE - ANGLE OF ATTACK

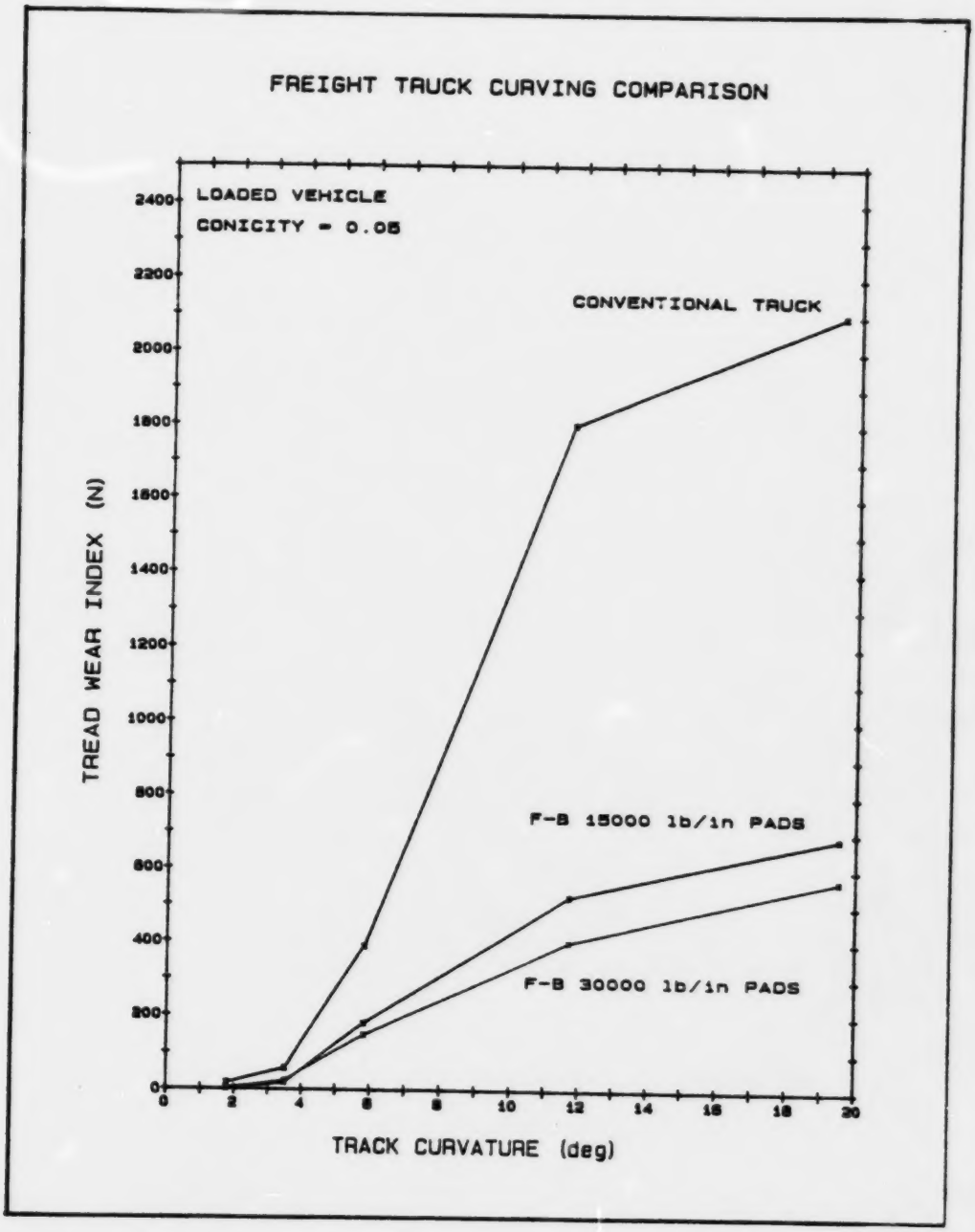

FIGURE 7.1-9: LOADED CAR ANALYTICAL CURVING PERFORMANCE - TREAD WEAR INDEX

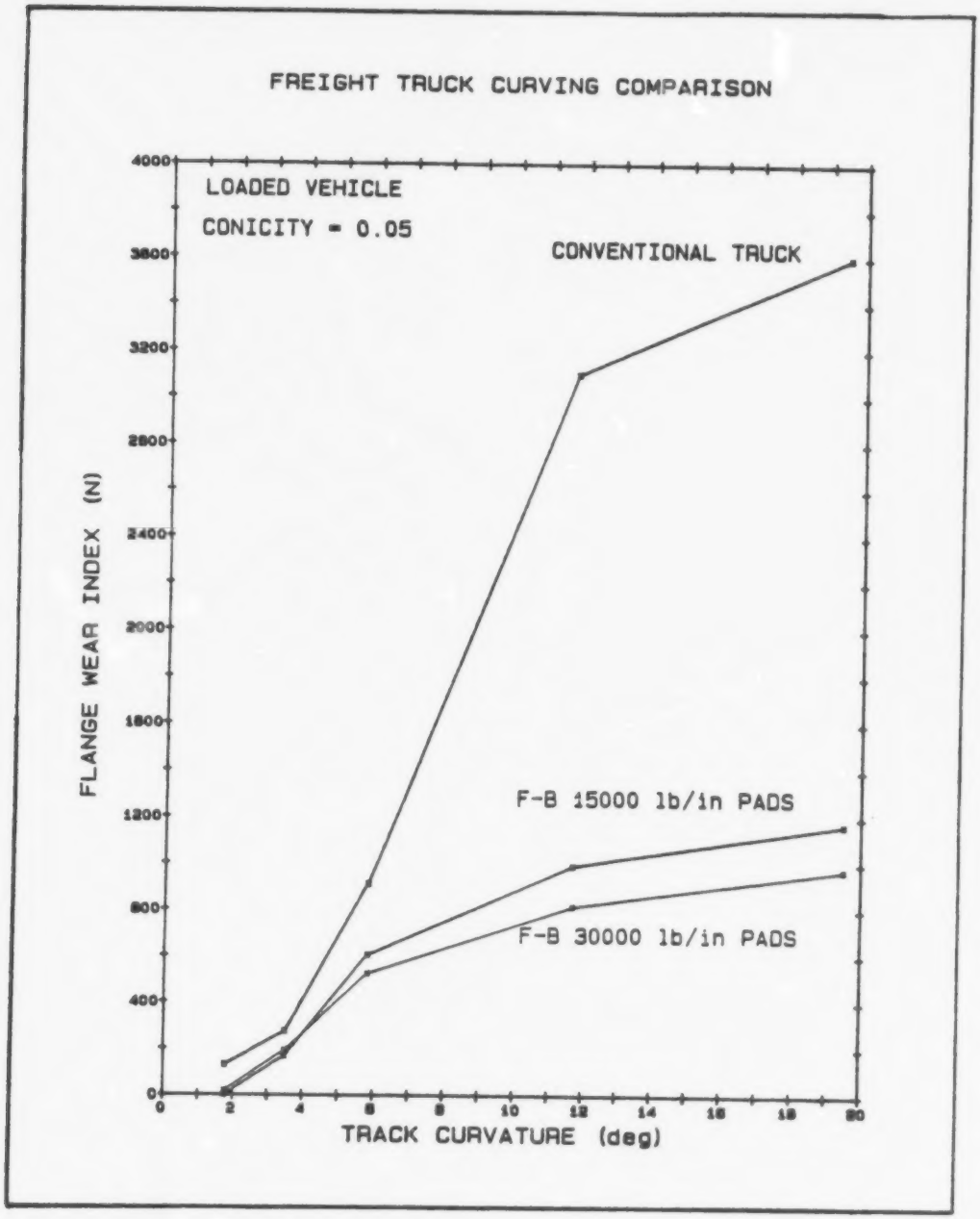

FIGURE 7.1-10: LOADED CAR ANALYTICAL CURVING PERFORMANCE - FLANGE WEAR INDEX

7.2 TEST RESULTS

7.2.1 Truck Mass, Moment of Inertia, Stiffness

The results of these tests were definitive only for masses and moments of inertia. The tests for component stiffness at ONTC were not successful in that the experimental bracing set-up proved inadequate. At one point in the shear stiffness test, the complete unit shifted, zeroing the force reading.

The mass and inertia data collected were as follows and as shown in Table 7.2-1:

- o bolster mass = 645.5 kg (1423 lb)
- o sideframe mass = 476.3 kg (1050 lb)

Unit	Mode	Pendulum Length (m / in)	Period (sec)	Moment of Inertia (kg s/m)
Bolster	Yaw	1.433 / 56.41	2.61	159.6
Sideframe	Yaw	1.098 / 43.21	2.38	75.03
Sideframe	Roll	0.3325 / 13.09	1.37	7.529

TABLE 7.2-1: INERTIA TEST DATA

A subsequent test to determine the truck shear and bending stiffnesses was carried out at the NRC Railway Laboratory. The results of this test was

that the axle shear or lateral stiffness was determined to be 10,000 lb/in (1,751,000 or $10^{6.24}$ N/m) while the interaxle yaw stiffness was determined to be 33 x 10^6 in/radian (3,736,086 or $10^{6.57}$ Nm/rad).

The test reports appear as Appendix H.

7.2.2 Truck Clearance and Low Speed Yard Tests

These initial tests showed that the welded sideframe brackets infringed on the 70 mm (2.75 in) AAR clearance requirements. The trucks were disassembled and a redesign completed. The brackets were shortened and tilted 2 degrees and the braces bent 2 degrees to accommodate the bolster. Upon reassembly and test, all clearance requirements were met.

7.2.3 High Speed Mainline Tests

The results of these tests showed a stable vehicle up to and including 27 m/s (60 mph) as shown typically in Figure 7.2-1. The recorded traces are as follows:

- Channel 1 - longitudinal accelerations, leading axle, modified truck, 2 g per division,

- Channel 2 - longitudinal acceleration, leading axle, standard truck 4 g per division,

- Channel 3 - lateral acceleration, bolster, frame braced truck, not working, not shown
- Channel 4 - lateral acceleration, bolster, standard truck, 0.2 g per division,
- Channel 5 - strain gauge, frame brace, 400 lb per division,
- Channel 6 - strain gauge, other frame brace, 400 lb per division,
- Channel 7 - spare; and,
- Channel 8 - event marker (data correlation only, not shown)

The Channel 1 trace shows oscillatory action peaking at 8 g for the frame-braced axle while Channel 2 shows near twice that value. Channel 1 shows a somewhat repeatable oscillation pattern for the modified truck while the Channel 2 trace appears to have a somewhat random oscillatory pattern.

The Channel 4 trace of the standard truck bolster lateral acceleration shows peak-to-peak values of 2.4 g and steady state near 1.4 g. The frame-braced truck bolster accelerometer ceased to operate during the test. Its record was to be Channel 3.

The brace forces recorded on Channels 5 and 6 were reduced and plotted against rail curvature, as peak (high and low) and mean forces. These results are

shown in Figures 7.2-2 and -3. The curves are second order least squares curve fits.

For the empty car (Figure 7.2-2) the largest force recorded at 18 m/s (40 mph) was 21000 N (4800 lb) on a 6 deg curve, while the smallest force was 1800 N (400 lb) on a 5.5 + deg curve.

For the loaded car (Figure 7.2-3) the largest force recorded was near 41000 N (9200 lb) on a curve of 6.25 deg while the smallest force recorded was near 8000 N (1800 lb) on a curve just over 5 deg.

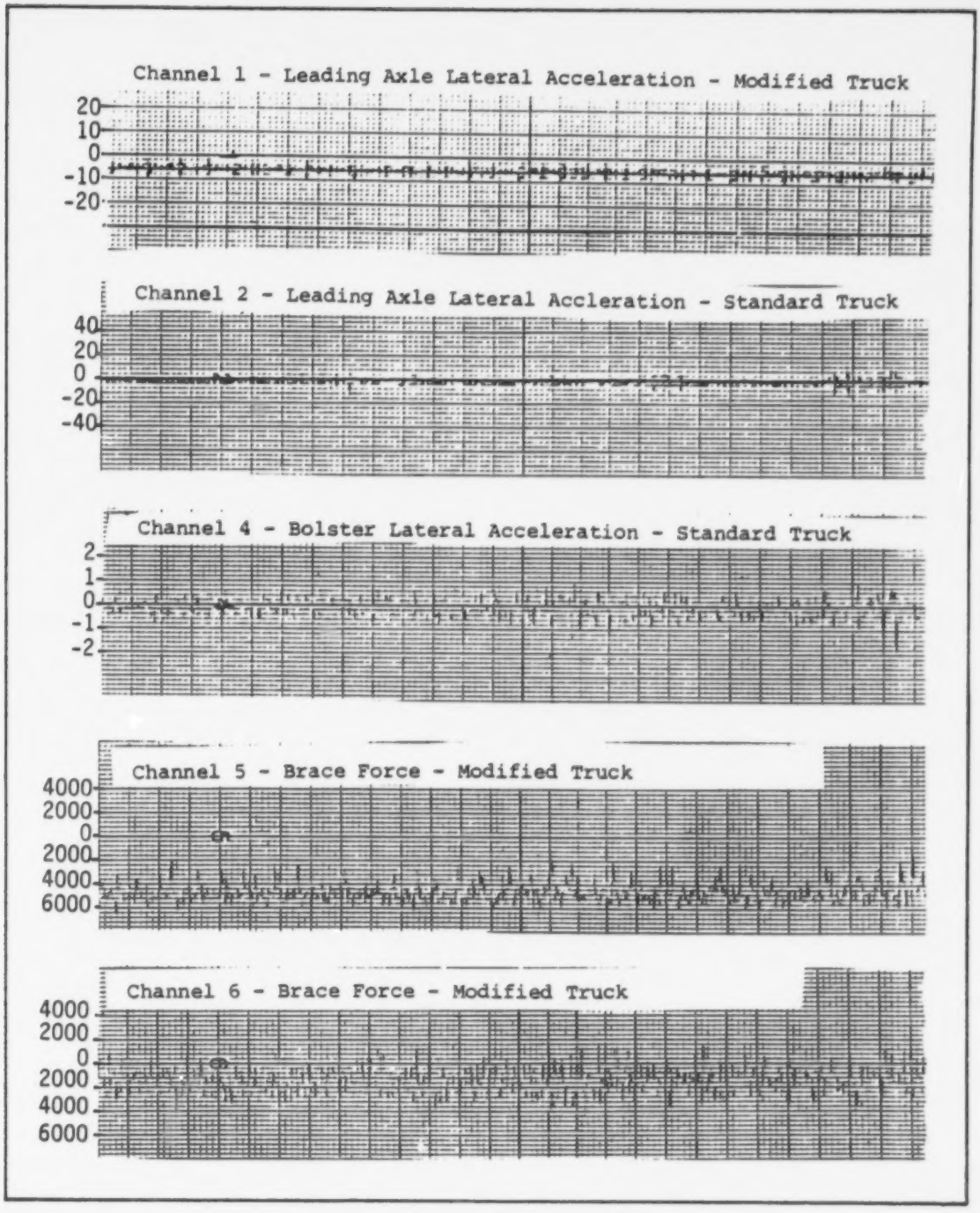

FIGURE 7.2-1: CHART RECORDER READOUT - 60 MI/HR

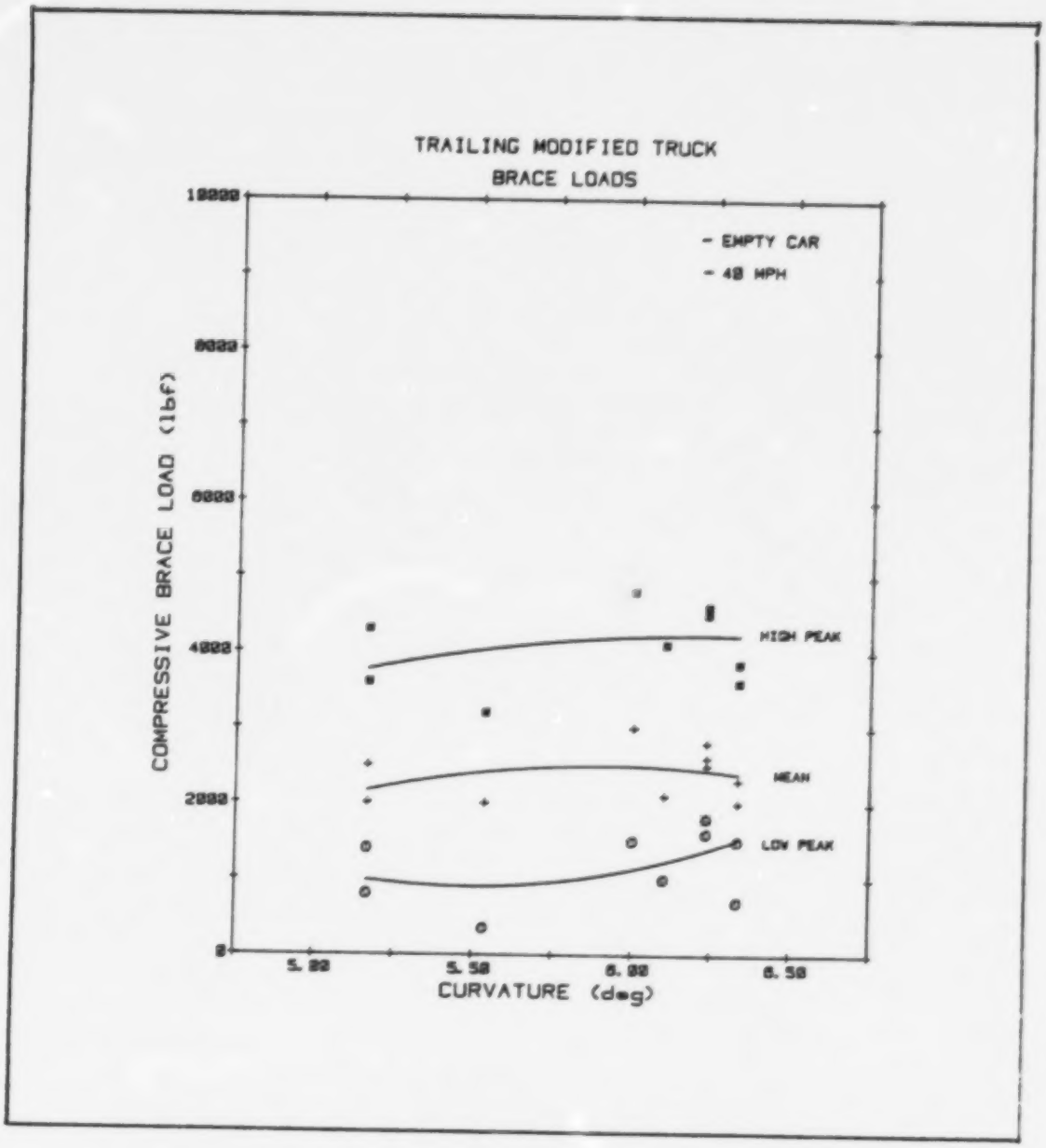

FIGURE 7.2-2: BRACE FORCES VS. TRACK CURVATURE, EMPTY CAR

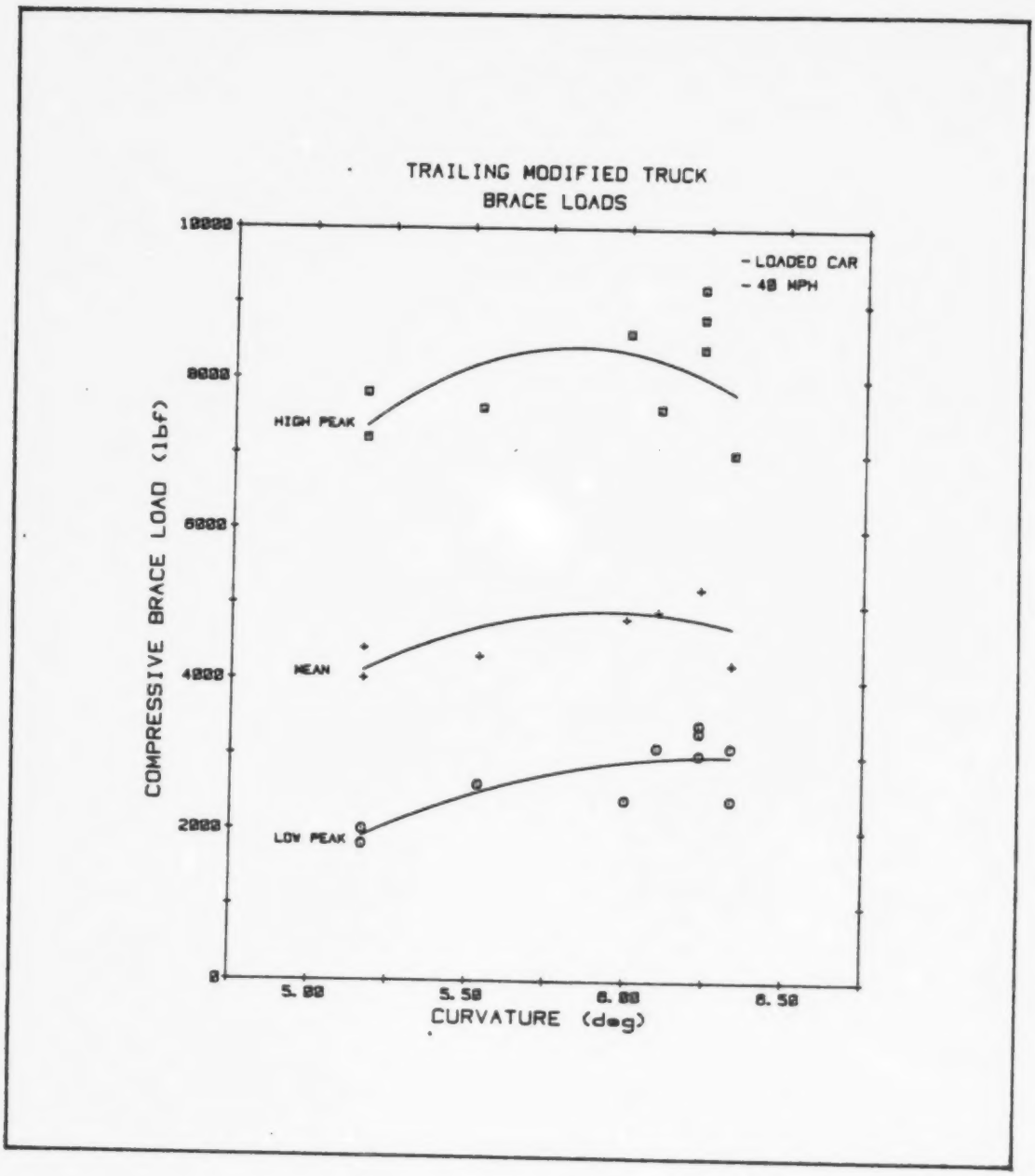

FIGURE 7.2-3: BRACE FORCES VS. TRACK CURVATURE, LOADED CAR

A subsequent stability test was carried out at CP Rail using a bathtub gondola car and randomly-chosen worn wheels. The results of this test (Figure 7.2-4) show that the trailing frame-braced truck achieved acceleration levels lower than any other truck except at 40 mph. It can also be seen that the leading frame-braced truck achieved lower levels of acceleration than the trailing reference truck at all speeds except 40 and 65 mph. It would appear that the critical speed is between 45 and 55 mph.

A complete set of test results is contained in Appendix I.

7.2.4 Low Speed Small Radius Curve Angle of Attack

Figure 7.2-5 shows typical results of the low speed angle of attack tests on a 19 deg curve for both the frame-braced and the standard trucks.

These results show the angles for the standard truck ranging from near 1.8 deg at 1 m/s to about 1.4 deg at just over 1 m/s. The trend, by first order least square curve fit, is towards smaller angles of attack as speed increases.

The results also show that the frame-braced truck achieved angles of attack in the range of near 1.3 deg below 1 m/s to a low of near 1 deg at a speed slightly greater than 1 m/s. As with the standard truck, the behaviour is towards decreasing angles of attack as speed increases.

A complete report on these tests has been published as Report No. TP 4869E, Axle Angle of Attack Comparison, Frame-Braced versus Conventional Freight Truck.

A subsequent angle of attack test was carried out at CP Rail near Calgary on a 5.5 degree curve. The trucks were fitted with new Heumann profile wheels and the cars loaded.

The results (Figure 7.2-6) show that the largest understeer angle of attack measured on the frame-braced truck was 16.2 minutes (0.27 deg) when eastbound and wyed, whereas the smaller angle was recorded as 0.5 minute (0.0083 deg) when westbound unwyed. The largest difference between the leading and trailing axle angles of the frame-braced truck was 8.5 minute (0.1417 deg).

Table 7.2-2 shows clearly that at balance speed of 37 mph, the frame-braced truck outperformed the reference truck by a factor of 4.5:1 to 6.5:1.

7.2.5 Modified Brake Performance Test

The results of the test were:

- o the brake shoes with the modified brake beam conformed under pressure to the tread;

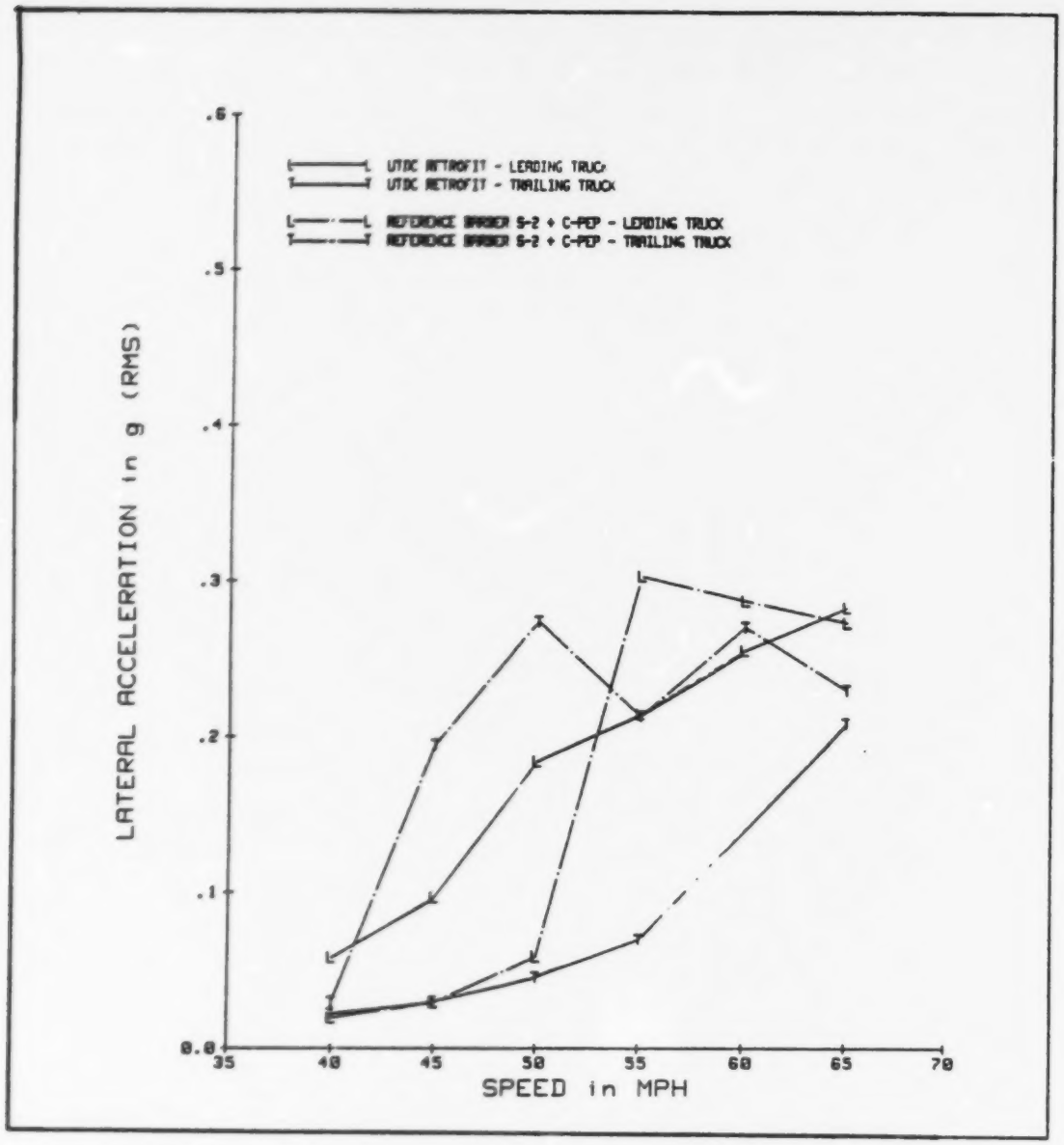

FIGURE 7.2-4: LATERAL ACCELERATION ON LEAD AXLE BEARING ENDCAP VERSUS SPEED FOR TRUCKS WITH SERVICE WORN WHEELS ON EMPTY 100-TON BATHTUB COAL CARS

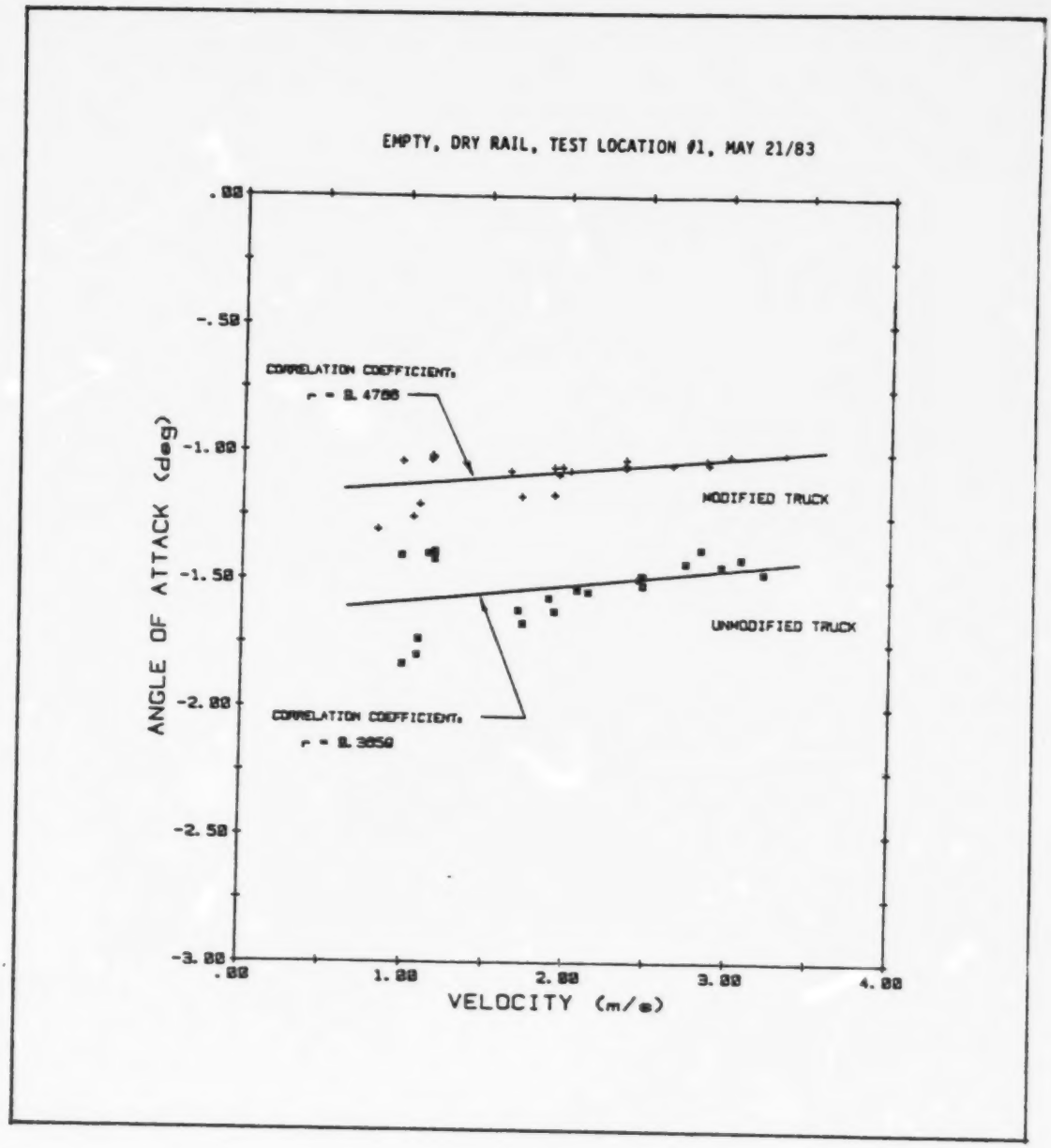

FIGURE 7.2-5: ANGLE OF ATTACK TEST COMPARISON FRAME-BRACED TO STANDARD TRUCK

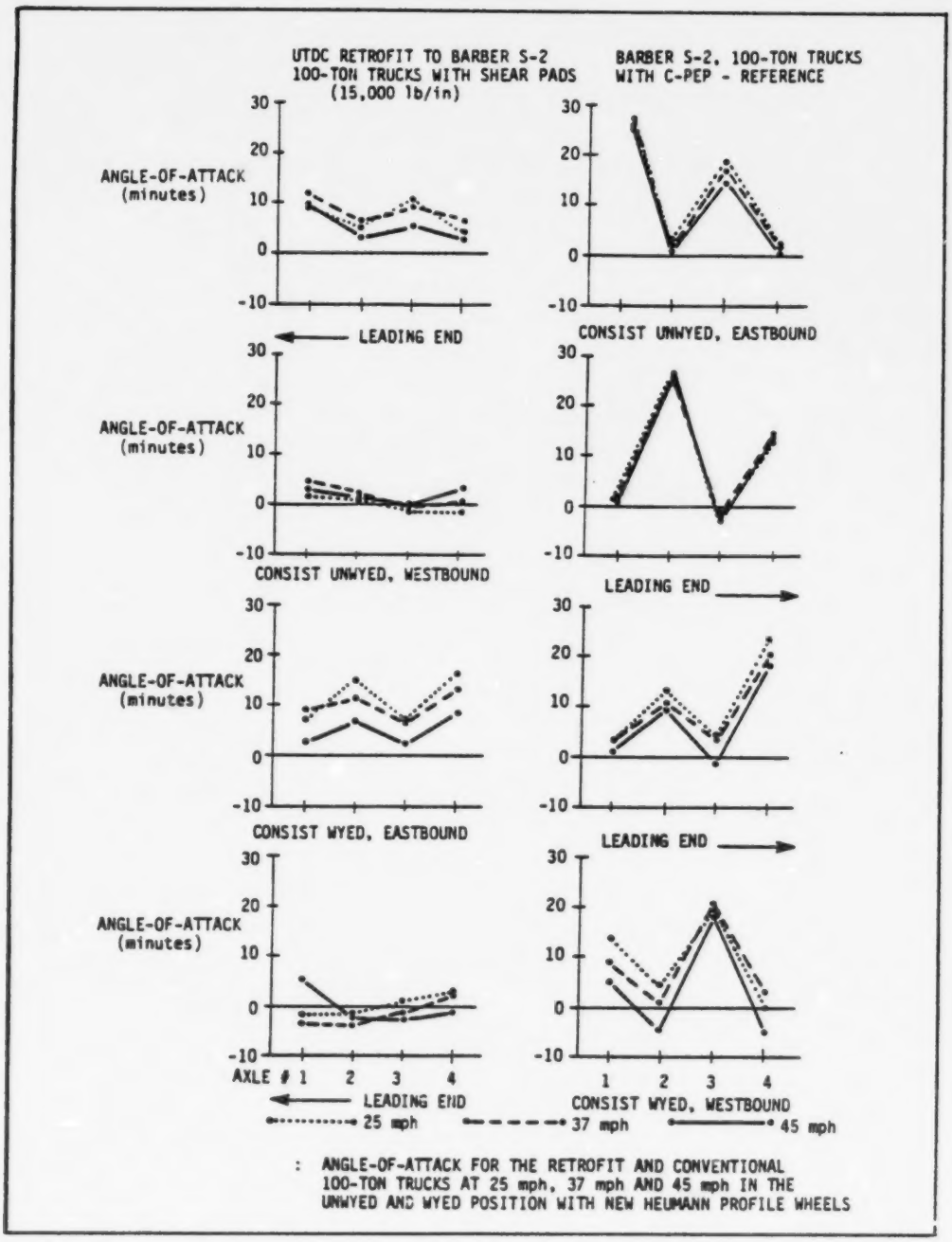

: ANGLE-OF-ATTACK FOR THE RETROFIT AND CONVENTIONAL 100-TON TRUCKS AT 25 mph, 37 mph AND 45 mph IN THE UNWYED AND WYED POSITION WITH NEW HEUMANN PROFILE WHEELS

FIGURE 7.2-6: ANGLE OF ATTACK, 100-TON TRUCKS, 3 SPEEDS

Consist	Direction	Angle-of-Attack (Minutes)							
		UTDC Retrofit (100-Ton Bathtub Coal Car)				Reference BS-2 With C-Pep (100-Ton Bathtub Coal Car)			
Unwyed	Eastbound	11.8	6.1	9.2	6.2	26.7	2.2	17.1	2.1
	Δ_1	5.7		3.0		24.5		15.0	
	Westbound	4.3	2.3	-0.7	0.6	1.7	25.8	-1.7	14.4
	Δ_2	2.0		1.3		24.1		16.1	
Wyed	Eastbound	9.0	11.7	6.7	13.3	2.9	10.9	3.5	20.5
	Δ_3	2.7		6.6		8.0		17.0	
	Westbound	-3.7	-3.9	-1.2	2.3	9.3	0.3	20.6	3.3
	Δ_4	0.2		3.5		9.3		17.3	
$\sum_1 \frac{\Delta_1}{4}$		2.6		3.6		16.9		16.35	

Δ_1 - difference in angle-of-attack for the 2 axles in each truck.

100-Ton Bathtub laden cars with new Heumann profile wheels

TABLE 7.2-2: ANGLE OF ATTACK OF LEADING AND TRAILING AXLES MEASURED AT 37 MPH

- the brake beams moved along the guide slot with no interference;

- the effectiveness of the brakes appeared to be that of the standard brakes; and

- the ONTC was satisfied that brake operation was not comprimised.

7.2.6 Wheel Profile Measurements

An example of the results of these measurements is shown in Figure 7.2-7. The quantitative results are contained in Table 7.2.3.

After some 24,358 km (15,139 mi) the modified truck wheel shows some wear on either side of the flange throat, but a portion of the throat remains unworn.

After some 23,812 km (14,799 mi) the standard truck wheel profile shows wear over the entire tread and down the flange.

A full set of profiles for cars 5021, 5029 (standard) and 5022, 5093 (frame-braced) appears as Appendix J.

Quantitatively for married pair 1, (Table 7.2-3), the wheels on Car 5021 have lost 3.2 kg less metal than Car 5022 which is modified. These cars began with wheels which had been reprofiled once, hence started with a diameter of 889 mm (35 inch).

For Married Pair 2, Car 5093, which was modified, lost 5.78 kg less metal than Car 5029. These cars began with new 914 mm (36 inch) diameter wheels.

As a percentage, modified Cars 5022 and 5093 lost 25.3 and 30.7 percent less metal than did Cars 5021 and 5029.

A computer-generated overlay of tracings of a Burlington Northern new wheel, an F-B demonstration wheel, and a conventional truck wheel is shown in Figure 7.2-8.

Very little tread wear has occurred on either wheel but the flange wear difference is clearly evident at the root.

A complete set of tracings is contained in Appendix K.

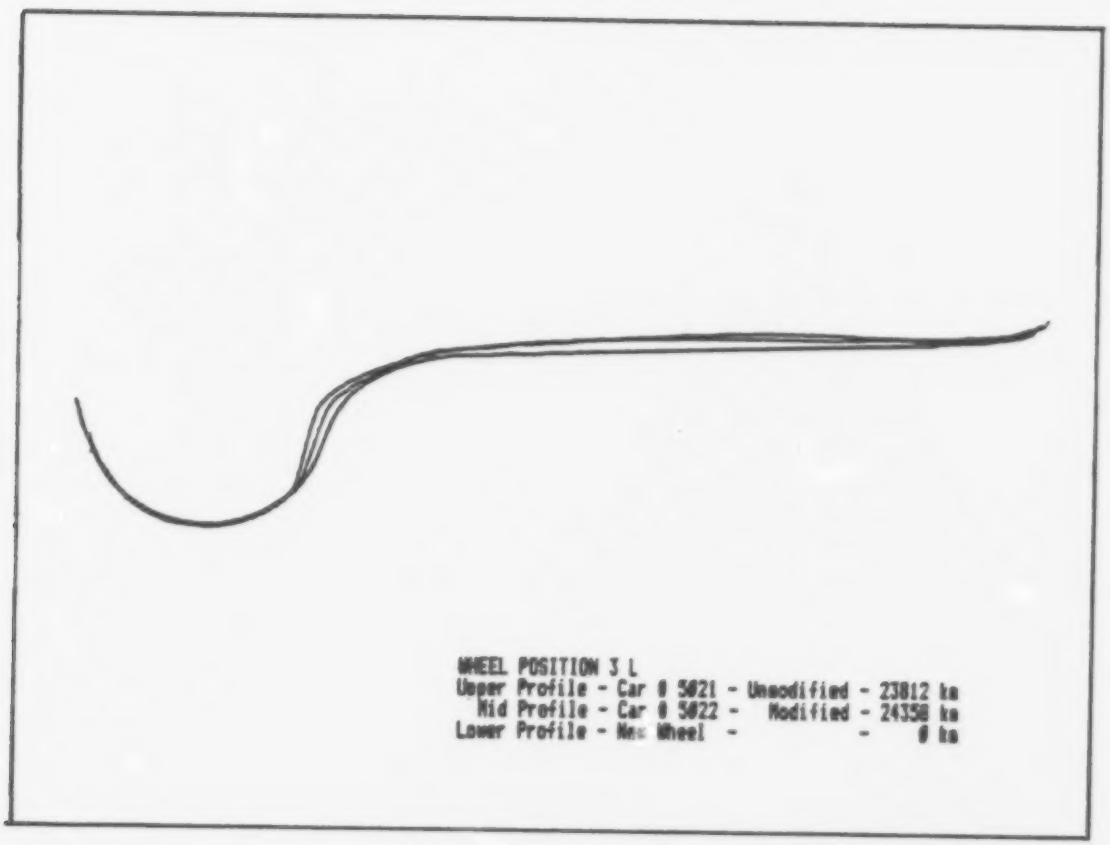
WHEEL POSITION 3 L
Upper Profile - Car # 5021 - Unmodified - 23812 km
Mid Profile - Car # 5022 - Modified - 24358 km
Lower Profile - New Wheel - - 0 km

FIGURE 7.2-7: OVERLAY OF WHEEL PROFILES, WHEEL POSITION 3L, FIRST MARRIED PAIR AT ONTC

WHEEL WEAR ON ONR CARS

Car No.	Status	Distance Travelled Miles	Kilometers
5021	CONV1	14882	23960
5022	FB 1	15223	24509
5029	CONV2	13096	21087
5093	FB 2	12244	19712

MASS OF METAL REMOVED TO 84.12.11 (kg)

Wheel Location	Car #5022	Car #5021	Car #5093	Car #5029
Axle 1 LH	.93	1.93	.83	1.84
Axle 1 RH	1.06	1.47	.59	1.88
Axle 2 LH	1.39	1.99	1.37	.94
Axle 2 RH	1.30	1.63	1.22	2.10
Axle 3 LH	1.52	1.78	1.22	1.62
Axle 3 RH	1.13	1.42	1.32	1.64
Axle 4 LH	1.38	1.24	.73	1.72
Axle 4 RH	1.54	2.00	.86	2.20
	10.25	13.45	8.13	13.91

MASS REMOVED PER 1000 KILOMETERS (kg)

Car #5022	Car #5021	Percent Reduction	Car #5093	Car #5029	Percent Reduction
.0378	.0805	53.0	.0419	.0872	51.9
.0432	.0614	29.6	.0299	.0883	66.1
.0565	.0829	31.8	.0694	.0443	-56.6
.0532	.0681	21.9	.0618	.0993	37.8
.0620	.0740	16.2	.0619	.0767	19.3
.0461	.0593	22.3	.0670	.0779	14.0
.0563	.0515	- 9.3	.0370	.0813	54.5
.0529	.0834	36.6	.0433	.104	58.5
.0510	.0701	25.3	.0515	.0824	30.7

TABLE 7.2-3: QUANTITATIVE WHEEL WEAR RESULTS

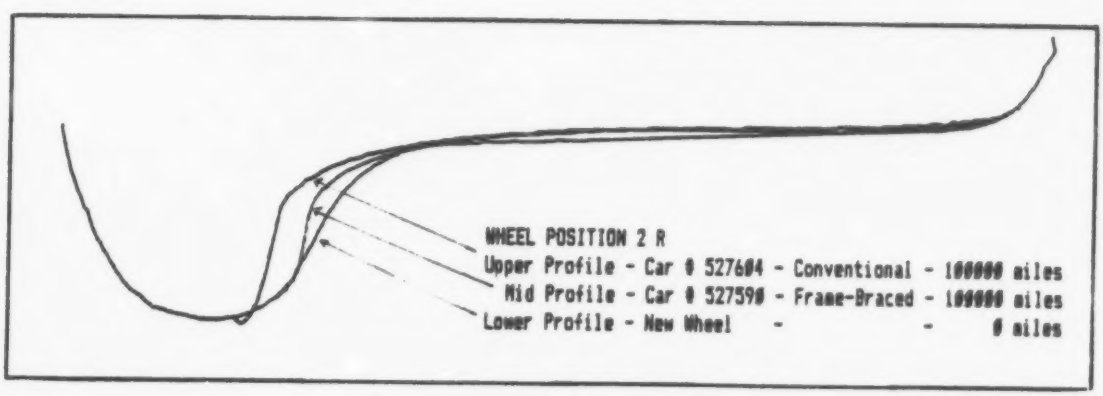
WHEEL POSITION 2 R
Upper Profile - Car # 527604 - Conventional - 100000 miles
Mid Profile - Car # 527598 - Frame-Braced - 100000 miles
Lower Profile - New Wheel - - 0 miles

FIGURE 7.2-8: OVERLAY OF WHEEL PROFILES, BN CARS, 100,000 MILES

8.0 DISCUSSION

8.1 STABILITY AND CURVING ANALYSIS

The analytical predictions were the results of many iterations on values of spring stiffnesses that could be altered, i.e., primary and brace rubber units. The intent was then to get the best of curving (angle of attack) and stability performance. The final result was in the specification for primary horizontal shear stiffness of 4.4×10^6 N/m (25000 lb/in) and a brace bushing axial stiffness of 2.5×10^7 N/m (140000 lb/in), which together yielded an interaxle bending stiffness K_B of $10^{6.64}$ Nm/rad (4.37×10^6 Nm/rad, 3.22×10^6 lbft/rad) and an interaxle shear stiffness K_S of $10^{6.25}$ N/m (1.78×10^6 N/m, 1.22×10^5 lb/ft)), values which could be found on all of the classical K_S/K_B performance plots.

From the stability curves (Fig. 7.1-1) which are based on worst case conditions, i.e, empty car and worn wheel conicity of 1:5, the critical speed of the frame braced truck is 22 percent higher than that of the conventional truck. The friction damping present at the bolster/sideframe interface and the carbody/bolster interface would tend to increase that critical speed.

The analytical empty car curving performance of the frame-braced design shows a 36 percent decrease in angle of attack over the conventional truck at a wheel conicity of 1:20 and upwards of 33 percent

with 1:5 worn wheels, both on a 300 m radius curve (5.8 degree).

Because of the improvement in angle of attack, it follows that the Tread Wear Index should be improved as well as the Flange Wear Index. Tread wear improves by some 50 percent at 0.05 conicity and near 21 percent at a wheel conicity of 0.20. Since the tread wear index is a product of tread force and angle of attack, both of which would be reduced through better wheel/rail alignment, it follows that the percent reduction in index would be somewhat greater than the angle of attack alone.

Also as a result of the improvement in angle of attack, the Flange Wear Index of the frame-braced truck is also improved. With the modified truck exhibiting a Flange Wear Index of near 27.5 N versus the conventional truck at more than 45 N, the improvement exceeds 39 percent, a significant improvement especially for those operators that reject the majority of their wheelsets for thin flange.

The loaded car curving performance shows that the improvement in angle of attack brought about by frame-bracing is some 49 percent on a 300 m curve and 67 percent on the 90 m curve. It must be noted that the mathematical model did not include provision for physical displacement stops such as at the bolster/sideframe and the sideframe/bearing adaptor interfaces, which would have yielded a smaller angle of attack for the conventional truck especially on the 90 m curve.

With respect to Tread Wear, the indices calculated for the frame-braced truck are some 54 percent less than the conventional truck on the 300 m curve and 67 percent better on the 90 m curve. Again, because the Tread Wear Index is a function of Angle of Attack, the index for the conventional truck on the 90 m curve is considered high.

The Flange Wear indices follow the Angle of Attack and Tread Wear trends. The frame-braced truck achieves indices some 33 to 67 percent lower than the conventional truck, i.e. and improvement factor between 1.5 and 3 to 1.

It is interesting to note that on curved track of less than 300 m radius (5.82 deg) the performance of the frame-braced truck with the stiffer 30,000 lb/in pads is better than that with the softer pads. On any curve of radius 596 m or less, the wheels would be fully flanged at a conicity of 0.05, and on the 300 m curve, the wheel rail forces are approaching or have achieved saturation. Although no in-depth study of this has been undertaken, it would appear that the maintenance of truck squareness through the increased lateral shear stiffness of the LC pads is more important and effective than any longitudinal movement allowance of the axles.

Although the Tread Wear Index and the Flange Wear Index may not provide definitive wear quantities in actual practice, there is little dispute in the comparison of the two trucks as to the relative savings in wear to be expected.

8.2 TESTING

8.2.1 Mass, Moments of Inertia, Stiffness

The tests for mass, centres of mass and mass moments of inertia were highly successful and provided useful data. The tests for component stiffness at ONTC were not successful as reported in Section 7.2-1. The readings from the bending stiffness test showed a stiffness less than half of what was expected. As a result, it was decided to use scaled published stiffness values in all analyses.

The tests for shear and bending stiffnesses at NRC, yielded good results. Those results showed an interaxle shear stiffness, within 2% of the value used in the analyses, and an interaxle yaw or bending stiffness within 15% of that used in the analyses. Applying these measured values to the analytical results in Figure 7.1-2 might show a critical speed 1-2 m/s less than for the values used, not a significant change.

8.2.2 Truck Clearance and Low Speed Yard Tests

As explained, the clearance tests showed inadequate bracket/rail clearance. A measurement of the sideframes showed that the tolerance on the casting was maximum all-round, a condition not fully allowed for in the design. In addition, the primary suspension pad supplier substituted a new redesigned pad for the discontinued unit originally supplied for the NRC tests, which was some 6 mm thinner. The bracket and brace redesign adequately compensated for these conditions.

8.2.3 High Speed Mainline Tests

It is evident from these test results that the frame-bracing modification promotes stable truck performance. The longitudinal axle accelerations alone have been halved from near 16 g to 8 g. A cursory investigation of the time and speed elements show that the oscillatory pattern of the frame-braced truck conforms to the 12 m (39 ft) rail joint spacing.

Although the frame-braced truck bolster accelerometer did not function, it is safe to say that the bolster movement should be no worse than that of the conventional truck and is probably better in proportion to the relative axle behaviours (2:1). This would be mainly because of the softer connection between the axle and sideframe, and the intersideframe bracing.

The results of the stability tests run at CP illustrate the difficulty in correlating test data in the form of RMS g acceleration to critical speed curves based on system zero damping.

Since the worn wheelsets were chosen at random, it is unknown what wheel conicity each had. Because RMS g is the measurement, even a stable truck with low levels of system damping could generate sufficient bursts of energy to be misconstrued as being unstable. Suffice it to say that the CP Researchers considered the critical speed to be near 55 mph (25 m/s), a value near 11 percent lower than

the 27.5 m/s predicted. It would appear that something or some things about the system remain unknown.

An investigation of the brace forces show that they are no greater during normal curving than some 75 percent of the design force of 53000 N (12000 lb).

8.2.4 Low Speed Small Radius Curve Angle of Attack

The example of results in Figure 7.2-4 shows in excess of a 25 percent decrease in angle of attack attributable to frame bracing. This reduction is in agreement with the results of the curving analysis for wheels of 0.05 conicity irrespective of the curve radius as seen in Section 7.1.

The results of the test show a more significant difference between the modified and unmodified trucks than might be expected. It was originally considered that because the wheels on both measured axles would be flanged hard against the rail on a curve of such small radius, that the difference in angles would be small. That was not the case and clearly illustrates the effect of increasing the interaxle shear stiffness.

The results at CP using a new Heumann profile wheel showed, in one test run, a leading axle angle of attack of 11.8 minutes (Table 7.2-2) or 0.197 deg. The analytical result from Figure 7.1-9 showed for a 5.5 degree curve, an angle of attack near 0.25 deg for a new 1:20 wheel. The analytical results for an empty vehicle (Figure 7.1-4) show an angle of attack near 0.21 deg for a 1:5 wheel, a good agreement.

Concurrently, the unmodified vehicle leading axle experience an angle of attack of 26.7 minutes or 0.445 deg. Analytically, for the 300 m curve, the conventional wheelset would show an angle greater than 0.3 deg empty with 1:5 wheel (Fig 7.1-4) and near 0.62 deg loaded with a 1:20 wheel (Fig 7.1-9). Again, a reasonable agreement exists, displaying an improvement exceeding 2:1.

8.2.5 Modified Brake Performance Test

The reworking, as necessary, of the new brake beam ends is only for the retrofit systems. In most cases, the ends of used brake beams are sufficiently loose in the sideframe pockets to require no work at all to allow good brake shoe-to-wheel conformity. Any new design frame braced truck would consider the wheel-to-brake requirements.

8.2.6 Wheel Profile Measurements

It is quite evident that the wheels installed under frame braced trucks are exhibiting less wear than the control sets.

The main advantage appears at the flange and the flange root. The wear on the tread shows some small difference but not to the obvious extent of that at the flange area.

The results of the Burlington Northern wheel measurements, especially with the much larger travel distance, are much more definitive. The tread wear difference between the frame-braced truck and the

conventional is quite small and as previously mentioned, more tread brake related than angle of attack related. Conversely, the difference in flange wear is very pronounced where it would appear that the flange of the conventional wheel could never be restored to original whereas the frame-braced truck wheel appears to have sufficient metal to accomplish that.

Information from BN says that average wheel life approaches 250,000 miles. The profiles shown in Figure 7.2-8 would lead one to believe that the frame-brace truck wheel would exceed that life by more than two-fold in the flange area alone.

9.0 CONCLUSIONS

From the results of the analyses and tests performed as a part of this program, it can be concluded that:

- frame bracing increases the stability of the three-piece freight truck by a margin of 22 percent and more analytically, and up to 20 percent by test;

- frame bracing the three-piece freight truck decreases wheel/rail angle of attack by 55 percent by test and upwards of 60 percent by analysis;

- excluding wear attributable to the action of tread braking, frame bracing is predicted to decrease wheel tread wear by 40 to 75 percent for an unloaded car for an improvement ratio of 1.67 to 4 to 1;

- excluding wear attributable to the action of tread braking, frame bracing is predicted to decrease wheel tread wear by 62 percent on a 300 m curve for a loaded car: an improvement ratio of 2.6 to 1;

- frame bracing is predicted to decrease wheel flange wear by 36 to 38 percent for an unloaded car for an improvement ratio of 1.5 to 1.6 to 1;

- frame bracing is predicted to decrease wheel flange wear by 42 percent on a 300 m curve for a loaded car: an improvement ratio of 1.7 to 1;

- by measurement at ONTC, after only some 24,000 km of travel, frame bracing is seen to decrease total wheel wear by 25-30 percent for an improvement ratio of 1.34 to 1.44 to 1;

- by measurement at BN, after 100,000 miles (80,000 km) of travel, frame bracing is seen to provide a total wheel wear improvement of 2.2 to 1;

- by analysis, the effect of frame bracing on the fatigue life of the sideframe is small to negligible; and by test, insignificant;

- the frame bracing design hardware can be installed on 90 tonne (100 ton) Barber S-2 design trucks and provide normal AAR clearance;

- the frame braces perform as designed and within design loads; and,

- as low as a 2.5 year payback period is feasible for high mileage heavy haul car operators.

10.0 RECOMMENDATIONS

It is recommended that:

- the frame-braced and control trucks remain in revenue service so to accumulate more travel distance;
- the wheel wear be monitored periodically to continue the assessment of relative wear;
- the economic (cost/benefit) analysis be revised as new wheel wear benefits are determined; and,
- additional cars be modified to provide a larger test sample.

THIS PAGE LEFT BLANK INTENTIONALLY.

APPENDIX A

PROPERTIES

OF CROSS BRACED TRUCKS

THE AMERICAN SOCIETY OF MECHANICAL ENGINEERS
345 E. 47 St., New York, N.Y. 10017

82-WA/DSC-21

The Society shall not be responsible for statements or opinions advanced in papers or in discussion at meetings of the Society or of its Divisions or Sections, or printed in its publications. Discussion is printed only if the paper is published in an ASME Journal. Released for general publication upon presentation. Full credit should be given to ASME, the Technical Division, and the author(s). Papers are available from ASME for nine months after the meeting.
Printed in USA.

PROPERTIES OF CROSS-BRACED TRUCKS

Roy E. Smith
Project Chief Engineer, Advanced Trucks
Urban Transportation Development Corporation
Kingston, Ontario

and

Ronald J. Anderson
Assistant Professor
Department of Mechanical Engineering
Queen's University
Kingston, Ontario

ABSTRACT

The dynamic and curving behaviour of railroad trucks having direct interaxle connections (cross-bracing) is compared with those which do not. The generalized parameters K_S and K_B, the interaxle shear and bending stiffnesses, are used to characterize the trucks. The validity of this characterization is demonstrated by variation of a number of the component parameters. Targets for the criteria of curving behaviour and practical limits for certain of the parameters are established. It is shown that cross-bracing offers no inherent advantage compared with normal frame connections.

It is also shown that, in the case of a truck with very low shear stiffness (e.g., 3-piece trucks), the inclusion of cross-bracing improves behaviour substantially, but not beyond that which may be obtained by shear bracing of adequate resilience in the frame itself.

NOMENCLATURE

a	-	Half axle spacing
b	-	Half transverse span of primary springs
m	-	metres
f_{11}	-	longitudinal creep coefficient
f_{22}	-	lateral creep coefficient
F	-	a force
r	-	wheel radius
I_A	-	Alignment index Tracking index
K_B	-	Interaxle bending stiffness
K_S	-	Interaxle shear stiffness
K_x	-	Primary stiffness (longitudinal)
K_y	-	Primary stiffness (lateral)
K_{RS}	-	Interaxle connection shear stiffness
K_{RB}	-	Interaxle connection bending stiffness
L	-	Load on each wheel
N	-	Newtons
R	-	Curve radius
X_0	-	Axle radial offset for true rolling
X_1	-	Axle radial offset (actual)
α	-	angle of attack
λ	-	Conicity
δI_T	-	Change of tracking index due to δx
δx	-	Lateral offset from pure rolling position
θ_0	-	Interaxle angle for true radial alignment
θ_1	-	Interaxle angle (actual)

INTRODUCTION

Rail-borne vehicles are subject to dynamic instabilities as a result of the nature of the interaction of the wheels with the rails (known as the creep phenomenon)[1,2]. This behaviour is normally controlled by elastic constraints exercised between the axles and a truck frame. These same elastic constraints affect the behaviour of the wheelsets when negotiating curved track. This paper investigates the properties which affect these aspects of truck behaviour and in particular a technique, known as cross-bracing, which attempts to improve the limits of truck behaviour which can be achieved in practical designs.

In a conventional truck layout the axles are connected to a truck frame through elastic suspension elements and the frame is then pivotted to the car body. Each of the suspension elements has longitudinal and lateral stiffness and these interact to provide constraint for the axles laterally, longitudinally and in yaw. Cross-braced trucks have further elastic connections directly between the axles.

In one mechanism the diagonally opposite ends of each axle, or of a sub-frame attached to each axle, are joined by tension members. Another mechanism has yoke members attached rigidly to each axle, extending towards the middle of the truck, where they are joined to each other by a more or less flexible hinge or resilient joint. Since the 1880's many mechanisms have been proposed to accomplish steering of railway trucks, the above two are mentioned specifically here because they employ cross-bracing and are currently under development.

With both of these mechanisms the axles have some freedom to yaw out-of-phase with one another but are restrained from any other motion in the yaw direction. By itself this would appear to provide the freedom necessary for curving behaviour but further examination reveals limitations. One of the

possible modes of instability is out-of-phase yaw oscillations of both axles. Restraint against this mode must be provided through the connections to the truck frame or through yaw stiffness in the mechanism. This restraint then offers resistance to the desired curving behaviour.

ANALYSIS

In order to investigate the behaviour of the cross-braced truck and compare it to that of more conventional layouts it is necessary to formulate models which enable the dynamic and curving behaviour of the trucks to be calculated. It is also necessary to establish a format for display of these characteristics in terms which are comparable and significant.

It has been found [3] to be convenient to express truck characteristics in terms of the interaxle shear and interaxle bending stiffnesses (K_S and K_B) which are defined to be the elastic stiffness opposing relative shear (lateral) motion between the axles and the elastic stiffness opposing relative (out-of-phase) yaw motion between them.

Figure 1 shows a schematic of a truck which includes axle interconnections. In this case the model includes both bending and shear stiffness in these interconnections (K_{RB} and K_{RS}) for complete generality.

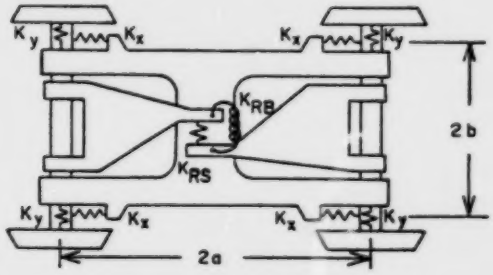

CONVENTIONAL ($K_{RS}=K_{RB}=0$)	CROSS-BRACED
$K_B = b^2 K_x$	$K_B = b^2 K_x + K_{RB}$
$K_S = \dfrac{b^2 K_x K_y}{b^2 K_x + a^2 K_y}$	$K_S = \dfrac{b^2 K_x K_y}{b^2 K_x + a^2 K_y} + K_{RS}$
$K_y = \dfrac{K_S K_B}{K_B - a^2 K_S}$	$\therefore K_S < \dfrac{1}{a^2} K_B$

FIGURE 1: CROSS-BRACED TRUCK SCHEMATIC

Interaxle shear is identical to in-phase axle yaw. This illustrates the significance of the values of K_S and K_B. K_S is a restraint preventing in-phase axle yaw motions and K_B prevents out-of-phase axle yaw motions. These are the two principal modes of truck instability. A third mode can occur in which the whole truck is in yaw oscillation as an assembly. This occurs when K_S and K_B are both very high, locking both axles together so that they move as a unit. Out-of-phase yaw motions are those required for good curving and it therefore appears that a low value of K_B is required if a truck is to achieve good alignment of wheels with rails without demanding excessive forces at the wheels.

The Limit Line

There is a significant factor to be noticed from examination of the formulae for K_S and K_B. There is an upper bound to the value of K_S for any given value of K_B if a conventional truck construction is to be used. This upper bound can be expressed in the form of a limit line in the K_S-K_B field. It is impossible for a conventional truck to achieve values of K_S above the line $K_S = (1/a^2)K_B$.

The techniques used in the analysis were straight-forward and will not be described in detail. A mathematical model of the vehicle and trucks was formulated and a set of equations of motion generated describing the motion of each component in the assembly. These equations of motion included the creep forces generated at the rails. This set of simultaneous differential equations was then solved for a series of different values of K_S and K_B and for different velocities. By plotting modal damping versus velocity, the critical velocity (at which the first mode becomes unstable) was obtained for each case.

The Curving Model

The same model with a revised, nonlinear, formulation for the creep forces (incorporating adhesion limits) and with limits on axle lateral excursion, to account for gauge clearance, was used in a curving analysis [4]. Wheel/rail forces, angle-of-attack, tracking index, alignment index and wear index were calculated. Three curves were used, having radii of 30m, 300m and 1000m. A worn wheel conicity of 0.20 (1/5) is used in this paper. In [5], a new wheel conicity of 0.05 (1/20) is also considered. The ranges of values of K_S and K_B were:

$$10^5 \leqslant K_S \leqslant 10^8 \quad \text{N/m}$$
$$10^5 \leqslant K_B \leqslant 10^8 \quad \text{N-m/rad}$$

Performance Criteria

The velocity at which hunting motions first begin is known as the critical velocity. Because the effects of hunting are extremely undesirable it is necessary to ensure that the critical velocity falls above the range of operating speeds. The variation of critical speed with K_S and K_B provides an indication of the proportions of K_S and K_B necessary to achieve design objectives with respect to this important stability criterion.

Good performance of the truck during curve negotiation is significant in improving noise, wear, and rolling resistance. Three independent measures of curving performance are considered as functions of K_S and K_B. The first of these is the angle-of-attack of the leading axle with respect to the rail. The others are the tracking index and alignment index as described below.

For a pair of coned wheelsets running on curved track two conditions must be met in order for pure rolling to be possible (see Figure 2). An angle must exist between the two axles and the centre of each of the axles must be offset from the centre of the rails by a certain amount.

The tracking index I_T is a measure of the correctness of the axle offset and the alignment index I_A describes the angular deflection. These indices are defined in Figure 2.

For perfect rolling the value of I_T will be 1.0, any other value (either lesser or greater) is

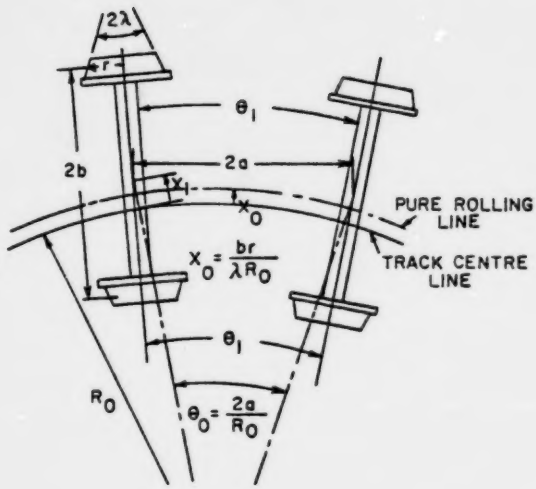

$$\text{TRACKING INDEX} = \frac{X_1}{X_0}$$

$$\text{TRUCK ALIGNMENT INDEX} = \frac{\theta_1}{\theta_0}$$

FIGURE 2: DEFINITION OF CURVING INDICES

an indication of a condition in which slip is occurring.

A value of 1.0 for I_A indicates a perfect steering angle and zero indicates that the axles have remained perfectly parallel. A value of 1.0 is not sufficient to show proper alignment with the rails however as both axles may take the same angle-of-attack to the rails and still maintain an alignment index of 1.0. If the alignment index is 1.0 and the leading axle angle of attack is 0.0 then true radial alignment will exist and if the tracking index is also 1.0 then pure rolling will occur.

Another criterion for judging truck performance is tread wear. To give some indication of the level of tread wear which might be expected to take place with any given truck design a tread wear index has been devised. This index is a measure of the work done against friction during sliding contact of the wheel treads with the rails. By multiplying the creep forces by the rate of creep (the ratio of the slip speed to the linear velocity) a measure of the work done per metre travelled is obtained. This index ignores the effects of spin at the point of contact and the microslip which occurs in the contact area due only to the contact elastic deformations. It represents nevertheless, an indication of the likely tread wear rate. No direct correlation of the rate of metal removal with the work done at the contact patch has been able to be made and there are no doubt a number of crucial factors which will influence any correlation which exists. It is not unreasonable even so to expect that, all other things being equal, a higher level of work done at the interface will result in more rapid removal of material.

Results

The variation of truck performance criteria with K_S and K_B are presented here. Each of the characteristic stiffnesses is varied over a range of three decades and results are presented both below and above the limit line for conventional trucks and those with cross-bracing. Figures 3 through 17 present the data in graphical form. The shaded area in these figures represents an operating condition without flange contact.

In making changes to the stiffness parameters, no changes to the masses of components (such as truck frame, axles, etc.) were made. It could reasonably be argued that the addition of cross-bracing is bound to increase the mass and inertia of the wheelsets. It was felt to be best however, to leave the mass values static so as to illustrate clearly the effect of the stiffnesses.

Critical Velocity

Figure 3 shows the characteristic curves of critical velocity for a wheelset conicity of 0.2. This takes the form which would be expected from a logical review of the properties of railway wheelsets. Increasing the level of stiffness in each direction will result in an increase in the critical velocity up to some point. After this point no further increase in critical velocity occurs because the unstable mode has become that which is affected by the other stiffness parameter. Increasing stiffness in the other direction is then the only way to gain an increase in critical velocity. It can be seen however, that in each direction, as stiffness is increased towards the right hand upper corner of the field a peak of critical velocity is reached and further increases will result in reduced critical velocity. This is the result of the stiffness becoming so high that the truck begins to act more and more like a rigid single axle and the interaxle motions are of less significance than truck yaw and lateral motions. It can be seen that the peak values for critical velocity are very similar for the conventional area of the field and the cross-braced area and indeed the characteristics are almost mirror images on either side of the limit line. It can also be seen that the peak value occurs in the cross-braced case at a lower value of K_B than for the conventional case. It is evident that by increasing K_S and reducing K_B it is possible to arrive at a point above the limit line with the same critical velocity as that obtained below the line. It is this which gives rise to the hope that some improvement in curving behaviour can be achieved by designing above the limit line.

Angle of Attack

For the small curve radius of Figure 4 we can see that increasing the value of K_S, particularly in the left hand side of the field, results in decreased angle of attack. The decrease is substantial along the $K_B = 10^5$ line but becomes rapidly less important as K_B is increased. For values of K_B above 10^6 the reduction in angle of attack obtained by using values of K_S above the limit line becomes very small.

For the intermediate curve radius (Figure 5) a different situation prevails. In the left side of the field, at low values of K_S and K_B, very low values of angle of attack are achieved, as K_S is

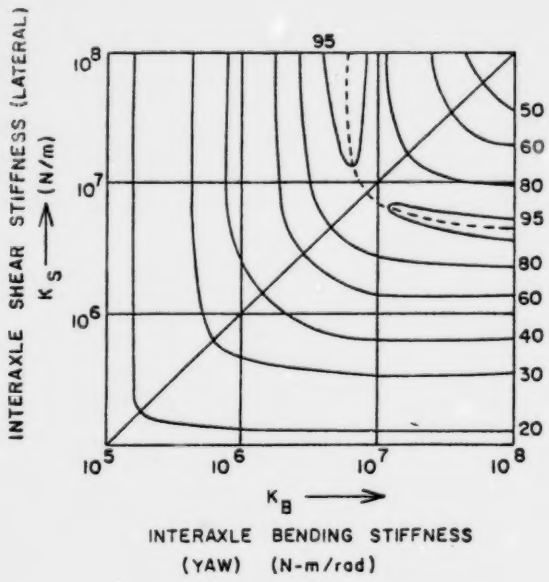

FIGURE 3: CRITICAL SPEED CHARACTERISTICS (m/sec)
UNSTEERED TRUCKS (λ =-.2)

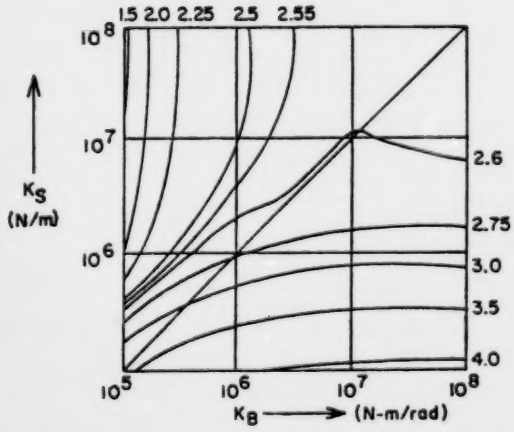

FIGURE 4: ANGLE OF ATTACK (DEGREES)
λ = 0.20, R = 30M , LEADING AXLE.

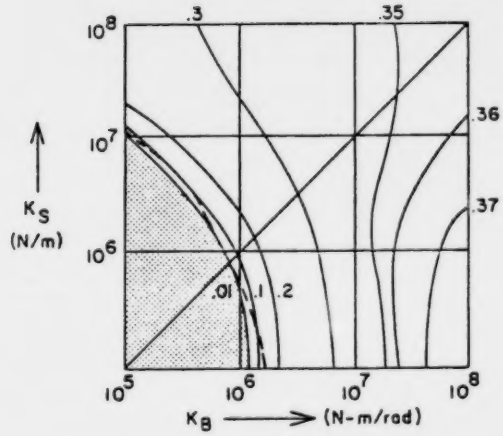

FIGURE 5: ANGLE OF ATTACK (DEGREES)
λ = 0.20, R = 300 M , LEADING AXLE.

increased however, the angle of attack becomes worse. This trend continues through the centre of the field up to $K_B = 10^7$. At that point the angle of attack is more-or-less constant regardless of the value of K_S. In the right hand side of the field, for values of K_S below the limit line very small improvements in the angle of attack can be seen, above the limit line no improvement is seen.

For the large curve radius (Figure 6) the result is very similar to that of Figure 5. In the low to middle range for K_B, increasing K_S makes the angle of attack worse while in the high K_B range it makes matters slightly better, except above the limit line where no improvements are seen. Cross-bracing then either makes matters worse or at best it simply doesn't affect the situation.

Flange Force

Figures 7 to 9 show the contours of flange force for the three curve radii. At the small radius (Figure 7) it can be seen that the flange force varies very little with changes in K_B. For very low values of K_S the lowest forces are experienced these rise rapidly to a peak near $K_S = 5 \times 10^5$ and thereafter are virtually constant.

For the intermediate radius (Figure 8) in the lower left hand corner of the field, no flange contact exists. As K_S is increased in this area flange contact eventually occurs and flange forces thereafter build up. Similarly, as K_B is increased, flange contact eventually occurs and flange forces build up. In the right hand side of the field increasing K_S gives a reduction in flange force, as the limit line is crossed however the flange force reduction becomes less significant.

For the larger curve radius (Figure 9) the same effect is even more pronounced. Here flange contact exists only in the lower right hand corner of the field and flange contact has been lost well before the limit line is reached.

Tracking Index

The tracking index contours for the leading axle are shown in Figures 10 and 11. For the small curve radius the tracking index is constant across the entire field, due to flange contact, so no figure is given.

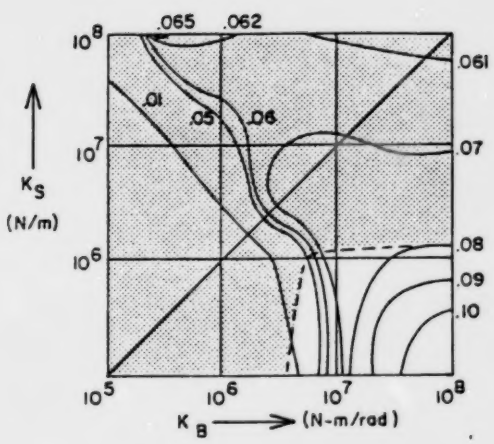

FIGURE 6: ANGLE OF ATTACK (DEGREES)
λ = 0.20, R = 1000M , LEADING AXLE

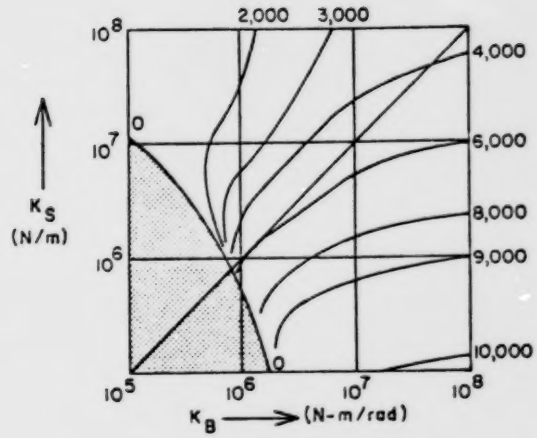

FIGURE 8: FLANGE FORCE (N), (LEADING AXLE)
λ = 0.20, R = 300 M

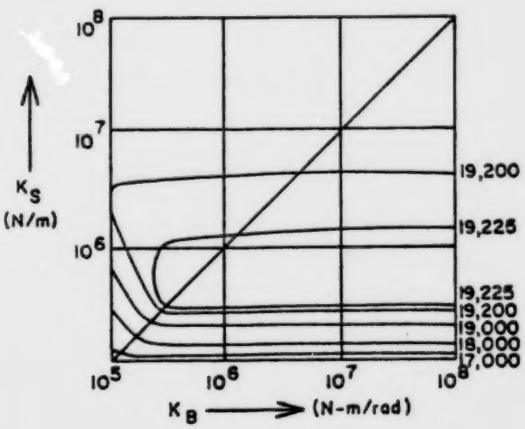

FIGURE 7: FLANGE FORCE (N), (LEADING AXLE)
λ = 0.20, R = 30 M

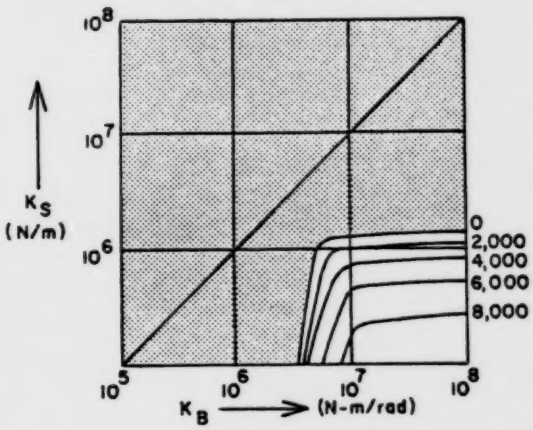

FIGURE 9: FLANGE FORCE (N), (LEADING AXLE)
λ = 0.20, R = 1000 M

For the case of intermediate curve radius (Figure 10) we can see that the bottom left hand

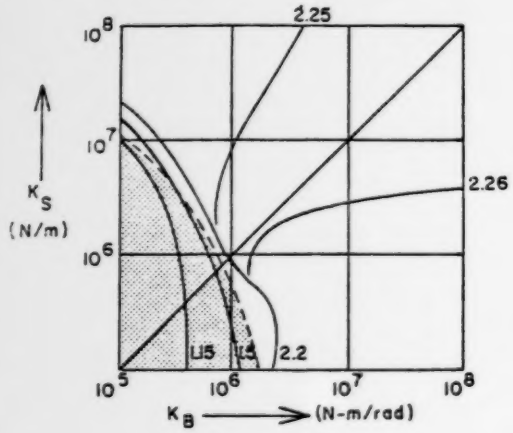

FIGURE 10: TRACKING INDEX (LEADING AXLE)
λ = 0.20, R = 300 M

corner of the field gives closest to the ideal value of 1.0, increasing either K_S or K_B gives worse values. No advantage can be seen to using values above the limit line.

The case of the large curve radius (Figure 11) presents a somewhat different situation. In the left hand portion of the field, curves very similar

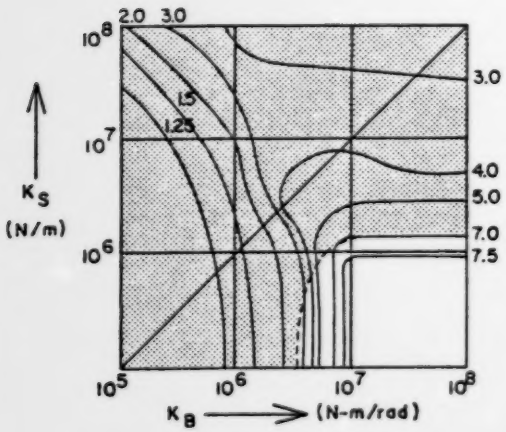

FIGURE 11: TRACKING INDEX (LEADING AXLE)
λ = 0.20, R = 1000 M

to those of the previous case are seen. Here increasing K_S, especially into the area above the limit line, worsens the values of the tracking index. For values of K_B close to the centre of the range it can be seen that increasing values of K_S initially result in increased values of tracking index and then as K_S increases further, the tracking index starts to decrease. As we move further into the right side of the field we see that increasing K_S results in steady reduction in the tracking index from very high values in the lower right hand corner to more moderate values in the upper right hand corner. Studying the portion of the field above the limit line it can be seen that, for low K_B, cross-bracing worsens the tracking index, for moderate K_B it provides some improvement and for high K_B it has very little effect.

Alignment Index

The alignment index contours are shown in Figures 12 to 14. For the case of the small curve radius (Figure 12) it can be seen that only very low

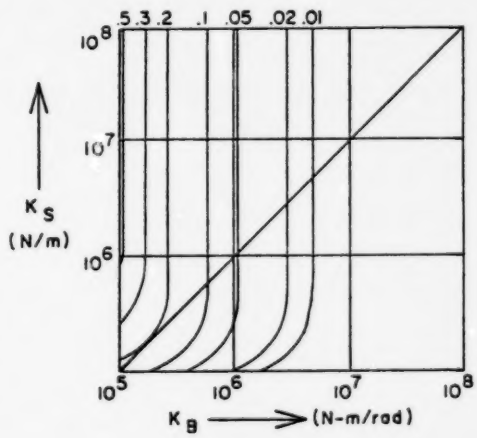

FIGURE 12: ALIGNMENT INDEX
λ = 0.20, R = 30 M

values of the alignment index are achieved anywhere within the field and that above the limit line no improvement in alignment index is seen by increasing K_S except for a small improvement in the extreme left hand side of the field.

For the intermediate curve radius (Figure 13) it can be seen that good values of alignment index occur in the lower left hand corner of the field and that increasing K_S always leads to lower (worse) values of alignment index throughout the field.

For the large curve radius (Figure 14) the situation is very similar to that of Figure 13. Increasing K_S, particularly to move into the area above the limit line, always produces a worsening of the alignment index. It can be seen in the upper right hand portion of the field of Figure 14 that the effect of increasing K_S is to actually cause a negative value for the alignment index.

Tread Wear Index

The tread wear index contours are shown in Figures 15 to 17. For the small curve radius (Figure 15) it can be seen that very little

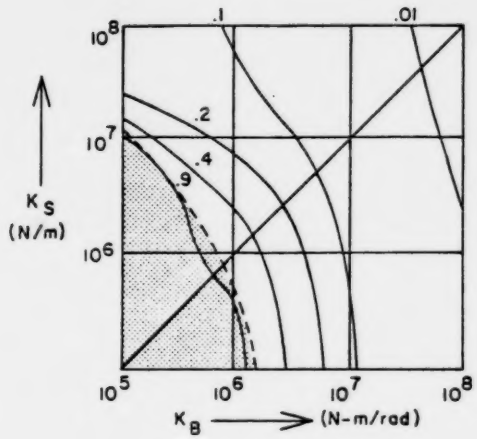

FIGURE 13: ALIGNMENT INDEX
$\lambda = 0.20$, R = 300 M

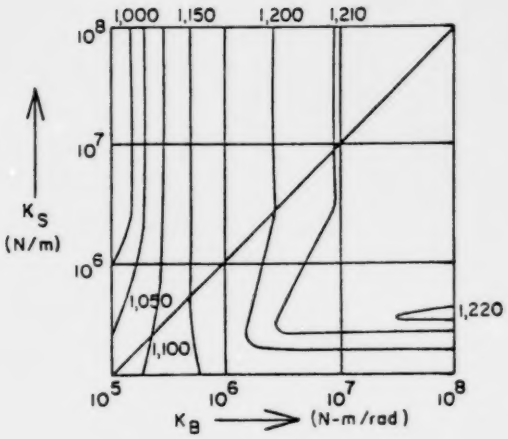

FIGURE 15: TREAD WEAR INDEX (m-N/m)
$\lambda = 0.20$, R = 30 M

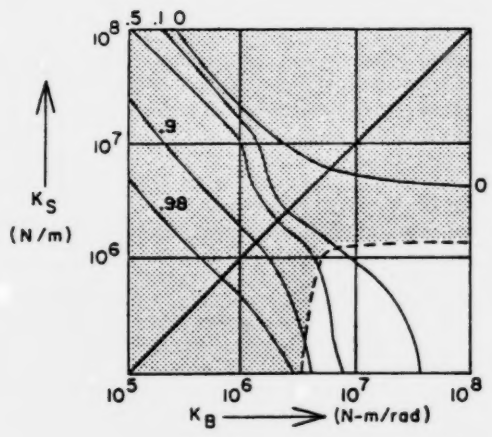

FIGURE 14: ALIGNMENT INDEX
$\lambda = 0.20$, R = 1000 M

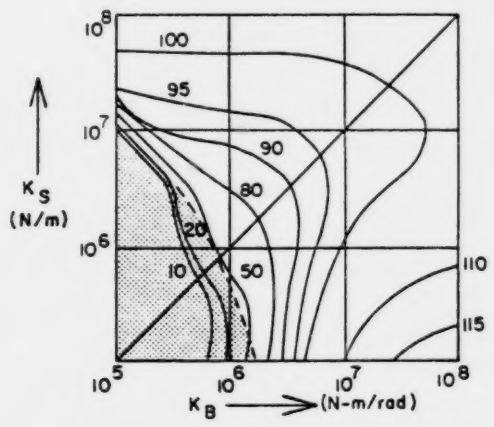

FIGURE 16: TREAD WEAR INDEX (m-N/m)
$\lambda = 0.20$, R = 300 M

variation in the index occurs across the entire field. In particular, it can be noted that above the limit line the contours are vertical, indicating that an increase in K_S will not affect the tread wear index.

For the intermediate radius (Figure 16), in the lower left hand corner of the field, low values of tread wear index are achieved. Increasing K_S in this area produces an increase in the wear index. This remains true throughout the field with the exception that, in the right hand side, increasing K_S results in a small decrease in the wear index followed by an increase. Throughout the field it can be seen that no reduction in wear index is achieved by moving into the area above the limit line (cross-bracing).

For the large curve radius (Figure 17) the situation is again similar to that of Figure 16 with the exception that a maximum occurs in the right hand field below the limit line. This has the effect of very slightly decreasing the wear index above the limit line for a part of the right hand field.

DISCUSSION

Before discussing the design implications of the results given above it is necessary to examine two aspects of the variables used to obtain these results. Since K_S and K_B, the interaxle shear and bending stiffnesses, have been used to characterize the truck suspension properties, it is necessary to explore the validity of this. It is also necessary to investigate the practical limitations which must be put on the values of these parameters.

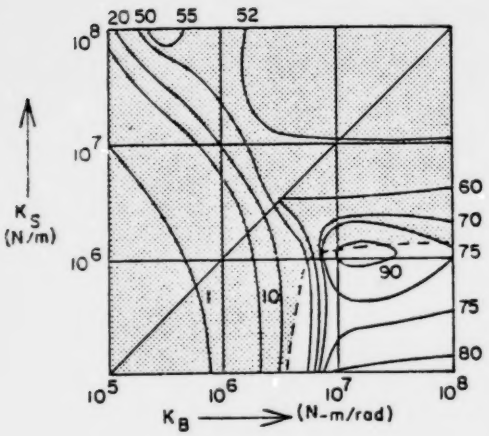

FIGURE 17: TREAD WEAR INDEX
$\lambda = 0.20$, R = 1000 M

K_S and K_B as Design Criteria

The validity of using only two stiffnesses to characterize a truck must be established. The expressions for K_S and K_B for a conventional truck (Figure 1) show that they constitute a simple, one-to-one replacement for the primary suspension stiffnesses K_x and K_y. For given values of K_S and K_B, there are unique values of K_x and K_y which must be used.

The case for the cross-braced truck is somewhat different. There are four independent stiffness parameters (K_x, K_y, K_{RB} and K_{RS}) in the cross-braced truck. That these four stiffnesses may be replaced by two, more general stiffnesses (K_S and K_B) was established by recalculating dynamic and curving performance for given values of K_S and K_B achieved through very different proportions of K_x, K_y, K_{RS} and K_{RB}.

The agreement was excellent for both critical velocity and curving performance variables [5].

Practical Limits

In all of the calculations performed for this analysis the values of K_x and K_y were allowed to vary throughout a range of three decades. It was felt that this range represented the range of stiffnesses practically achievable in the suspension components. There are other practical limits to the value which these may take however. In particular, the longitudinal stiffness, K_x, has a lower limit imposed upon it. The longitudinal forces of traction and braking must always pass from the axle to the truck frame through the stiffness K_x. Transmitting this force results in a displacement of the axle relative to the truck frame. In a real truck the amount of displacement which can be allowed is limited by practical considerations such as drive train clearances, brake mechanism motions, slack adjuster sensitivity, spring retention, bearing housing clearances, etc.

To estimate the allowable value for K_x let us make the practical assumption that a 30,000 kg vehicle decelerating at 0.4 g must give an axle-frame deflection of no more than 3mm. In this case the minimum value of K_x would be 4.9×10^6 N/m.

For an inboard bearing design the value of b is approximately 0.5m and K_B is thus limited to no less than 1.2×10^6 N-m/rad. For an outboard bearing design b is approximately 1.0m and therefore the limit is 4.9×10^6 N-m/rad. These calculations show that, for the configuration under consideration here, the left hand side of the $K_S - K_B$ field ($K_B < 10^6$) is not accessible in any practical sense.

One of the criteria used to examine the effectiveness of a truck in achieving good alignment of the axles on curved track is the angle of attack of the axle to the true perpendicular to the rail at the point of contact. Comparison of one truck against another gives a measure of relative merit but it is also necessary to keep in mind an absolute measure of "goodness". Clearly the ideal condition is for the angle of attack to be zero. Recognizing that this may not be attainable it is necessary to establish what would be an acceptable level.

An angle of attack, α, generates a lateral wheel/rail interaction force which is, for small angles, proportional to α. The constant of proportionality is the lateral creep coefficient f_{22} resulting in:

$$F = f_{22}\alpha \quad \ldots\ldots (1)$$

In order not to allow this lateral force to absorb a large proportion of the available friction at the wheels we must limit its value. A reasonable limit is one third of the available friction force.

$$F \leqslant \frac{\mu L}{3} \quad \ldots\ldots (2)$$

where L is the normal force on the wheel.

The result is:

$$\alpha \leqslant \frac{\mu L}{3 f_{22}} \quad \ldots\ldots (3)$$

For practical values of the variables, the limit on angle of attack is approximately 0.01 degrees.

It is possible to similarly determine a range for the value of the tracking index which will ensure a limitation of the longitudinal creep rate and thus a limitation on the amount of available adhesion utilized by the lack of (or excessive amount of) lateral wheelset offset. If we again arbitrarily set the limit on the induced creep force to one third of the maximum available we can derive the equation

$$f_{11}\frac{\lambda \delta x}{r} \leqslant \frac{\mu L}{3} \quad \ldots\ldots (4)$$

we can also derive

$$\delta I_T = \frac{\lambda \delta x}{r} \cdot \frac{R}{b} \quad \ldots\ldots (5)$$

from which $\delta I_T \leqslant \frac{\mu L R}{3 f_{11} b}$ $\ldots\ldots (6)$

which, for practical values of the variables, gives:

$$\delta I_T \leqslant .000242\ R \quad \ldots\ldots (7)$$

For various curve radii then the allowable range of values of I_T is given in Table 1.

TABLE 1

R = 30m	$0.993 \leq I_T \leq 1.007$
R = 50m	$0.988 \leq I_T \leq 1.012$
R = 100m	$0.976 \leq I_T \leq 1.024$
R = 300m	$0.927 \leq I_T \leq 1.073$
R = 1000m	$0.758 \leq I_T \leq 1.242$

Figures 10 and 11 show that these target values for the tracking index are never even closely approached except at large radii and in areas of the field where the stability is insufficient. It seems then that for any practical truck design, on curves which are of practical interest, the longitudinal creep rate at the wheels will always make excessive demands on the adhesion.

Cross-Bracing Effects

In order to illustrate the effect of cross-bracing some of the results have been cross-plotted. By superimposing the critical velocity curves over those for each of the other parameters it is possible to determine the best achievable value for any of these parameters versus the design critical speed. In general it can be expected that different values will be found for the cross-braced case (above the limit line) than for the more restrictive conventional case.

Figure 18 shows the variation of leading axle

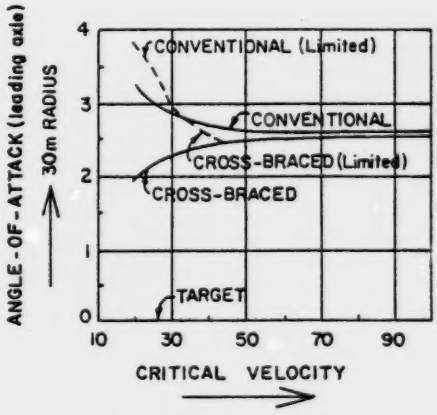

FIGURE 18: TRADE-OFF CURVES ANGLE-OF-ATTACK (DEGREES) 30 M RADIUS

angle of attack with design critical speed for 30m radius curves and 0.2 conicity. It can be seen that in the unlimited case cross-bracing offers a small advantage over the conventional truck as long as the desired critical speed is low. For the case where the value of K_B is limited to the practical region the variations are as shown in the dotted lines. (N.B. the lower limit for K_B was set at 1×10^6 N-m/rad rather than 1.2×10^6 as calculated). It can be seen that in this case there is very little difference between the conventional and the cross-braced trucks at any speed. In neither case does the angle-of-attack approach the desired value of 0.01 deg.

Figure 19 shows similar plots for a curve radius of 300 m. In this case it can be seen that the angle of attack gets steadily worse with increasing design critical speed. It can also be seen that the cross-braced design is very slightly better than the conventional except at very low critical speeds. Also the target value for angle-of-attack can only be reached at very low critical speeds and for the practical region it cannot be reached at all.

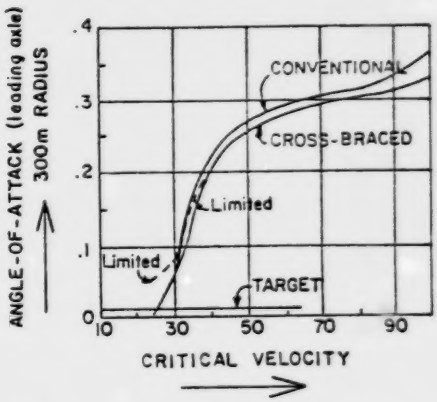

FIGURE 19: TRADE-OFF CURVES ANGLE-OF-ATTACK (DEGREES) 300 M RADIUS

Figure 20 shows similar plots again but this

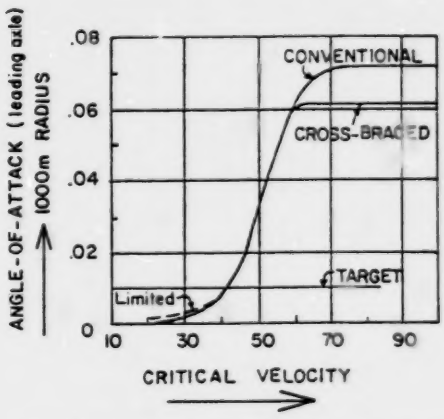

FIGURE 20: TRADE-OFF CURVES ANGLE-OF-ATTACK (DEGREES) 1000 M RADIUS

time for a curve radius of 1000m. In this instance it can be seen that there is very little difference between the two cases except at very high critical speeds where the target value is greatly exceeded for either case.

It was mentioned earlier that the assumption that wheelset inertia remains the same for a cross-braced truck is optimistic. The realistic case would give that design a higher wheelset inertia and thus lower critical speeds. Taking this into account any small advantages which might appear to accrue to the cross-braced design will be reduced or eliminated.

The Paradox Explained

The results obtained in this analysis are apparently paradoxical. We saw earlier that by venturing into the cross-braced area of the K_S - K_B field we could expect to achieve a given value of critical speed with a significantly lower value of K_B. The curving results do not show the improvement in curving behaviour which we might have expected from this. To understand why this is so we must examine more closely the behaviour of wheelsets.

In [6] it is shown that the wheelset lateral force is proportional to the yaw displacement and the yaw couple is proportional to the lateral displacement. For a truck in a curve the axles must take up a position yawed with respect to each other in order to be aligned with curved track. Because there exists an interaxle yaw stiffness, K_B, the axles must develop equal and opposite yaw torques to provide the required deflection. Equal and opposite lateral displacements (leading axle outwards and trailing axle inwards) must occur in order for these torques to be developed. For these lateral displacements to occur the interaxle lateral stiffness, K_S, must be overcome. This means that equal and opposite lateral forces must be developed and this requires yaw displacements of the axles relative to the rail. The leading axle must yaw towards the outer rail and the trailing axle towards the inner rail to produce the required forces. This is in opposition to the direction required to produce alignment.

This explains why the curving behaviour of trucks does not get significantly better when we enter the cross-braced regime of the K_S - K_B field even though we may well be able to operate at lower values of K_B. The increased K_S counteracts the decreased K_B and prevents improved alignment.

CONCLUSIONS

The design criteria which govern the performance of railway trucks are principally the values of K_S and K_B. It can be seen from all of the above that it is advisable to choose values as close to the so-called "limit line" as possible.

The results of this analysis demonstrate quite conclusively that self-steering (the ability of the railway wheelset to align itself to curved track) is only a practical feature in trucks which negotiate very large curve radii. Cross-bracing, whether it be done to achieve K_S - K_B values outside the range available to conventional design, or whether it be done within the conventional range, does not significantly improve the potential performance of the railway truck. Self-steering, or radial action (a description sometimes applied to trucks of this configuration), is therefore a misnomer.

For the same reasons that cross-bracing does not achieve significant improvement in the design of the railway truck it cannot be expected to achieve much in improving the performance of a well designed rigid frame truck as a retrofit modification.

The Effect of Modifying 3-Piece Freight Trucks

The typical North American freight car truck of 3-piece construction holds the axles firmly parallel to one another but is very free to "lozenge". In other words, it has a very high value of K_B and a low value of K_S. This puts it in the lower right hand corner of the K_S - K_B field. It can be seen that from such a position the only way to improve either the critical speed or the curving behaviour (or both of them) is to increase the value of K_S. Addition of cross-bracing will achieve this and thus improve the performance of the truck by improving its critical speed and reducing or eliminating flange forces on large radius curves.

In noting the improvement to be expected in a 3-piece truck by increasing substantially the value of K_S it should also be seen that there is little or no value to be gained from increasing K_S to a point above the conventional limit line. This means that there is no need to obtain the increased K_S through direct axle interconnections, improved truck frame shear stiffness will be just as effective.

It should be noted that the characteristics established in this paper are based on mass and dimension values typical for a small transit vehicle. For a freight car the values would be significantly different and therefore one can expect the absolute values of such items as critical velocity and wheel flange force to be different. It can be expected however, that the same trends will be evident for a freight truck as are true for the model studied here. This has been confirmed, at least in part, by analysis of other truck models.

Alternative Configurations

It has been emphasized throughout that the premise on which all of the analysis and its conclusions are based is that the truck structure is of the conventional form. This means that a truck frame exists to carry the vehicle load out to the axle bearings. The bearings are located close to the wheels and a primary suspension exists which elastically connects the axle bearings to the truck frame.

This sort of model is representative of the physical reality of most railway trucks. For sound structural reasons it is typical practice to mount the axle bearings close to the wheels (either inboard or outboard), this keeps bending moments on the axles to a minimum. The truck frame then spans between the bearings in either an "H" configuration or as two side frames (beams) and a bolster (the 3-piece truck). With this type of construction the practical limits on the achievable value of K_B mentioned here are applicable.

A method of circumventing the problem of providing for the transmission of brake forces is to provide links directly from the axle bearings to the car body. To achieve the required curving results however, these links must not interfere with the ability of the axles to align with the rails or the truck to swivel under the car body. In order to achieve this they would have to be arranged such that one end follows the motions of the axle bearings whilst the other end follows the motions of the car body. This implies a mechanism which applies a steering law between the axles and the car body. Such a mechanism, because of the stiffness required to transmit the braking forces, would enforce the steering law and assure axle alignment. Steering motions would be forced, against any restraint between axle and truck frame.

In such a mechanism the yaw restraint between the axle and the truck frame can be eliminated and there will nevertheless remain a stabilizing influence through the linkage. Elimination of the frame constraint will mean moreover that no force will be required to align the axles with the rails (assuming the truck is free to swivel under the car.) The term guided steering has been coined to distinguish mechanisms which fall into this category from those which require substantial force to be generated in the steering linkage.

Because the steering mechanism introduces an additional stabilizing constraint on the axles and, particularly in the guided steering case, because this stabilizing constraint is independent of the curving behaviour, it can be seen that the traditional curving/stability trade-off no longer exists. Also, because of the direct axle yaw/body yaw connection provided through the steering mechanism a large number of potential new modes of instability exist, somewhat different in nature from those of trucks without body connections.

For the above reasons the behaviour of vehicles with steered axle trucks is dramatically different from those without such provision. The K_S and K_B values, so useful in characterizing the unsteered case, are no longer applicable to the steered one. Instead of just two fundamental axle modes there are now eight. This means that there are eight fundamental interaxle stiffnesses. The chances of characterizing the behaviour of such a system through simple universal parameters seems quite remote. Certainly those used for the unsteered case will not be sufficient.

SUMMARY

We have seen that systems of interaxle connections within a truck do not significantly improve the curving performance which can be achieved. The terms "self-steering" or "radial" are therefore misleading when applied to such trucks. We have also seen that the application of cross-bracing can retrieve a poorly performing design, if the problem is caused by low shear stiffness, but not beyond that which can be achieved with good rigid frame design.

It is clear that if improvements are to be made beyond the potential of the rigid frame truck in the areas of wheel wear, rail wear, noise, energy consumption, etc., through better wheel/rail alignment, they will not be made through interaxle connections or other internal truck modifications. Positive steering of the axles through links to the car body might provide a breakthrough in the quest for improvements. This has been investigated and will be the subject of further reports.

ACKNOWLEDGEMENTS

The authors wish to thank UTDC R&D Ltd. for permission to publish this paper and acknowledge with thanks the support provided by the Natural Sciences and Engineering Research Council of Canada under grant A1615.

REFERENCES

1. Carter, F.W., "On the Action of a Locomotive Driving Wheel", Proceedings Royal Society of London, Series A, Vol. 112, 1926, pp. 151-157.

2. Kalker, J.J., "On the Rolling Contact of Two Elastic Bodies in the Presence of Dry Friction", Doctoral Dissertation, Technische Hogeschool, Delft, Netherlands, 1967.

3. Pollard, M.G., "The Development of Cross-Braced Freight Bogies", Rail International, September 1979.

4. Anderson, R.J., "A Non-Linear, Steady-State Curving Model for Steerable-Axle Railway Vehicles", 10-th IMACS World Congress on System Simulation and Scientific Computation, Montréal, Canada, August, 1982.

5. Smith, R.E. and Anderson, R.. "Properties of Cross-Braced Trucks", Internal Report, Urban Transportation Development Corporation.

6. Newland, D.E., "Steering a Flexible Railway Truck on Curved Track" ASME 69-RR-5. Joint Railroad Conference, Montréal, 1969.

THIS PAGE LEFT BLANK INTENTIONALLY.

APPENDIX B

FRAME-BRACED MODIFICATION PARTS LIST

This appendix contains the parts list for a retrofit kit to fit four sideframe patterns of 100-ton trucks. It accommodates both rod under and rod through brake systems.

APPENDIX B

This appendix contains a complete list of parts necessary to incorporate the modification on one truck. The items with Part Numbers 42-7100-XXX are those designed or modified by UTDC R&D Ltd. Other part numbers are those of commercial suppliers.

UTDC R&D LTD.

FRAME-BRACED FREIGHT TRUCK PARTS LIST

ITEM	QUANTITY	PART NUMBER	DESCRIPTION
		42-7100-040	Installation - Frame Brace
1	4		LC Pad, J12695-8
2	2	42-7100-004	Frame Brace
2-1	1	42-7100-028	Frame Brace Weldment
2-1-2	2	42-7100-000	End Block
3	1		Clamp, HAS128
4	4	42-7100-026	Flat Washer with C'Bore
5	8	CBB 45-1-15	Mounting-Centre Bonded, CBB 45-1-15
6	4	42-7100-003	Flat Washer
7	4		Bolt with Wire Hole, SA253
8	2	42-7100-042	Mounting Brkt Weldment RH
8-1	1	42-7100-044	Channel
8-1-2	1	42-7100-001	Holding Ring
8-2	1	42-7100-043	Base Mounting Brkt Detail RH
9	2	42-7100-041	Mounting Brkt Weldment LH
9-1	1	42-7100-045	Channel
9-1-2	1	42-7100-001	Holding Ring
9-2	1	42-7100-043	Base
10	4	42-7100-033	Support Plate (Bracket)
13	1	42-7100-050	Frame Brace-Upper
14	A/R		Locking Wire-Stainless, SAE 30304

APPENDIX C

TEST PLANS

MASS, MOMENT OF INERTIA, STIFFNESS TESTING

K_s K_b STIFFNESS MEASUREMENT

TEST PLAN
MASS INERTIA AND STIFFNESS MEASUREMENTS OF CERTAIN COMPONENTS OF THE BARBER S-2 TRUCK

REPORT NO.: 42-TP-7100-001

ISSUE NO.: 1

COPY NO.:

RELEASE DATE:

B.H. Willoughby
Originator

Date: 82.10.07

Project Engineer

Date: 82-10-12

Program Manager

Date: 82.10.12

SUMMARY

The accuracy of the computer analyses on the Barber S2 truck depends on the accuracy of the information used to construct the model.

Since mass inertia and stiffness data is apparently not available elsewhere it is planned to obtain this information by direct measurement. It is proposed to use the facilities and equipment, insofar as possible, at the ONR in North Bay, Ontario to gather this information.

This test plan outlines the method proposed to collect this data.

TABLE OF CONTENTS

	TITLE	PAGE
1.0	BACKGROUND	
2.0	PURPOSE	
3.0	EXAMINATION OF APPROACHES	
3.1	Mass	
3.2	Centre of Mass	
3.3	Inertia	
3.4	Stiffness	
4.0	SAFETY CONSIDERATIONS	
5.0	TEST VARIABLES	
5.1	Mass	
5.1.1	Primary Test Variable	
5.1.2	Secondary Test Variable	
5.2	Centre of Mass	
5.3	Mass Moment of Inertia	
5.3.1	Primary Test Variable	
5.3.2	Secondary Test Variable	
5.4	Stiffness Measurements	
5.4.1	Primary Test Variables	
5.4.2	Secondary Test Variable	
6.0	MEASUREMENT OF TEST VARIABLES	
6.1	Mass	
6.2	Mass Moment of Inertia	
6.3	Stiffness Measurements	
7.0	TEST PARAMETERS	
8.0	INSTRUMENTATION CONSIDERATIONS	
9.0	TEST PLAN	
9.1	Mass Measurement	
9.2	Mass Inertia Measurement	
9.3	Stiffness Measurement	
9.3.1	Inter Axle Shear Stiffness	
9.3.2	Inter Axle Bending Stiffness	
9.3.3	Bolster Lateral Stiffness	
10.0	SCHEDULE	

THIS PAGE LEFT BLANK INTENTIONALLY.

1.0 BACKGROUND

Since the mass inertia and stiffness data on the Barber S-2 truck is apparently not available, it was decided to gather this information directly. This data can be obtained by relatively simple lab test methods providing the components to be measured are available in the ONR workshops in North Bay, Ontario.

2.0 PURPOSE

The reason for the requirement of accurate data is to construct a mathematical model and perform a computer analysis of this truck with and without truck frame bracing.

3.0 EXAMINATION OF APPROACHES

3.1 MASS

The method used for mass measurement will be to weigh each component involved.

3.2 CENTRE OF MASS

Each component will be suspended statically from a variety of points to determine the position of the centre of mass.

3.3 INERTIA

Inertia information will be gathered by suspending the components involved and timing the pendulum movements in each of the required planes.

3.4 STIFFNESS

Stiffness data will be obtained by applying a measured force to certain components and measuring displacement obtained by

4.0 SAFETY CONSIDERATIONS

Standard industrial safety practices will be observed.

5.0 TEST VARIABLES

5.1 MASS

5.1.1 Primary Test Variable

- Weight.

5.1.2 Secondary Test Variable

- Unequal weight in different test samples.

5.2 CENTER OF MASS

5.3 MASS MOMENT OF INERTIA

5.3.1 Primary Test Variables

- Distance from fulcrum to mass center.
- Time period of oscillation.

5.3.2 Secondary Test Variable

- Mass center location in different test samples.

5.4 STIFFNESS MEASUREMENT

5.4.1 Primary Test Variables

- Force applied.
- Displacement.

5.4.2 Secondary Test Variable

- Unequal displacements vs force applied in different test samples.

6.0 MEASUREMENT OF TEST VARIABLES

6.1 MASS

- Load cells will be used to weigh the mass in each sample.

6.2 MASS MOMENT OF INERTIA

- Tape measure will be used to measure distance from fulcrum to mass center.
- Stop watch will be used to measure the time period of oscillations.

6.3 STIFFNESS MEASUREMENT

- Applied force will be measured by a load cell located between a hydraulic jack and the component being tested.
- Displacement will be measured by dial gauges.

7.0 TEST PARAMETERS

To avoid possible weather problems with equipment, this test should be carried out indoors.

8.0 INSTRUMENTATION CONSIDERATIONS

The following instruments are required to complete this test.

- Electronic weighing kit
- 10 m measuring tape

- Stop watch
- Dial gauges

9.0 TEST PLAN

9.1 MASS MEASUREMENT

Mass measurement will be obtained from the following sequence of events.

- Weigh kit will be set at zero.
- Load cells will be prepositioned.
- Test component will be lowered onto load cells (see Figure 1 and 2).
- Component will be weighed and the weight recorded.
- Mass center will be calculated from the weight and location of each load cell used.
- Rotate component 90° and repeat for C of G height.

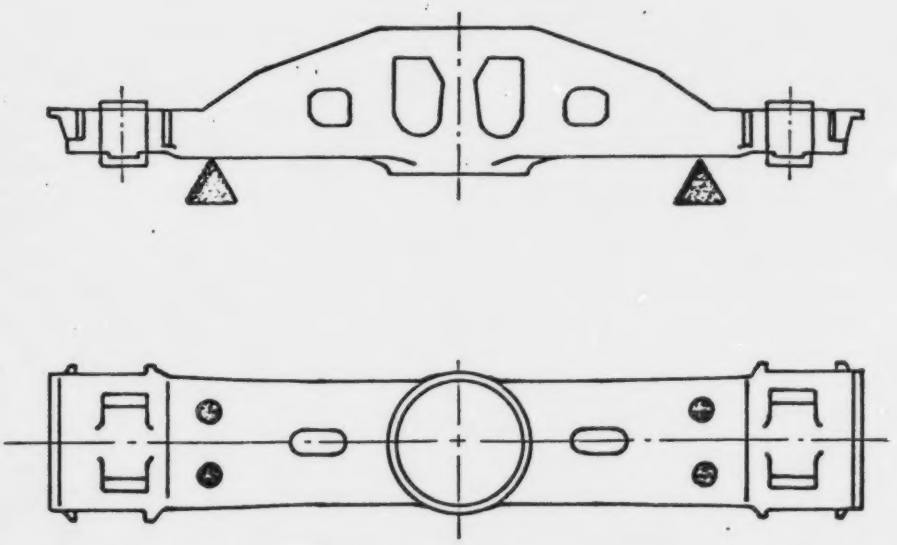

Figure 1

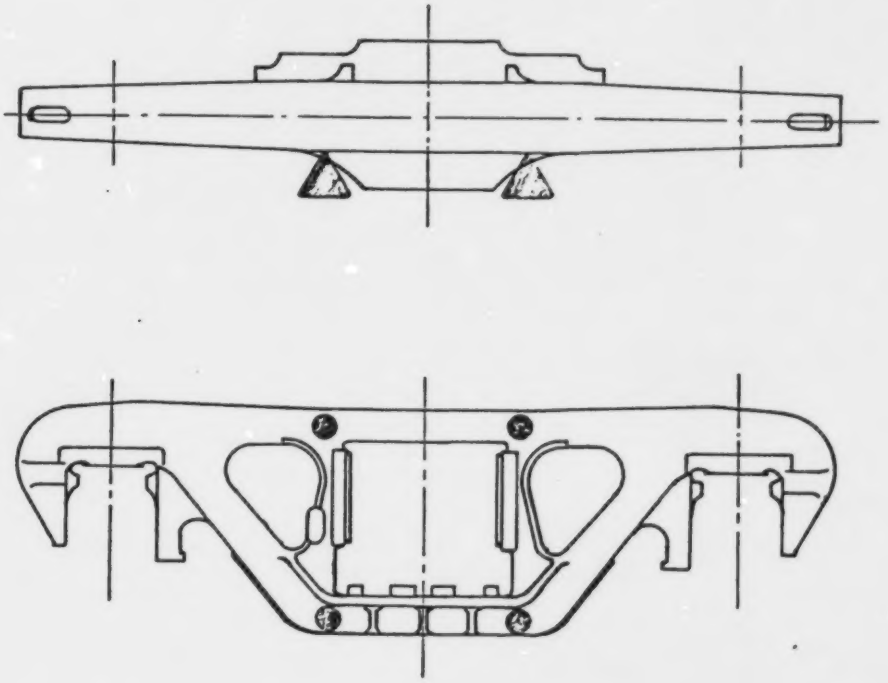

Figure 2
Sideframe Load Cell Locations

9.2 MASS INERTIA MEASUREMENTS

Mass inertia will be obtained from the following sequence of events:

- Calculate mass inertia of pendulum (if necessary).
- Attach component to pendulum (see Figure 3 and 4).
- Measure distance from fulcrum to mass center.
- Time oscillations.
- Calculate mass inertia.

Mass Inertia Test Arrangement

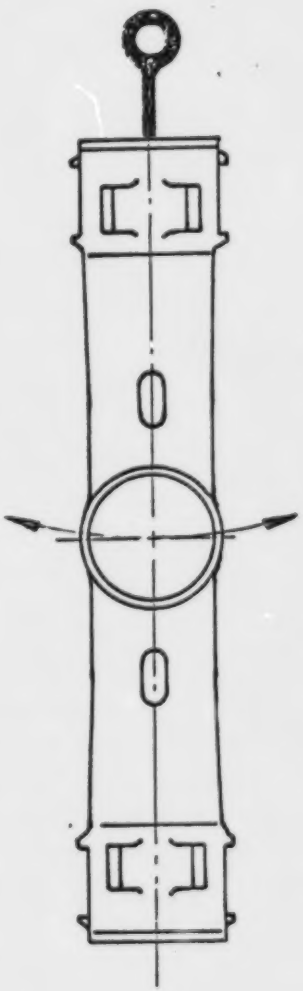

Figure 3
Bolster
(Yaw)

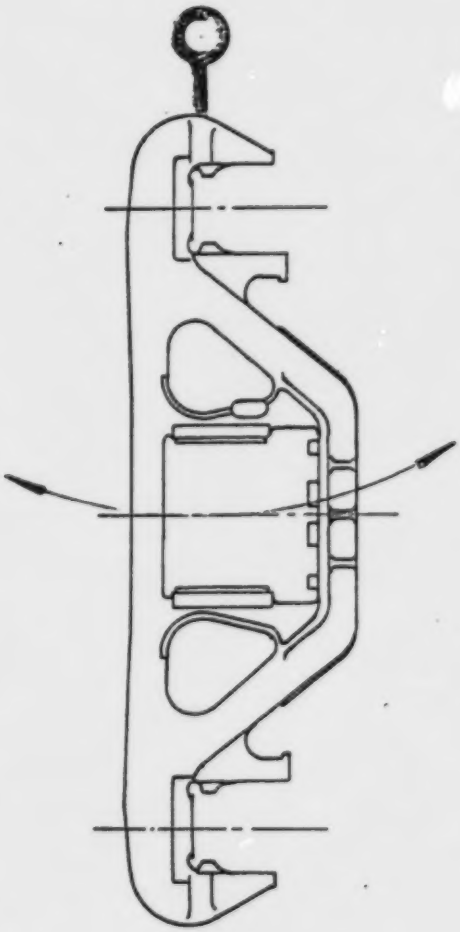

Figure 4
Sideframe
(Yaw and Roll)

9.3 STIFFNESS MEASUREMENTS

9.3.1 Inter Axle Shear Stiffness

- Fix one axle.
- Install roller plates under opposite axle wheels.
- Apply lateral force to opposite axle (1000 lb, 2000 lb, 3000 lb, 4000 lb, 5000 lb).
- Measure displacement at each 1000 lb force.
- Release force to 4000 lb, 3000 lb, 2000 lb, 1000 lb, 0 lb.
- Measure displacement at each force stop.

9.3.2 Inter Axle Bending Stiffness

- Fix one axle.
- Install roller plates under opposite axle wheels.
- Apply longitudinal force to one wheel of opposite axle (1000 lb, 2000 lb, 3000 lb, 4000 lb, 5000 lb).
- Measure displacement at each 1000 lb force.
- Release force to 4000 lb, 3000 lb, 2000 lb, 1000 lb, 0 lb.
- Measure displacement at each force stop.

9.3.3 Bolster Lateral Stiffness

- Apply lateral force to bolster (200 lb increments).
- Measure displacement at each 200 lb between bolster and sideframes.
- Release lateral force to bolster (200 lb increments).
- Measure displacement at each 200 lb between bolster and sideframe.

All of the above to be done with car empty and loaded.

10.0 SCHEDULE

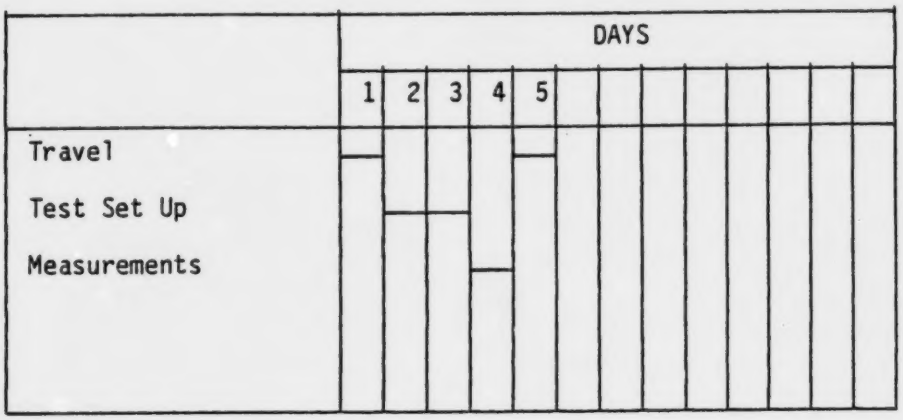

11.0 MATERIAL

Material required for this test will include:

- Load cell interface material.
- Pendulum attachments to test samples.
- Suitable jack.

12.0 LABOUR AND RESOURCES

ONR labour and resources will be utilized as much as possible.

K_s K_b STIFFNESS MEASUREMENT TEST PLAN

Report No.: 42-TP-7100-020

Issue No.: 1

Copy No.:

B. Willoughby

B.H. Willoughby

Originator

Project Engineer

Date: 85.06.26

Project Manager

Date: 26 June/85

REVISIONS

ISSUE NO.	DATE	DESCRIPTION	PAGES AFFECTED
1	85.06.25	NC	-

SUMMARY

Before conducting more line tests with the Barber S-2 trucks modified with UTDC frame bracing, CP Rail have requested K_s and K_b data from frame braced trucks.

Since stiffness data are not available, it is planned to acquire these data at the NRC facilities in Ottawa.

This test plan outlines the method proposed to collect this information.

CONTENTS

SECTION		TITLE	PAGE NO.
		COVER	i
		REVISIONS	ii
		SUMMARY	iii
		CONTENTS	iv
1.0		BACKGROUND	1
2.0		PURPOSE	1
3.0		EXAMINATION OF APPROACHES	1
4.0		SAFETY CONSIDERATIONS	1
5.0		TEST VARIABLES	1
	5.1	Primary Test Variables	1
	5.2	Secondary Test Variables	1
6.0		MEASUREMENT OF TEST VARIABLES	2
7.0		TEST PARAMETERS	2
8.0		INSTRUMENTATION CONSIDERATIONS	2
9.0		TEST PLAN	3
	9.1	Inter-Axle Shear Stiffness	3
	9.2	Inter-Axle Bending Stiffness	3

1.0 BACKGROUND

Since stiffness data on the frame braced Barber S-2 truck are not available, it was decided to gather this information directly. The data can be obtained by relatively simple lab test measurements, using an available frame braced truck atthe NRC facilities in Ottawa.

2.0 PURPOSE

The reasons for gathering the data is to fulfill a request from CP Rail for this information, and to confirm computer calculations.

3.0 EXAMINATION OF APPROACHES

Stiffness data will be obtained by applying a measured force to certain components and measuring the resulting displacement by these forces.

4.0 SAFETY CONSIDERATION

Standard industrial and NRC safety practices will be observed.

5.0 TEST VARIABLES

5.1 PRIMARY TEST VARIABLES

- Force applied;
- Displacement.

5.2 SECONDARY TEST VARIABLE

- Unequal displacements versus force in different test samples;

- Weight of carbody on truck;

- Friction between wheelset, on which force is applied, and the ground.

6.0 MEASUREMENT OF TEST VARIABLES

- Applied force will be measured;

- Resultant displacement will be measured;

- Unequal displacments versus force will be averaged;

- Weight of carbody on truck;

- Low friction devices to be installed under wheelset on which force is applied to eliminate friction between wheels and ground.

7.0 TEST PARAMETERS

To avoid possible weather problems with equipment, this test should be carried out indoors.

8.0 INSTRUMENTATION AND EQUIPMENT CONSIDERATIONS

The following instrumentation and equipment is required for this test:

- Hydraulic jack to apply force to components;

- Dial gauges to measure displacements;

- Load cell to measure applied force;

- 10 m measuring tape;
- Stop watch;
- Low friction devices;
- Tie down equipment (chain tensioner etc.).

9.0 TEST PLAN

9.1 INTER-AXLE SHEAR STIFFNESS (See Figure 1)

- Fix one axle;
- Install low friction device under opposite axle wheels;
- Apply lateral force to opposite axle (1,000 lb, 2,000 lb, 3,000 lb, 4,000 lb, 5,000 lb);
- Measure displacement and record at each stop;
- Release force to 4,000 lb, 3,000 lb, 2,000 lb, 1,000 lb;
- Measure displacement and record at each stop;
- Repeat five times.

9.2 INTER-AXLE BENDING STIFFNESS (See Figure 2)

- Fix one axle;
- Install low friction devices under opposite axle wheels;

- Apply longitudinal force to one end of opposite axle 1,000 lb, 2,000 lb, 3,000 lb, 4,000 lb, 5,000 lb;

- Measure displacement and record at each stop;

- Release force to 4,000 lb, 3,000 lb, 2,000 lb, 1,000 lb;

- Measure displacement and record at each stop;

- Repeat five times.

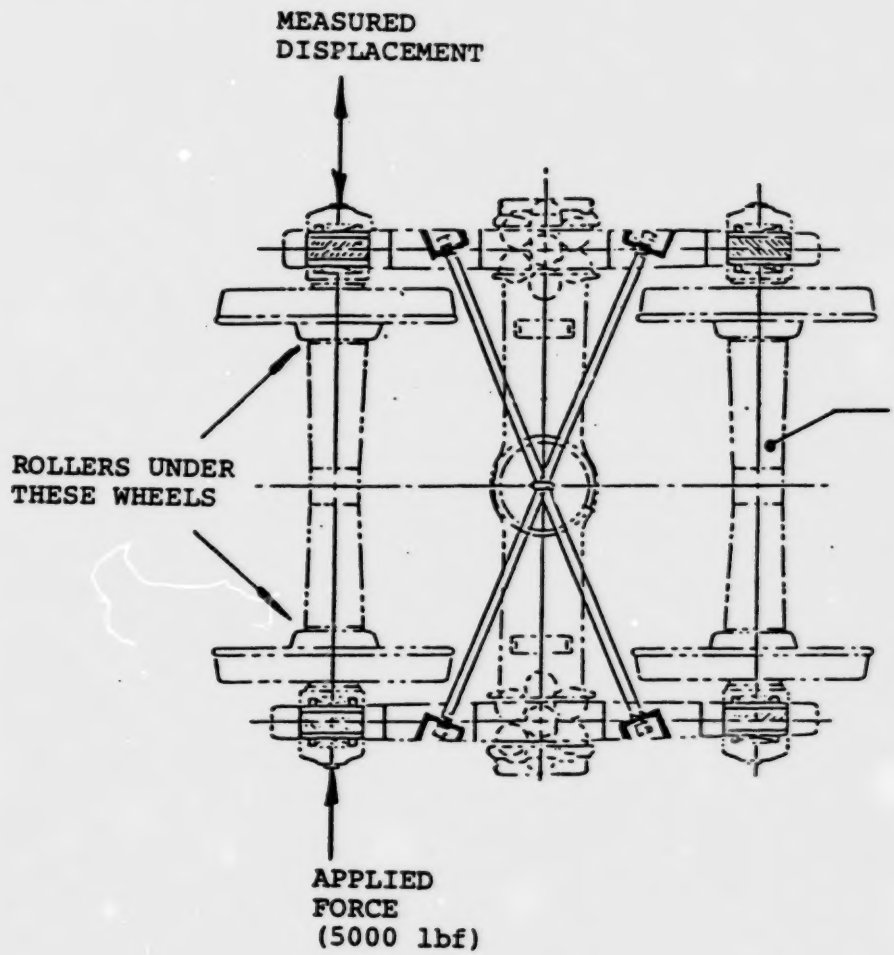
MEASURED
DISPLACEMENT
ROLLERS UNDER
THESE WHEELS
THIS AXLE
HELD RIGID
APPLIED
FORCE
(5000 lbf)

FIGURE 1

APPENDIX D

TEST PLAN

STATIC AND DYNAMIC TESTING OF THE

FRAME BRACED BARBER S-2 FREIGHT TRUCKS

TEST PLAN
STATIC AND DYNAMIC TESTING OF THE FRAME-BRACED BARBER S-2 FREIGHT TRUCKS

REPORT NO.: 42-TP-7100-002

ISSUE NO.: 1

COPY NO.:

RELEASE DATE:

B.H. Willoughby
Originator

Date: 83.02.16

John W. Howard
Project Engineer

Date: 83.02.21

SUMMARY

This test plan was created as a guide for the static and dynamic tests to be carried out on experimental and control trucks to be mounted under a test train consist at the ONTC facilities in North Bay.

Testing will be carried out on a married pair of gondola cars. One car will have experimental truck sets installed and the other will have a controlled truckset. In this report the experimental truck sets are referred to as modified trucks and the control truck sets are referred to as unmodified trucks.

A second married pair of gondola cars will be formed as a back-up if for some unforeseen reason, wheel wear testing cannot be continued on the first pair.

TABLE OF CONTENTS

	TITLE	PAGE
1.0	BACKGROUND	1
2.0	PURPOSE	1
3.0	EXAMINATION OF APPROACHES	1
3.1	Wheel Wear	1
3.2	Dynamic Performance	2
3.3	Modified Truck Structural Integrity	2
4.0	SAFETY CONSIDERATIONS	2
5.0	TEST VARIABLES	2
5.1	Primary Test Variables	2
5.2	Secondary Test Variables	2
6.0	MEASUREMENT OF TEST VARIABLES	3
6.1	Measurement of Primary Test Variables	3
6.2	Measurement of Seondary Test Variables	3
7.0	TEST PARAMETERS	3
7.1	Commissioning	3
7.2	High Speed Empty	4
7.3	High Speed Loaded	4
8.0	INSTRUMENTATION CONSIDERATIONS	4
9.0	TEST PLAN	5
9.1	Test Train Consist	5
9.2	Test Equipment	5
9.3	Commissioning, Low and Moderate Speed Tests	5
9.4	High Speed Empty Test	5
9.5	High Speed Loaded Test	6
10.0	ADDENDA	6
10.1	Schedule	6
10.2	Labour and Resources	6

THIS PAGE LEFT BLANK INTENTIONALLY.

1.0 BACKGROUND

UTDC has proposed a practical method of reducing wheel/rail wear on the Barber S-2 truck. This relatively inexpensive method involves, modifying the truck by:

- o Adding elastomeric pads between the axle bearing housings and the truck sideframes to allow the axles to self steer in curves; and
- o Bracing the sideframes to prevent lozenging of the truck in curves.

2.0 PURPOSE

The primary purpose of these tests is to demonstrate improved wheel wear when the modified truck wheelset wear is compared to the unmodified truck wheelset wear.

The secondary purpose of these tests is to demonstrate:

- o No degradation of dynamic performance of the modified trucks; and
- o No degradation of structural integrity of the modified truck sideframes.

3.0 EXAMINATION OF APPROACHES

3.1 WHEEL WEAR

Wheel profile measurements from modified truck wheelsets will be compared to profile measurements taken from unmodified truck wheelsets with the same aggregate distance travelled.

3.2 DYNAMIC PERFORMANCE

Dynamic performance will be demonstrated by measuring and comparing the performance of a modified truck with an unmodified truck.

3.3 MODIFIED TRUCK STRUCTURAL INTEGRITY

Modified truck frame bracing strain will be measured directly during dynamic testing.

Modified and unmodified truck frame strain will be measured at similar points and compared.

4.0 SAFETY CONSIDERATIONS

Standard industrial and ONTC safety practices will be adhered to.

5.0 TEST VARIABLES

5.1 PRIMARY TEST VARIABLES

The primary test variable is the wheel wear on unmodified and modified truck sample wheels.

5.2 SECONDARY TEST VARIABLES

The secondary test variables are:

- o Lateral acceleration of the leading axle of the modified truck sets, and unmodified truck sets during dynamic testing.

- Lateral accelerations of the leading truck bolster of the modified truck sets and the unmodified truck sets during dynamic testing.

- Strain in the frame-bracing of the leading modified truck set.

- Strain in the sideframe at a brace connection to the sideframe on the leading truck of the modified set and at a corresponding location on the leading truck of the unmodified set during dynamic testing.

6.0 MEASUREMENT OF TEST VARIABLES

6.1 MEASUREMENT OF PRIMARY TEST VARIABLES

Wheel tread/flange profile will be measured and recorded before dynamic tests and periodically throughout the program.

6.2 MEASUREMENT OF SECONDARY TEST VARIABLES

Secondary test variables will be measured during dynamic tests to be carried out after truck set modifications and test train consist is formed.

7.0 TEST PARAMETERS

7.1 COMMISSIONING (AFTER WHEEL PROFILE MEASUREMENT)

Speeds - low to moderate
Location - on or near ONTC North Bay facilities
Direction - forward

7.2 HIGH SPEED EMPTY

Speeds - 40 to 65 mph in 5 mph increments (minimum 5 miles at each speed)
Location - between North Bay and Temagami on ONTC track
Direction - forward

7.3 HIGH SPEED LOADED

Speeds - 40 to 65 mph in 5 mph increments (minimum 5 miles at each speed).
Location - between Kid Creek and Noranda on ONTC track.
Direction - forward

8.0 INSTRUMENTATION CONSIDERATIONS

- Wheel Wear -Tread wear measuring device
- Aggregate Distance -Hubodometer mounted on one axle of each car
- Accelerometers -one lateral 2 g. on modified leading truck bolster
  -one lateral 2 g. on unmodified leading truck bolster.
  -one lateral 100 g. on modified leading truck leading axle.
  -one lateral 200 g. on unmodified leading truck leading axle.
- Strain gauges -one linear mounted on the brace rod, leading truck
  -two rosettes on truck frame near brace bracket weld on modified leading truck
  -two rosettes mounted on truck frame on

unmodified leading truck at corresponding location to modified truck.

- o Power Supplies
- o Recording Equipment
- o Cables and Connections
- o Communication Equipment

9.0 TEST PLAN

9.1 TEST TRAIN CONSIST

The consist will be formed as shown in figure 1.

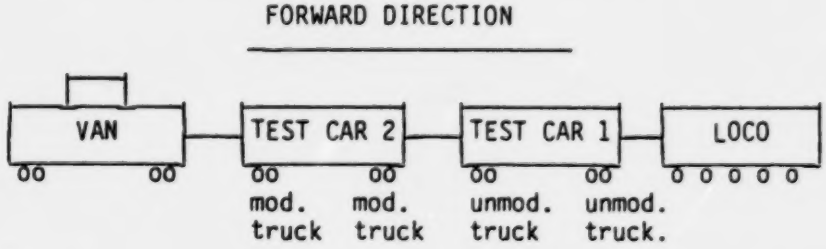

9.2 TEST EQUIPMENT

Test equipment will be installed and calibrated as required.

9.3 COMMISSIONING, LOW AND MODERATE SPEED TESTS

As per 7.1.

9.4 HIGH SPEED EMPTY TEST

As per 7.2.

9.5 HIGH SPEED LOADED TEST

As per 7.3.

10.0 ADDENDA

10.1 SCHEDULE

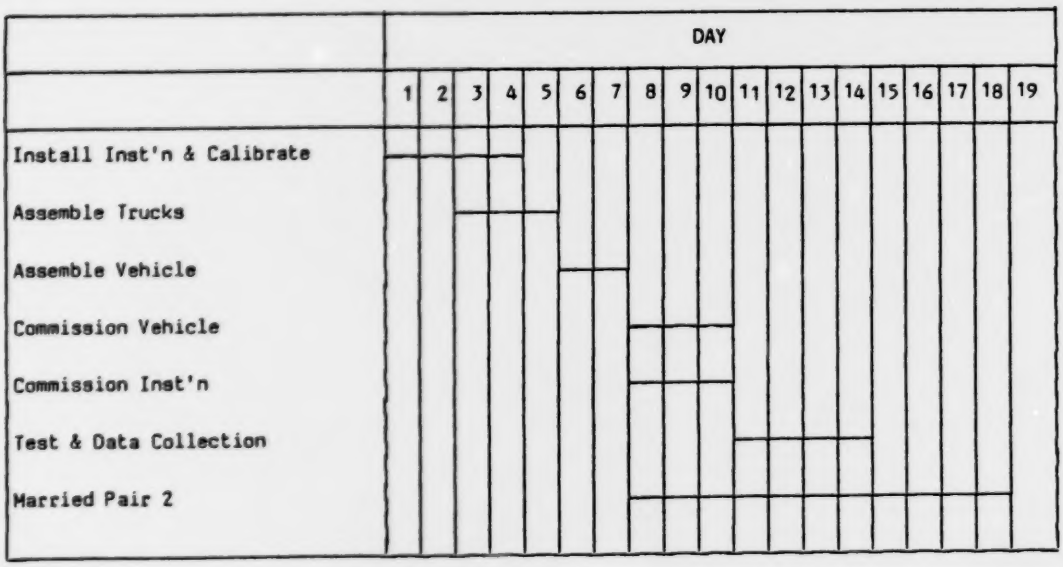
DAY
1 2 3 4 5 6 7 8 9 10 11 12 13 14 15 16 17 18 19
Install Inst'n & Calibrate
Assemble Trucks
Assemble Vehicle
Commission Vehicle
Commission Inst'n
Test & Data Collection
Married Pair 2

10.2 LABOUR AND RESOURCES

ONTC labour and resources will be utilized as much as possible.

APPENDIX E

FATIGUE ANALYSIS OF THE FRAME BRACED TRUCK

FATIGUE TEST OF CROSS BRACED TRUCK

Chadwick
Engineering Ltd

FATIGUE ANALYSIS of

FRAME-BRACED TRUCK
(Barber S-2 100-ton)

Prepared by: T. Martin
T. Martin, Engineer,
Chadwick Engineering.

Approved by: D. Chadwick
D. Chadwick, P. Eng.,
President,
Chadwick Engineering.

Date: 18 July 1983

2D Sherwood Avenue, Amherstview, Ontario K7N 1N2 (613) 384 2866

TABLE OF CONTENTS

1.0	INTRODUCTION	5.
2.0	DESCRIPTION OF MODIFICATION	5.
3.0	DATA COLLECTION	5.
4.0	THEORY OF FATIGUE	8.
5.0	FAILURE CRITERIA	10.
6.0	EVALUATION OF ENDURANCE LIMIT	11.
7.0	SPECIFICATION OF ENDURANCE LIMIT	14.
8.0	STATIC DATA ANALYSIS	15.
9.0	DYNAMIC DATA ANALYSIS	19.
9.1	Stress Range and Frequency	21.
10.0	LIFE CALCULATIONS - Cumulative Fatigue Damage	21.
11.0	RECOMMENDATIONS	24.
12.0	CONCLUSIONS	26.

LIST OF FIGURES

Figure 1	FRAME-BRACED TRUCK RETROFIT	6.
Figure 2	FRAME-BRACE BRACKET/GAUGE LOCATION & GEOMETRY	7.
Figure 3	STRESS-CYCLE RELATIONSHIP FOR FERROUS METALS	9.
Figure 4	MODIFIED GOODMAN DIAGRAM	10.
Figure 5	FACTORS OF SAFETY	20.
Figure 6	MANSON'S METHOD	23.

LIST OF TABLES

Table 1	STRAIN ROSETTE READINGS - Static Tests	15.
Table 2	TRUE STRAIN STATES - Static Tests	16.
Table 3	PRINCIPAL STRAINS - Static Tests	17.
Table 4	PRINCIPAL STRESSES - Static Tests	18.
Table 5	von MISES STRESSES - Static Tests	19.
Table 6	DYNAMIC TEST - Data Reduction.	22.

1.0 INTRODUCTION

The standard 3-piece freight truck has almost no shear stiffness between its side frames. This allows the truck to parallelogram when negotiating curves, producing large angles of attack between the axles and the rails. This results in poor performance and high wheel and rail wear rates. This low shear stiffness also degrades the dynamic performance of the truck. The UTDC patented frame-bracing significantly increases this shear stiffness and enhances truck performance while reducing the wheel/rail wear rates.

This report presents a fatigue analysis of the side frame in the area of the Modification, using data collected from tests on the Ontario Northland Railway.

2.0 DESCRIPTION OF MODIFICATION

The General arrangement of the frame-braced Modification is shown in Figure 1. Two rods span diagonally between four rod attachment brackets welded to the side frames. The diagonal rods are connected to the brackets through rubber bushings to allow for angular motion due to side frame pitching. The standard cast bearing adapter is augmented by a rubber covered steel pad.

3.0 DATA COLLECTION

Data used in this report was gathered by UTDC Technicians during tests run on the Temagami subdivision of the Ontario Northland Railway. Two test sections were used; one from Mile 30 to Mile 43, and the second from Mile 52 to Mile 62.5. Testing was performed on two, 100-ton, Barber Model S-2 Trucks; one with the Modification and one 'as is'. The tests were run with the trucks mounted on both empty and fully-loaded Gondola cars. Data was collected in the form of strip-charts calibrated so that strains could be read directly.

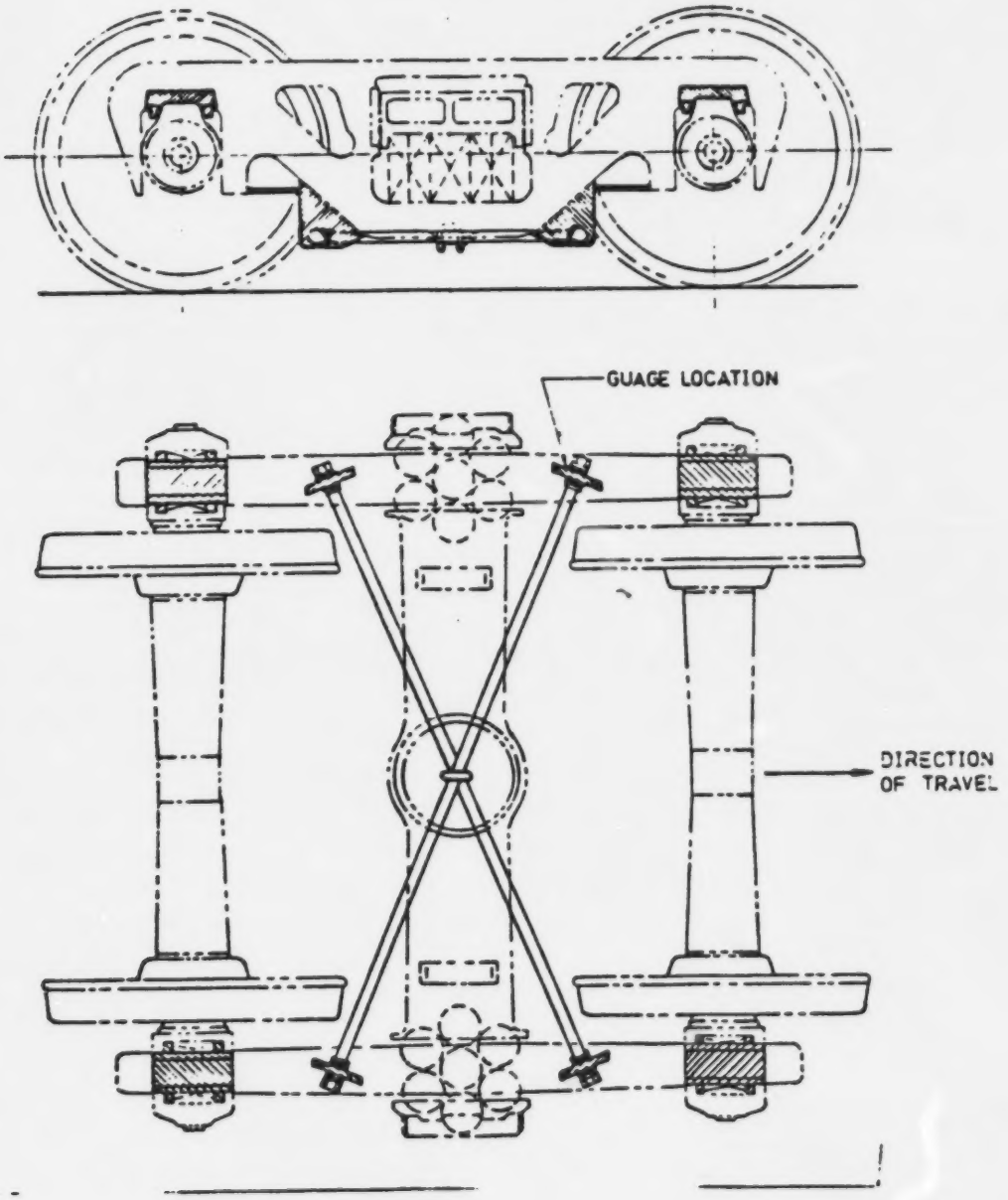

FIG. 1 : FRAME-BRACED TRUCK RETROFIT

Two strain gauge rosettes, were fixed to both a modified and unmodified truck. Each rosette consists of three strain gauges at 45° to one another. In all cases, the gauges were fixed to the forward area of the left-hand sideframe of the lead truck. The location and orientation of the gauges is as shown in Figure 2

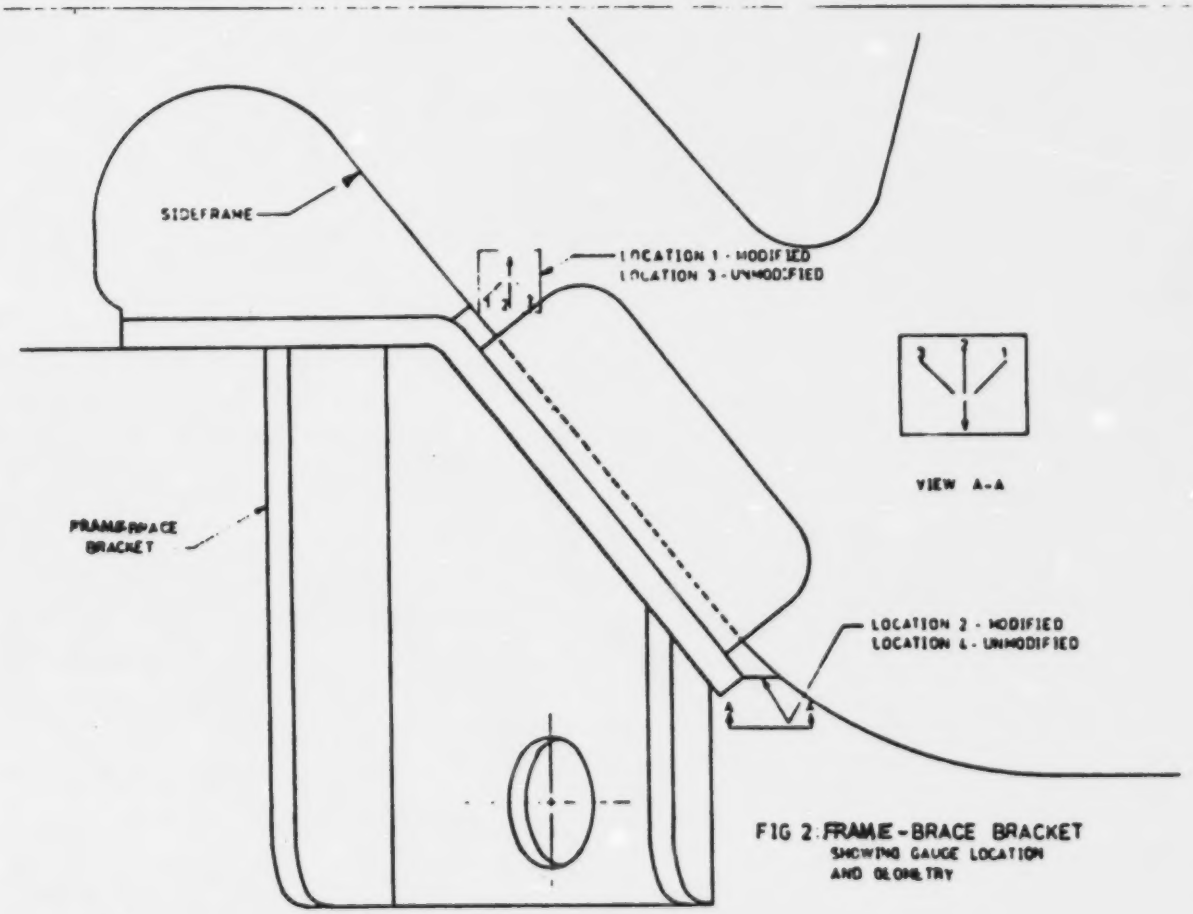

FIG 2: FRAME-BRACE BRACKET SHOWING GAUGE LOCATION AND GEOMETRY

The individual gauges in the rosettes are identified by the numbers 1, 2 and 3 as shown in Figure 2. The rosette location and truck are identified as shown.

1. - modified truck upper location
2. - modified truck lower location
3. - unmodified truck upper location
4. - unmodified truck lower location

The individual gauge, location and truck are indentified by a two digit number formed from the previous identification digits.

For example:

42. - unmodified truck, lower location
gauge #2 in the rosette.

4.0 THEORY OF FATIGUE

Fatigue is a low stress failure that occurs when a member is subjected to cyclic loading. Although the exact mechanism by which failure occurs is not known, empirical relationships have been developed for design purposes. The term endurance limit results from the fact that ferrous materials do not fail by fatigue when stesses are kept below a certain level. The general relationship between stress and cycles to failure is shown in Figure 3.

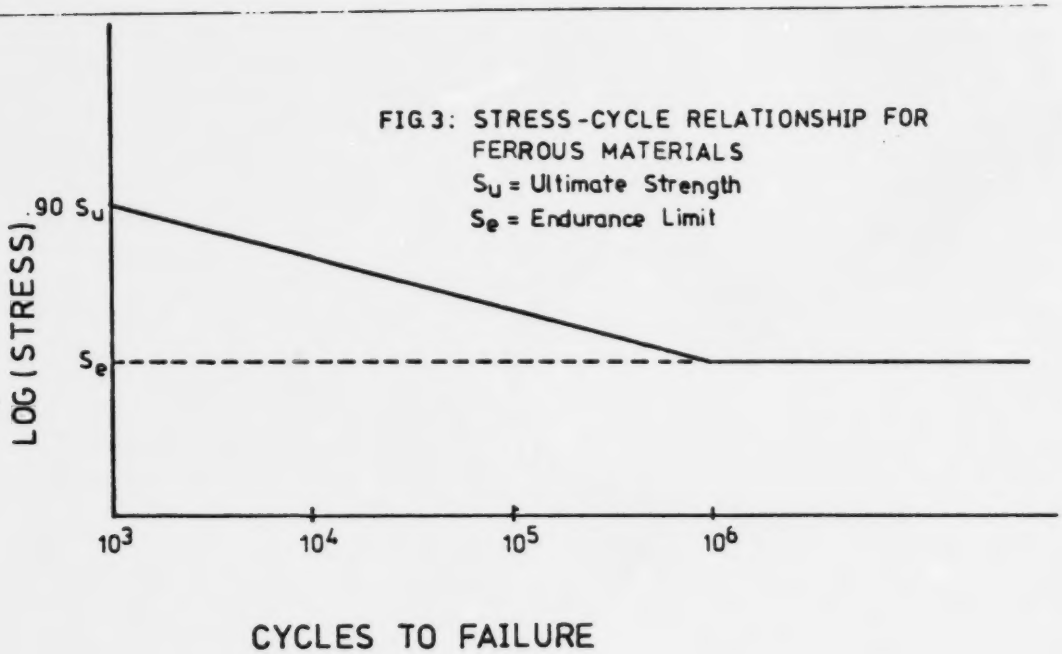

FIG.3: STRESS-CYCLE RELATIONSHIP FOR FERROUS MATERIALS
S_u = Ultimate Strength
S_e = Endurance Limit

Any member that is subjected to complete reversal of stress at a peak stress lesss than the Endurence Limit ,Se, will not fail in fatigue.

When a cyclic load is superimposed over a static load, the allowed stress level, although dependant on Se, is not limited by it. The relationship is best described by a graphical construction known as a modified Goodman Diagram, Figure 4, where the shaded area represents the safe zone.

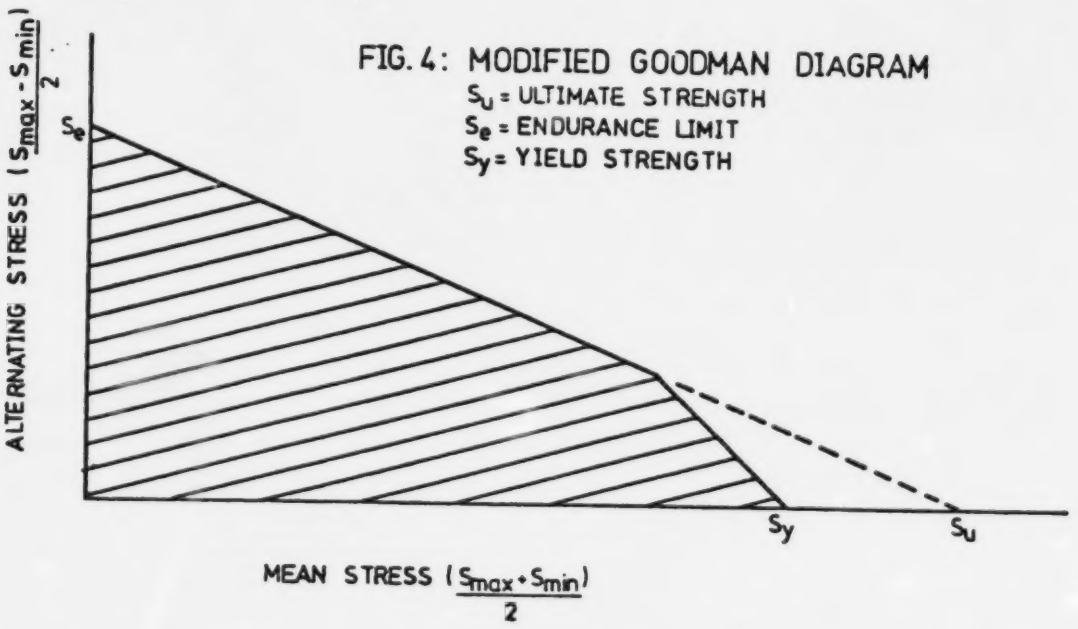

FIG. 4: MODIFIED GOODMAN DIAGRAM
S_u = ULTIMATE STRENGTH
S_e = ENDURANCE LIMIT
S_y = YIELD STRENGTH

Any load which results in combination of a mean and alternating stress in this zone will be unlikely to fail through fatigue. This relationship applies only to a member whose mean stress is tensile.

5.0 FAILURE CRITERIA

The stress used to evaluate the fatigue properties of the member is developed from the maximum normal stress by the distortion energy theorem. For a two-dimensional stress element with maximum normal stresses & , the stress produced by this theory (known as the von Mises stress) is given by the relation:

$$\sigma' = \sqrt{\sigma_1^2 - \sigma_1 \sigma_2 + \sigma_2^2}$$

This method produces results closest to those found by experimentation.

6.0 EVALUATION OF ENDURANCE LIMIT

A method of arriving at the endurance limit, Se, from the ultimate strength Su, of the material has been developed empirically and proven in practice. It should be noted, however, that because the pattern of fatigue failures for a sample of given Su assumes a Weibull distribution, a failure is still possible when calculations indicate an adequate margin of safety. It is therefore a recommended practice to quote factors of safety at some given level of reliability.

The endurance limit for a particular element is developed from the endurance limit of a rotating-beam specimen through a series of factors that take into account size, surface finish, etc. The generally accepted method of determining the limit for the rotating beam specimen is:

For Su = 1380 N/mm^2 (200,000 psi)
Se = 0.5 Su

And For Su = 1380 N/mm^2 (200,000 psi)
Se = 690 N/mm^2

ENDURANCE LIMIT MODIFICATION

The endurance limit for a particular specimen is developed from Se' by the relation:

$$Se = kakbkckdkekfSe'$$

where
- Se' = endurance limit of rotating-beam specimen
- Se = endurance limit of mechanical element
- ka = surface factor
- kb = size factor
- kc = reliability factor
- kd = temperature factor
- ke = stress concentration factor
- k_f = miscellaneous factor(s)

1. **Surface Factor-** fatigue cracks will start from small defects in the surface of a member. These small defects serve to concentrate stresses in the area in which they occur. They range from a value of 1.0 for a polished surface, to as low as .20 for a high-strength forging. For both the modified and unmodified truck, a factor of .65 will be used.

2. **Size Factors-** larger members will have a more linear stress distribution, resulting in faster propogation of fatigue cracks. The factors generally accepted are:

- kb = 1.0 for $d \leq$ 8mm where 'd' is section depth
- kb = .75 - .90 for d 8mm $< d <$ 50mm
- kb = .60 - .75 for $d \geq$ 50mm

3. Reliability Factor- In order to account for the statistical spread in the rotating beam specimens, a reliability factor is included. For convenience, the distribution is assumed normal, and testing has shown that a standard deviation of 8% is a reasonable assumption. The factor ke is developed from the relation:

$$kc = 1.0 - 0.08Zr$$

where Zr is a standardized variable corresponding to a given reliability. For a reliability of .99,Zr = 2.326, & kc = .814. Because there will be less consistency in welds a value of kc for the modified construction of .702 will be used, corresponding to a reliablility of .9999, (ie., one in ten thousand)

4. Temperature Factor- Materials yield more easily at higher temperatures. Because of this, a temperature factor for steels of:

$$kd = 620/(460 + T), \qquad T > 160°F \text{ is assumed.}$$

Because the member under consideration will be operating at less than 160°F, kd =1.0

5. Stress Concentration Factor- Large scale discontinuities (ie. welds, changes in section, etc.,) result in localized areas of high stress. The effect of these discontinuities is dependant on two factors; one is the theoretical stress concentration factor Kt, which is dependant on geometry, and the other is the sensitivity of the material to notches q. The actual stress concentration factor, Kf, is given by:

$$Kf = 1 + q(Kt-1)$$

If conservative results are desired, (or q is uncertain) the full theoretical stress concentration factor is recommended. For the modified member, Kf =1.5 to 2.0 is generally accepted for fillet welds resulting in ke = 1/Kf =.5 to .67 (The higher stress concentration will be used in this analysis.) For the unmodified member ke = 1.0.

6. Miscellaneous Effects- This factor is intended to take into account such things as residual stresses, directional characteristics, corrosion and surface treatments (ie. case-hardening, plating, etc.) For the members under consideration kf will be taken as being 1.0.

Caution:

The factors developed above represent statistical averages of observed data. It is always accompanied by the caution that results of tests are preferred under all circumstances. There are simply too many variables involved to give truly accurate values of the endurance limits of particular specimens.

7.0 SPECIFICATION OF THE ENDURANCE LIMIT

Dofasco recommends using an endurance limit for the side frame material, cast steel, Grade 'B', AAR Spec M-210 of 110 N/mm^2(16000psi). This includes modifying factors for surface (.65) and reliability (.70). For a member of this size, an additional modifying factor (kb = .70) must be included. This gives a fatigue limit of 77N/mm^2 for the unmodified member. When the stress concentration factor for the fillet weld is included (.50), the fatigue limit for the modified member becomes 38.5 N/mm^2(5600psi). These are conservative values, but, because of the nature of fatigue, failure at stress levels that are calculated to be safe are still possible.

8.0 STATIC DATA ANALYSIS

Table 1. lists results from the static tests conducted.

TABLE 1 - STRAIN GAUGE READINGS, STATIC TEST

	STRAIN ($\mu\epsilon$)							
Location	1		2		3		4	
Load condition	L(Load)	E(Empty)	L	E	L	E	L	E
Gauge #1	-40	-8	-12	-3	-45	-8	-23	-3
Gauge #2	25	3	-33	-5	-11	-2	-17	-6
Gauge #3	80	13	-12	-3	100	20	-23	-3

In order to be of use, these strain readings must be transformed to the actual strain experienced at the gauge location. The formulae for this transformation are:

$\epsilon_x = \epsilon_3$ (Strain at gauge 3)

$\epsilon_y = \epsilon_1$ (Strain at gauge 1)

$$\gamma_{xy} = 2\epsilon_2 - (\epsilon_1 + \epsilon_3)$$

where γ_{xy} is the shear strain

Results from this transformation are listed in Table 2.

TABLE 2 - TRUE STRAINS, STATIC TESTS

	STRAIN ($\mu\epsilon$)							
Location	1		2		3		4	
Load condition	L	E	L	E	L	E	L	E
ϵ_x	80	13	-12	-3	100	20	-23	-3
ϵ_y	-40	-8	-12	-3	-45	-8	-23	-3
γ_{xy}	10	1	-42	-4	-77	-16	12	-6

TRANSFORMATION TO CONDITIONS OF MAXIMUM NORMAL STRESS

As listed, the results in Table 2 reflect the strain state at an orientation of 45° to the direction of the strain gauge (see Figure 2). This is not, however, the peak normal strain, which occurs when the shear strain is zero. These maximum strains are given by the equation:

$$\epsilon_{1,2} = \frac{\epsilon_x + \epsilon_y}{2} \pm \sqrt{\left(\frac{\epsilon_x - \epsilon_y}{2}\right)^2 + \left(\frac{\gamma_{xy}}{2}\right)^2}$$

Results from the application of this to Table 2 are listed in Table 3 along with the angle of orientation of ϵ_1, which is given by:

$$\phi = \text{Tan}^{-1}\left(\frac{\gamma_{xy}/2}{\frac{(\epsilon_x - \epsilon_y)}{2}}\right)$$

TABLE 3 - PRINCIPAL STATIC STRAINS

Location	1		2		3		4	
Load condition	L	E	L	E	L	E	L	E
ε_1 ($\mu\varepsilon$)	80	13	9	-1	110	22	-17	0
ε_2 ($\mu\varepsilon$)	-40	-8	-33	-5	-55	-10	-29	-6
φ	2.4°	1.4°	-45°	-45°	-14°	-15°	45°	-45°

These principle strains may be transformed to principle stresses by the relation:

$$\sigma_1 = \frac{E}{1-\nu^2}\left(\varepsilon_1 + \nu\varepsilon_2\right)$$

where E = YOUNG'S MODULUS
$= 207 \times 10^3 \ N/mm^2$
ν = POISSON'S RATIO
$= .265$

The results of this calculation are listed in Table 4. The angle ϕ, in this case, represents the rotation from the axes of the strain gauge (in a clockwise direction).

TABLE 4 - PRINCIPLE STRESSES, STATIC TESTS

Location		1		2		3		4	
Load condition		L	E	L	E	L	E	L	
∇_1	N/mm	15.5	2.41	0	-.52	21.4	4.28	-5.5	-
	(psi)	(2240)	(350)	(0)	(-75)	(3100)	(620)	(-800)	(-5
∇_2	N/mm	-4.14	-1.03	-6.83	-1.17	-5.73	-.93	-7.45	-
	(psi)	(-600)	(-150)	(-990)	(-170)	(-830)	(-135)	(-1080)	(-2
φ	Degrees	47°	46°	0°	0°	31°	30°	90°	

CALCULATION OF MISES STRESS

The Mises stress results from use of the maximum distortion energy theorem of failure. This is given by:

$$\nabla' = \sqrt{\nabla_1^2 - \nabla_1 \nabla_2 + \nabla_2^2}$$

This formula yields results that are closest to experimental data. These results are listed in Table 5.

TABLE 5 - MISES STRESS, STATIC TEST

Location		1		2		3		4	
Load condition		L	E	L	E	L	E	L	E
∇'	N/mm	17.9	3.04	6.83	1.03	24.8	4.83	6.69	1.24
	(psi)	(2600)	(440)	(990)	(150)	(3600)	(700)	(970)	(180)

INTERPRETATION OF RESULTS

Because most fatigue failures start from zones in tension, location 2 & 4 may be assumed to be safe. In addition, stresses at these points show many inconsistencies. Analysis will therefore be concentrated on a comparison of stresses at locations 1 & 3.

9.0 DYNAMIC DATA ANALYSIS

It has been assumed that the Mises stress at the gauge points may be scaled directly from the strains by taking the ratio of dynamic strain over static strain and multiplying by the static stress. This was made necessary because gauges 11 and 33 were not functioning during the dynamic tests. The transfer equations used are:

TRUCK/LOCATION 1

$$\text{MISES STRESS} = \frac{\text{PEAK STRAIN}}{80} \times 17.9 \text{ N/mm}^2$$

TRUCK/LOCATION 3

$$\text{MISES STRESS} = \frac{\text{PEAK STRAIN}}{-45} \times 24.8 \text{ N/mm}^2$$

Because of the orientation of the rosette used at locations 1 and 3, gauge 1 in the rosette is perpendicular to the principle stress direction, and gauge 3 is parallel to this direction. Because of this orientation of gauges the level of confidence in the scaled stresses is not high. Development of factors of safety are drawn from the modified Goodman diagram. We have assumed a constant mean stress, and will define the factor of safety as, $n = \frac{S_a}{\sigma_a}$, where S_a is the maximum allowable stress for infinite life with a mean stress of σ_m. This is illustrated in Figure 5.

FIG 5: FACTORS OF SAFETY

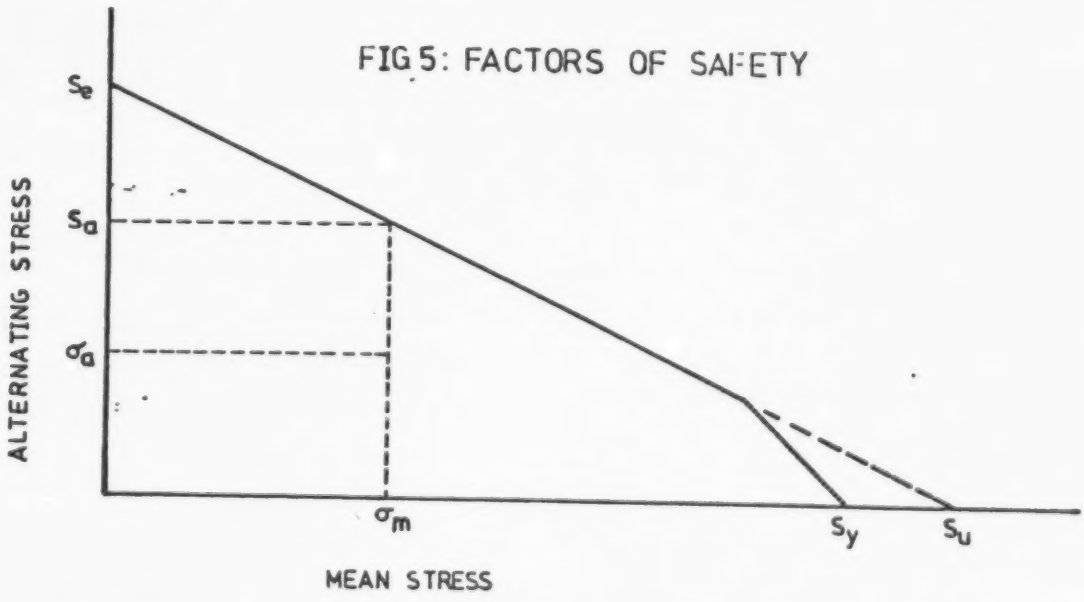

Table 6, Dynamic Analysis-Data Reduction, has been arranged to allow rapid comparisons to be made between the modified and unmodified trucks for a variety of track geometries and speeds. In general, factors of safety were significantly higher for the unmodified truck, due entirely to the stress concentrating effect of the transverse weld. It should also be noted that no allowance was made for residual tensile stresses in these welds. It has been assumed that these stresses will be relieved by heat treatment.

9.1 Stress Range and Frequency

The strip charts from the dynamic tests show there are two principal frequencies of vibration in the system. The lower frequency appears to be the dominant one, causing much higher strains than the high frequency component. It is this lower frequency that is recorded in Table 6. It should be noted that all stresses observed occur at a frequency that requires infinite fatigue life to avoid failure. Strains for the high frequency (approx 20Hz) component appear to be in the range of 3 to 5 μE, or 150 psi, not high enough to cause damage in the side frame.

10.0 LIFE CALCULATIONS - CUMULATIVE FATIGUE DAMAGE

When a member is subjected to a level of stress that is outside the envelope of the modified Goodman diagram, the life expectancy of the member is reduced by an amount that depends on the ratio n/N, where n is the number of cycles experienced at stress level , and N is the number of cycles required to produce a fatigue failure. When this overstressing is repeated at several different levels, failure will eventually occur. The criterion that is most often used to determine cycles-to-failure is known as Miner's Rule, and, expressed mathematically, this is:

$$n1/N1 + n2/N2 + \ldots\ldots ni/Ni = C$$

where the constant C is determined by experimentation and has usually been found to be in the range:

$$0.7 \leq C \leq 2.2$$

For random loading, most authorities recommend using C = 1.

TABLE 6 - DYNAMIC TEST DATA, Data Reduction

Track Geometry	Rosette location and Truck Configuration	Speed (mph)	Peak Strain (με)	Mises Stress N/mm² (psi)	Factor of Safety	Mile Marker	Frequency (Hz)	Load Condition
6° CL (curve left)	1	40	30	6.73 (975)	5.5	32	1.35	Loaded 100 ton
	3		-10	5.52 (800)	13.1			
Tangent	1	40	30	6.73 (975)	5.5	33	1.35	Loaded
	3		-25	13.8 (2000)	5.25			
6° CR (curve right)	1	40	80	17.9 (2600)	2.1	35	1.35	Loaded
	3		-50	27.6 (4000)	2.6			
Tangent	1	50	40	8.97 (1300)	4.2	37	1.7	Loaded
	3		-20	11.0 (1600)	6.6			
2° CL	1	60	10	2.24 (325)	16.6	39	2.0	Loaded
	3		-15	8.28 (1200)	8.75			
Tangent	1	61	35	7.86 (1140)	4.7	40.5	2.0	Loaded
	3		-20	11.0 (1600)	6.6			
6° CR	1	40	80	17.9 (2600)	2.1	52.5	1.35	Loaded
	3		-45	24.8 (3600)	2.9			
6° CR	1	40	110	24.8 (3600)	1.5	54.5	1.35	Loaded
	3		-45	24.8 (3600)	2.9			
4° CR	1	50	60	13.5 (1950)	2.8	58.5	1.7	Loaded
	3		-35	19.3 (2800)	3.8			
4° CR	1	58	90	20.2 (2930)	1.8	61	2	Loaded
	3		-55	30.4 (4400)	2.4			
6° CR	1	40	40	8.97 (1300)	4.2	35	1.35	Empty
6° CR	1	40	50	11.2 (1625)	3.5	35	1.35	Empty
Tangent	1	50	20	4.48 (650)	11.1	35.7	1.7	Empty

Unfortunately, Miner's Rule has not been verified by experiment for two important points. First, the theory states that the static strength Su is decreased because of the application of the overstress. Experiments show no such decrease. Secondly, Miner's Rule does not take into account the order in which stresses are applied, and therefore ignores any stress less than Se0, the endurance limit of the virgin material. A graphical approach, known as Manson's Method, has been developed to deal with these deficiencies and is shown in Figure 6, where Se1, represents the endurance limit of the specimen after overstressing.

FIG. 6: MANSON'S METHOD

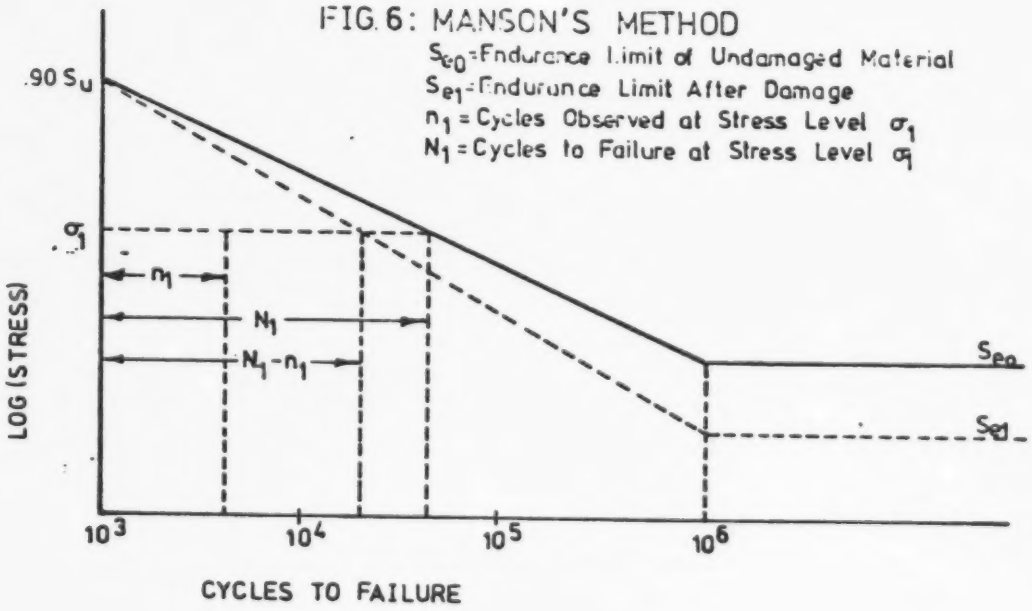

In addition, **Manson's Method** results in a lower value of Sel, & is therefore more conservative than **Miner's Rule.**

The results produced by either method cannot be considered complete and accurate solutions, but function as guides only. The problem of cumulative damage has not been completely solved, and both methods are simply approximations of experimental results. There has been no approach reported that is in consistent agreement with experiment.

Because analysis of the member under consideration here shows no such over-stressing there will be no cumulative damage experienced in the side frame material at the rosette locations.

11.0 RECOMMENDATIONS

i) When applying strain gauges to a structural member it is almost impossible to determine the point of maximum stress unless the member geometry is rather simple and the loading is well defined. In a complex structure subject to loads which are not well defined some method must be used to locate the areas of high stress and determine the direction of this stress so that the strain gauge location and orientation can be determined.

The most popular method to accomplish this is to apply a thin coat of brittle lacquer to the surface of the member. This lacquer can be formulated to crack at specific levels of strain. The member is loaded causing the lacquer to crack. The area were cracks first appear is the area of maximum stress. The gauge orientation is defined since the cracks will be perpendicular to the direction of maximum strain.

We recommend that this method be used to ensure that the strains measured are indeed the maximum strains in the area of interest.

ii) The fatigue life of structural joint is very dependant on the joint geometry and means of connection. In this case, welding is the only practical means to make the connection between the frame-brace bracket and the sideframe, and, the most practical joint, results in the use of fillet welds. In general, fillet welds result in larger stress concentration than full penetration groove welds. The analysis shows that these fillet welds will result in an adequate fatigue life of the structure but the fatigue life could be improved with some modifications.

We recommend that all fillet welds perpendicular to the principal direction of strain be eliminated. In all other fillet welds, the weld surface should be smooth and blend with the structure. Care should be taken at the ends of the welds to ensure all craters are filled and the ends also blend with the structure.

iii) We recommend an analysis be done to determine if the joint side plate is required. We suspect this plate is redundant and could be eliminated resulting in a smoother stress flow and longer fatigue life.

12.0 CONCLUSIONS

The modified member has an infinite fatigue life with a factor of safety of 1.5 for the worst loads recorded. This is to be compared to the unmodified member which has a factor of safety of 2.4 (all factors of safety quoted are at a reliability of .9999 ie., 1 sample in 10,000 will have a lower endurance limit). It is probable that, through previously recommended changes, a stress concentration factor of 1.2 to 1.5 can be achieved. This would result in factors of safety of 2.3 to 2.7, assuming stress levels remain constant. It is more probable that stresses will be slightly higher, and a factor of safety of 2.0 to 2.4 is more likely.

The stresses and factors of safety relate to gauge locations only. These locations are not necessarily the points of highest stress, and safety factors could be lower than those quoted above at some other location.

NS NORFOLK SOUTHERN

The Thoroughbred

FATIGUE TEST OF CROSS BRACED TRUCK

DESIGNED BY
UTDC RESEARCH & DEVELOPMENT, LTD.

Research & Tests Laboratory
Alexandria, Virginia

August 1985
Revised October 15, 1985

FATIGUE TEST OF CROSS BRACED TRUCK
DESIGNED BY UTDC RESEARCH & DEVELOPMENT, LTD.

I. Introduction -

This report covers fatigue testing of side frames modified by application of cross bracing rods, as shown on UTDC R&D Drawing 42-7100-078 (Attachment A).

Two side frames were tested simultaneously:

(1) A 100-ton Grade B side frame cast by American Steel Foundries in March 1963, Pattern No. 22052-D.

(2) A 100-ton Grade C quenched and tempered side frame, cast by Scullin Steel in August 1973, Pattern No. 8358-A

The test side frames were selected from storehouse stock of used side frames, and were sent to the Burlington Northern for application of the cross bracing brackets. The Grade B side frame was tested in the as-welded condition without heat treatment; the Grade C casting was tempered after welding by Buckeye Steel Castings Company.

II. Test Procedure -

The purpose of this test was to simulate the combinations of vertical load and the cross brace load input to detect any possible fatigue problems which could be produced by multiple load application in the area of the cross brace brackets.

Attachment B shows the test set-up. Two vertical 100,000# cylinders were used to apply a total load range of 50,000 to 190,000# in a sinusoidal wave form at a frequency of 0.65 Hz. The maximum 190,000# load represents 156% of the static load based on 263,000# gross rail

loading. Pieces of steel tubing were used in place of truck springs to reduce the pump capacity requirements to produce the required loading. No friction wedges or side springs were installed.

The cross bracing system was exercised by applying a longitudinal load to the corner of the Grade B side frame, while the Grade C side frame was held secure. The Grade B side frame was allowed to move longitudinally on nylatron pads under the pedestals, but were restrained from moving laterally.

Strain gages were applied to the cross brace rods to measure tension and compression. The longitudinal cylinder was operated on a "stroke control" sine wave cycle which produced a maximum cross brace rod tension of 9,000#. A frequency of 0.10 Hz on the longitudinal cylinder with a stroke of 1-3/8" was chosen as the optimum test condition. This was the maximum frequency which could be sustained on this cylinder without exceeding oil capacity of the system, and being out of phase with the vertical cylinders exposed the side frames to a full range of load combinations. Attachment C illustrates the recorded rod forces for a full cycle of vertical and longitudinal force combinations.

The bolts securing the cross brace rods to the side frames were tightened to 200 ft.lbs. per manufacturer's recommendations. Tightening the bolts was found to cause a 600# tensile preload in the rods.

III. Test Results and Conclusions -

The side frames were loaded as described for a total of 1,000,000 vertical load cycles and 153,750 longitudinal load cycles.

At the end of the test, a visual inspection of the side frames was made, paying particular attention to the welds at the cross brace brackets. The welds of the brackets to the side frame were sound, as were the welds joining the bracket sub-assemblies. Failure was noted, however, on several welds securing the washer to the bracket (see photograph, Attachment D). In one location, a crack initiated in the weld and propagated to the edge of the bracket. The location and condition of each of the washer welds is as follows, as related to the geographical position of the side frames in the test fixture, and with 12:00 being vertical:

Grade B (South) Side Frame -

SE Inside: 7:00 weld cracked 100%.
10:00 weld cracked 1/4".
2:00, 4:00 welds O.K.

SE Outside: 2:00, 4:00, 10:00 welds O.K.
8:00 weld cracked 100%.

SW Inside: 8:00, 11:00 welds O.K.
2:00 weld cracked 100%.
4:00 weld cracked 100% with crack propagated into bracket plate to edge of plate.

SE Outside: All welds O.K.

Grade C (North) Side Frame -

NE Inside: 11:00 weld cracked 1/4".
All other welds O.K.

NE Outside: 4:00 weld cracked 1/4".
All other welds O.K.

NW Inside: All welds O.K.

NW Outside: All welds O.K.

Temperature of the rubber bushings was monitored during the test, and was found not to rise above ambient during the testing.

Torque of the cross brace bolts was checked with a torque wrench after testing was complete. Torque to rotate three of the bolts was in excess of 200 ft.lbs.; the fourth was rotated at 150 ft.lbs.

In summary, the modified side frames passed the fatigue test satisfactorily with the exception of the welds of the washers to the bracket.

ATTACHMENT A

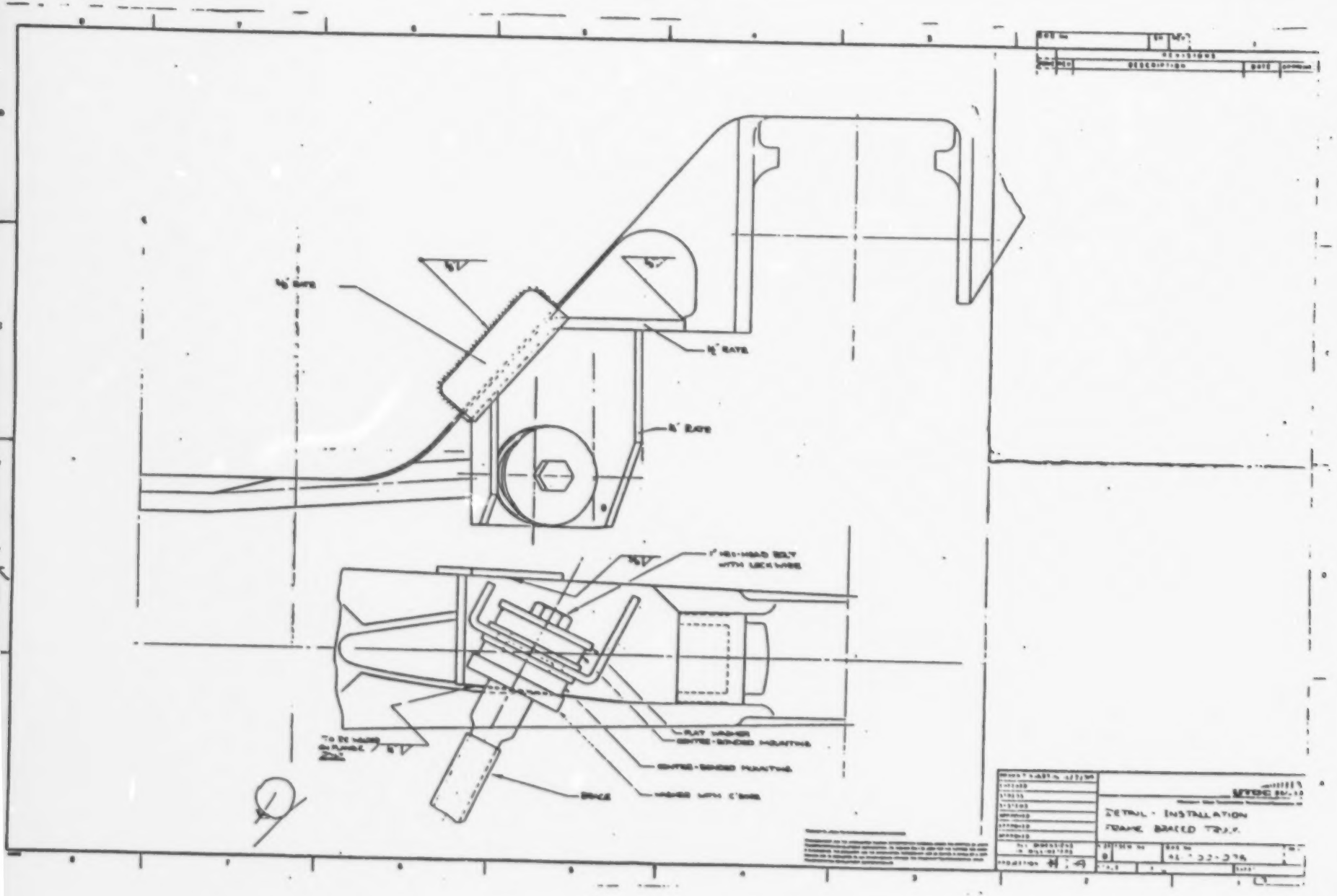

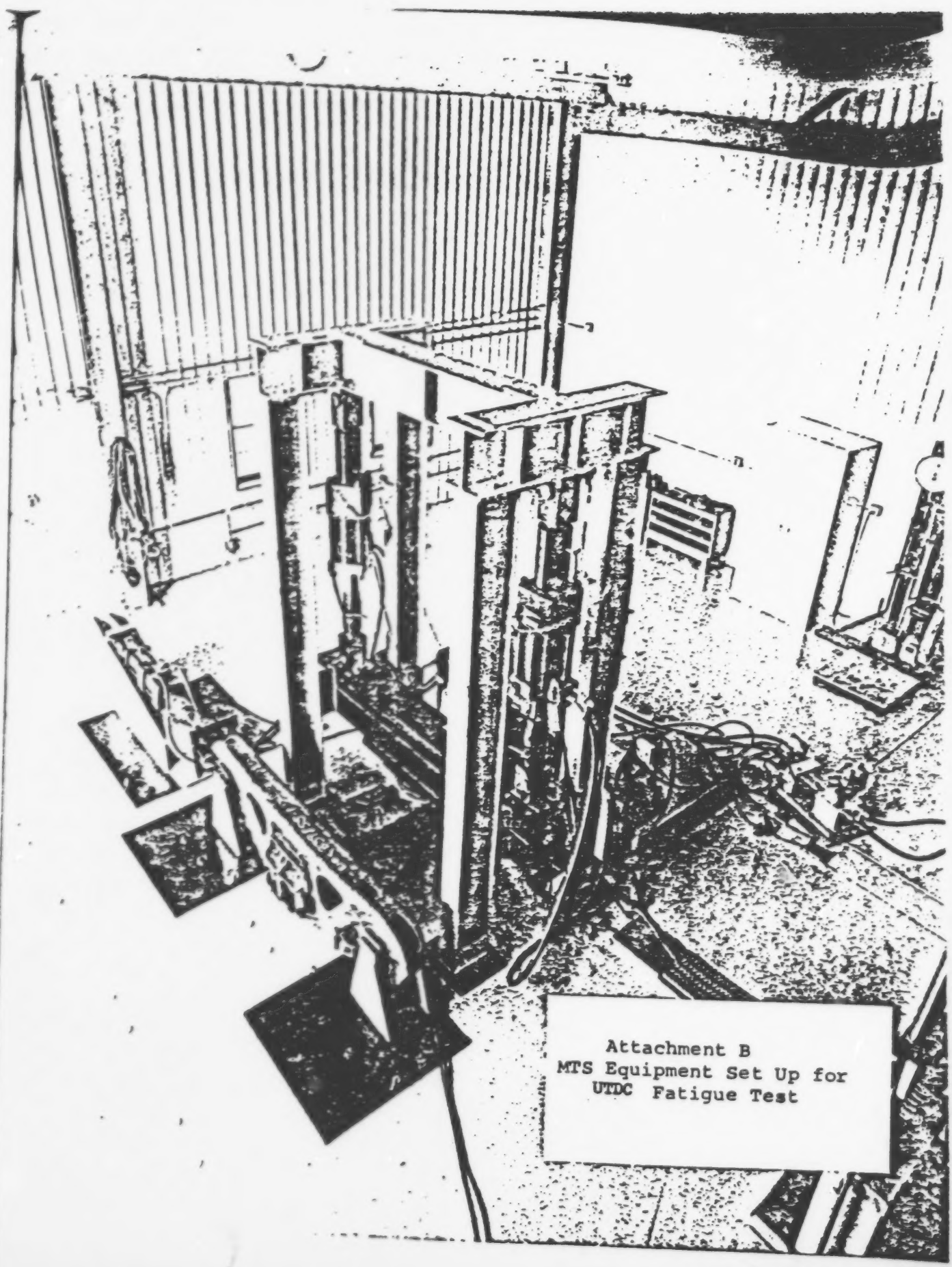

Attachment B
MTS Equipment Set Up for
UTDC Fatigue Test

Attachment C
Typical Load Pattern on Cross Rods

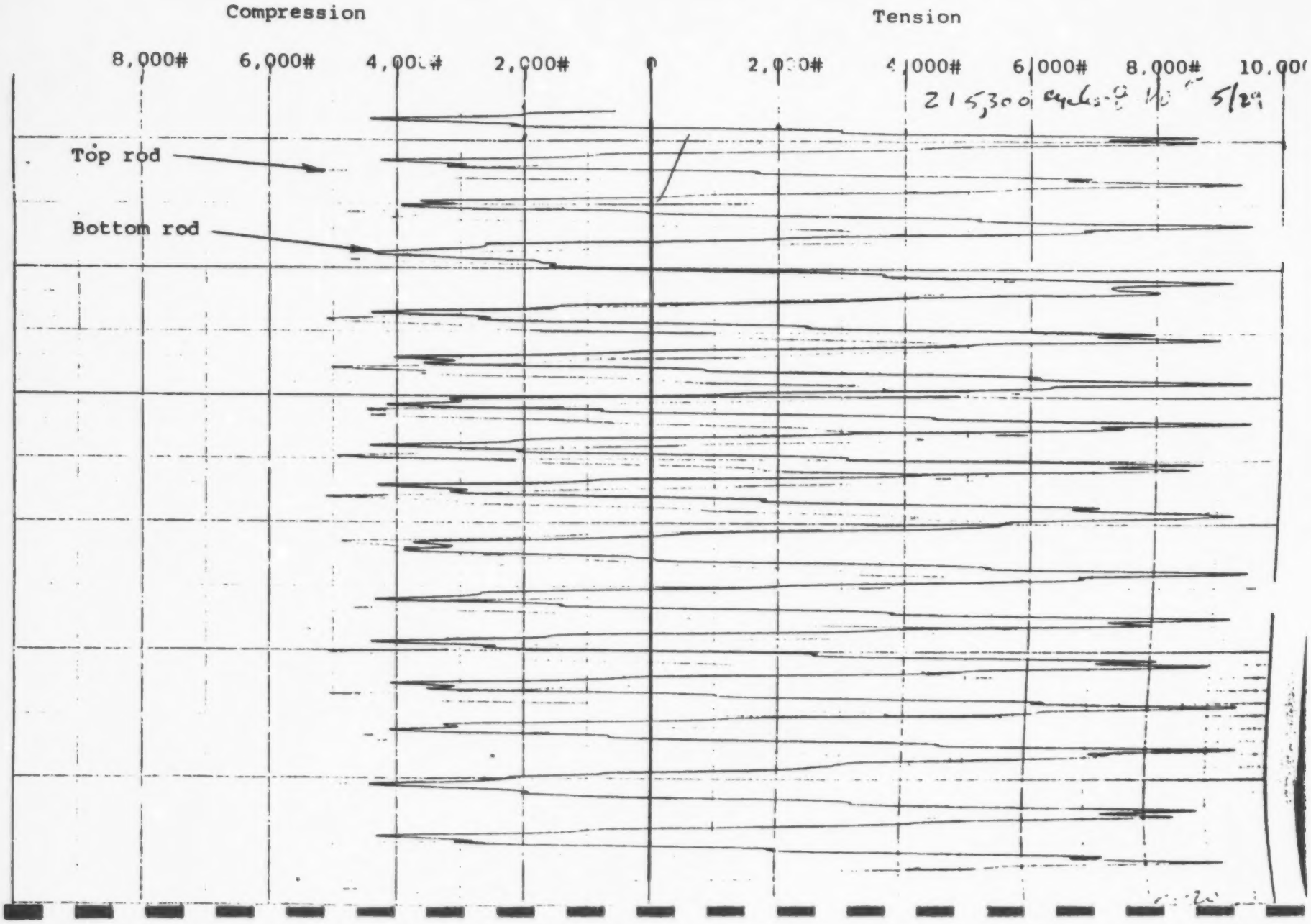

ATTACHMENT D

Arrow indicates crack of weld securing washer to bracket.
Red and white appearance is caused by dye penetrant.

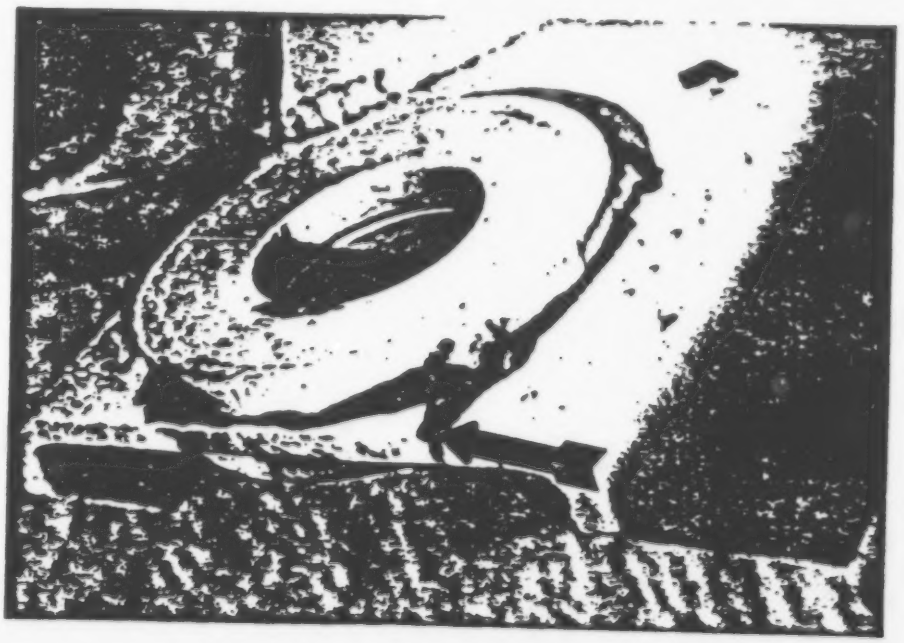

Inside SW, 4:00 location, showing crack (arrow) originating in weld,
which progressed to edge of bracket.

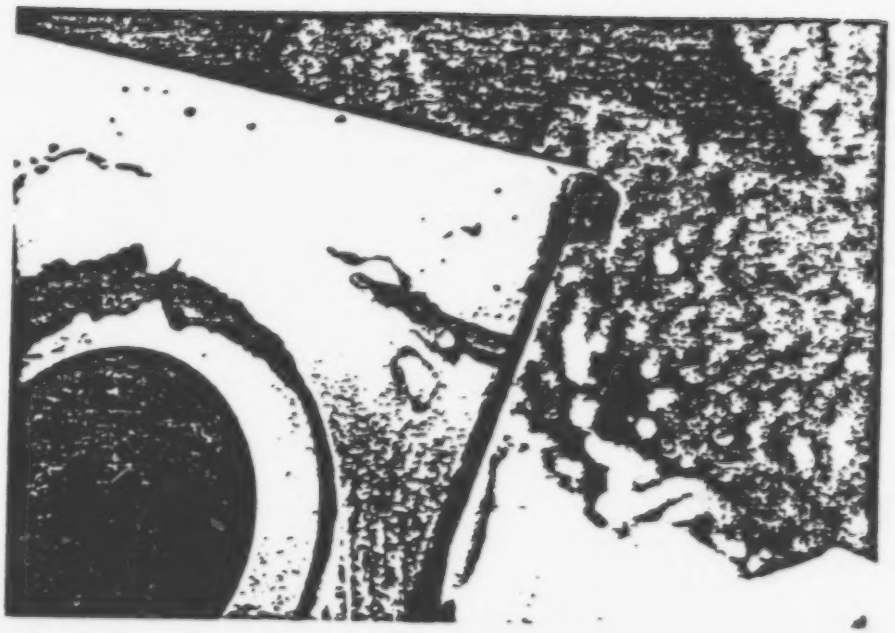

Inside SW, 4:00 location, with washer removed.
Note crack in plate did not progress to inside toward hole.

APPENDIX G

RESULTS

OF THE

STABILITY AND CURVING

ANALYSES

APPENDIX G
RESULTS OF STABILITY AND CURVING ANALYSIS

This appendix contains the results of the dynamic stability and curving performance computer analyses carried out for the 100 ton gondola car used in this project. Those results are shown graphically in Figure G-1 through G-12.

The stability results are shown in Figure G-1. This plot shows curves of constant critical speed against shear stiffness (k_s) and bending stiffness (k_B). The dashed curves represent constant sideframe-to-bolster torsional stiffness: a combination of the normal bolster/spring cluster/sideframe stiffness plus the effects of the frame braces. The upper left region remains blank since no practical results can occur in that region using an unconnected axle set truck design.

The plot itself shows that the higher attainable critical speed is slightly more than 37.5 m/s (84 mi/hr) for log k_s greater than 6.5 and for log k_B between 6.4 and 6.9. This represents a k_s of 3.16×10^6 N/m (18000 lb/in) and K_B between 2.51×10^6 and 7.94×10^6 N/m (14300 and 45300 lb/in).

Because this program was hardware oriented, the availability of hardware to approach the required theoretical stiffnesses determined the actual point on the plot where the frame braced truck could perform. The shear and bending stiffnesses were determined from:

$$k_s = \frac{b^2\, kx\, ky}{a^2\, Ky + b^2\, kx + \frac{2a^2b^2kxky}{K_t}}$$

$$k_B = b^2\, kx$$

where b = ½ the sideframe separation
a = ½ the truck wheelbase
k_x = primary longitudinal stiffness
k_y = primary lateral stiffness
k_T = bolster-sideframe torsional stiffness

The torsional stiffness K_T of the sideframe is calculated as:

$$K_T = K_{s-b} + K_b \frac{(2C_1C_2)}{(2C_1)^2 + (2C_2)^2}$$

where K_{s-b} is the torsional stiffness of the sideframe-to-bolster connection;
k_B is the tensile stiffness of the brace;
C_1 is the longitudinal distance between the bolster centre and the brace attachment bracket centre; and
C_2 is the lateral distance from the truck centre to the brace attachment bracket centre.

The results of the analyses of both the conventional truck and the frame-braced are shown in the table below.

	K_s (N/m)	KB (N/m)
Conventional	$10^{5.5}$	10^{8}
Frame-Braced	$10^{6.25}$	$10^{6.64}$

TABLE G-1: VALUES OF SHEAR AND BENDING STIFFNESS - FREIGHT TRUCKS

Placing these points on Figure G-1 shows a value of critical speed for the conventional truck as off the scale in the lower right corner and less than 22.5 m/s (49.5 mi/hr). Conversely, the critical speed for the frame braced trucks would be

between 27.5 and 30 m/s (60.5 and 66 mi/hr). The actual critical speeds should be higher because frictional damping at the sideframe/bolster interface has not been included in either the conventional or the frame-braced linear analysis.

The curving analysis produced results (Figure G2 - G12) form of:

- angle of attack;
- tread wear index; and
- flange wear index

Applying the values of K_S and K_B as shown in Table G-1, the angle of attack predicted for the conventional truck occur at the extreme lower right corner of each plot.

The conventional angle of attack (Figures G-2, G-3) would be greater than 0.55 degrees for a concity of 0.05 and a curve of 300 m radius, greater than 0.08 for the curve of radius 1000 m. The frame-braced truck would achieve angles of attack less than 0.35 deg on the 300 m curve and near 0.06 deg on the 1000 m curve, improvements of 25% or more.

For a conicity of 0.2, Figures G-4 and G-5 show improvements of 30 percent and more on curves of 300 m and 1000 m radius.

For the tread wear index, Figures G-6 and G-7 show that the conventional truck predictions are 70+ N and 5.00+ N respectively while for the frame-braced truck they are 35.00 N and slightly greater than 3.00 N, improvements exceeding 30%.

At a conicity of 0.2, the improvements (Figures G8, G9) are in excess of 20 percent.

For the flange wear index, the results in Figures G-10 and G-11 show 140 N and more than 27.5 N for the conventional truck on 300 m and 1000 m radius curves for a wheel conicity of 0.05 while predictions for the frame-braced truck are less than 90 N and near 16 N respectively showing improvements in excess of 25%.

For a wheel concity of 0.2 and a curve radius of 300 m (Figure G-12) and improvement in performance exceeds 30%. There is no predicted flange contact for either the frame-braced trucks or the conventional truck on a 1000 m radius curve.

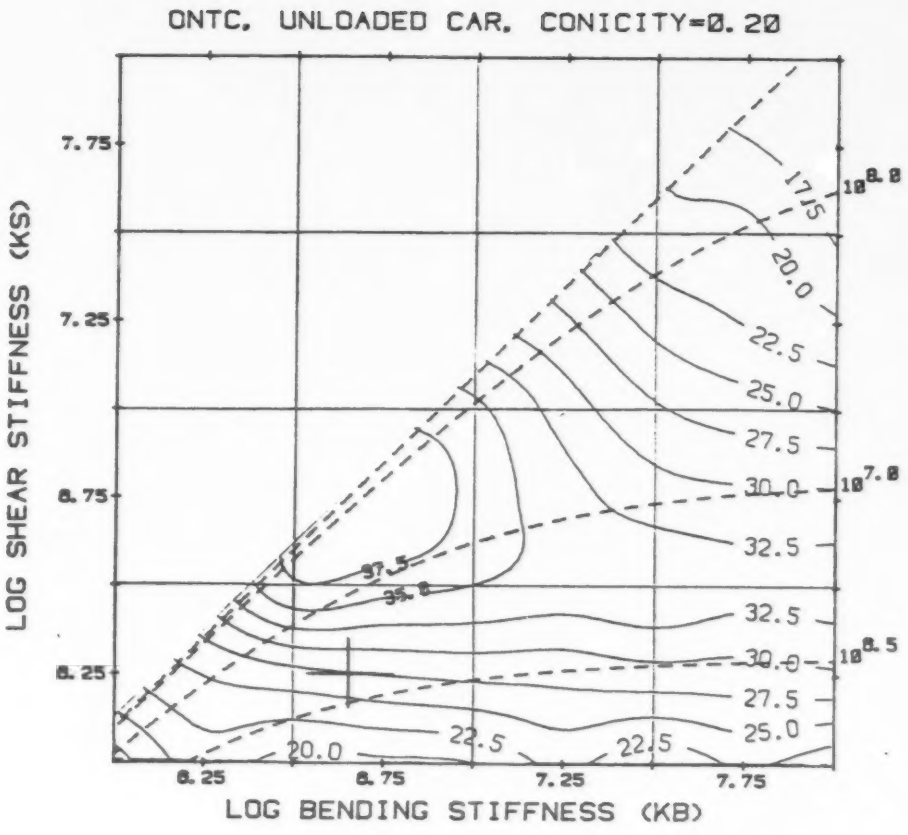

FIGURE G-1: CRITICAL SPEED VS. K_S/K_B

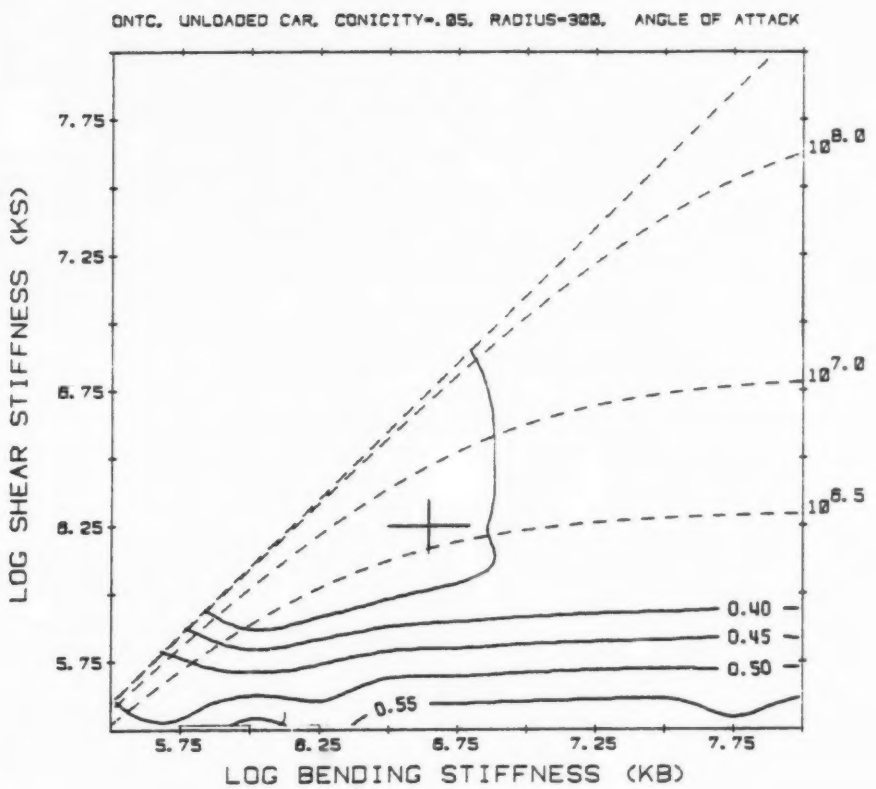

FIGURE G-2: ANGLE OF ATTACK, 300 M RADIUS CURVE

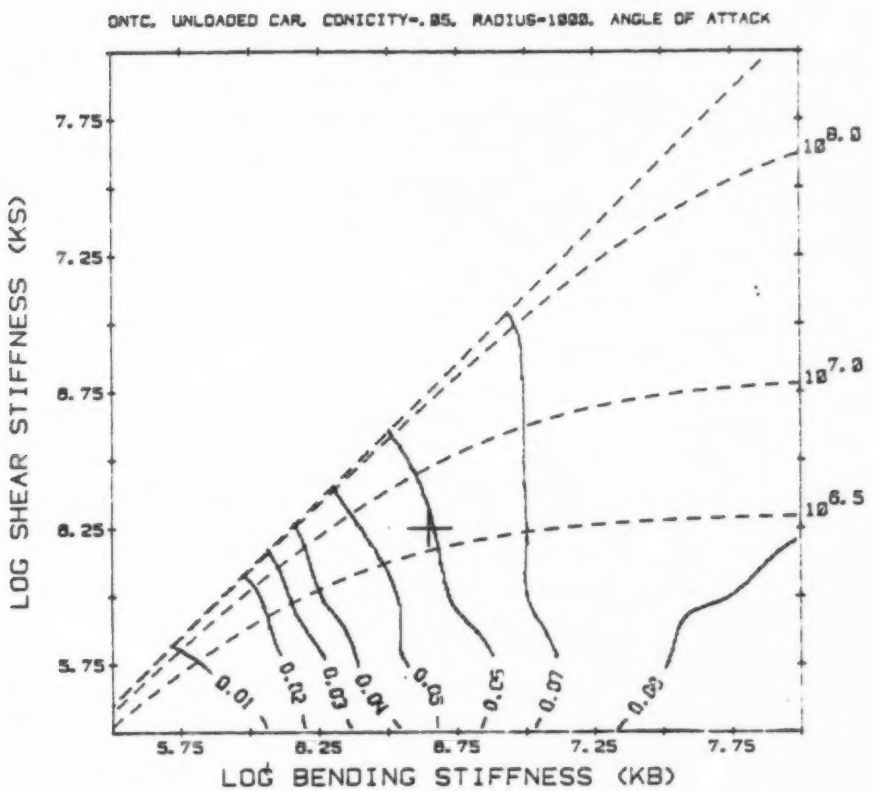

FIGURE G-3: ANGLE OF ATTACK FOR 1000 M RADIUS CURVE

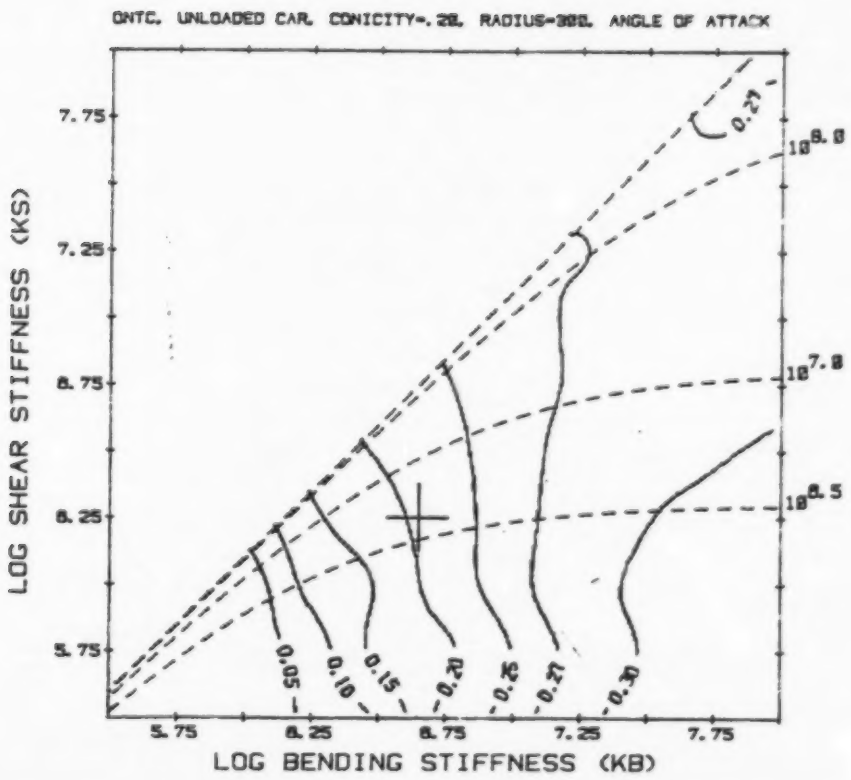

FIGURE G-4: ANGLE OF ATTACK, 300 M RADIUS CURVE, CONICITY OF 0.2

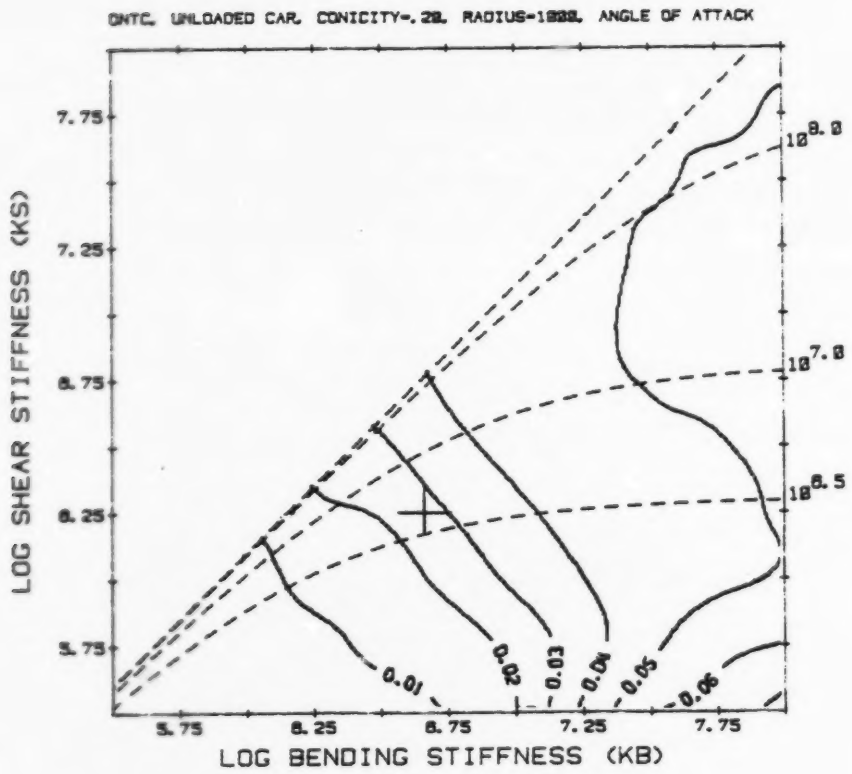

FIGURE G-5: ANGLE OF ATTACK, 1000 M RADIUS CURVE, CONICITY OF 0.2

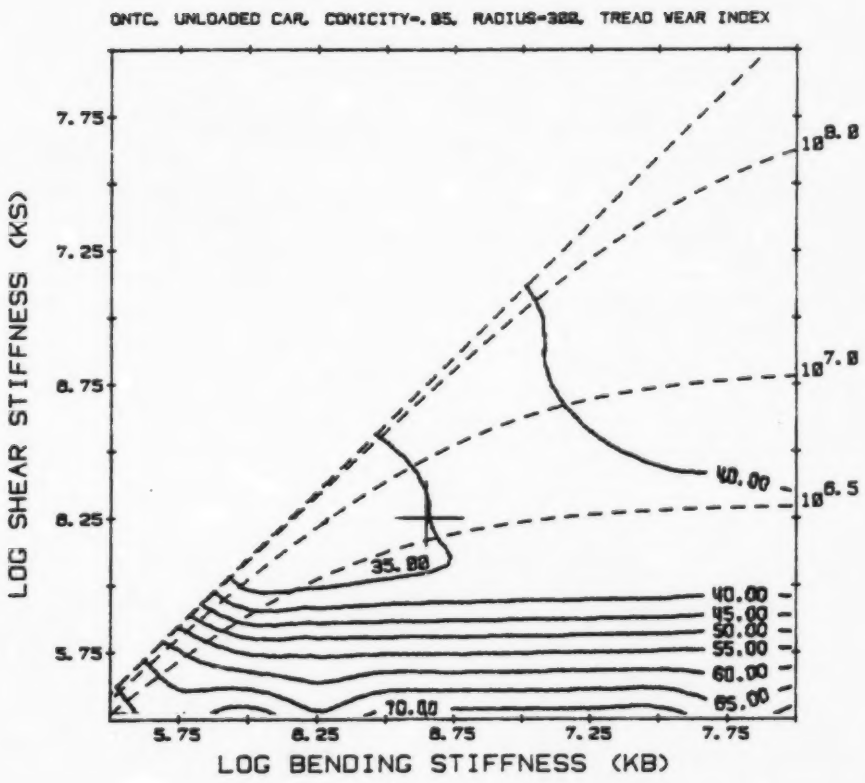

FIGURE G-6: TREAD WEAR INDEX, 300 M CURVE, CONICITY OF 0.05

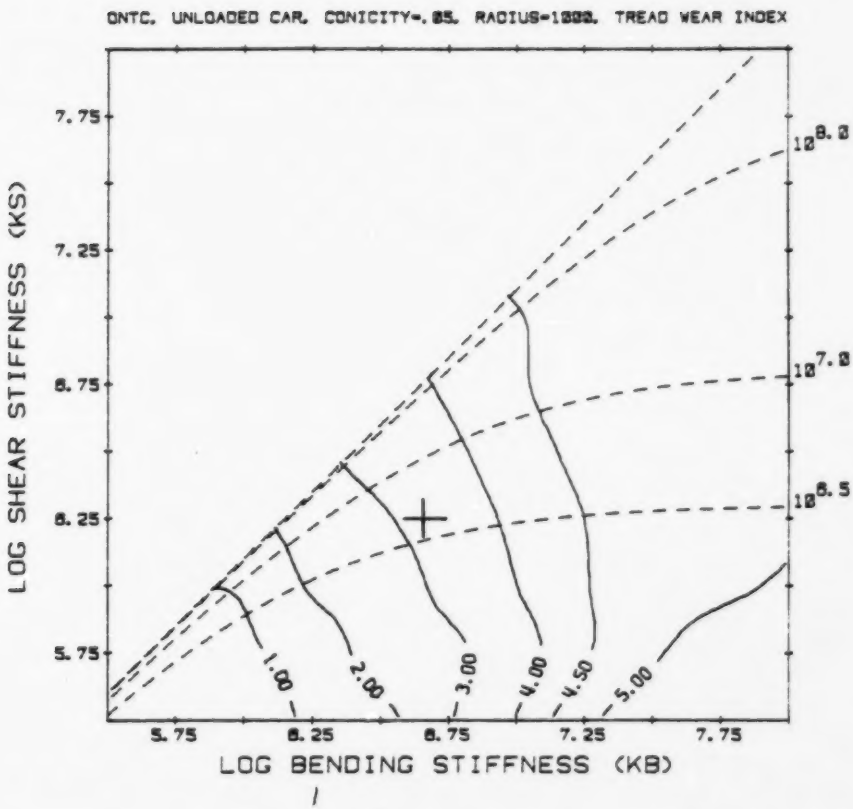

FIGURE G-7: TREAD WEAR INDEX, 1000 M CURVE, CONICITY OF 0.05

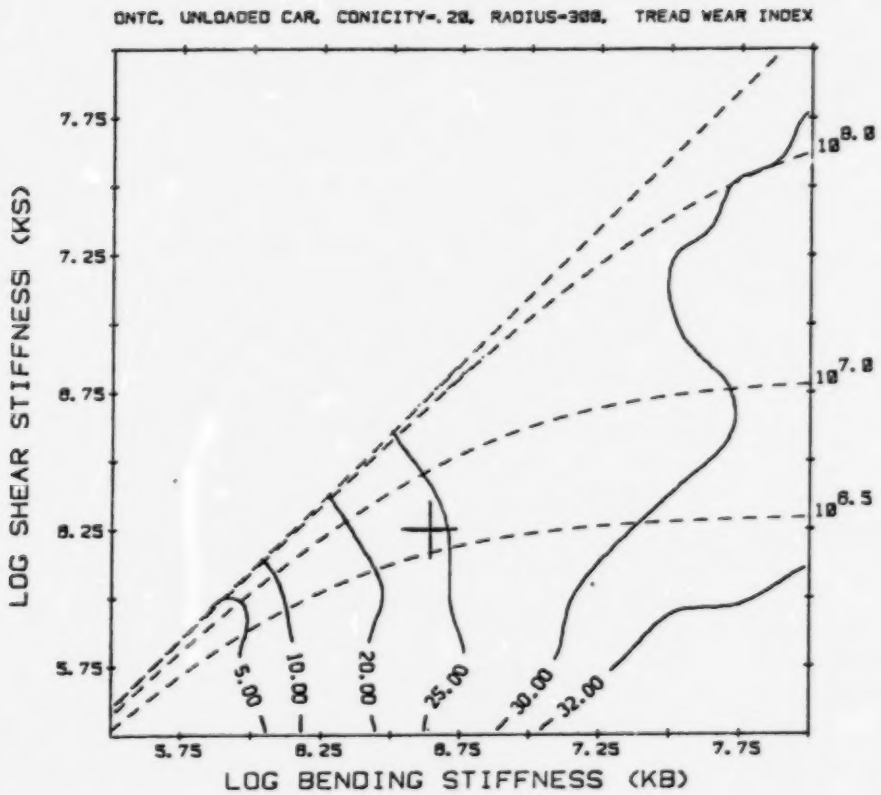

FIGURE G-8: TREAD WEAR INDEX, 300 M CURVE, CONICITY OF 0.2

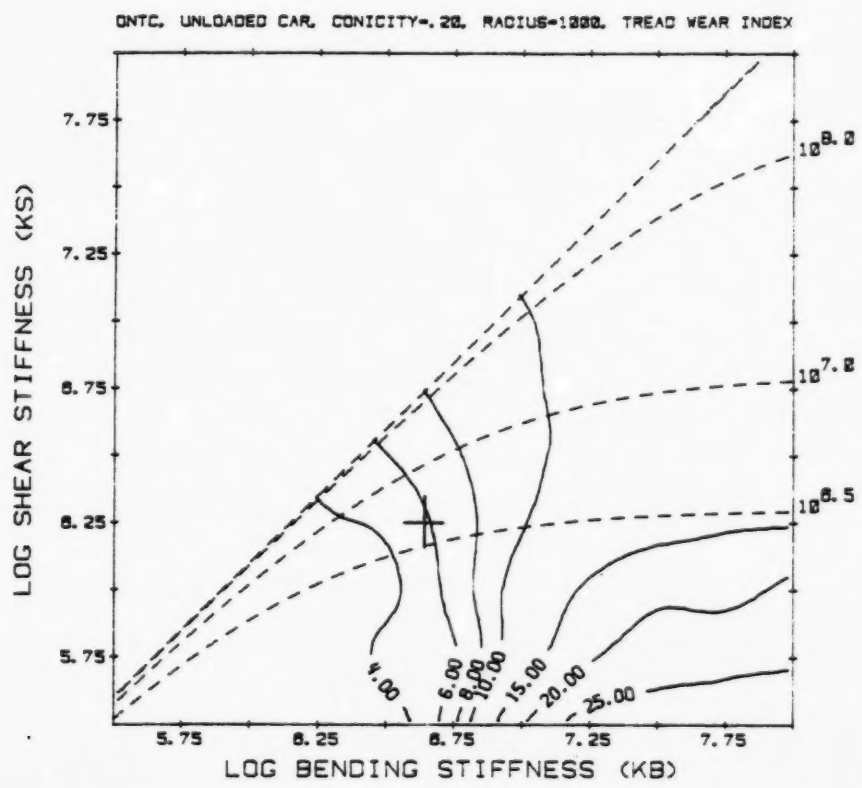

FIGURE G-9: TREAD WEAR INDEX, 1000 M CURVE, CONICITY OF 0.2

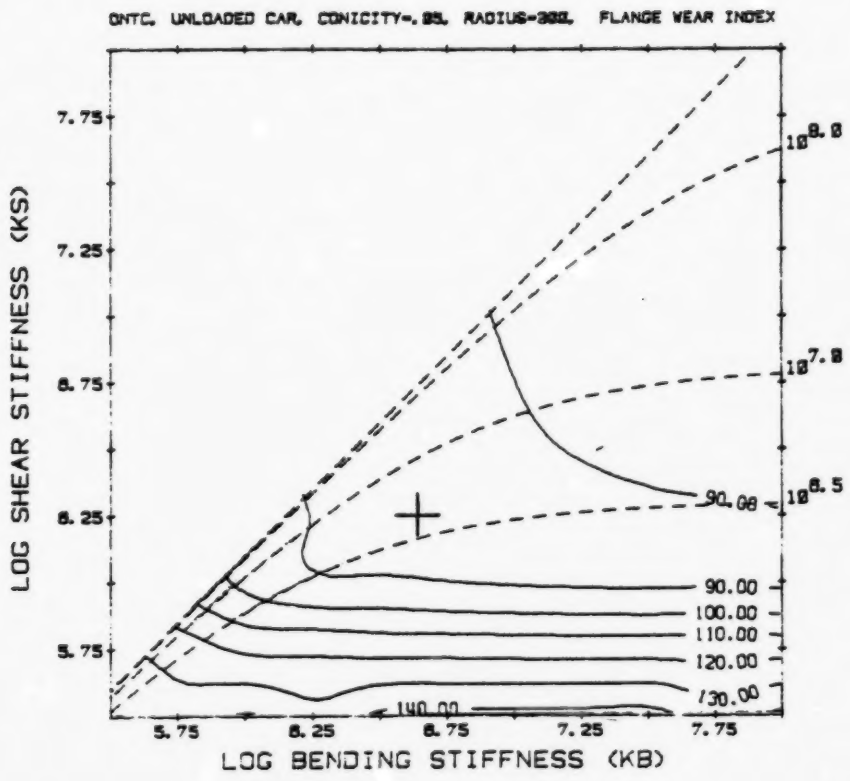

FIGURE G-10: FLANGE WEAR INDEX, 300 M RADIUS CURVE, CONICITY OF 0.05

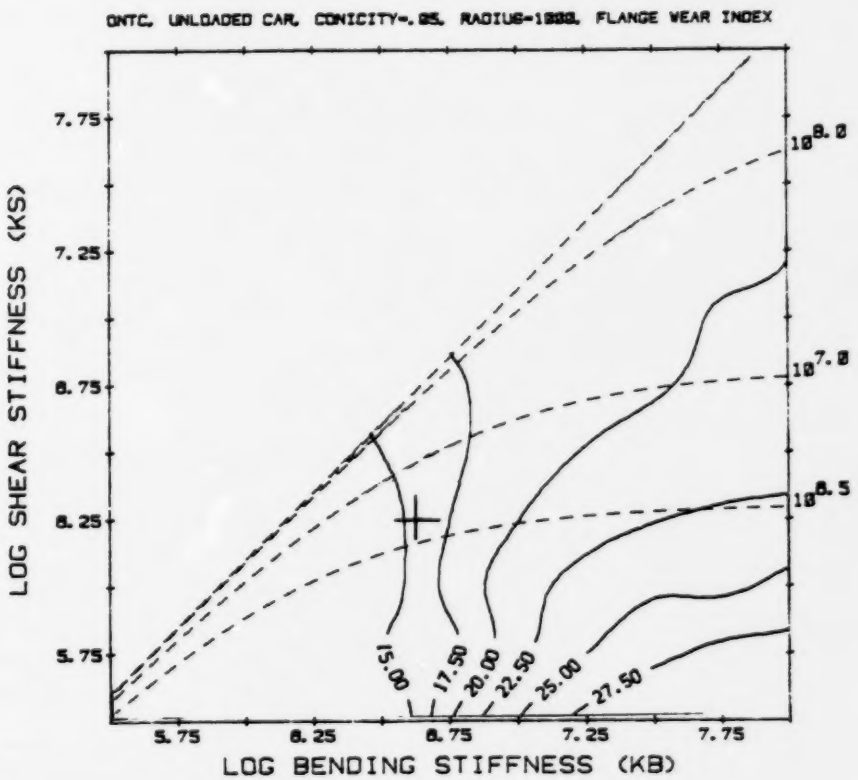

FIGURE G-11: FLANGE WEAR INDEX, 1000 M RADIUS CURVE, CONICITY OF 0.05

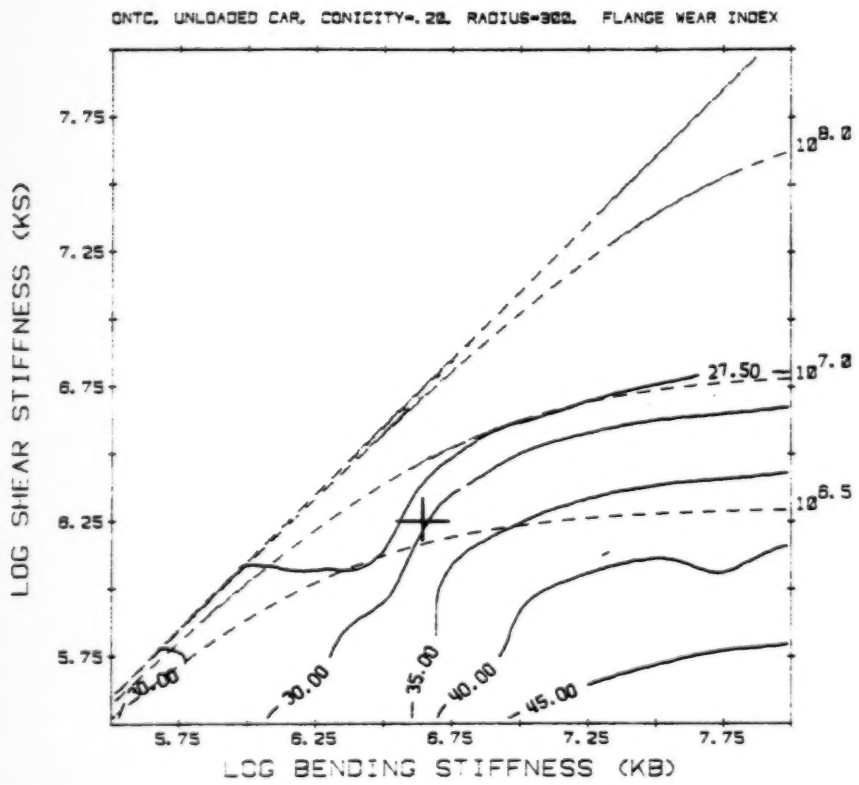

FIGURE G-12: FLANGE WEAR INDEX, 300 M RADIUS CURVE, CONICITY OF 0.2

APPENDIX H

REPORT ON MASS INERTIA, LINEAR AND STIFFNESS

MEASUREMENT TESTS

UTDC RESEARCH & DEVELOPMENT LTD.
INTER OFFICE MEMORANDUM

To: [redacted]

cc: R.E. Smith
T. Warhurst

From: B. Willoughby

Date: 28 October 1982

File: 42-7100

Subject: MASS, INERTIA, LINEAR AND STIFFNESS MEASUREMENT TESTS ON THE BARBER S-2 TRUCK AT ONR NORTH BAY.

---

1. Introduction and Background

To acquire the subject measurements a test plan (42-TP-7100-003) was produced and permission obtained from ONR to conduct these tests in their facilities at North Bay, Ontario.

T. Warhurst and I proceeded to North Bay to carry out these tests on 17 Oct. 82. Linear measurements and photographs were taken on 18 Oct. 82. Mass and Inertia measurements were taken 19-20 Oct. 82. Stiffness measurements were taken 21-22 Oct. 82. We departed North Bay for Kingston on 23 Oct. 82.

The ONR car house employees, Dave Stevens (General Foreman), Rollie Laland (Heavy Equipment Foreman) and Russel Ratz (Lead Hand) gave us excellent co-operation and assistance in collecting the data.

The testing for the mass measurements was hampered by not having more load cells. (ICTS weighing programs required the four-cell weighing kit).

2. Tests Conducted and Measurement Methods

a. Linear

Linear measurements were taken directly.

b. Mass

Mass centre was determined by weighing a sideframe and a bolster.

c. Inertia

Inertia was obtained by timing the pendulum action of the mass and measurement of distance between mass centre and pivot point.

Sideframe was measured for yaw and roll. Bolster was measured for yaw only.

d. Stiffness

Stiffness was measured using trucks mounted under an empty car (approx 62,000 lb) and a full car (approx 260,000 lb). Three tests were carried out on one truck of each for K_s, K_b, and bolster lateral stiffness, on one truck at each load.

K_s data was obtained by fixing one axle, applying lateral force to the other and measuring inter axle displacement.

K_b data ws obtained by fixing one axle, applying longitudinal force to one side of the other axle and measuring inner axle displacement.

Bolster lateral data was obtained by applying lateral force to the bolster and measuring displacement between bolster and each sideframe, and bolster and ground.

3. Results

The following are the preliminary results of the tests. Final results will be given in test report 42-TP-7100-003.

a. Mass

Bolster weight = 1,423 lb.

Sideframe weight = 1,050 lb.

b. Inertia

Bolster Yaw:
Fulcrum to centre of mass = 56.41"
Time interval per cycle = 2.61 sec.

Sideframe Yaw:
Fulcrum to centre of mass = 43.21"
Time interval per cycle = 2.38 sec.

Sideframe Roll:

Fulcrum to centre of mass = 13.09"
Time interval per cycle = 1.37 sec.

Truck K_S

Empty car (approx 62,000 lbs).

Locations
- Lateral force against unfixed axle
- D_1-Lateral movement of unfixed axle
- D_2-Lateral movement of fixed axle
- D_3-Longitudinal movement of fixed wheel diagonally opposite force applied
- Inter axle measured outboard of wheels between two centerpunched indents.

Force Applied (lb)	Movement in 1000			Inter Axle (in)	
	D1	D2	D3	Force Side	Other Side
0	0	0	0	65 3/4	66 11/16
500	8.5	0.75	0		
1,000	26.0	1.5	0.7	65 25/32	66 5/8
1,500	64.2	5.0	2.0		
2,000	110.0	5.8	3.8	65 3/4	66 9/16
2,500	160.0	11.0	3.8		
2,600	*500.0+	15.0	5.5		
3,000	Rezeroed	15.8	4.1	65 3/4	66 9/16
3,500	381.0	21.0	2.5		
3,500	384.0	21.2	2.0		
4,000	578.0	27.5	15.0	65 13/16	66 9/16
	592.00***				
	Rezeroed				
4,000	6.0	28.0	15.0		
4,500	119.0	31.0	22.0		
5,000	235.0	37.2	34.0	65 7/8	66 7/8
0	258.0	27.0	31.0		

* Truck Jumped
** Repeat
*** After 20 min.

Truck$_S$

Full car (aprox 260,000 lb)

Locations same as empty car

Force Applied (lb)	Movement in 1000			Inter Axle (in)	
	D_1	D_2	D_3	Force Side	Other Side
0	0	0	0	65 1/2	65 5/8
500	0	0	1.3		
1,000	0	0.4	2.8	65 5/8	65 19/32
1,500	0	0.6	4.8		
2,000	0	0.9	6.9	65 9/16	65 9/16
2,500	0.1	1.0	9.5		
3,000	0.25	1.1	12.2	65 9/16	65 19/32
3,500	0.25	1.5	16.0		
4,000	0.5	1.8	19.4	65 5/8	65 21/32
4,500	0.7	2.0	23.6		
5,000	0.8	2.4	27.3	65 19/32	65 21/32
0	0.3	1.1	13.0	65 1/2	65 9/16

Truck K_b

Empty car (approx 62,000 lb)

Locations

- Longitudinal force against one end of unfixed axle.
- D_1-Longitudinal movement of fixed wheel on force side.
- D_2-Lateral movement of force axle.
- D_3-Longitudinal movement of unfixed wheel on opposite end of unfixed axle.
- Inter axle measurement outboard of wheels between two centerpunched indents.

Force Applied (lb)	Movement in 1000			Inter Axle (in)	
	D_1	D_2	D_3	Force Side	Other Side
0	0	0	0	65 3/4	66 5/8
500	4.5	0	-5.0		
1,000	8.4	0	-8.1	65 3/4	66 5/8
1,500	12.5	0.5	-11.1		
2,000	16.1	0.5	-15.0	65 13/16	66 5/8
2,500	22.0	-.75	-20.7		
3,000	34.0	-1.0	-33.0	65 3/4	66 19/32
3,500	53.5	-4.8	-50.3		
4,000	89.5	-6.5	-75.0	65 31/32	66 5/8
4,500	396.0	-12.0	-140.0		

Truck K_b

Full car (approx 260,000 lb)

Locations-same as empty car

Force Applied (lb)	Movement in 1000			Inter Axle (in)	
	D_1	D_2	D_3	Force Side	Other Side
0	0	0	0	65 1/2	65 5/8
500	1.0	0.2	-0.8		
1,000	2.0	0.5	-1.1	65 15/32	65 9/16
1,630	4.0	0.5	-2.1		
2,000	5.0	0.1	-2.8	65 15/32	65 19/32
2,500	7.0	-1.0	-3.6		
3,000	9.0	-1.0	-5.0	65 15/32	65 19/32
3,500	11.0	-1.0	-6.2		
4,000	13.0	-1.0	-7.5	65 1/2	65 19/32
4,500	15.0	-1.8	-11.4		
5,000	17.0	-1.8	-9.6	65 15/32	65 5/8
0	8.8	-1.2	-5.0	65 15/32	65 19/16

Bolster Lateral

Empty Car (approx 62,000 lb)

Locations D_1-Force side between bolster and force side sideframe, lateral displacement.

D_2-Opposite side between bolster and other side sideframe, lateral displacement.

D_3-Bolster lateral displacement to ground.

Force Applied (lb)	Movement in 1000		
	D_1	D_2	D_3
0	0	0	0
500	0	0	1.0
1,020	0	.5	1.8
1,500	1	1.4	4.1
2,000	3.5	3.2	7.2
2,500	5.2	5.6	10.6
3,000	6.2	11.8	14.5
3,500	7.9	10.8	11.8
4,000	9.3	12.8	23.0
4,500	11.3	15.0	27.5
5,000	19.5	23.0	37.0
0	13.8	18.8	25.0

Bolster Lateral

Full car (approx 260,000 lb)

Locations-same as for empty car.

Force Applied (lb)	Movement in 1000 D_1	D_2	D_3
0	0	0	0
500	0	0	1.0
1,000	0	0	1.8
1,500	0	0	2.5
2,000	0	0	3.2
2,500	0	0	4.5
3,000	0	0	5.8
3,500	0	0	7.0
4,000	0	0	8.9
4,500	0	0	10.6
5,000	0	0	12.6
0	0	0	16.5*

* Bolster Creaked

4. Discussion of Results

These results are preliminary and are subject to changes. A test report, 42-TR-7100-003 will be produced to give final figures for this test.

5. Recommendations

More load cells would have cut test time and made the mass measuremetns much less awkward.

B. Willoughby

/sa

Distribution CONTROLLED

Classification UNCLASSIFIED

Division of Mechanical Engineering

Division de génie mécanique

Pages 2

Fig. Diag. 7

Tables 2

CALIBRATION ANALYSIS AND TEST REPORT

RAPPORT D'ÉTALONNAGE D'ANALYSE ET D'ESSAI

CAT-RW-014

RAILWAY LABORATORY

Date 08/85

Lab. Order Comm. Lab. 22597

File Dossier 3730-3

For Pour: Urban Transportation Development Corporation
Kingston, Canada

Reference Référence: NRC32 signed by Acting Director of Programs

Title/Titre: MEASURED VALUES OF INTER-AXLE LATERAL AND YAW STIFFNESS FOR THE UTDC CROSS-BRACED TRUCK

Approved Approuvé: C.A.M. Smith
Laboratory Head
Chef de laboratoire

Author Auteur: C.A.M. Smith and Ron Koopman

This report may not be published wholly or in part without the written consent of the Division of Mechanical Engineering.

Ce rapport ne doit pas être reproduit, ni en entier ni en partie, sans une autorisation écrite de la Division de génie mécanique.

Copy No.
Copie N° _____

Measured Values of Inter-axle Lateral and Yaw Stiffness for the UTDC Cross-braced Truck

Introduction: Stiffness Measurements for Railway Trucks

From mathematical modeling studies of railway truck hunting phenomena (Refs 1,2) it has become clear that the ratio of inter axle shear stiffness Ks to the inter axle bending stiffness Kb is a critical determination in the predition of the threshold speed above which the truck is unstable. The N.R.C. vibration facilities hitherto used for railway car truck responses to track irregularities have recently been put to use to measure these parameters Ks and Kb. Fig. 1 shows the cross section of track which is supported by 24 1 inch diameter steel balls suitably caged to remain between horizontal flat steel plates attached to the underside of the rail structures and the upperside of the support frame allowing the rail structure freedom in the horizontal plane. Fig. 1 also shows that a longitudinal pivoted bar takes away the longitudinal freedom leaving only lateral and yaw. By clamping one axle set's wheels to this moving frame and the other to terra firma and using a hydraulic actuator as a quassi static bi-directional jack applying a lateral force to the moving frame axle set as shown in Fig. 2 we can measure Ks. Similarly Fig. 3 shows how by moving the jack to the frame and installing a second constraining bar, Kb can be measured. Since the term shear stiffness implies a uniform parallel shear throughout a solid and we suspect the shearing in a freight truck is not uniform (ie quite low at the bearing pads) we will use the term interaxle lateral stiffness with the units of lbs/inch. Similarly the Bending characteristic will be referred to as interaxle yaw stiffness in inch lbs/radian.

Apparatus

One MTS model 204.63 - actuator was mounted as shown in figs 2 and 3 to sequentially cycle the forced axle through the desired range. Dial indicators were set up to measure all axle movements necessary to calculate relative lateral displacement and relative yaw angle.

Results

Table I contains the results of three consecutive experiment where the axle on the platform was forced laterally and the inter axle Lateral Displacement (q1 - q3 in fig 5) is plotted in fig 6 vs Lateral Force.

Table II contains the results of three consecutive experiment where the axle on the platform was torqued about its vertical axis and the inter-axle yaw angle (q2 - q4 in fig 5) is plotted with respect to the applied torque.

Conclusion

With the axles forced into relative lateral displacements and relative yaw angles by a single by-directional jack constrained as shown the "eye averaged" lateral stiffness was 10,000 lbs/inch and the "eye averaged" yaw stiffness was 33 X 10^6 inch lbs/radian.

Since the curves are consistent and non linear with hysterises, curve fitting may be justified. Damping ratios may also be determined.

Recommendations

Having explored the single jack possibilities for truck stiffness measurements and found good repeatability it now seems appropriate to adapt a two jack system to the NRC rig so the two parameters are completely separated by the forced geometry of the moving platform. The simple experiments as performed are very useful for comparisons and give a reasonably good figure for the parameters.

References

1. Wickens, A.H. "Steering and Dynamic Stability of Railway Vehicles". Vehicle System Dynamics Volume 5, 1975-76 pages 15 - 46

2. Marcotte, P. Caldwell, W.N. List, H.A. "Performance Analyses and Testing of a Conventional Three-piece Freight Car Truck Retrofitted to provide Axle Steering". Presented at ASME Winter Annual Meeting of December 1978

TABLE I

Run 1701 Results			Run 1702 Results			Run 1703 Results		
Force F lbs	Inter axle lateral displacement q1 - q3 inches	relative yaw q2 - q4 radians	Force F lbs	Inter axle lateral displacement q1 - q3 inches	relative yaw q2 - q4 radians	Force F lbs	Inter axle lateral displacement q1 - q3 inches	relative yaw q2 - q4 radians
0	0	0	0	0	0	0	0	0
1000	0.0481	0.00029	1000	0.0600	0.0005	1000	0.0594	0.00041
2000	0.1161	0.00121	2000	0.1367	0.00143	2000	0.1424	0.00145
3000	0.2346	0.00295	3000	0.2710	0.00319	3000	0.2730	0.00321
4000	0.3625	0.00477	4000	0.3966	0.00503	4000	0.3994	0.00502
5000	0.4307	0.00546	5000	0.4728	0.00574	5000	0.4778	0.00572
4000	0.4134	0.00546	4000	0.4516	0.00573	4000	0.4562	0.00572
3000	0.3489	0.00473	3000	0.3839	0.00501	3000	0.3879	0.00497
2000	0.2441	0.00318	2000	0.2781	0.00351	2000	0.2826	0.00340
1000	0.1239	0.00155	1000	0.1612	0.00176	1000	0.1648	0.00175
0	0.0188	0.00007	0	0.0603	0.00041	0	0.0611	0.00036
-1000	-0.0440	-0.00074	-1000	-0.0110	-0.00057	-1000	-0.0113	-0.00064
-2000	-0.1595	-0.0 196	-2000	-0.1296	-0.00171	-2000	-0.1251	-0.00175
-3000	-0.2489	-0.00277	-3000	-0.2148	-0.00247	-3000	-0.2109	-0.00251
-4000	-0.3063	-0.00288	-4000	-0.2726	-0.00255	-4000	-0.2692	-0.00259
-5000	-0.3564	-0.00285	-5000	-0.3220	-0.00254	-5000	-0.3203	-0.00256
-4000	-0.3361	-0.00288	-4000	-0.3017	-0.00266	-4000	-0.2989	-0.00259
-3000	-0.3121	-0.00292	-3000	-0.2740	-0.00259	-3000	-0.2698	-0.00263
-2000	-0.268	-0.00273	-2000	-0.2298	-0.00244	-2000	-0.2294	-0.00246
-1000	-0.1954	-0.00214	-1000	-0.1520	-0.00179	-1000	-0.1604	-0.00188
0	-0.0813	-0.00098	0	-0.0496	-0.00075	0	-0.0446	-0.00078

Displacement results from this table plotted in fig 6

TABLE II

Run 1901 Results			Run 1902 Results			Run 1903 Results		
Force F lbs	Inter axle lateral displacement q1 - q3 inches	relative yaw q2 - q4 radians	Force F lbs	Inter axle lateral displacement q1 - q3 inches	relative yaw q2 - q4 radians	Force F lbs	Inter axle lateral displacement q1 - q3 inches	relative yaw q2 - q4 radians
0	0	0	0	0	0	0	0	0
1000	-0.0070	0.00086	1000	-0.0091	0.00061	1000	-0.0074	0.00056
2000	-0.0401	0.00202	2000	-0.0415	0.00169	2000	-0.0412	0.00166
3000	-0.0840	0.00337	3000	-0.0825	0.00295	3000	-0.0811	0.00291
4000	-0.1371	0.00503	4000	-0.1359	0.00458	4000	-0.1366	0.00462
5000	-0.1740	0.00622	5000	-0.1678	0.00575	5000	-0.1692	0.00580
6000	-0.1990	0.00706	6000	-0.1958	0.00680	4000	-0.1572	0.00542
7000	-0.2231	0.00802	5000	-0.1876	0.00648	3000	-0.1254	0.00448
6000	-0.2229	0.00792	4000	-0.1684	0.00586	2000	-0.0838	0.00323
5000	-0.2030	0.00727	3000	-0.1341	0.00483	1000	-0.0343	0.00172
4000	-0.1820	0.00657	2000	-0.0875	0.00344	0	-0.0078	0.00038
3000	-0.1396	0.00525	1000	-0.0397	0.00192	-1000	-0.0253	-0.00110
2000	-0.0976	0.00403	0	-0.0062	0.00042	-2000	-0.0545	-0.00260
1000	-0.0512	0.00253	-1000	-0.0286	-0.00102	-3000	-0.0781	-0.00430
0	-0.0148	0.00088	-2000	-0.0541	-0.00241	-4000	-0.0645	-0.00565
-1000	-0.0135	-0.00042	-3000	-0.0803	-0.00407	-5000	-0.0694	-0.00664
-2000	-0.0520	-0.00195	-4000	-0.0652	-0.00547	-4000	-0.0643	-0.00641
-3000	-0.0759	-0.00349	-5000	-0.0696	-0.00653	-3000	-0.0483	-0.00587
-4000	-0.0775	-0.00479	-6000	-0.0714	-0.00692	-2000	-0.0280	-0.00516
-5000	-0.0906	-0.00568	-5000	-0.0716	-0.00689	-1000	-0.0070	-0.00397
-6000	-0.0827	-0.00621	-4000	-0.0647	-0.00660	0	-0.0384	-0.00255
-7000	-0.0643	-0.00645	-3000	-0.0441	-0.00592			
-6000	-0.0646	-0.00645	-2000	-0.0207	-0.00515			
-5000	-0.0644	-0.00643	-1000	-0.0172	-0.00385			
-4000	-0.0600	-0.00624	0	-0.0453	-0.00241			
-3000	-0.0411	-0.00559				Yaw results from this table plotted in fig 7		
-2000	-0.0173	-0.00481						
-1000	-0.0183	-0.00366						
0	-0.0485	-0.00221						

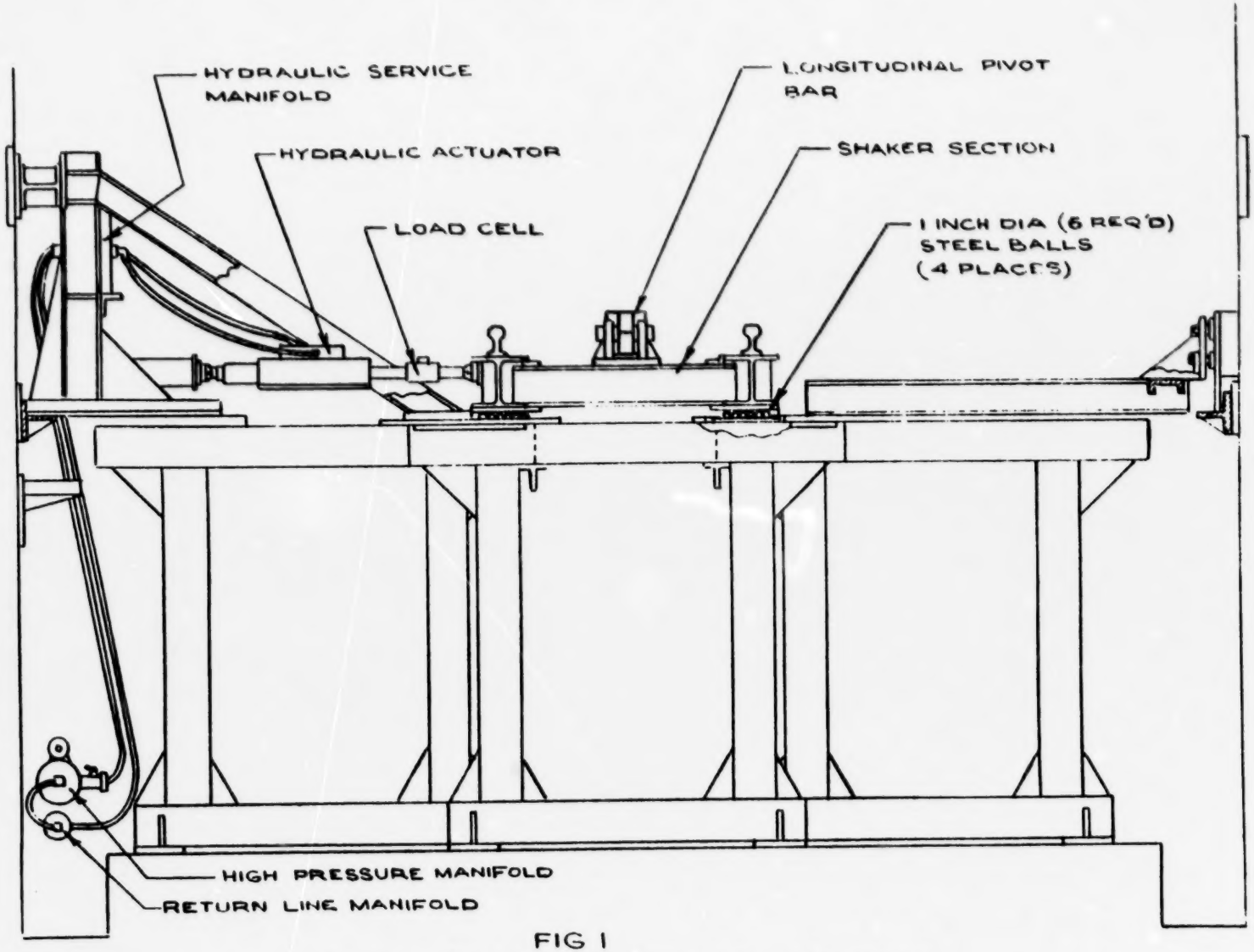

FIG 1

CROSS SECTION OF LATERAL/YAW VIBRATION PLATFORM

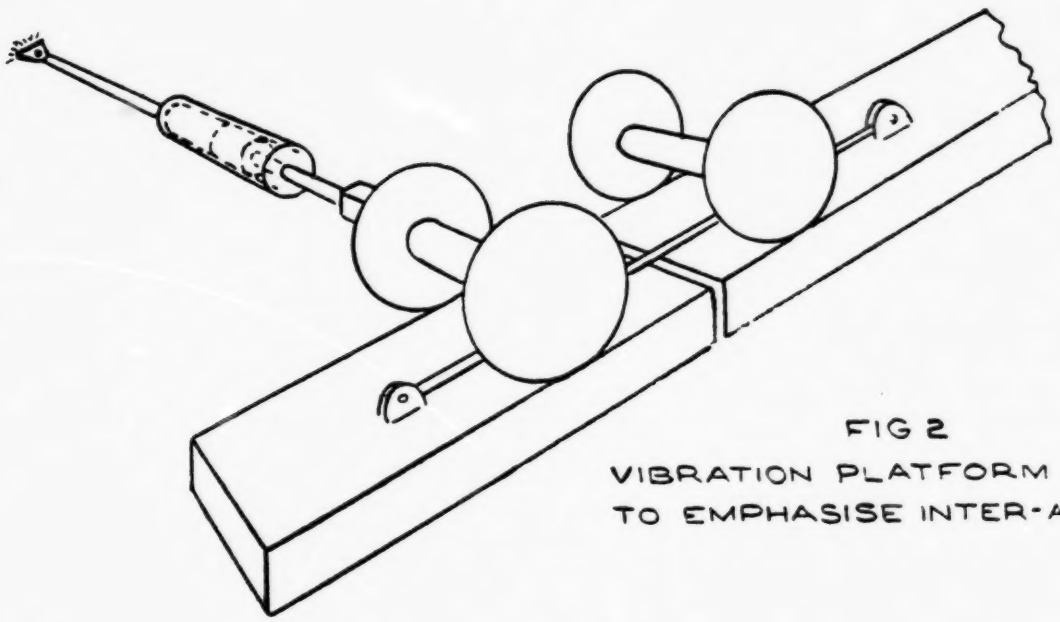

FIG 2
VIBRATION PLATFORM CONFIGURED
TO EMPHASISE INTER-AXLE LATERAL

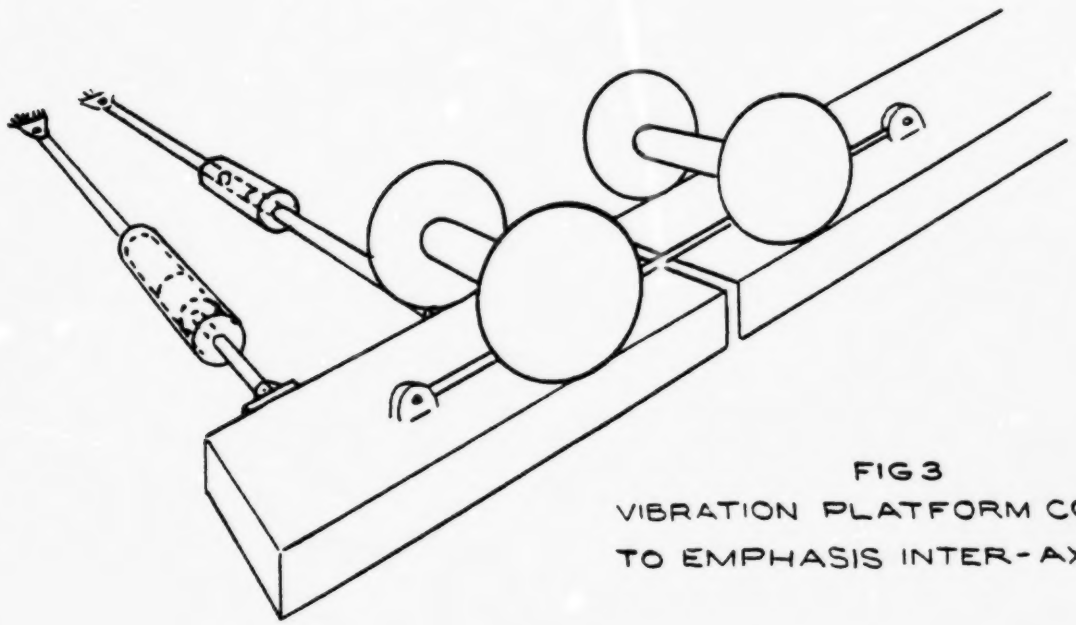

FIG 3
VIBRATION PLATFORM CONFIGURED
TO EMPHASIS INTER-AXLE YAW

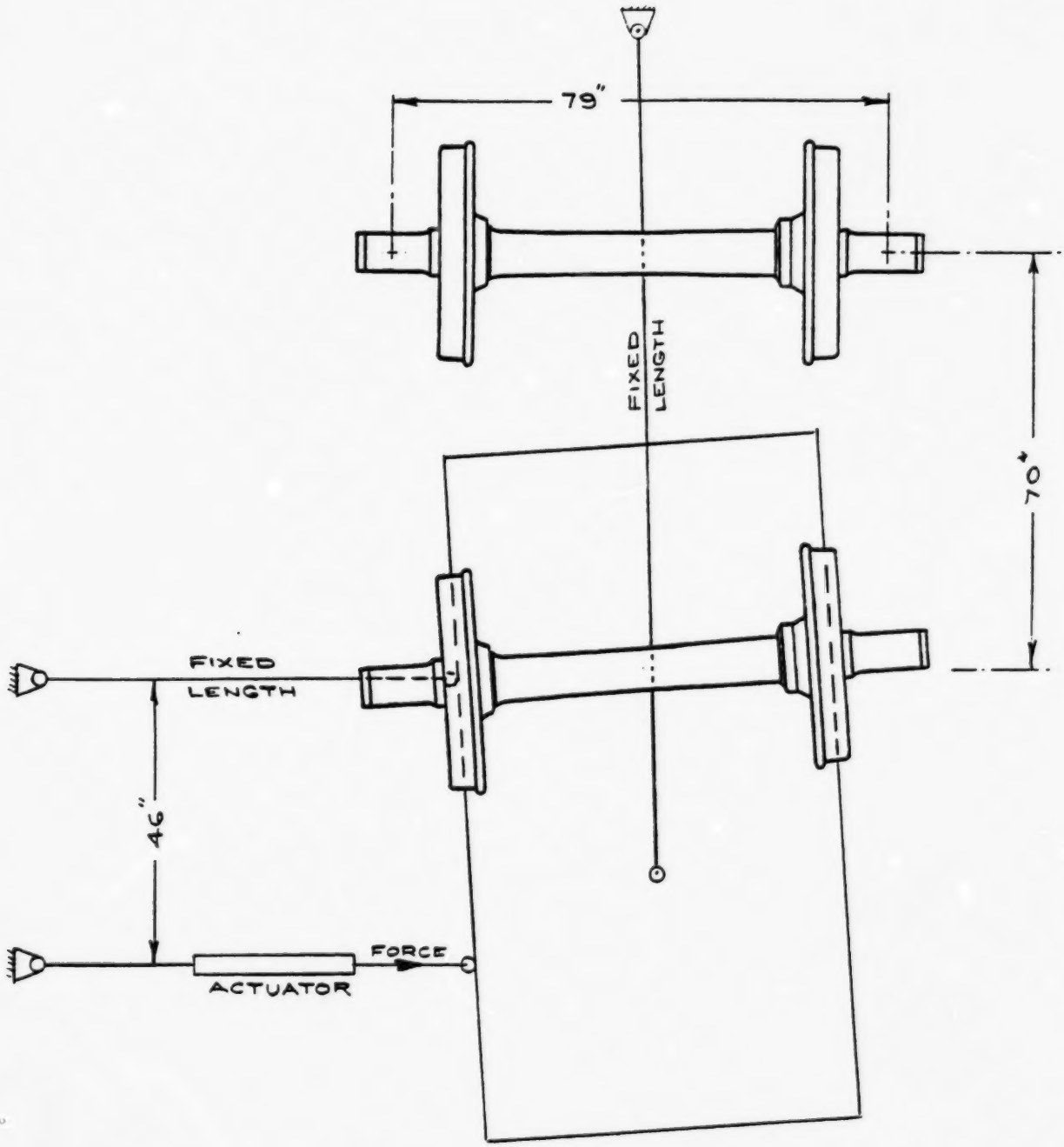

FIG 3A

PLAN VIEW OF SET UP OF FIG 3 SHOWING DISTANCES USED IN CALCULATION

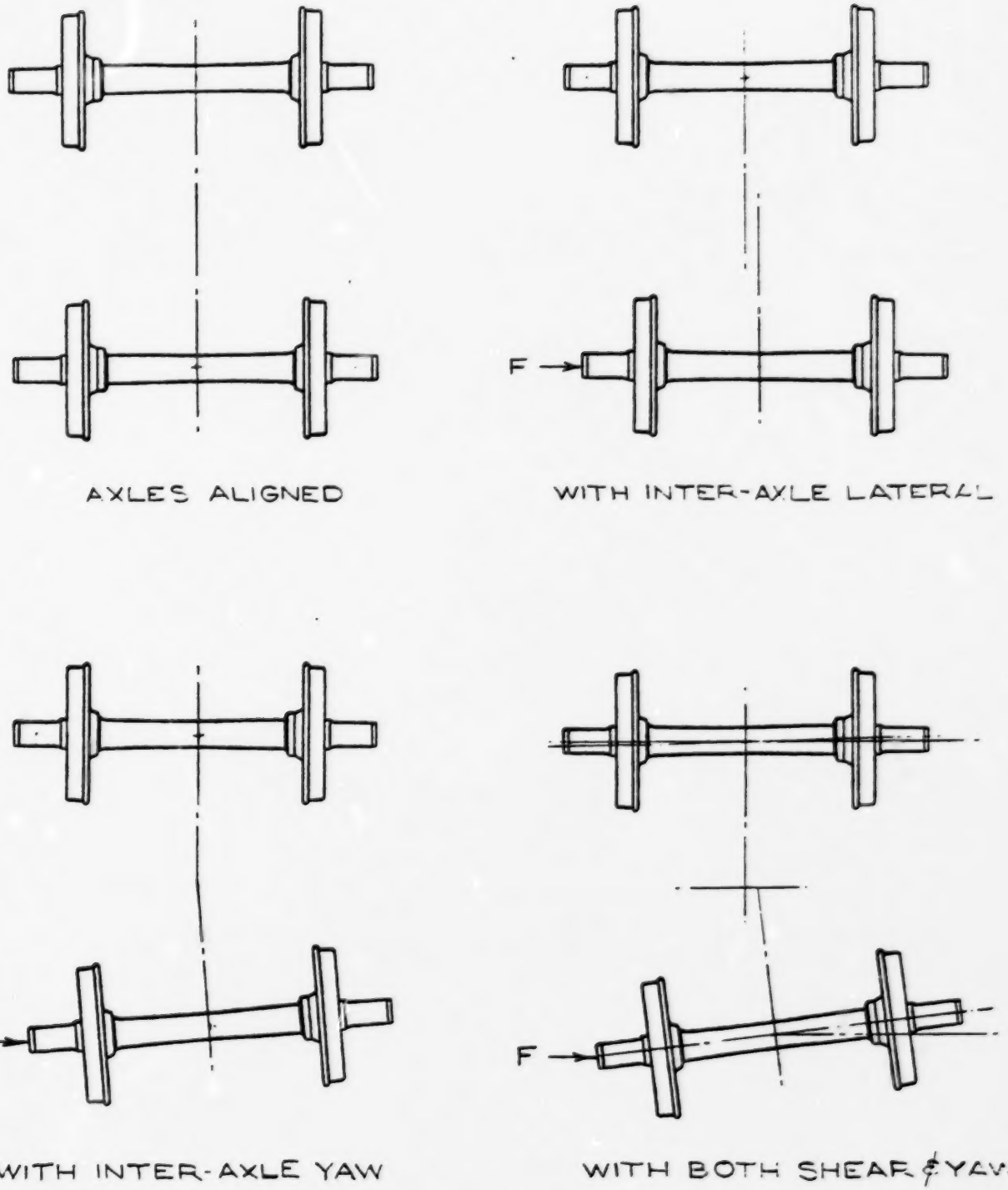

AXLES ALIGNED

WITH INTER-AXLE LATERAL

WITH INTER-AXLE YAW

WITH BOTH SHEAR & YAW.

FIG 4

ILLUSTRATING LATERAL PLUS YAW COMBINED MOVEMENTS

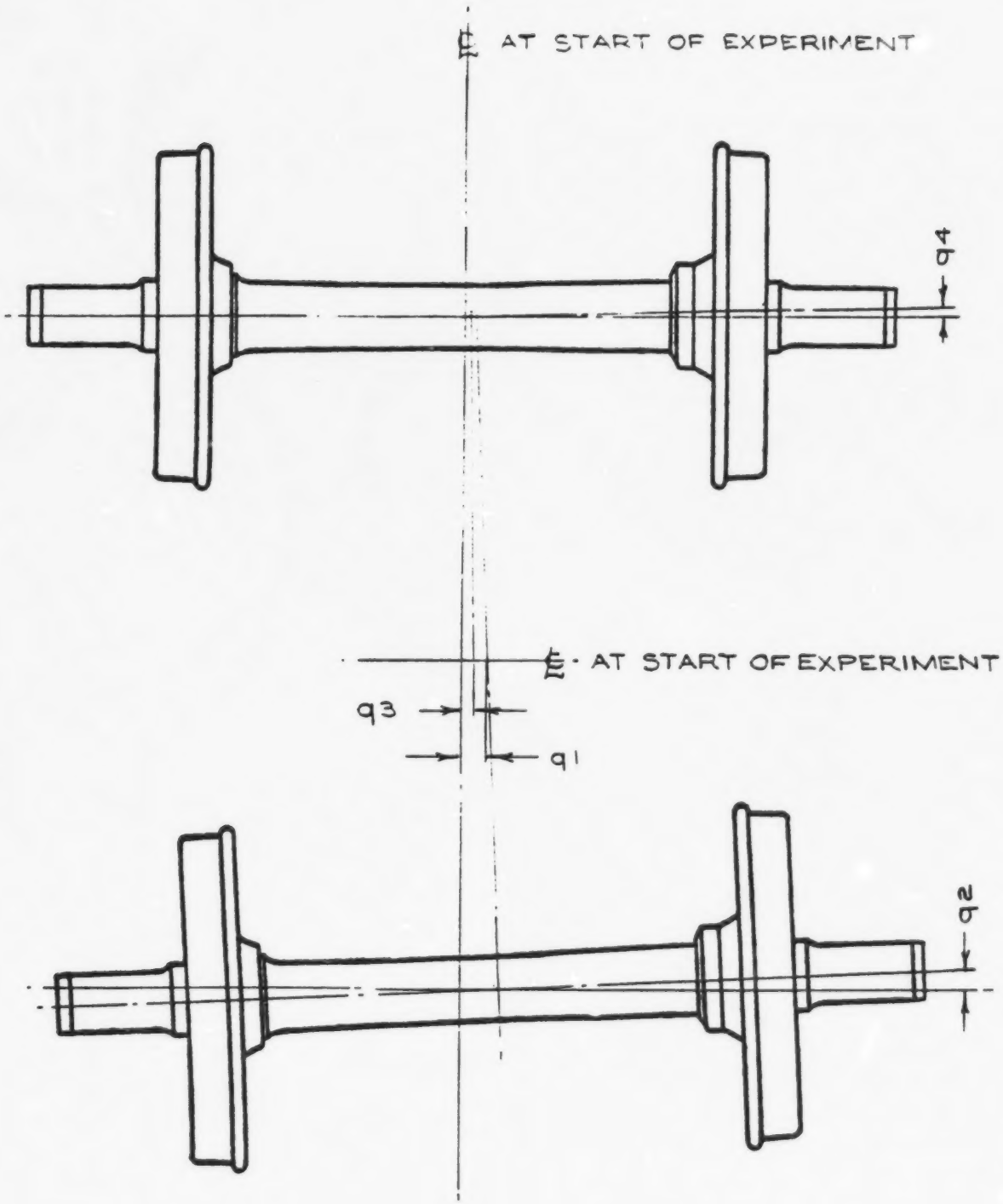

FIG 5
SEPARATING THE VARIABLES

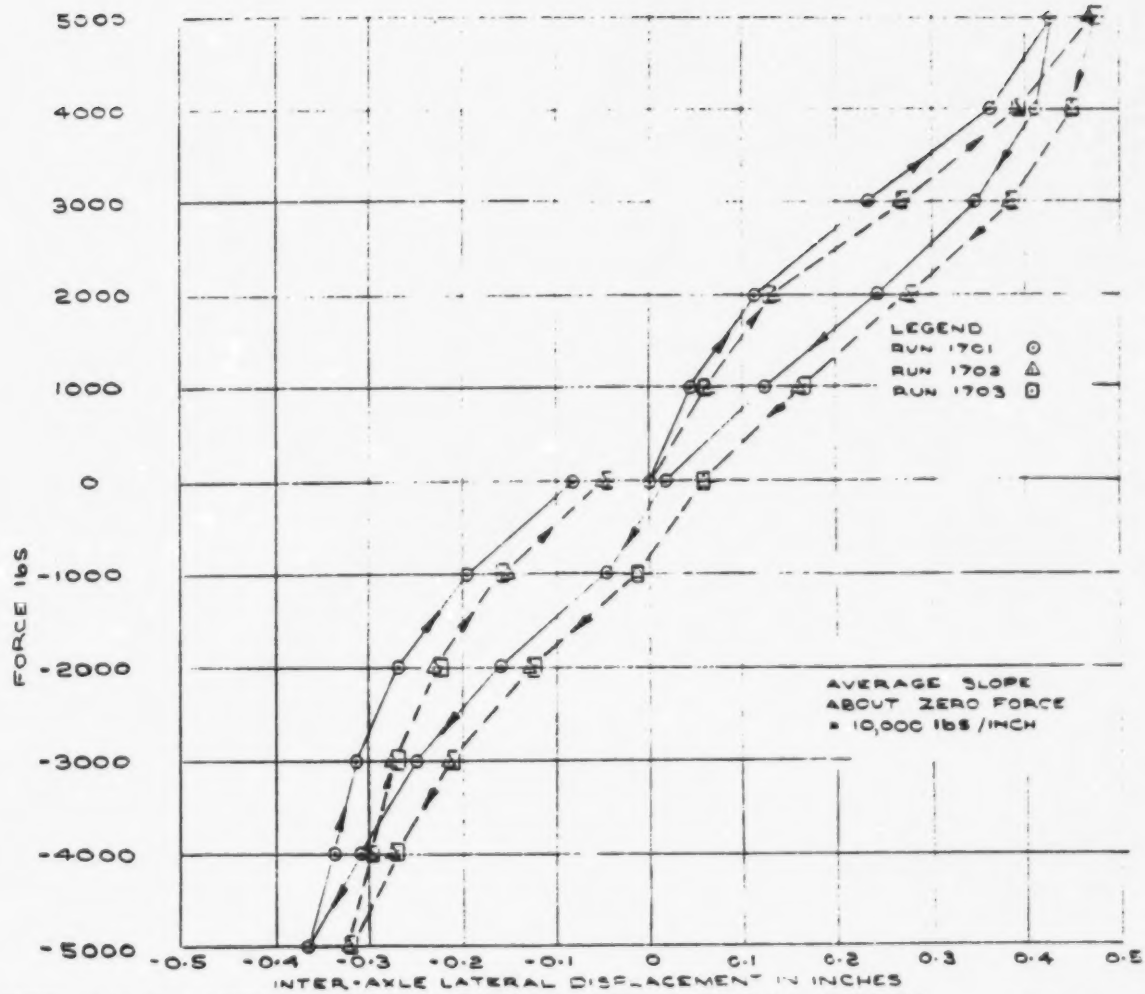

INTER-AXLE LATERAL DISPLACEMENT VS LATERAL FORCE
FOR U.T.D.C. TRUCK LIGHT CONDITION

FIG 6

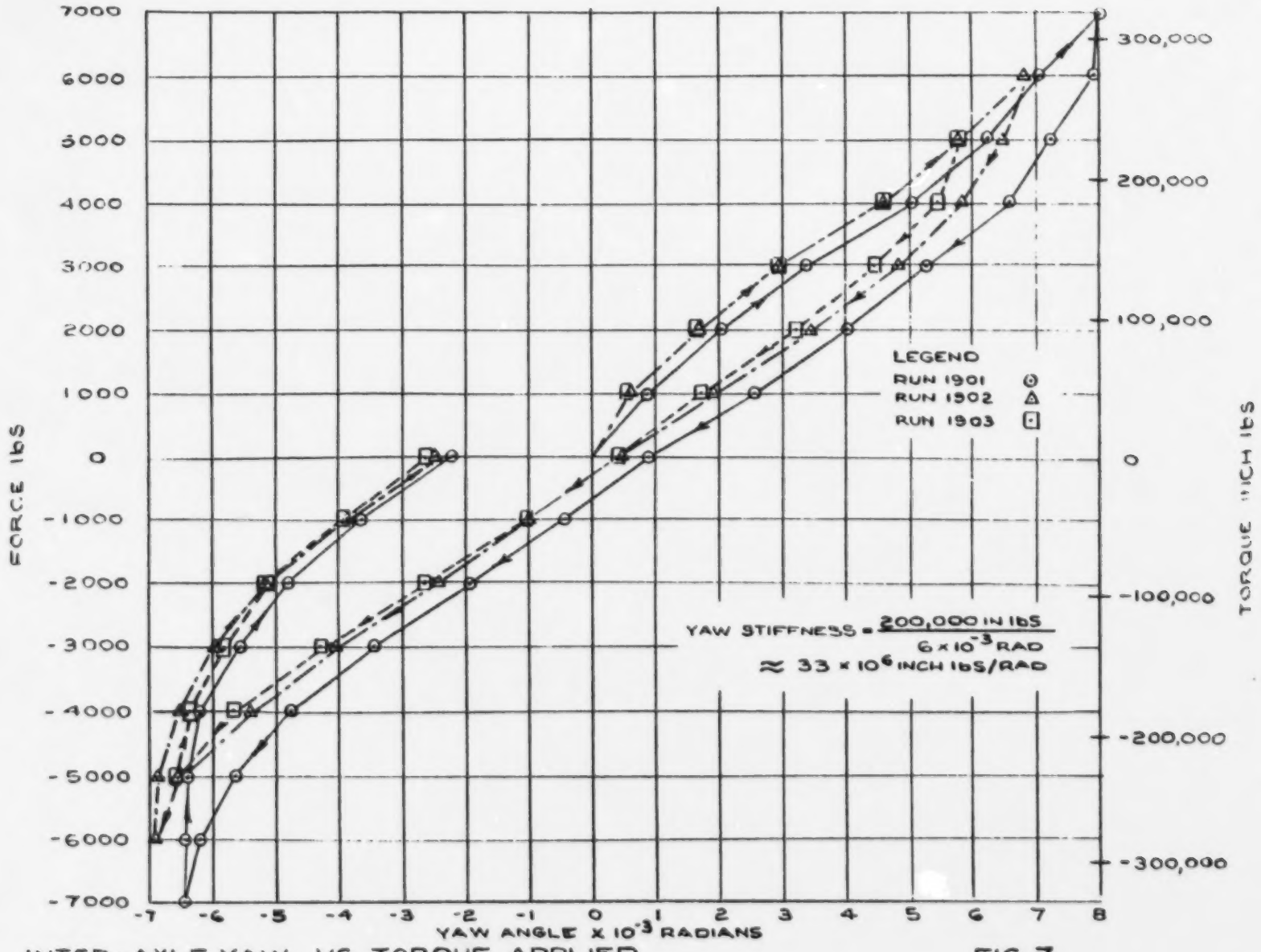

INTER-AXLE YAW VS TORQUE APPLIED
FOR U.T.D.C TRUCK LIGHT CONDITION

FIG 7

REPORT DOCUMENTATION PAGE/PAGE DE DOCUMENTATION DE RAPPORT

REPORT/RAPPORT	REPORT/RAPPORT
1a CAT-RW-014	1b
REPORT SECURITY CLASSIFICATION / CLASSIFICATION DE SÉCURITÉ DE RAPPORT	**DISTRIBUTION/DIFFUSION**
2 UNCLASSIFIED	3 CONTROLLED

TITLE/SUBTITLE/TITRE/SOUS-TITRE (CLASSIFICATION) UNCLASSIFIED

4 MEASURED VALUES OF INTER-AXLE LATERAL AND YAW STIFFNESS FOR THE UTDC CROSS-BRACED TRUCK

AUTHOR(S)/AUTEUR(S)

5 Smith, C.A.M. and Koopman, Ron

SERIES/SÉRIE

6

CORPORATE AUTHOR/PERFORMING AGENCY/AUTEUR D'ENTREPRISE/AGENCE D'EXÉCUTION

7 National Research Council, Railway Laboratory
Division of Mechanical Engineering

SPONSORING AGENCY/AGENCE DE SUBVENTION

8 Urban Transportation Development Corporation
Kingston, Ontario

DATE	FILE/DOSSIER	LAB. ORDER / COMMANDE DU LAB.	PAGES	DIAGS	REFS
9 1985/08	10 3730-3	11 22597	12a 2	12b 7	12c 2

NOTES

13

DESCRIPTORS(KEY WORDS)/MOTS-CLÉS

14 bending, shear, lateral, yaw stiffness

SUMMARY/SOMMAIRE

15 Use has been made of a lateral/yaw vibration table for full sized railway vehicles to obtain quassi static truck stiffness.

ADDRESS/ADRESSE

16 C.A.M. Smith, Railway Laboratory
Division of Mechanical Engineering
Ottawa, Ontario
K1A 0R6 (613) 998-9638

APPENDIX I

STABILITY AND CURVING TEST RESULTS

AT CANADIAN PACIFIC

P O Box 6042, Station "A"
Montreal, Quebec H3C 3E4
Tel (514) 395-5151, Telex 05-268576

DEC 3 1984

Canadian Pacific

R Klein
Assistant Vice President
Planning And Research
H H Benattar
Director
Administration
A E Bethune
Director
Technical & Operations Research
J M Konig
Director
Special Projects
J F Schulman
Director
Economics & Business Analysis
T W Phillips
Director
Cost Analysis

November 23, 1984

Q9-2-4-2

Mr. B. Caldwell
Executive Vice-President
UTDC Research & Development Ltd.
P.O. Box 160, Station A
Kingston, Ontario
K7M 6R1

Dear Brian:

This refers to our recent conversation relating to test results for the UTDC frame braced truck which were discussed with UTDC personnel at a meeting held at Canadian Pacific earlier this week.

As requested, attached are copies of the test results for the curving and stability performance of the UTDC and reference car trucks. The results are being provided on the understanding they will be used solely for internal use at UTDC.

Yours sincerely,

A.E. Bethune

Attach.

cc: Mr. W.S.C. McLaren

Co Originals to FWH
Copies to — QLA
SFS
RES.

John - please advise on your reaction.

BBC

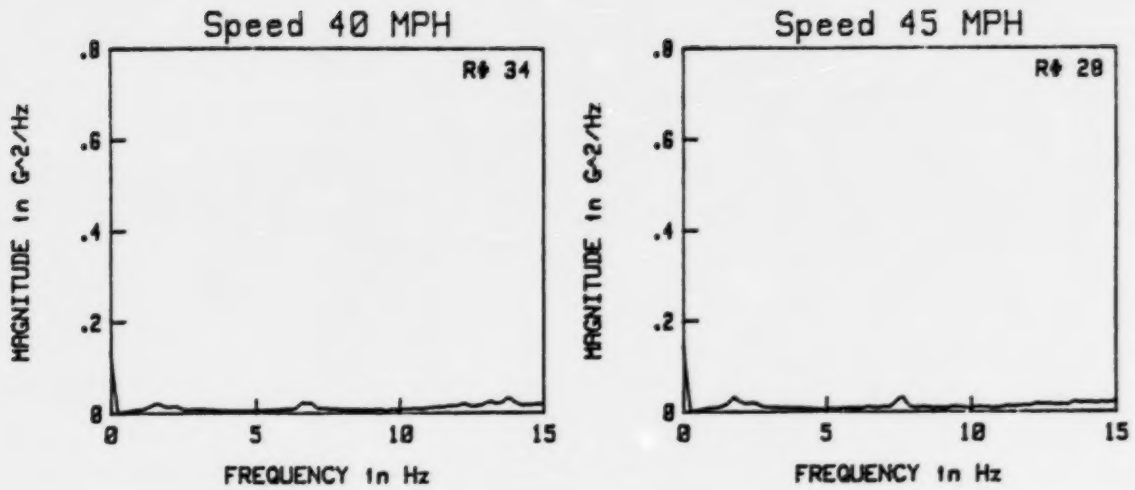

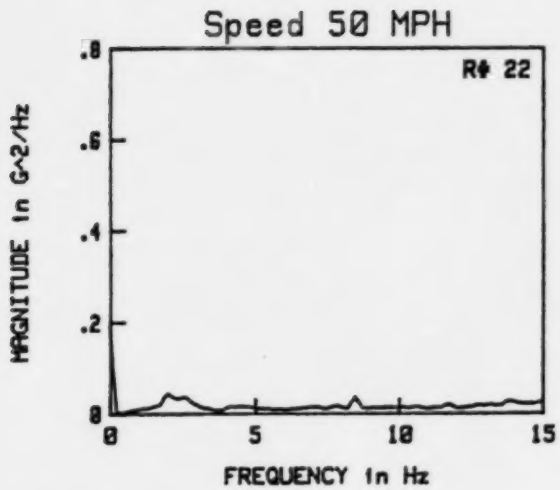

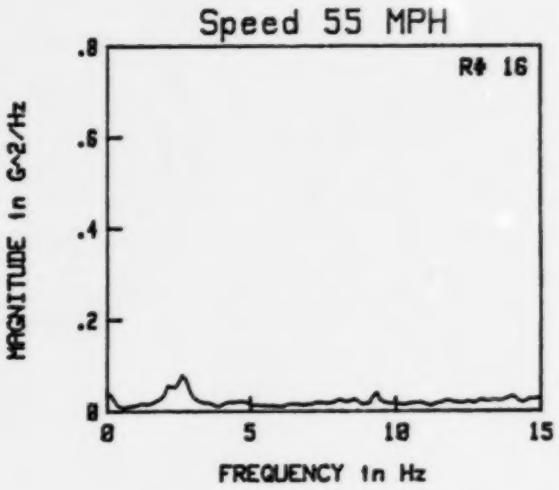

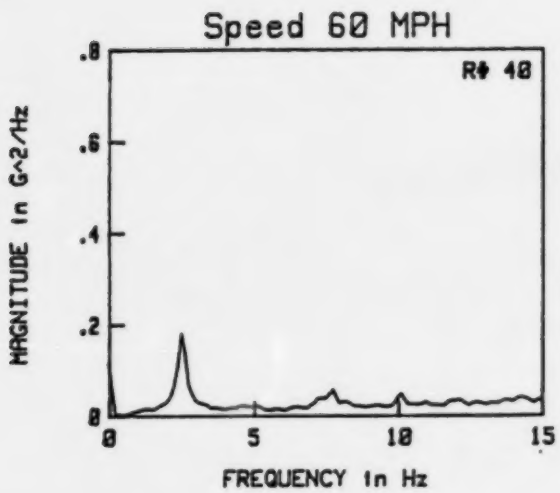

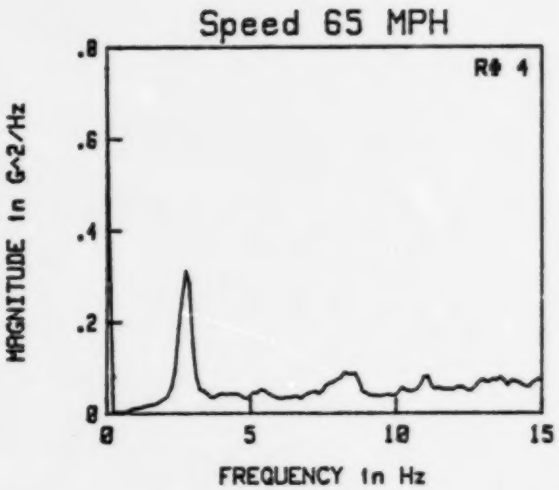

UTDC (RETROFIT) 100 TON TRAILING TRUCK

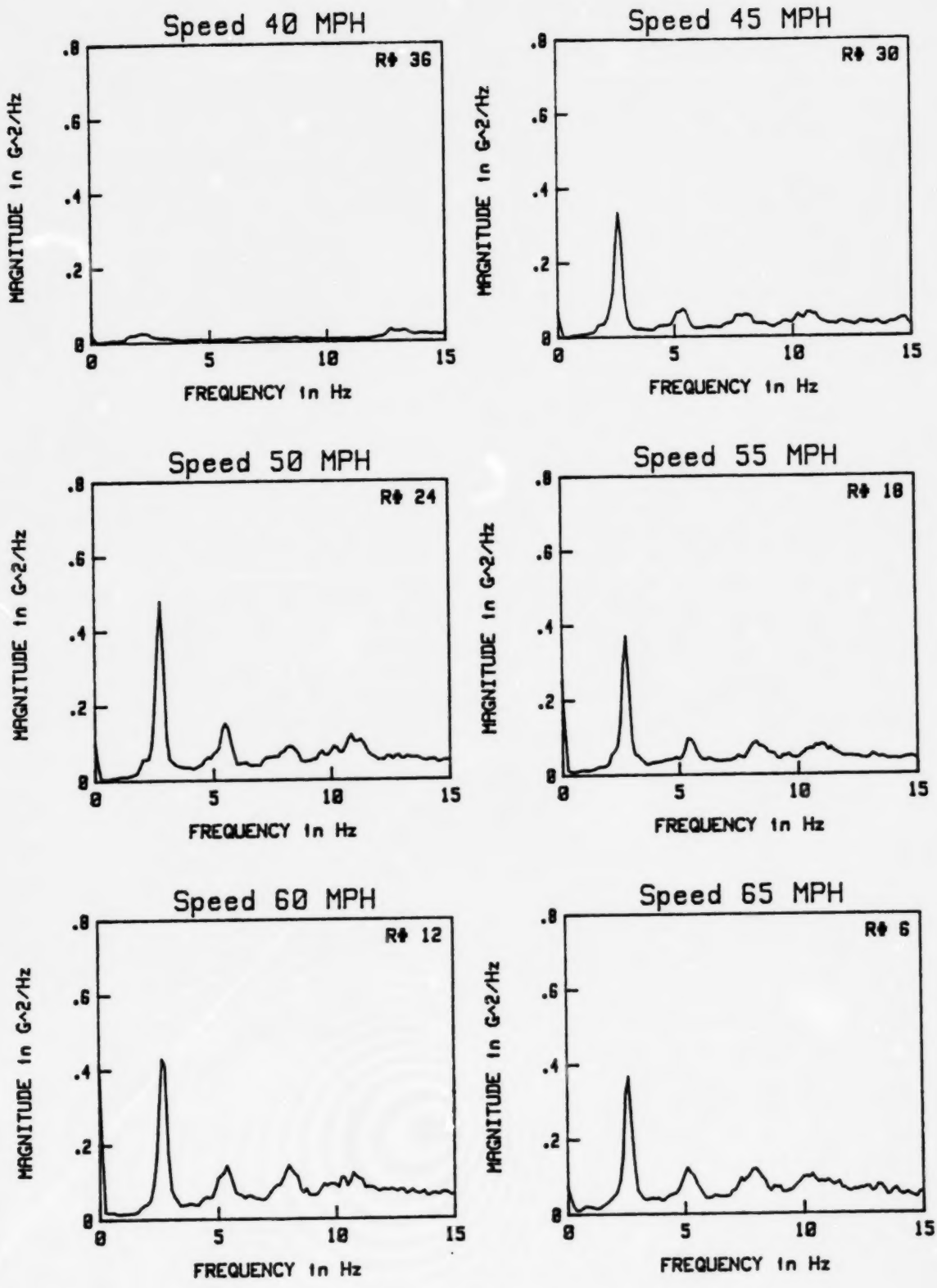

REFERENCE 100 TON TRAILING TRUCK

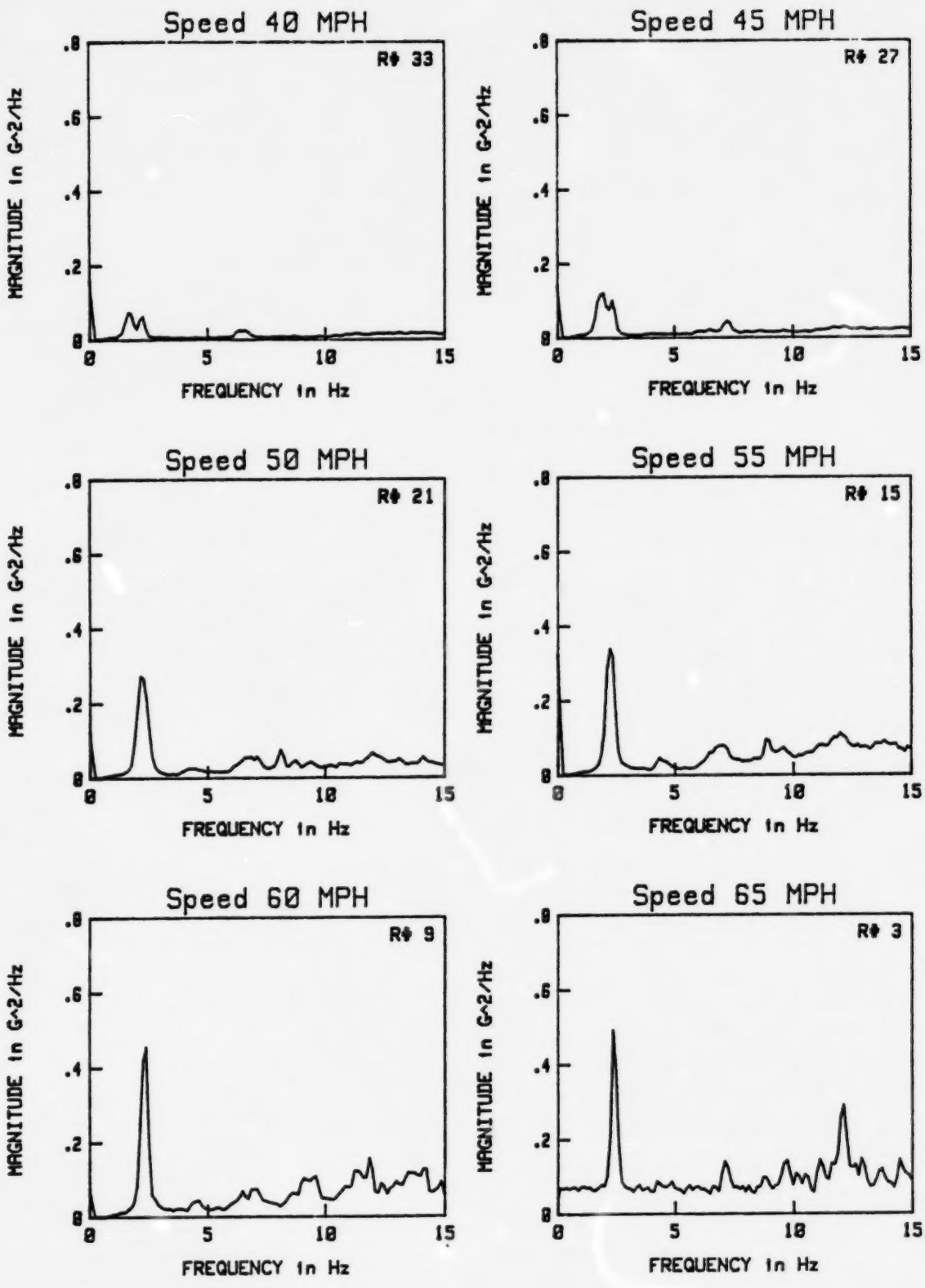

UTDC (RETROFIT) 100 TON LEADING TRUCK

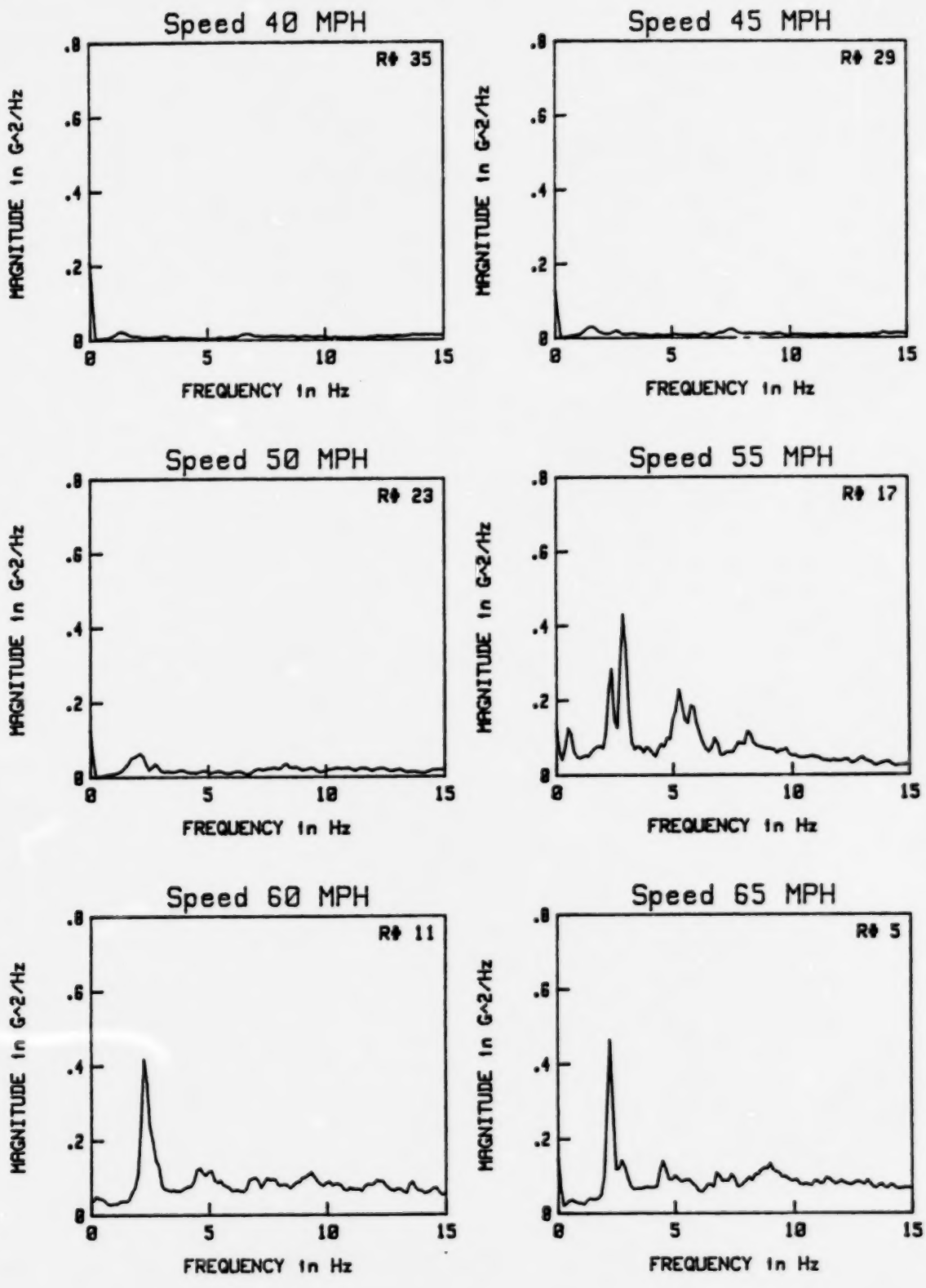

REFERENCE 100 TON LEADING TRUCK

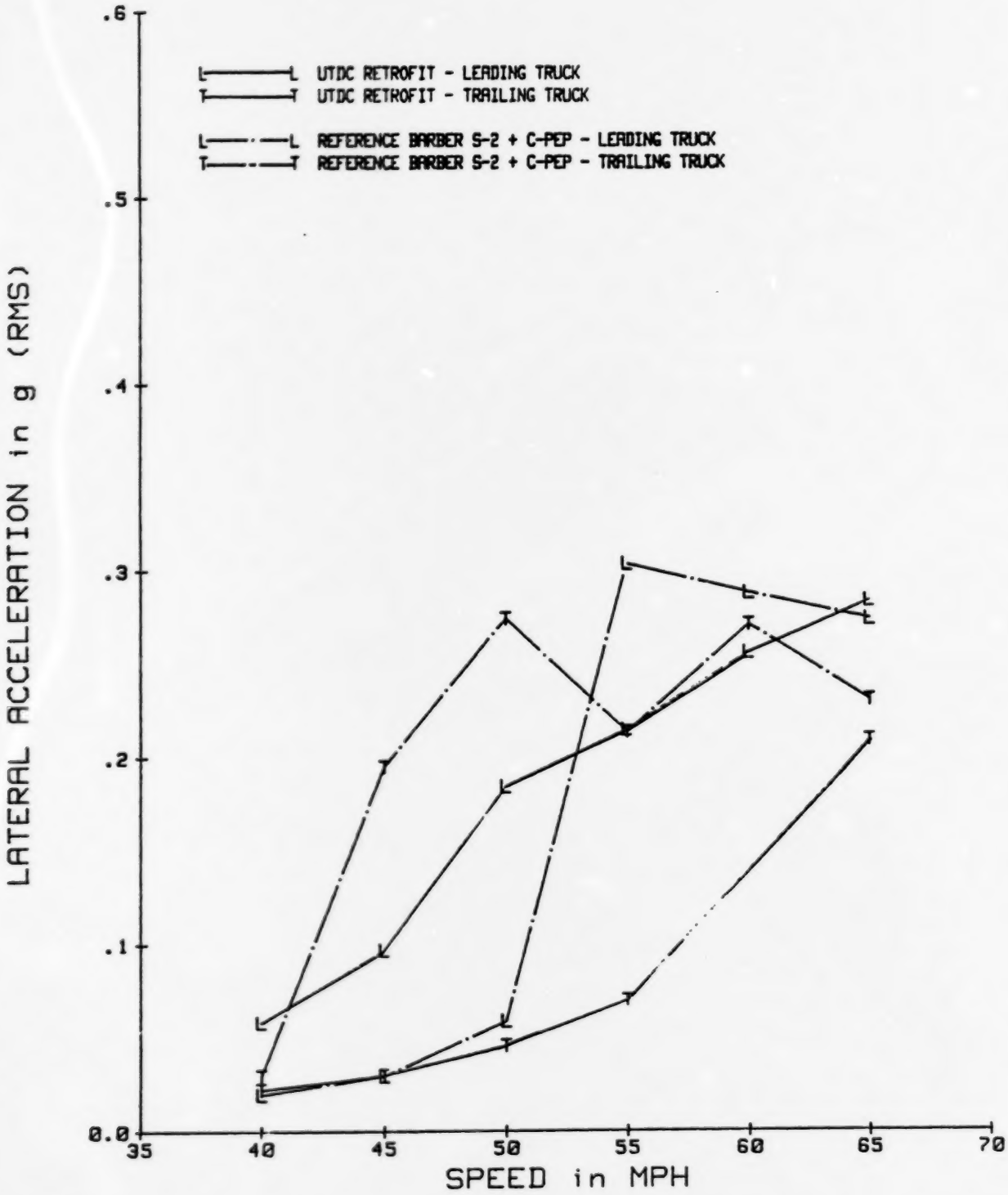

LATERAL ACCELERATION ON LEAD AXLE BEARING ENDCAP vs SPEED FOR TRUCKS WITH SERVICE WORN WHEELS ON EMPTY 100-TON BATHTUB COAL CARS

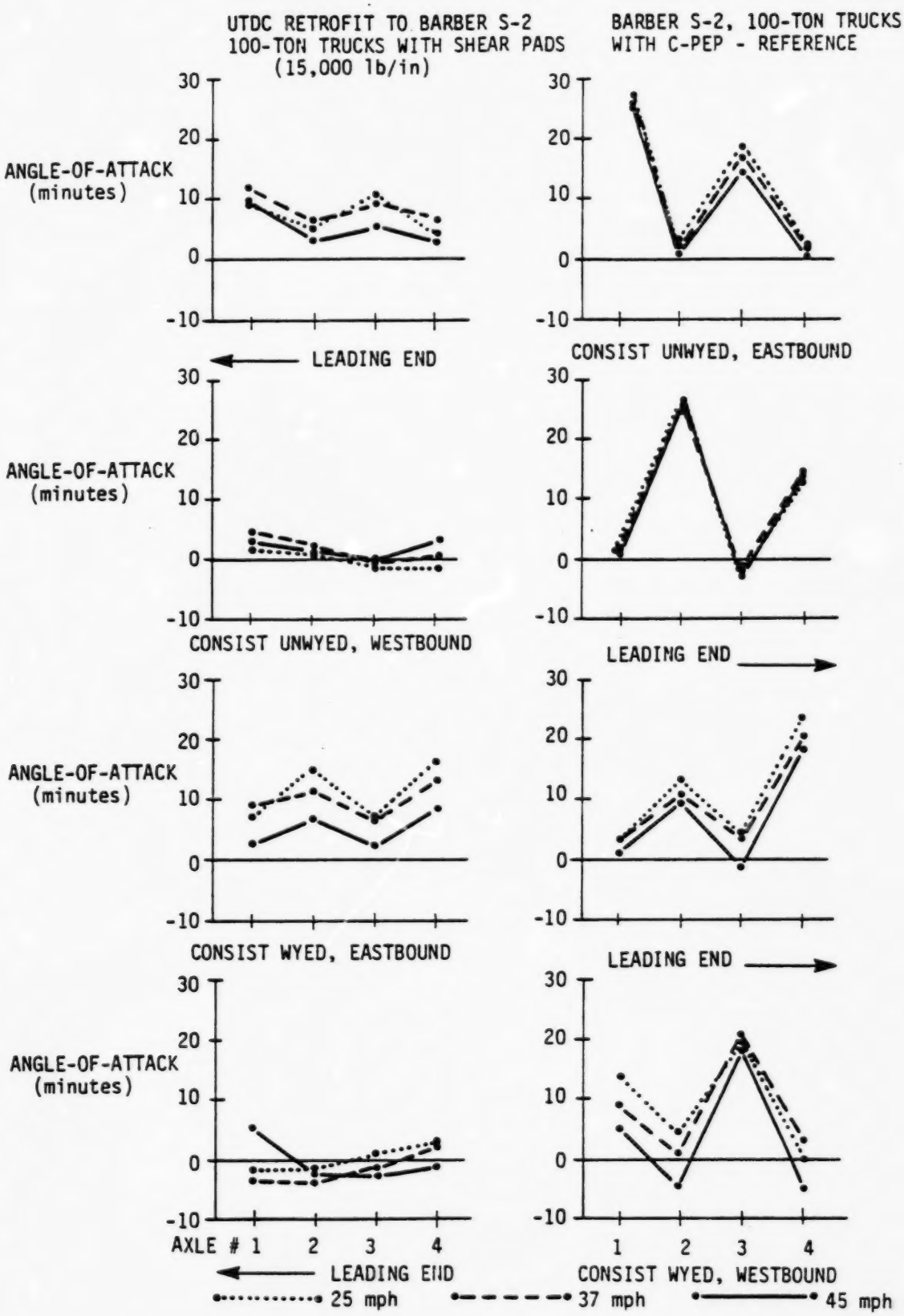

FIG. : ANGLE-OF-ATTACK FOR THE RETROFIT AND CONVENTIONAL 100-TON TRUCKS AT 25 mph, 37 mph AND 45 mph IN THE UNWYED AND WYED POSITION WITH NEW HEUMANN PROFILE WHEELS

Consist	Direction	Angle-of-Attack (Minutes)							
		UTDC Retrofit (100-Ton Bathtub Coal Car)				Reference BS-2 With C-Pep (100-Ton Bathtub Coal Car)			
Unwyed	Eastbound	9.2	5.3	10.3	4.3	27.1	3.7	18.3	2.7
	Δ_1	3.9		6.0		23.4		15.6	
	Westbound	1.8	0.5	-1.2	-1.4	1.1	26.3	-2.5	13.5
	Δ_2	1.3		0.2		25.2		16.0	
Wyed	Eastbound	6.6	15.1	7.8	16.2	3.3	13.2	4.7	23.5
	Δ_3	8.5		8.4		9.9		18.8	
	Westbound	-1.4	-1.4	1.5	3.1	13.5	4.2	19.6	0.8
	Δ_4	0		1.6		8.3		18.8	
$\sum_i \frac{\Delta_i}{4}$		3.4		4.0		16.7		17.3	

Δ_i - difference in angle-of-attack for the 2 axles in each truck.

100-Ton Bathtub laden cars with new Heumann profile wheels

Angle-of-Attack of Leading and Trailing Axles Measured at 25 mph

Consist	Direction	Angle-of-Attack (Minutes)							
		UTDC Retrofit (100-Ton Bathtub Coal Car)				Reference BS-2 With C-Pep (100-Ton Bathtub Coal Car)			
Unwyed	Eastbound	11.8	6.1	9.2	6.2	26.7	2.2	17.1	2.1
	Δ_1	5.7		3.0		24.5		15.0	
	Westbound	4.3	2.3	-0.7	0.6	1.7	25.8	-1.7	14.4
	Δ_2	2.0		1.3		24.1		16.1	
Wyed	Eastbound	9.0	11.7	6.7	13.3	2.9	10.9	3.5	20.5
	Δ_3	2.7		6.6		8.0		17.0	
	Westbound	-3.7	-3.9	-1.2	2.3	9.3	0.3	20.6	3.3
	Δ_4	0.2		3.5		9.3		17.3	
$\sum_i \frac{\Delta_i}{4}$		2.6		3.6		16.9		16.35	

Δ_i - difference in angle-of-attack for the 2 axles in each truck.

100-Ton Bathtub laden cars with new Heumann profile wheels

Angle-of-Attack of Leading and Trailing Axles Measured at 37 mph

Consist	Direction	Angle-of-Attack (Minutes)							
		UTDC Retrofit (100-Ton Bathtub Coal Car)				Reference BS-2 With C-Pep (100-Ton Bathtub Coal Car)			
Unwyed	Eastbound	9.0	3.1	5.1	2.5	26.2	1.3	14.6	0.0
	Δ_1	5.9		2.6		24.9		14.6	
	Westbound	3.0	1.2	0.1	3.1	-0.6	24.6	-2.7	14.1
	Δ_2	1.8		3.0		25.2		16.8	
Wyed	Eastbound	2.9	7.0	2.1	8.1	0.8	9.7	-1.3	18.9
	Δ_3	4.1		6.0		8.9		20.2	
	Westbound	5.6	-2.1	-3.1	-1.0	5.7	-4.7	18.5	-4.2
	Δ_4	7.7		2.1		10.4		22.7	
$\sum_i \frac{\Delta_i}{4}$		4.8		3.4		17.3		18.5	

Δ_i - difference in angle-of-attack for the 2 axles in each truck.

100-Ton Bathtub laden cars with new Heumann profile wheels

Angle-of-Attack of Leading and Trailing Axles Measured at 45 mph

APPENDIX J

WHEEL PROFILES

FOR

REPROFILED AND WORN WHEELS

STANDARD AND MODIFIED TRUCKS

APPENDIX J

This appendix contains wheel profile tracings of the wheels under Cars Serial Number 5021 and 5093 equipped with standard Barber S-2 trucks, and Cars Serial Number 5022 and 5029 equipped with frame-braced modified Barber S-2 trucks.

All of the trucks were reconditioned and the sideframes matched button-for-button prior to assembly. The wheels of Cars 5021 and 5022 were reconditioned with the first wear reprofiling. Cars 5029 and 5013 were outfitted with new wheels.

Car 5021 currently has achieved 23,960 km (14,882 mi) of test and service usage. Car 5022 has achieved 24,509 km (15,223 mi) of test and service usage. Both cars were tested and began service running together.

Car 5029 has achieved 21,087 km (13,096 mi) while Car 5093 has achieved 19,591 km (12,712 mi) of test and service usage.

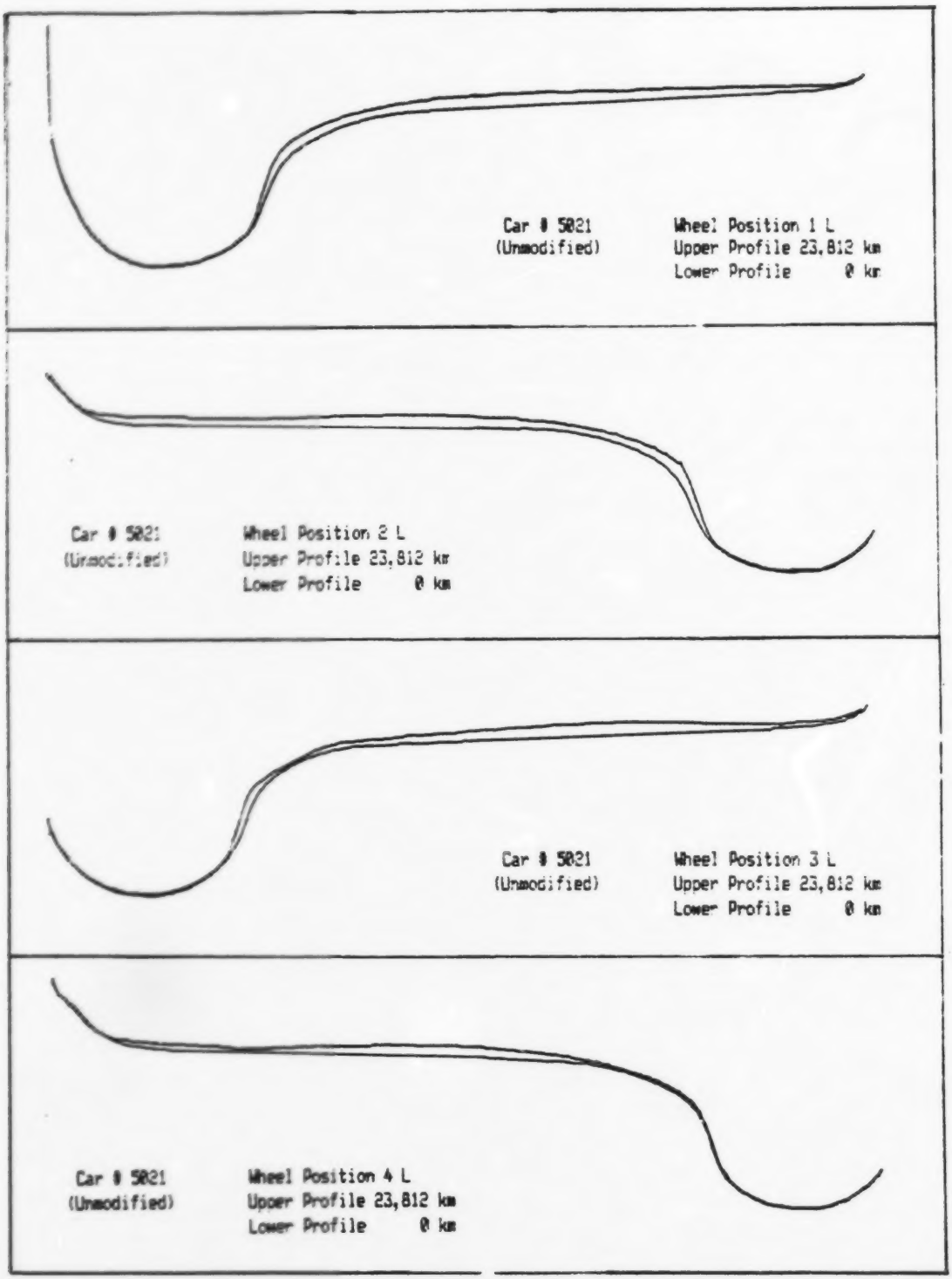
Car # 5021
(Unmodified)
Wheel Position 1 L
Upper Profile 23,812 km
Lower Profile 0 km
Car # 5021
(Unmodified)
Wheel Position 2 L
Upper Profile 23,812 km
Lower Profile 0 km
Car # 5021
(Unmodified)
Wheel Position 3 L
Upper Profile 23,812 km
Lower Profile 0 km
Car # 5021
(Unmodified)
Wheel Position 4 L
Upper Profile 23,812 km
Lower Profile 0 km

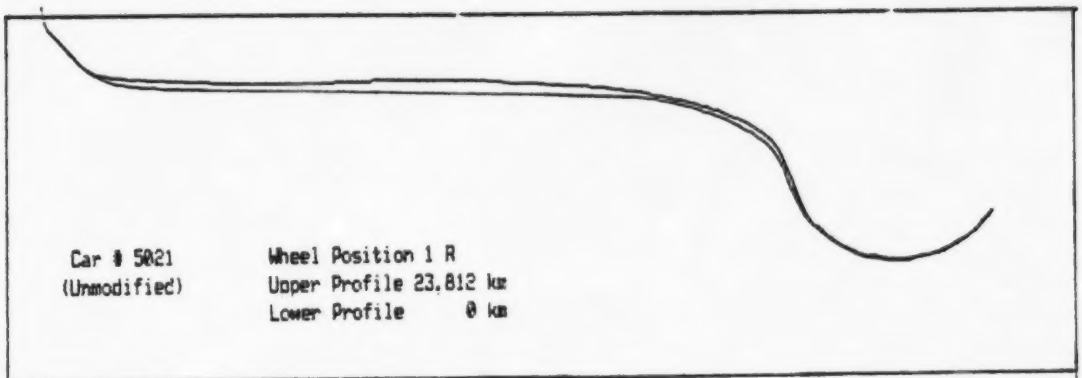

Car # 5021
(Unmodified)

Wheel Position 1 R
Upper Profile 23,812 km
Lower Profile 0 km

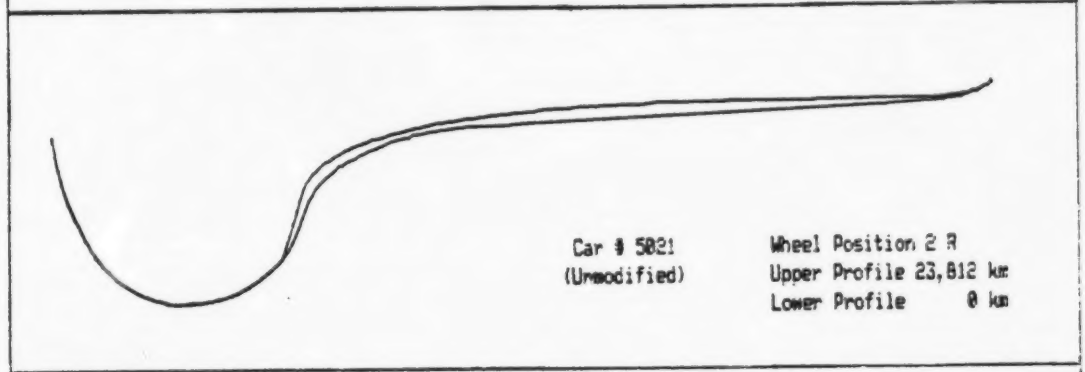

Car # 5021
(Unmodified)

Wheel Position 2 R
Upper Profile 23,812 km
Lower Profile 0 km

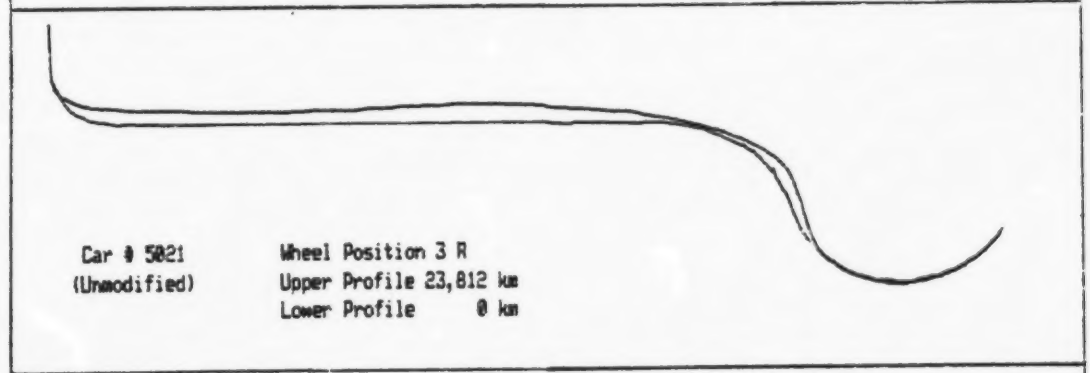

Car # 5021
(Unmodified)

Wheel Position 3 R
Upper Profile 23,812 km
Lower Profile 0 km

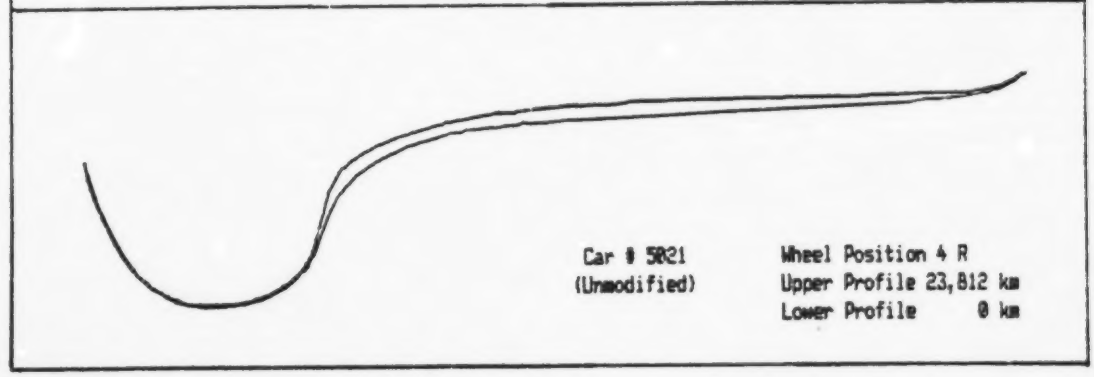

Car # 5021
(Unmodified)

Wheel Position 4 R
Upper Profile 23,812 km
Lower Profile 0 km

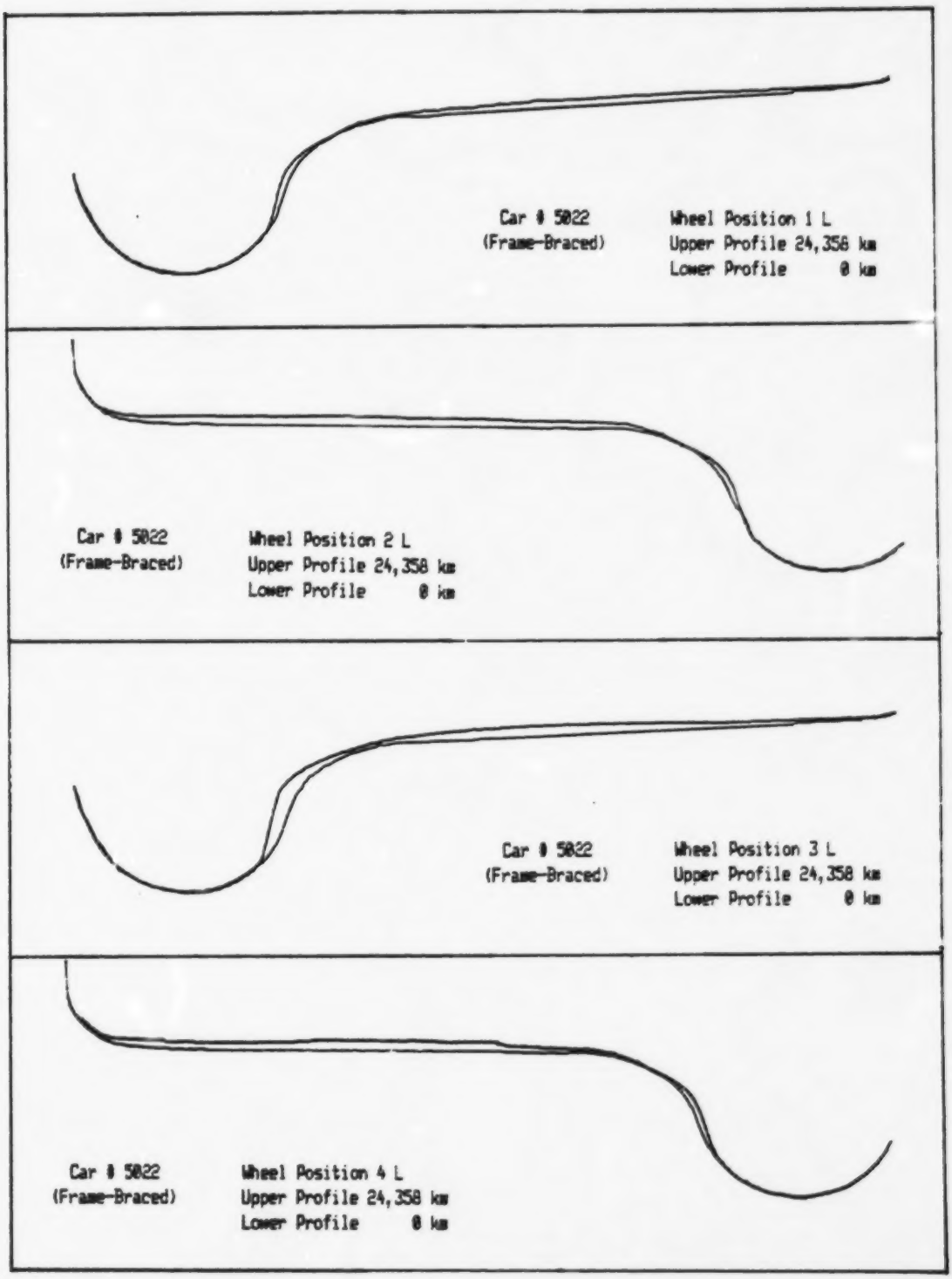
Car # 5022
(Frame-Braced)
Wheel Position 1 L
Upper Profile 24,358 km
Lower Profile 0 km
Car # 5022
(Frame-Braced)
Wheel Position 2 L
Upper Profile 24,358 km
Lower Profile 0 km
Car # 5022
(Frame-Braced)
Wheel Position 3 L
Upper Profile 24,358 km
Lower Profile 0 km
Car # 5022
(Frame-Braced)
Wheel Position 4 L
Upper Profile 24,358 km
Lower Profile 0 km

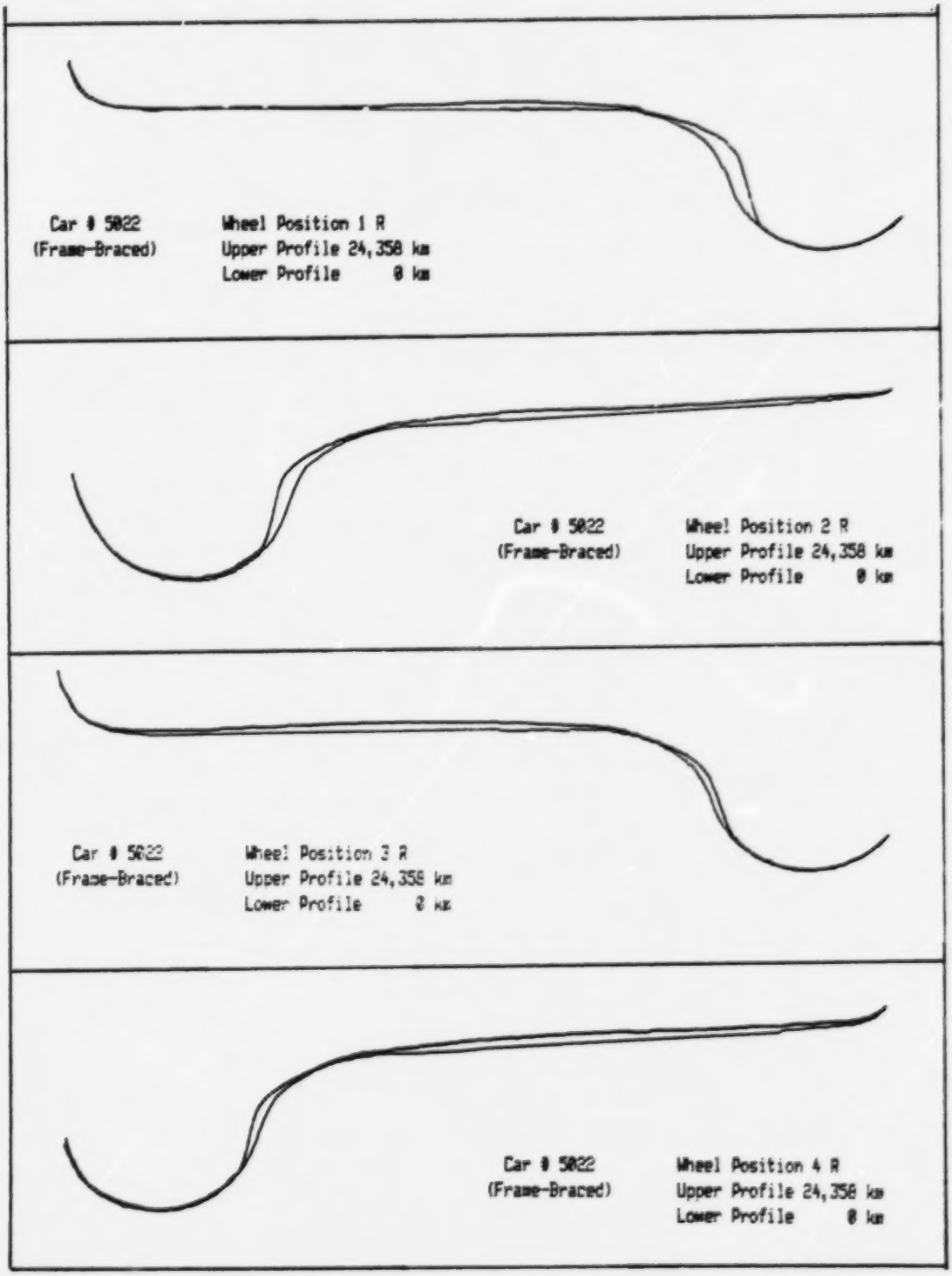
Car # 5022
(Frame-Braced)
Wheel Position 1 R
Upper Profile 24,358 km
Lower Profile 0 km
Car # 5022
(Frame-Braced)
Wheel Position 2 R
Upper Profile 24,358 km
Lower Profile 0 km
Car # 5022
(Frame-Braced)
Wheel Position 3 R
Upper Profile 24,358 km
Lower Profile 0 km
Car # 5022
(Frame-Braced)
Wheel Position 4 R
Upper Profile 24,358 km
Lower Profile 0 km

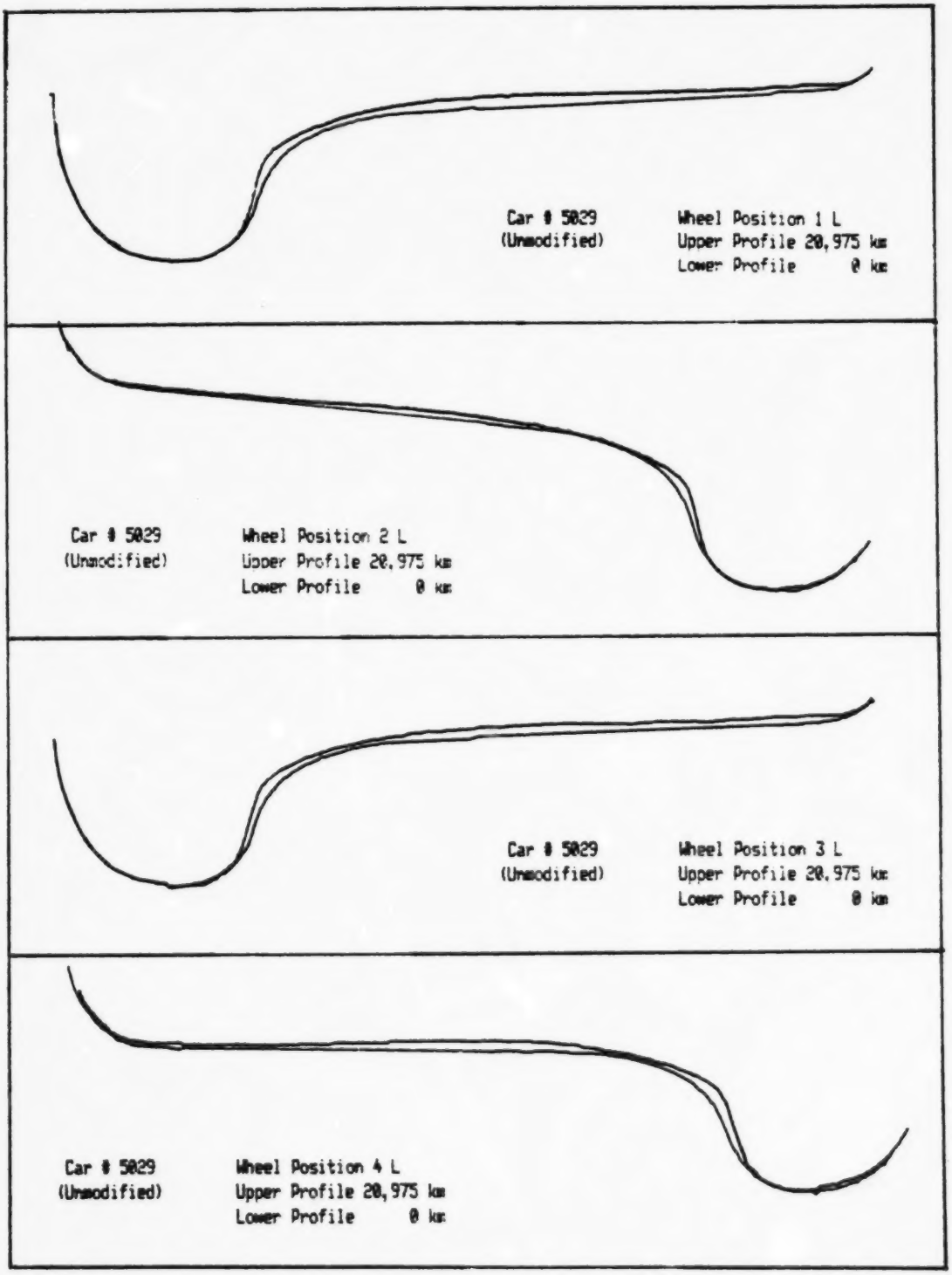
Car # 5029
(Unmodified)
Wheel Position 1 L
Upper Profile 20,975 km
Lower Profile 0 km
Car # 5029
(Unmodified)
Wheel Position 2 L
Upper Profile 20,975 km
Lower Profile 0 km
Car # 5029
(Unmodified)
Wheel Position 3 L
Upper Profile 20,975 km
Lower Profile 0 km
Car # 5029
(Unmodified)
Wheel Position 4 L
Upper Profile 20,975 km
Lower Profile 0 km

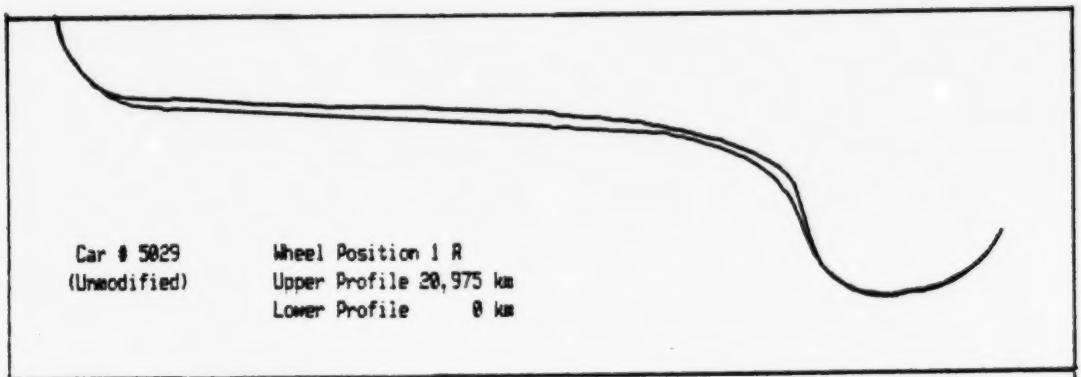
Car # 5029
(Unmodified)
Wheel Position 1 R
Upper Profile 20,975 km
Lower Profile 0 km

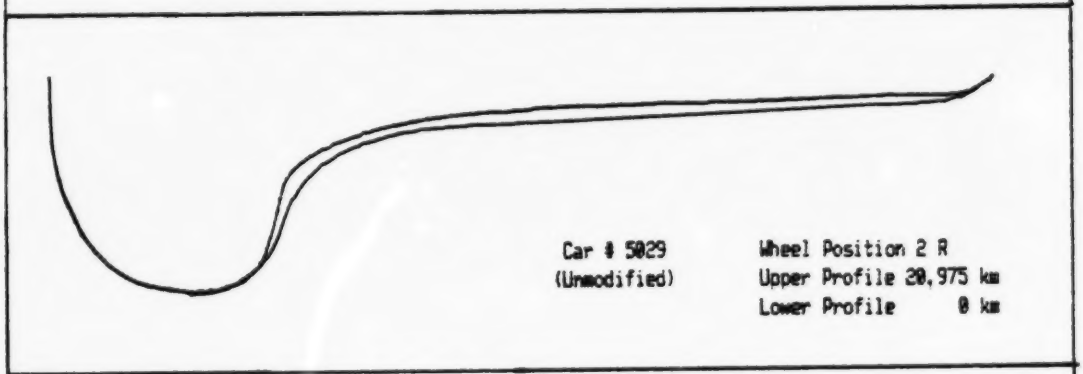
Car # 5029
(Unmodified)
Wheel Position 2 R
Upper Profile 20,975 km
Lower Profile 0 km

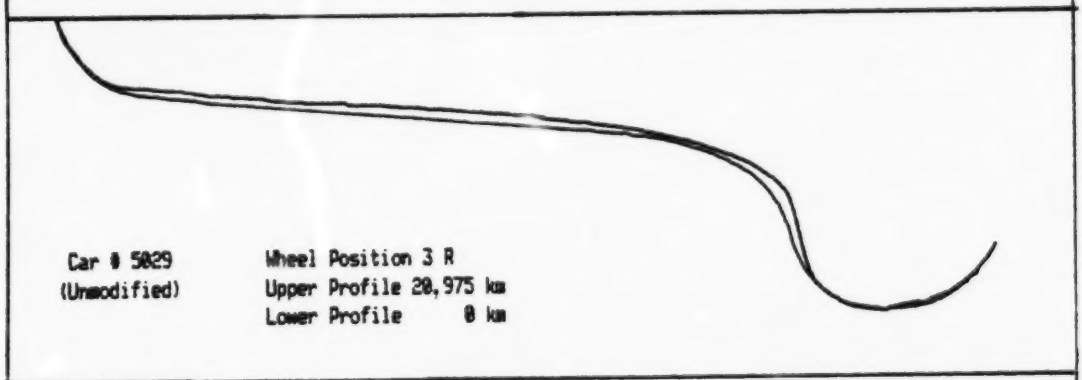
Car # 5029
(Unmodified)
Wheel Position 3 R
Upper Profile 20,975 km
Lower Profile 0 km

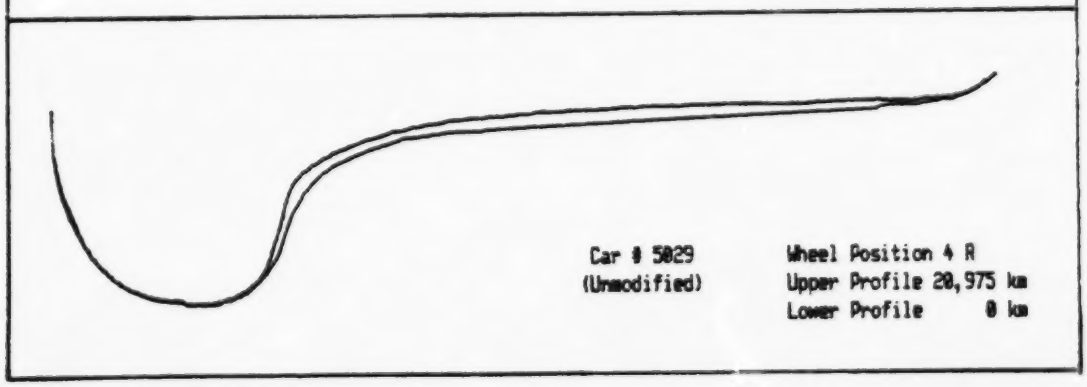
Car # 5029
(Unmodified)
Wheel Position 4 R
Upper Profile 20,975 km
Lower Profile 0 km

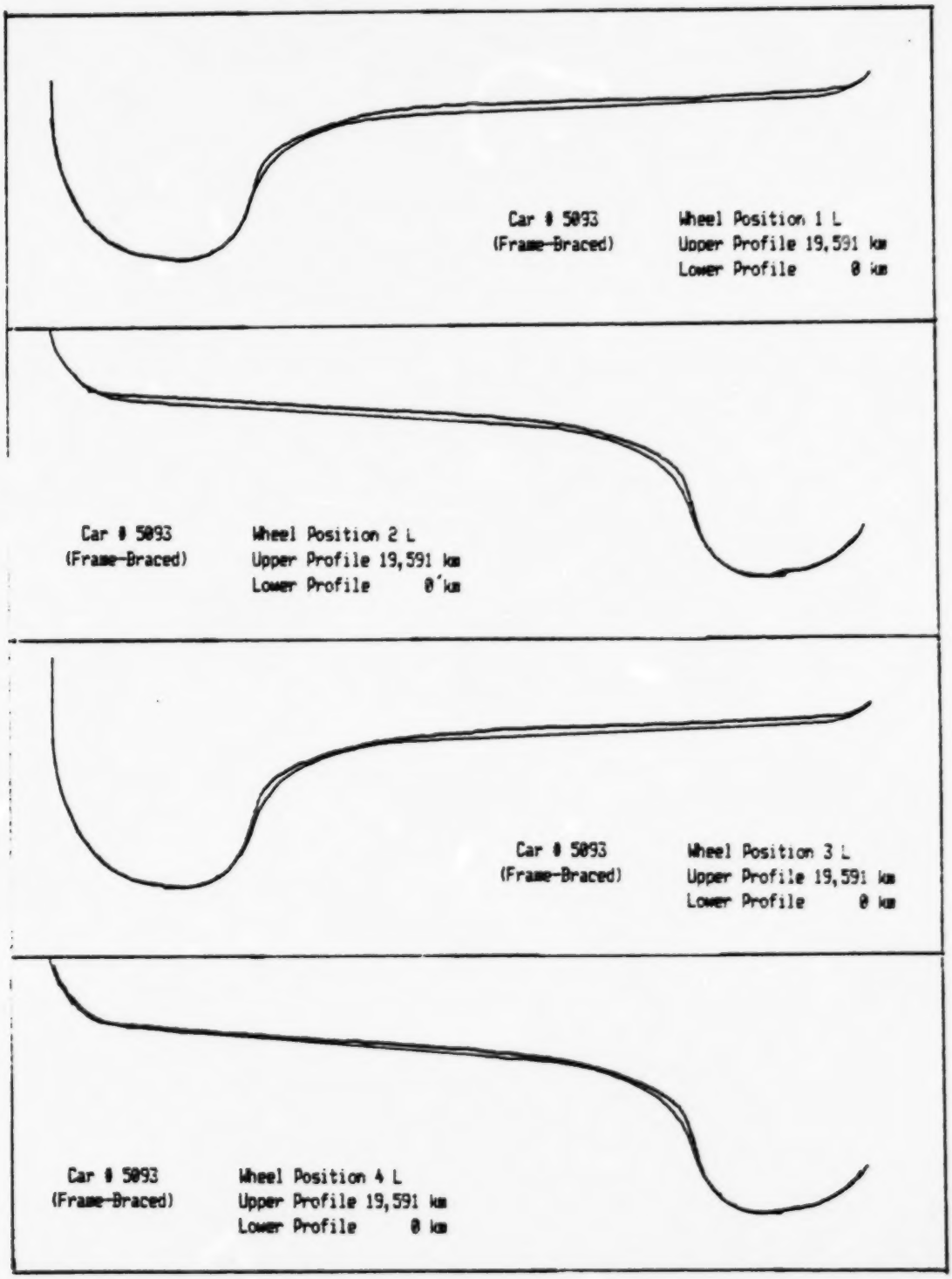
Car # 5093
(Frame-Braced)
Wheel Position 1 L
Upper Profile 19,591 km
Lower Profile 0 km
Car # 5093
(Frame-Braced)
Wheel Position 2 L
Upper Profile 19,591 km
Lower Profile 0 km
Car # 5093
(Frame-Braced)
Wheel Position 3 L
Upper Profile 19,591 km
Lower Profile 0 km
Car # 5093
(Frame-Braced)
Wheel Position 4 L
Upper Profile 19,591 km
Lower Profile 0 km

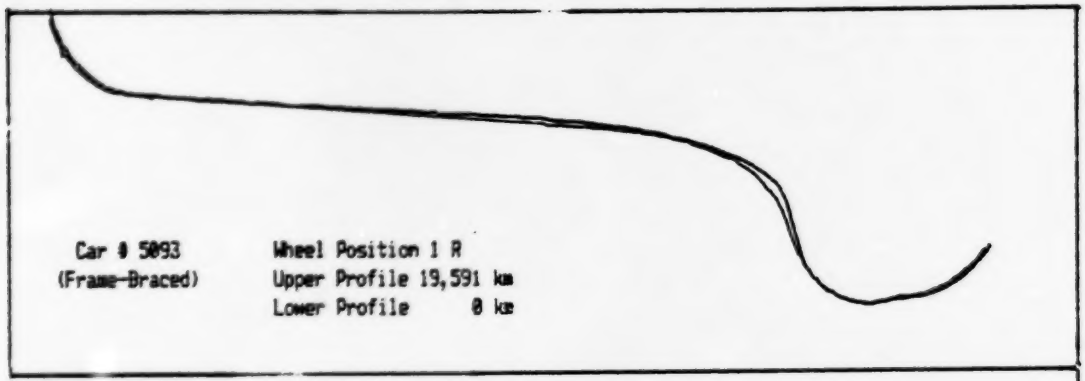

Car # 5093
(Frame-Braced)

Wheel Position 1 R
Upper Profile 19,591 km
Lower Profile 0 km

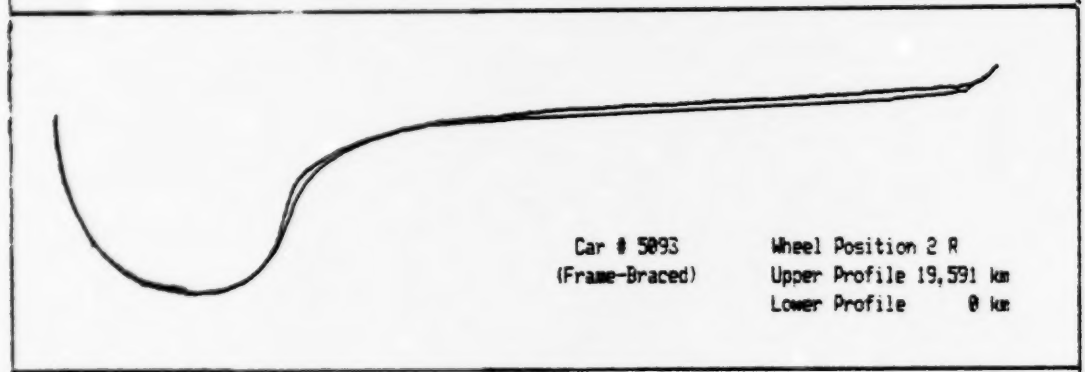

Car # 5093
(Frame-Braced)

Wheel Position 2 R
Upper Profile 19,591 km
Lower Profile 0 km

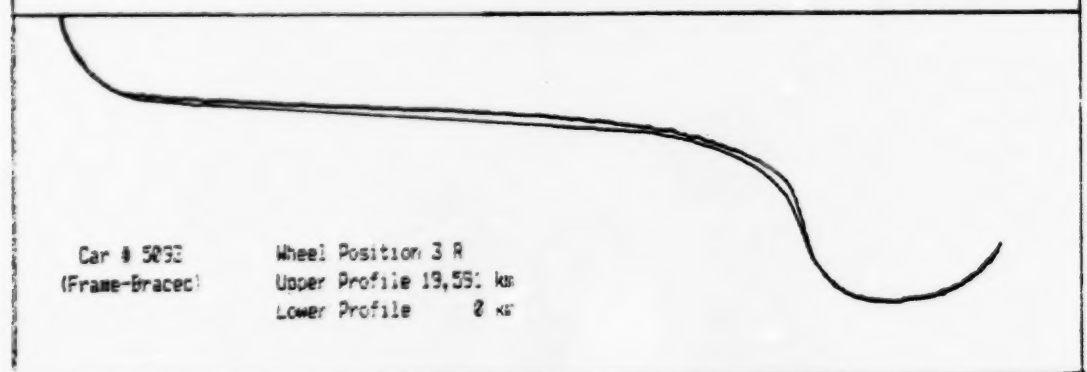

Car # 5093
(Frame-Braced)

Wheel Position 3 R
Upper Profile 19,591 km
Lower Profile 0 km

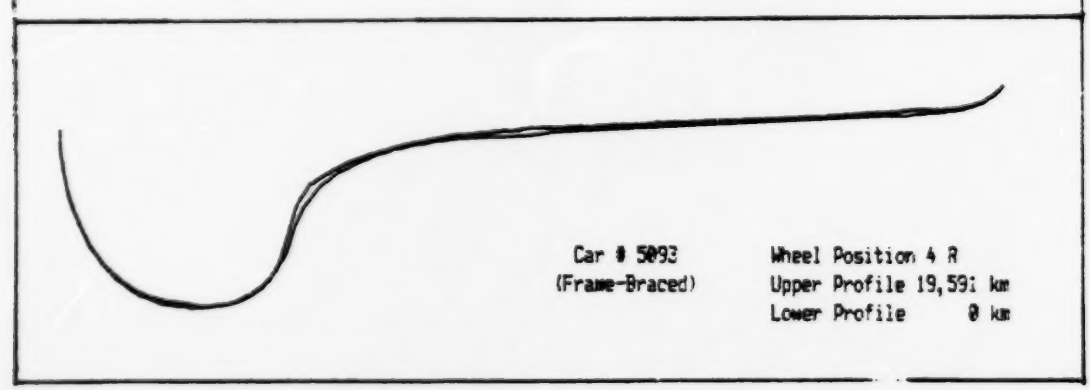

Car # 5093
(Frame-Braced)

Wheel Position 4 R
Upper Profile 19,591 km
Lower Profile 0 km

APPENDIX K

WHEEL PROFILES FROM BURLINGTON NORTHERN

COAL CARS

APPENDIX K

This appendix contains the results of wheel wear monitoring of the Frame Braced trucks installed under three 100 ton coal cars on the Burlington Northern Railroad. Specifically, the frame bracing has been retrofitted to the following trucks.

- American Steel Foundries Ride Control (Car 527590);
- Barber S-2-C (car 528015); and
- National Castings Incorporated Super C-1 (Car 527563).

Pages 1 through 6 contain computer regenerated wheel profiles taken at 100,000 miles (160,000 km), 50,000 miles (80,000 km) and new (top to bottom of each) for the three test cars. It is clearly evident that the wear in all cases between 50,000 and 100,000 miles is extremely small and in some cases barely evident.

Pages 7 through 9 contain computer regenerated wheel profiles taken at 100,000 miles for the test cars and the comparable control cars (527604/Asiz, 528009/Barber, 567607/NCI). In all cases but one, the control (non-frame-braced) car wheel profile is above that of the frame-braced unit, showing significantly more wear especially at the flange. The exception (marked with an asterisk *) is wheel 3R of Cars 527563 and 527607 where the wheel on the frame-braced truck wheel has worn more than that on the conventional truck. No reason has been found for this apparent anomaly.

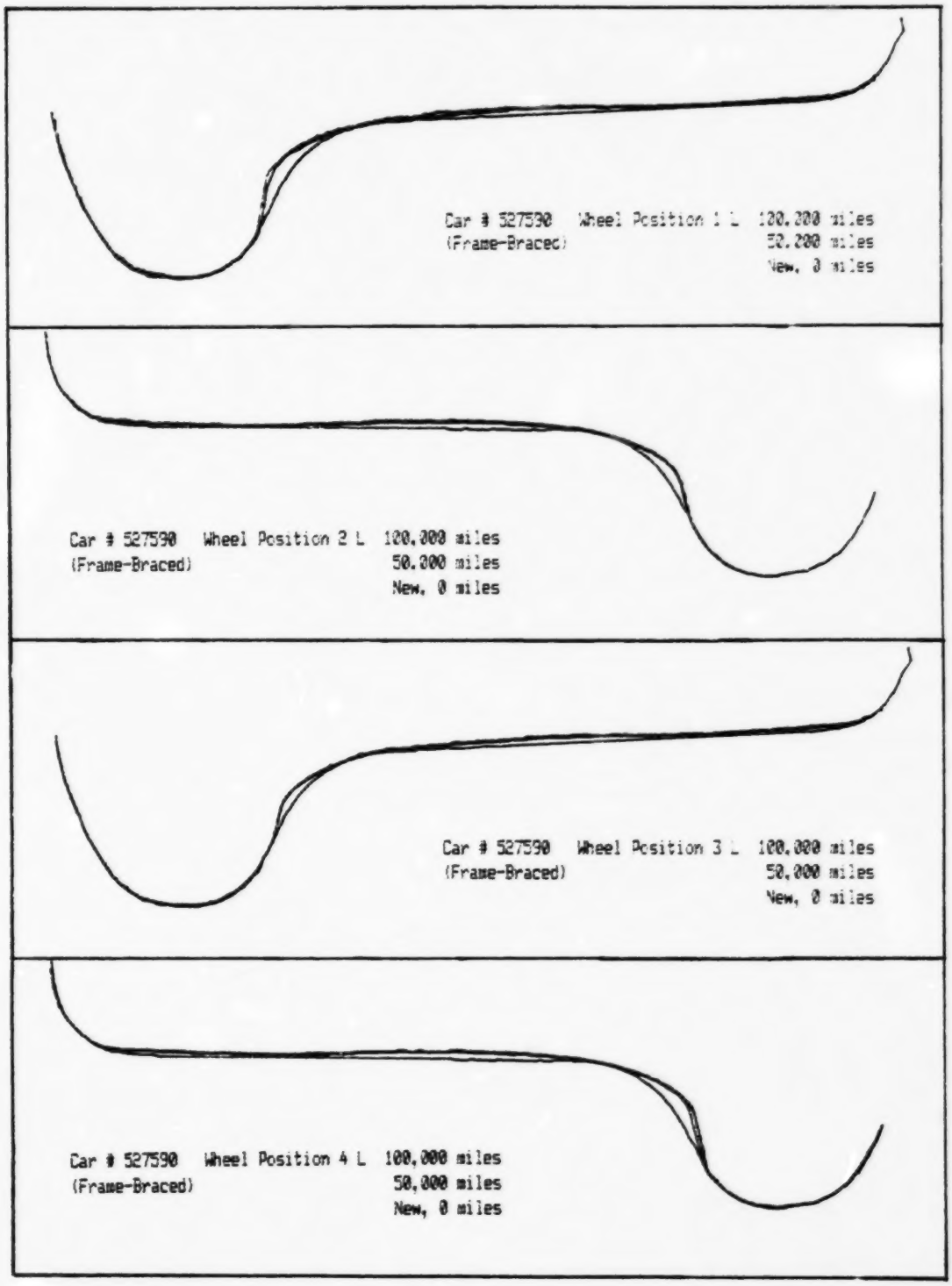
Car # 527590 Wheel Position 1 L 100,000 miles
(Frame-Braced) 50,000 miles
New, 0 miles
Car # 527590 Wheel Position 2 L 100,000 miles
(Frame-Braced) 50,000 miles
New, 0 miles
Car # 527590 Wheel Position 3 L 100,000 miles
(Frame-Braced) 50,000 miles
New, 0 miles
Car # 527590 Wheel Position 4 L 100,000 miles
(Frame-Braced) 50,000 miles
New, 0 miles

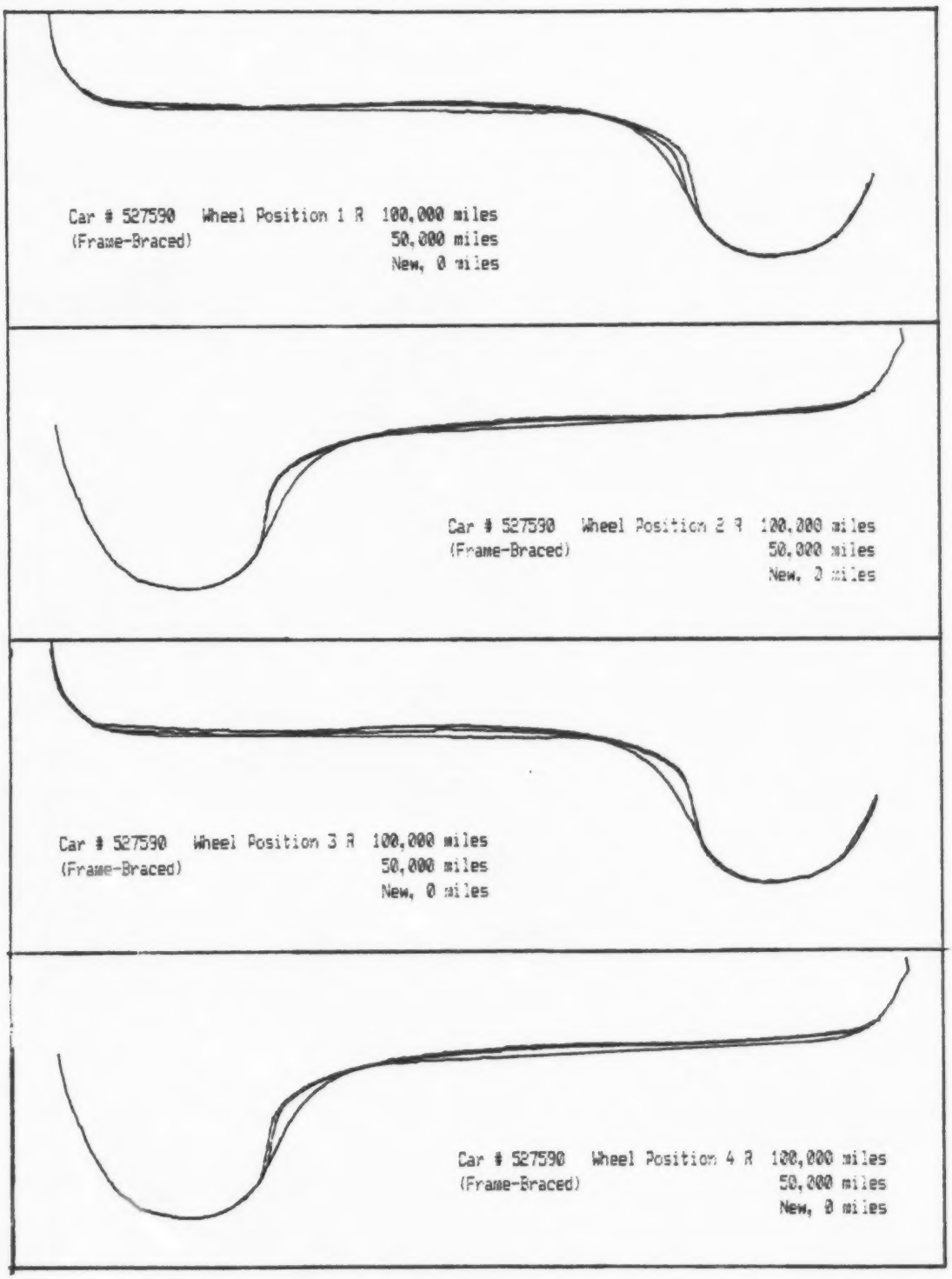
Car # 527590 Wheel Position 1 R 100,000 miles
(Frame-Braced) 50,000 miles
New, 0 miles
Car # 527590 Wheel Position 2 R 100,000 miles
(Frame-Braced) 50,000 miles
New, 0 miles
Car # 527590 Wheel Position 3 R 100,000 miles
(Frame-Braced) 50,000 miles
New, 0 miles
Car # 527590 Wheel Position 4 R 100,000 miles
(Frame-Braced) 50,000 miles
New, 0 miles

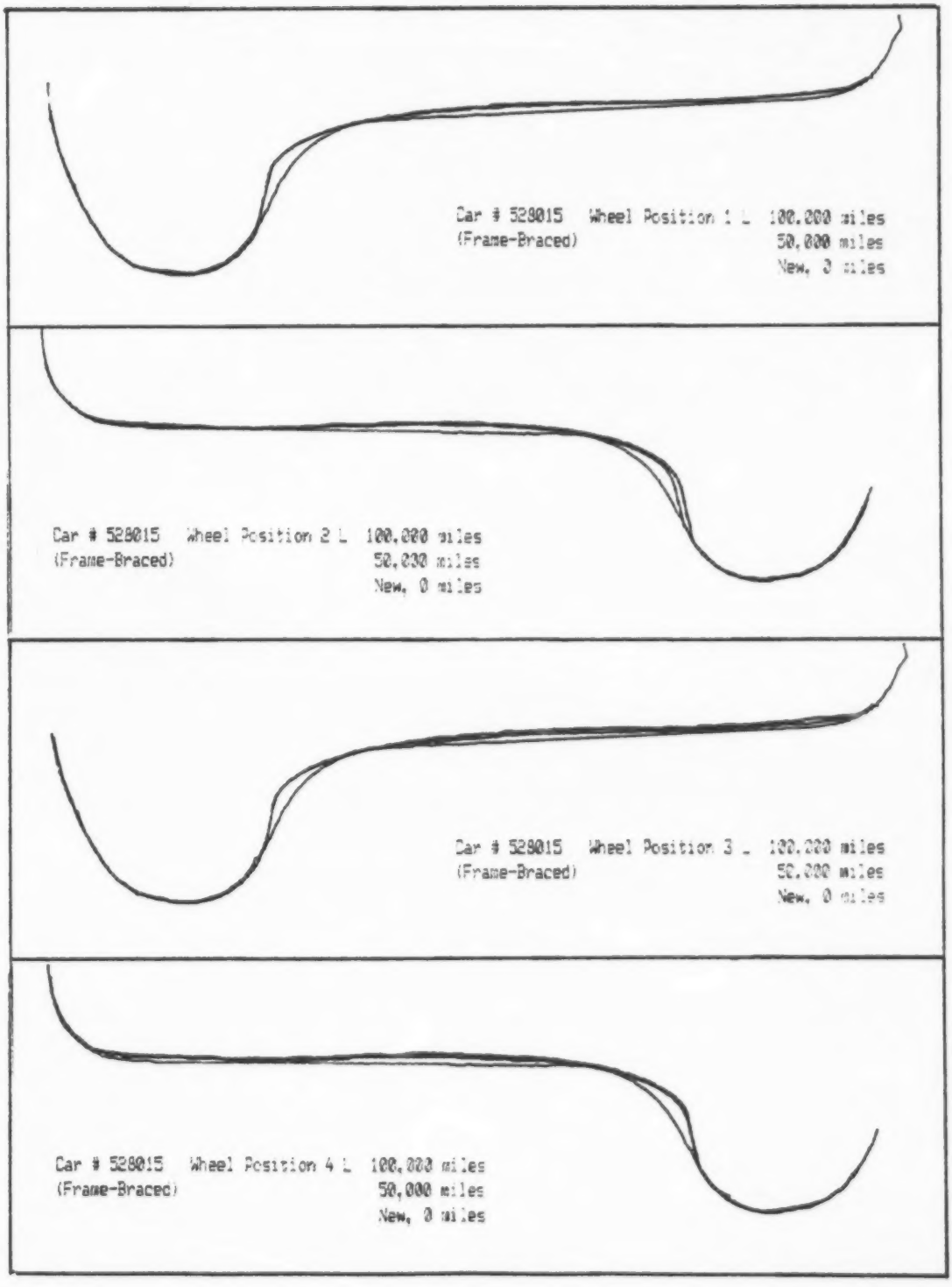
Car # 528015 Wheel Position 1 L 100,000 miles
(Frame-Braced) 50,000 miles
New, 0 miles
Car # 528015 Wheel Position 2 L 100,000 miles
(Frame-Braced) 50,000 miles
New, 0 miles
Car # 528015 Wheel Position 3 L 100,000 miles
(Frame-Braced) 50,000 miles
New, 0 miles
Car # 528015 Wheel Position 4 L 100,000 miles
(Frame-Braced) 50,000 miles
New, 0 miles

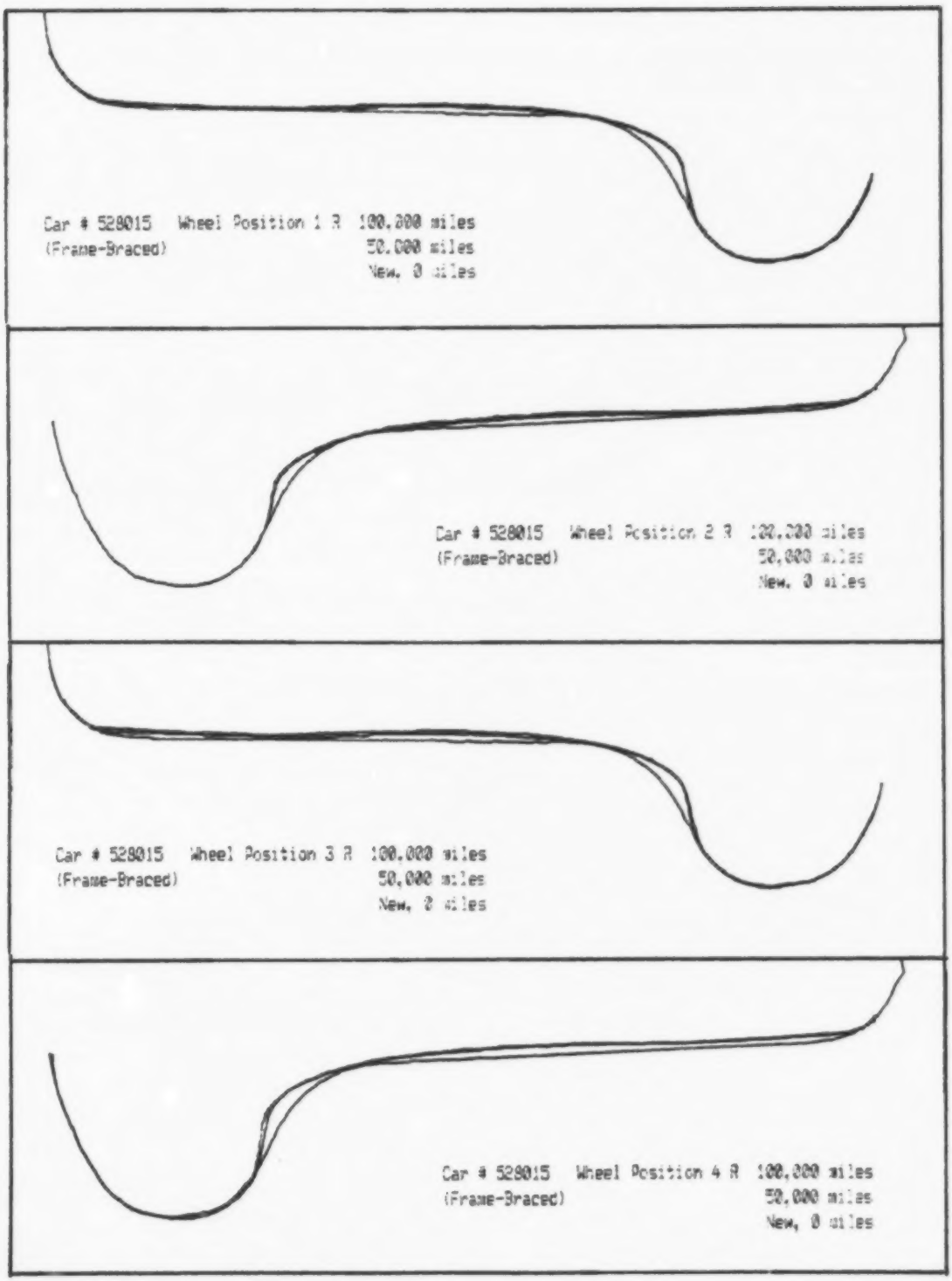
Car # 528015 Wheel Position 1 R 100,000 miles
(Frame-Braced) 50,000 miles
New, 0 miles
Car # 528015 Wheel Position 2 R 100,000 miles
(Frame-Braced) 50,000 miles
New, 0 miles
Car # 528015 Wheel Position 3 R 100,000 miles
(Frame-Braced) 50,000 miles
New, 0 miles
Car # 528015 Wheel Position 4 R 100,000 miles
(Frame-Braced) 50,000 miles
New, 0 miles

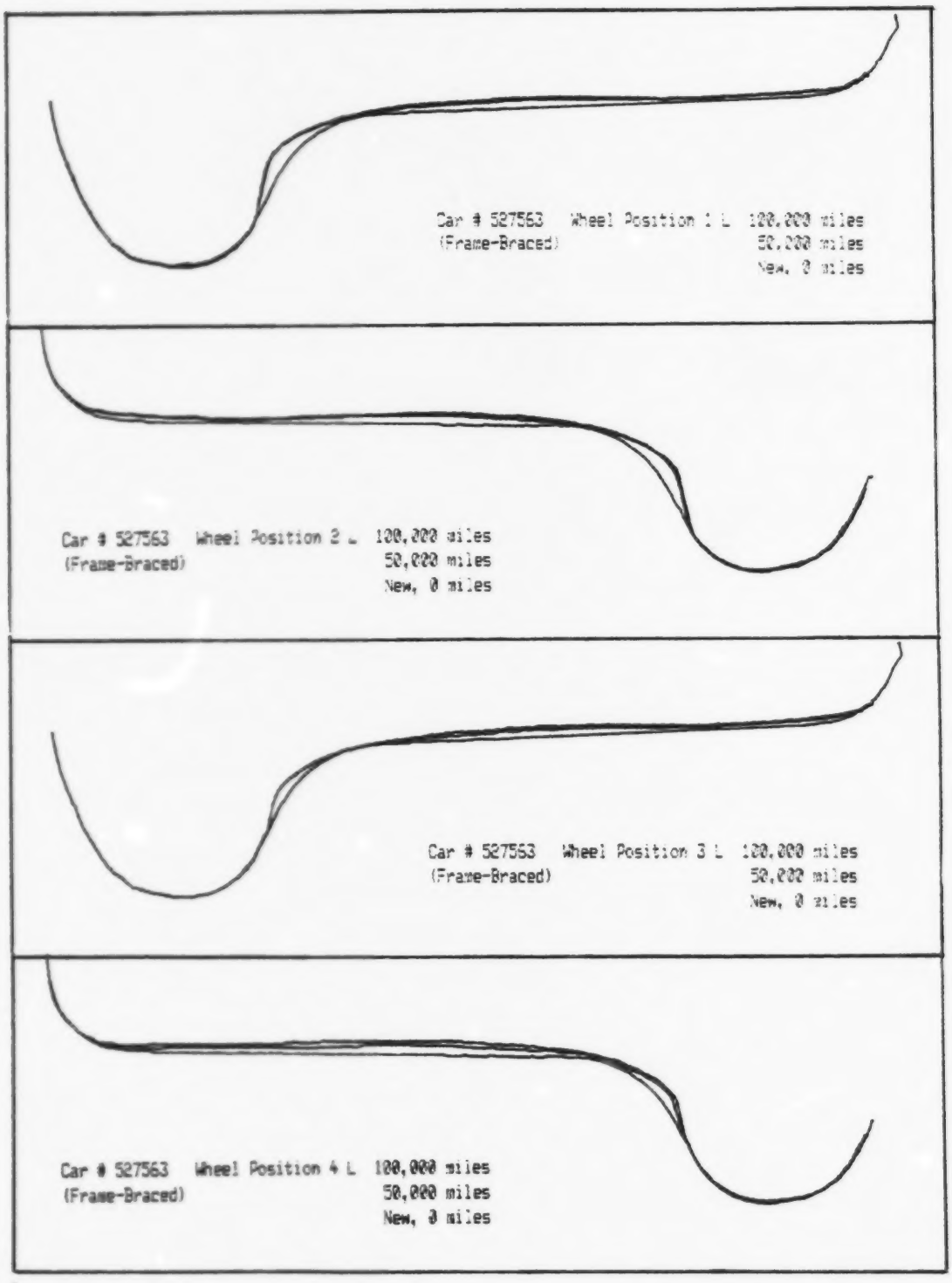
Car # 527563 Wheel Position 1 L 100,000 miles
(Frame-Braced) 50,000 miles
New, 0 miles
Car # 527563 Wheel Position 2 L 100,000 miles
(Frame-Braced) 50,000 miles
New, 0 miles
Car # 527563 Wheel Position 3 L 100,000 miles
(Frame-Braced) 50,000 miles
New, 0 miles
Car # 527563 Wheel Position 4 L 100,000 miles
(Frame-Braced) 50,000 miles
New, 0 miles

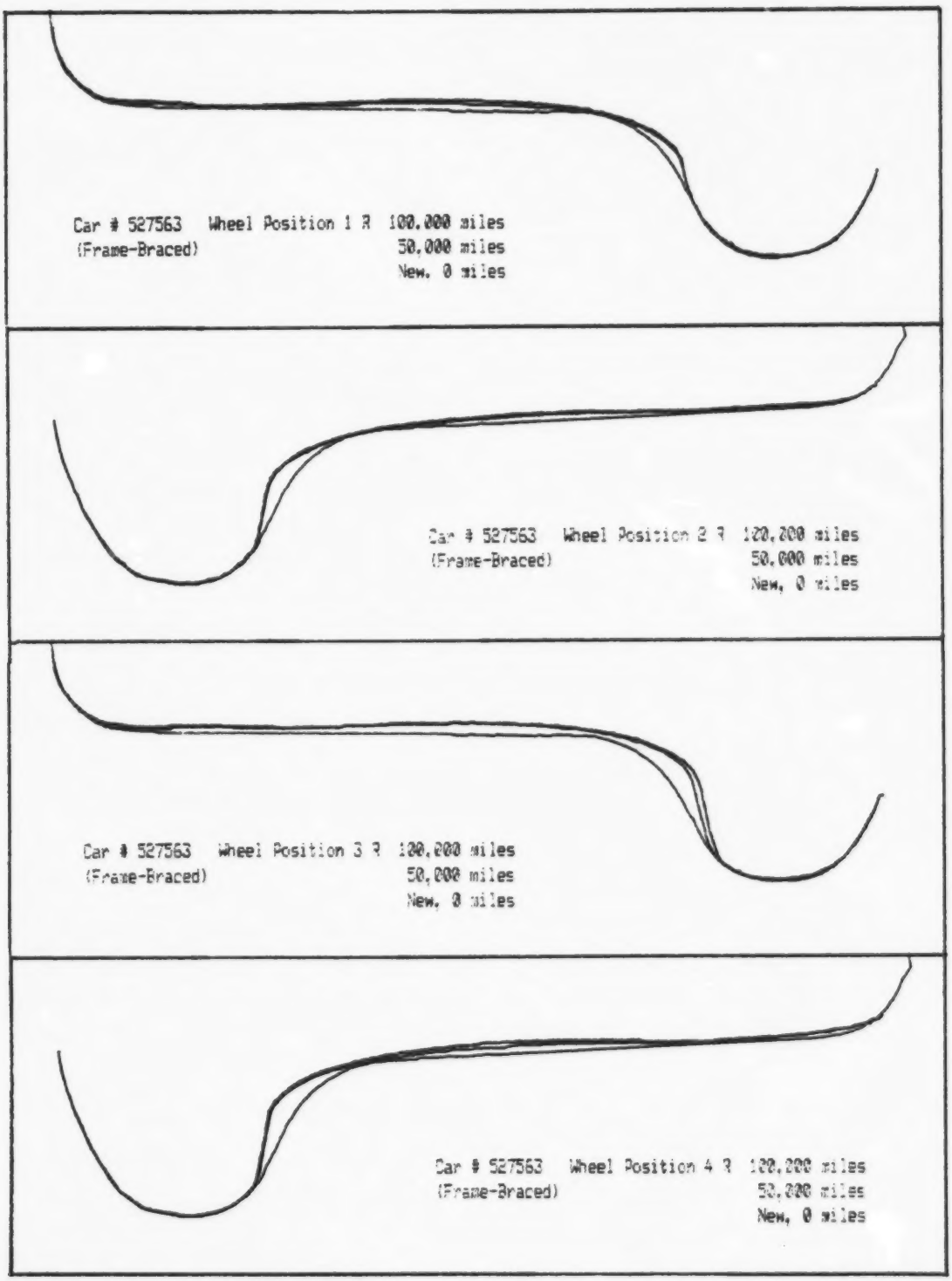
Car # 527563 Wheel Position 1 ? 100,000 miles
(Frame-Braced) 50,000 miles
New, 0 miles
Car # 527563 Wheel Position 2 ? 100,000 miles
(Frame-Braced) 50,000 miles
New, 0 miles
Car # 527563 Wheel Position 3 ? 100,000 miles
(Frame-Braced) 50,000 miles
New, 0 miles
Car # 527563 Wheel Position 4 ? 100,000 miles
(Frame-Braced) 50,000 miles
New, 0 miles

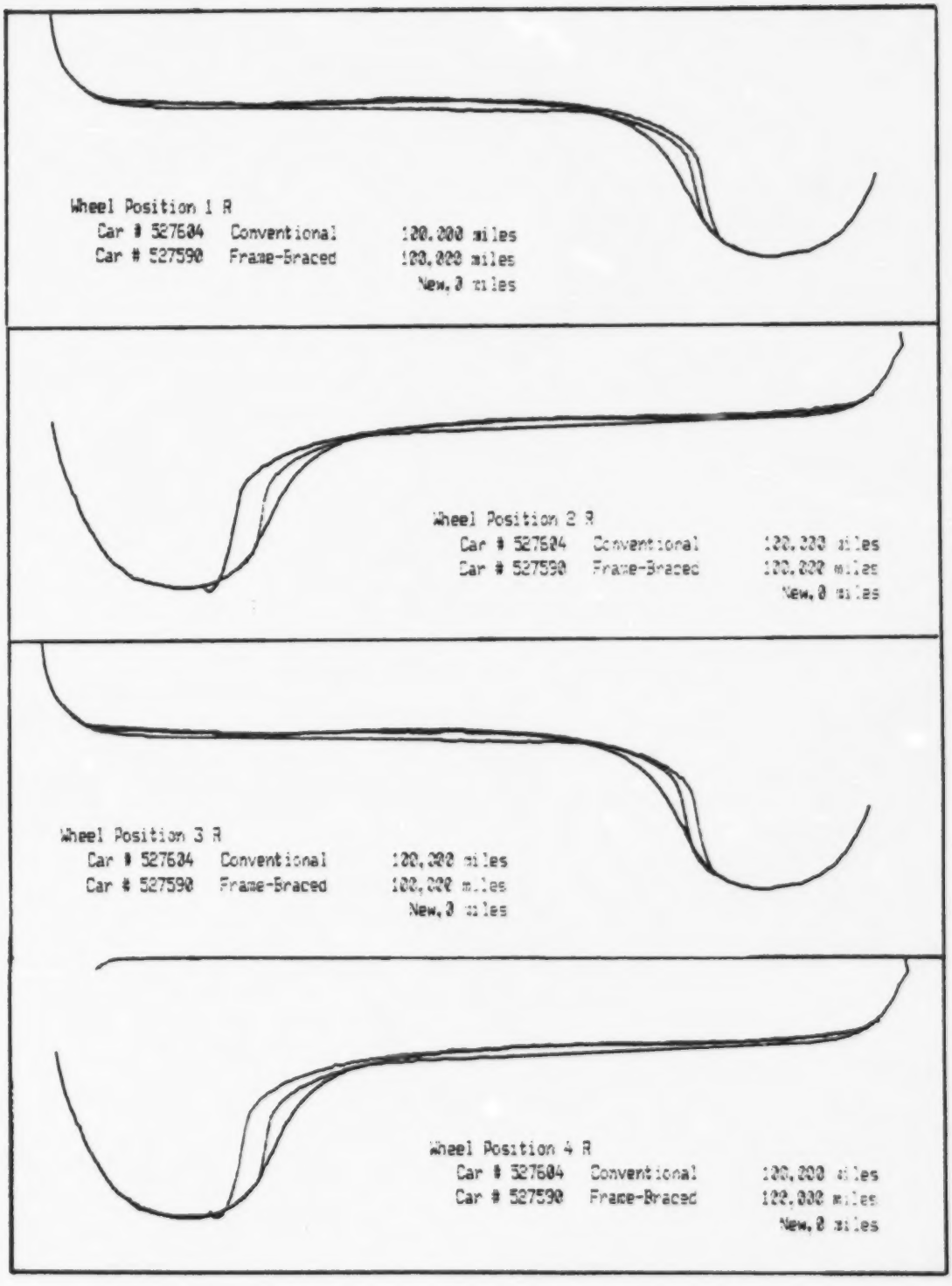
Wheel Position 1 R
Car # 527604 Conventional 120,000 miles
Car # 527590 Frame-Braced 120,000 miles
New, 0 miles
Wheel Position 2 R
Car # 527604 Conventional 120,000 miles
Car # 527590 Frame-Braced 120,000 miles
New, 0 miles
Wheel Position 3 R
Car # 527604 Conventional 120,000 miles
Car # 527590 Frame-Braced 120,000 miles
New, 0 miles
Wheel Position 4 R
Car # 527604 Conventional 120,000 miles
Car # 527590 Frame-Braced 120,000 miles
New, 0 miles

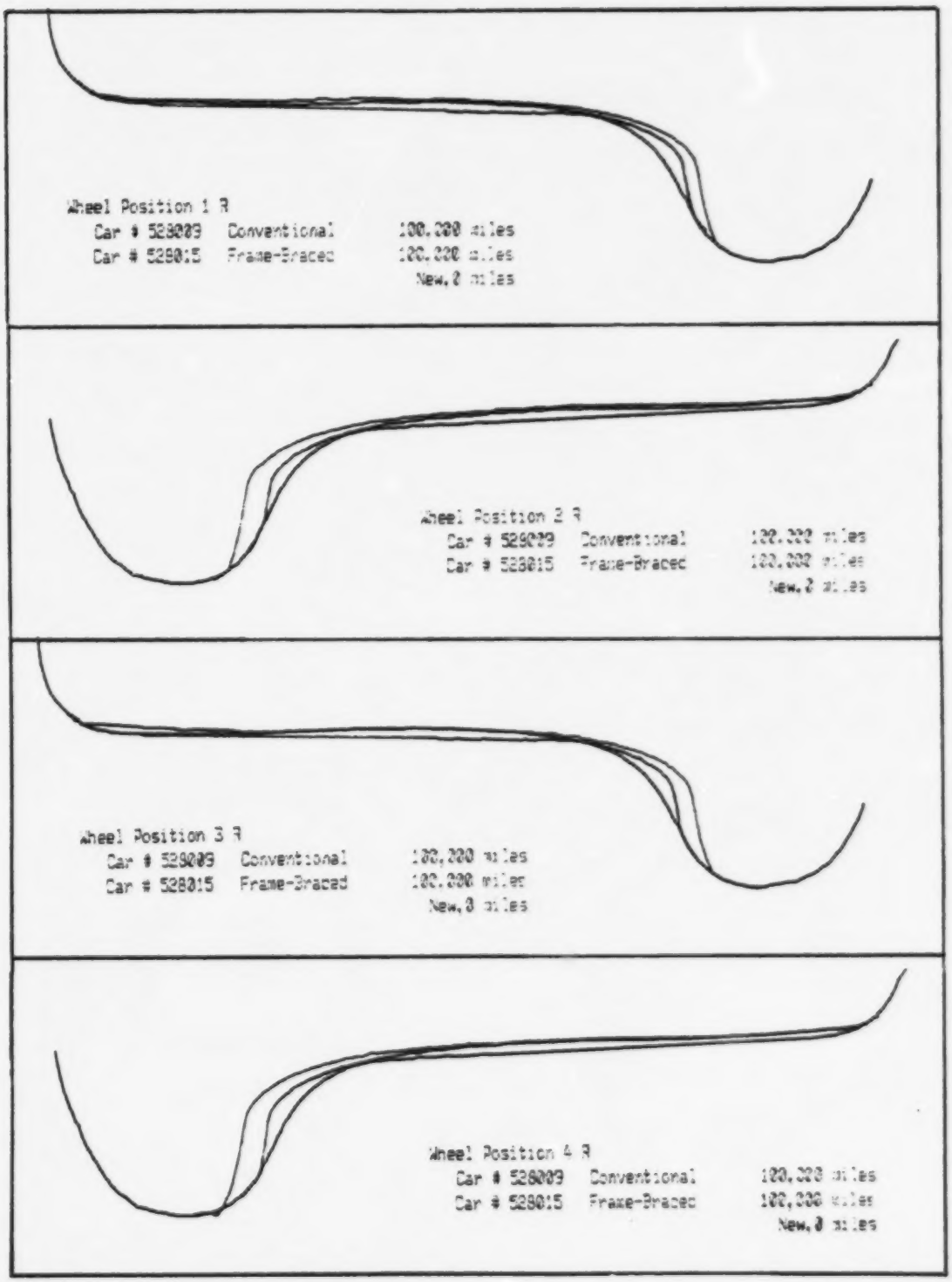
Wheel Position 1 R
Car # 528009 Conventional 100,000 miles
Car # 528015 Frame-Braced 100,000 miles
New, 0 miles
Wheel Position 2 R
Car # 528009 Conventional 100,000 miles
Car # 528015 Frame-Braced 100,000 miles
New, 0 miles
Wheel Position 3 R
Car # 528009 Conventional 100,000 miles
Car # 528015 Frame-Braced 100,000 miles
New, 0 miles
Wheel Position 4 R
Car # 528009 Conventional 100,000 miles
Car # 528015 Frame-Braced 100,000 miles
New, 0 miles

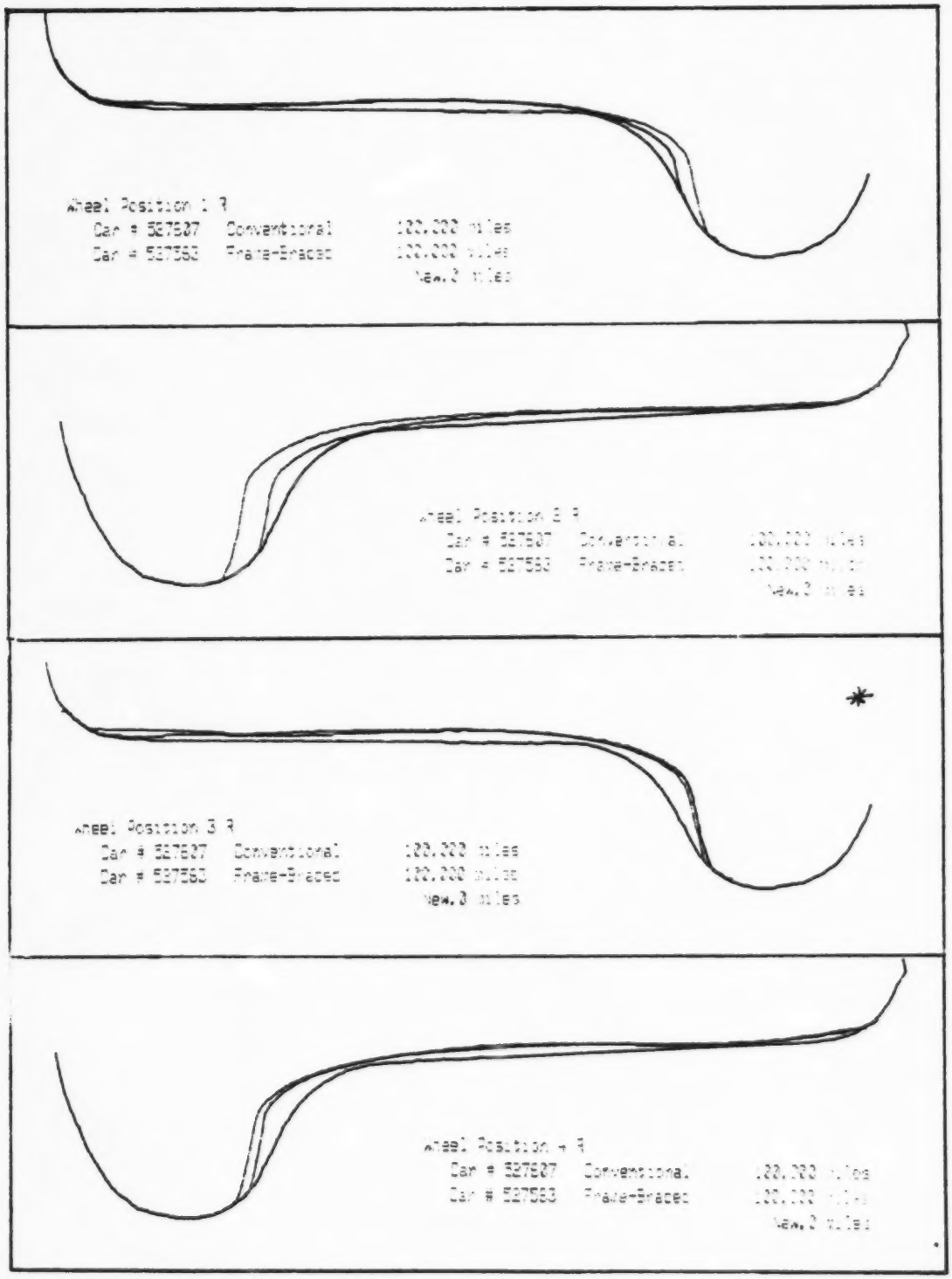
Wheel Position 1 ?
Car # 527537 Conventional 120,000 miles
Car # 527563 Frame-Braced 120,000 miles
New,? miles
Wheel Position 2 ?
Car # 527537 Conventional 120,000 miles
Car # 527563 Frame-Braced 120,000 miles
New,? miles
Wheel Position 3 ?
Car # 527537 Conventional 120,000 miles
Car # 527563 Frame-Braced 120,000 miles
New,? miles
Wheel Position 4 ?
Car # 527537 Conventional 120,000 miles
Car # 527563 Frame-Braced 120,000 miles
New,? miles